संपादक
डॉ. गिरिराजशरण अग्रवाल
डॉ. मीना अग्रवाल

ISSN 0975-735X

शोध दिशा

58

UGC APPROVED CARE LISTED JOURNAL

रेणु के निबंधों में साहित्यकारों की भूमिका

डॉ॰ पोर्शिया सरकार
सहायक अध्यापिका
निस्तारिणी कॉलेज, पुरुलिया (पश्चिम बंगाल)

उन्नीसवीं शताब्दी के अंत तक अनेक नवीन वैचारिक भावनाओं के संप्रेषण की आवश्यकता नए रूप में महसूस की गई। नवजागरण, राष्ट्रीय मुक्ति आंदोलन, जनवादी आंदोलन आदि ने लेखकों और पाठकों को करीबी रिश्तों में बाँध दिया। ऐसे ही अवस्था में निबंध साहित्य का जन्म हुआ। वैसे यदि हम रेणु के निबंध साहित्य का अवलोकन करेंगे, तो हम पाएँगे कि रेणु ने कुल आठ निबंधों की रचना की है। उनमें कुछ निबंध काफी महत्त्वपूर्ण हैं। रेणु की समस्त रचनाओं में देश की मिट्टी, उसमें बसे लोग और उनका जीवन ही झलकता है। रेणु स्वीकार करते हैं कि उनकी प्रतिबद्धता मात्र मनुष्य के प्रति है। उनका मूल मंत्र, उनकी मूल चेतना है–'सबार ऊपरे मानुष सत्य'। इसलिए उनकी रचनाओं में भी यह आदर्श पूरी तरह से घुल-मिल गया है। उन्होंने अपने विचारों को अपने निबंधों में ठूँसने का कार्य नहीं किया है, ना ही अपनी रचनाओं को बौद्धिकता से प्रांजल बनाया है। उनका साहित्य वैचारिक क्लिष्टता से मुक्त है।

रेणु के निबंधों में 'सामाजिक कार्यकर्त्ता से दो शब्द', 'उतरी स्वप्न-परी-हरी-क्रांति', 'पतियाते हैं तो मानिए आंचलिकता भी एक विधा है', 'उलझे हुए रिश्ते : सुलझे हुए विचार', 'तीसरी कसम को जानबूझ कर फेल किया गया था' आदि निबंधों को देखा जा सकता है। इन निबंधों में उनके सामाजिक दायित्वबोध को देखा जा सकता है।

रेणु राजनीति से जुड़े हुए थे, पर स्वाधीनता-प्राप्ति के पश्चात राजनीति से उनका मोहभंग हो गया। समाज पर राजनीति के पड़नेवाले प्रभाव को वे भली-भाँति समझते थे। स्वाधीन भारत में विकास के लिए कई कदम उठाए जा रहे थे, परंतु वे सारे प्रयत्न कितने कारगर थे इसका अंदाजा रेणु जैसे सजग साहित्यकार को था। रेणु ने अपने दो निबंधों में समाज के प्रति साहित्यकारों की भूमिका को अंकित किया है। 'राष्ट्र-निर्माण में लेखक का सहयोग' नामक निबंध में रेणु की समाज के प्रति सजगता साफ झलकती है। स्वतंत्रता-प्राप्ति के पश्चात स्वतंत्र भारत की प्रमुख समस्याओं में से एक समस्या थी राष्ट्र-निर्माण की समस्या। रेणु यह महसूस कर रहे थे कि समाज और राष्ट्र नाना वैज्ञानिक अनुसंधानों, योजनाओं एवं परियोजनाओं की उड़ान भरने के लिए तैयार जरूर था, परंतु जनता की मानसिकता में वैज्ञानिक चेतना का नितांत अभाव था। उनका मानना था कि 'तरह-तरह के वैज्ञानिक प्रतिष्ठानों के द्वारा सर्वसाधारण के बीच विज्ञान का प्रसाद वितरण कर देने से कुछ नहीं होगा। जन साधारण की वैज्ञानिक दृष्टि को खोलने की आवश्यकता है। वैज्ञानिक संपद-लाभ करने के साथ-साथ वैज्ञानिक दृष्टि-लाभ श्रेयस्कर है। देश की खर-श्रोता नदियाँ के जल-श्रोत को विज्ञान कीशृंखला में बाँधकर, देश की बंजर और गैर-आबाद जमीन को शस्य-श्यामल बनाने के साथ-साथ मानसिक दुर्भिक्षग्रस्त राष्ट्र की चित्र-भूमि को उर्वर बनाने की

ISSN 0975-735X

आवश्यकता थी।" रेणु का मानना है कि बिजली की रोशनी बाहरी स्तर को रोशन कर सकती है लेकिन लोगों के दिलों में फैले अँधेरे को मिटाने के लिए वैज्ञानिक अनुसंधानों को सही अर्थ में लोगों की चेतना को जगाना होगा। लेखक का दायित्व अपनी रचनाओं के माध्यम से लोगों के दिलों में फैले अंधकार को दूर करना और नई सोच को जन्म देना है– 'विद्युत आलोक से गाँव-गाँव की गली-गली को आलोकित करने का क्या अर्थ, जबकि जनजीवन के मन के कोने में फिर अंधकार बद्धमूल हो रहा?'[2] वे "आत्मानुसंधान, तीव्र विचार-विमर्श को 'मानवता की सफलता और उन्नति के लिए न्यूनतम उपकरण" मानते हैं। सभ्यता के सभी उपकरण प्रस्तुत कर देने से ही लोगों के अंदर की स्वाधीनता को प्राप्त नहीं किया जा सकता है।

पंचवर्षीय योजनाओं का समुचित लाभ जनता को न मिलने के कारणों पर जब रेणु विचार करते हैं तब उन्हें लगता है कि स्वाधीन भारत में त्याग और सेवा का आदर्श भाव लोगों में से विलुप्त हो गया है। गाँधी के आदर्श जो कभी लोगों को मानसिक शक्ति प्रदान करते थे, वे भी लोगों के जीवन से विलुप्त हो चुके हैं। राष्ट्र को संगठित करने का जो प्रयास राष्ट्रनायकों ने आजादीपूर्व किया था, वह प्रचेष्टा आज समाप्त हो चुकी है, जबकि लोगों को संगठित करने की जरूरत आजाद भारत में और ज्यादा है। उज्ज्वल भविष्य के निर्माण के लिए कष्टमय वर्तमान को स्वीकार करना होगा। रेणु मानते हैं कि लोकतंत्र की रक्षा हर परिस्थिति में की जानी चाहिए। राष्ट्रनिर्माण में 'लेखक और कलाकार' दोनों ही सहयोगी बनकर महत्त्वपूर्ण भूमिका निभा सकते हैं वे इसे अनिवार्य मानते हैं। वे देश के भ्रष्ट नौकरशाहों पर प्रहार करते हैं जो लेखकों को दल-विशेष के नेताओं और विभिन्न सरकारी परियोजनाओं से जुड़े भ्रष्ट नौकरशाहों का गुणगान करने के लिए एकत्रित करते हैं। रेणु लेखकों से इस प्रकार के सहयोग की अपेक्षा नहीं करते हैं क्योंकि इससे न तो राष्ट्रनिर्माण का कार्य होता है और न ही साहित्य का ही मंगल होता है। वस्तुतः जनजीवन के सुख-दुःख से कटकर लिखनेवाला लेखक कभी भी जनजीवन को प्रभावित नहीं कर सकता है। उनका मानना है कि राष्ट्र के निर्माण के लिए राष्ट्रनायकों की जितनी जरूरत है, उतनी ही जरूरत है लेखकों की, जो निष्पक्ष होकर जनसाधारण की समस्याओं को उजागर करें। उन्हें पैसे और दूसरी चीजों के प्रलोभन से अपने को मुक्त करना होगा। रेणु का मानना है कि केवल साहित्यकार ही अपनी रचना से समाज के नवनिर्माण का कार्य नहीं करता है, बल्कि गाँव में रहनेवाला लुहार, किसान भी नवनिर्माण में अपने स्तर पर सहयोग करता है। वह अपने कार्यों से नई पीढ़ी के लिए प्रेरणा का स्रोत बन जाता है। रेणु कहते हैं कि 'क्या पता कि नवनिर्माण की तीव्र प्रेरणा कहीं किसान के बेटे को स्पंदित कर रही हो और वह अपनी अटपटी भाषा में मन के उल्लास को जोड़ने की चेष्टा कर रहा हो। दूर किसी गाँव में बैठा कोई बूढ़ा लुहार ट्रेक्टरों, बुल्डोजरों की गड़गड़ाहट को सुनकर फिर से जवान हो रहा हो, संभव है, साहित्यकारों की पंक्ति में उन्हें स्थान न मिले, किंतु, जनजीवन में नवीन प्रेरणा और आदर्श स्थापित करने का श्रेय उन्हीं कलाकारों का होगा।'[3]

देश की उन्नति के प्रति रेणु की जागरूकता को एक और निबंध में हम देख सकते हैं। वह है–'जनजागरण में साहित्यकार की भूमिका'। इसमें देश की सामाजिक समस्याओं के साथ रेणु ने राजनीतिक उतार-चढ़ाव को भी बहुत अच्छी तरह से दिखाया है। साहित्य-जगत में आने से पहले ही रेणु ने राजनीति को अपने जीवन में महत्त्वपूर्ण स्थान दिया था। उनका मानना है कि जनसाधारण की समस्याओं को समझने और दूर करने का सबसे बड़ा माध्यम राजनीति है। रेणु का राजनीति में प्रवेश सियासी शोहरत पाने के लिए नहीं था। शुरुआती दौर से ही उनके दिलोदिमाग में जनता ही

ISSN 0975-735X

सर्वोपरि थी। इसलिए सन् 1972 में वे बिहार विधानसभा के चुनाव में निर्दलीय प्रत्याशी के रूप में चुनाव लड़े। राजनीति के जरिए वे समाज में इंकलाब लाना चाहते हैं। वे समाज का समुचित विकास चाहते हैं। इसके लिए वे समाज में विभिन्न आंदोलनों की जरूरत को महसूस करते हैं, लेकिन वे आंदोलन के मूकद्रष्टा न थे। उन्होंने बाकायदा हाथ में बंदूक लेकर विभिन्न आंदोलनों में भाग लिया, जिसका एक उदाहरण सन् 1975 का बिहार-आंदोलन था, जिसमें उन्होंने भाग लिया था। रेणु लंबे समय से पेप्टिक अल्सर से पीड़ित थे, परंतु घर और अस्पताल का चक्कर लगाते समय उन्होंने अपने वतन और उसकी जरूरतों को कभी अनदेखा नहीं किया, वरन् अस्पताल में जब ऑपरेशन के लिए डॉक्टरों ने उन्हें मजबूर किया, तब वे ऑपरेशन की तारीख को आगे बढ़वाते रहे और आंदोलन में सक्रिय होकर भाग लेते रहे। जब राजनीति में असफलता मिली, तो उन्होंने साहित्य की शक्ति का उपयोग किया, पर उद्देश्य एक ही रहा–जनसाधारण की चेतना को जाग्रत करना। वे उस साहित्य को बकवास मानते हैं, जो समाज-हित में कार्य नहीं करता है। लेखन की सार्थकता तभी है, जब लेखक समाज के उपेक्षित, प्रताड़ित, प्रवंचित और दलित समुदाय की वास्तविकता को अपनी रचना में स्थान देता हो, वरना लेखन व्यर्थ है। इस निबंध में वे लिखते हैं–'आपने 'मैला आँचल' अगर पढ़ा हो तो आजादी के पूर्व की राजनीतिक, सामाजिक तथा आर्थिक झलक के साथ आपको आजादी के बाद की झलक भी मिली होगी।'[4] वस्तुतः 'मैला आँचल' लेखक की कल्पना नहीं बल्कि भारत की वास्तविक तस्वीर है। मैला आँचल का बावनदास आजाद भारत के नेताओं के घिनौने रूप को सामने लाते हुए कहता है–'अब तो सभी लोग 'मैले' (एम॰एल॰ए॰) बनना चाहते हैं। पटना में रहना चाहते हैं। अब जनता को कौन पूछता है।'[5] यही नहीं वह जातिवाद के दलदल में फँसे काँग्रेसियों पर प्रहार करता है और कहता है–'अब सभी काँग्रेसियों को अपनी-अपनी टोपियों पर अपनी जाति लिखवा लेना चाहिए...भूमिहार काँग्रेसी 'राजपूत काँग्रेसी', 'कायस्थ काँग्रेसी'।'[6] 'परती परिकथा' के संबंध में लेखक की स्वीकारोक्ति है–'परती परिकथा में मैंने जमीन, भूमिहीनों और खेतिहर मजदूरों की समस्या को लेकर बातें की। जातिवाद, भाई-भतीजावाद और भ्रष्टाचार की पनपती बेल की ओर मात्र इशारा नहीं किया था, इसे समूल नष्ट करने की आवश्यकता पर भी बल दिया था।'[7] वे अपनी अन्य कहानी के संबंध में कहते हैं–'मैंने निम्न मध्यवर्ग, पिछड़े लोगों, भूमिहीनों, खेतिहर मजदूरों तथा समाज के ऐसे लोगों का चित्रण किया जिन्हें हरिजन कहकर गौरवान्वित तो कर दिया गया, किंतु वे आजादी के बाद भी बे-जमीन, पिछड़े और अछूत एवं आक्रांत होते रहे। शोषण तो कभी बंद नहीं हुआ, बल्कि सारी विकृतियाँ दिन-दूनी, रात चौगुनी होकर समाज को ग्रसती गईं।'[8] रेणु को लगता है कि भारतीय समाज के नग्न चेहरे को अपने साहित्य में दिखाया जाए ताकि पाठकवर्ग समाज में बदलाव लाने के लिए कदम बढ़ाए, लेकिन ऐसा हुआ नहीं, इसलिए उन्हें पीड़ा होती है। वे कहते हैं–'तो क्या हुआ लिखकर यह सब? मैं सोचता हूँ कि लिखने के बजाय अगर मैं किसी लड़के पर मोटी रकम तिलक में गिनानेवाले पड़ोसी के दरवाजे पर सत्याग्रह करने बैठ जाता, अछूतों को सही जगह दिलाने के लिए कम-से-कम अपने ही गाँव में कोई प्रयत्न करता या जाति-पाँति के विरुद्ध अनशन करता तो अच्छा था। एक हजार से भी ज्यादा पृष्ठ लिखने और भूरी-भूरी प्रशंसा मिलने के बावजूद मुझे मिला-यह सड़ा हुआ बिहार।'[9] रेणु समाज में दहेजप्रथा के भयानक रूप को देखते हैं, जो कमने के बजाए पूरे समाज में फैलता ही जाता है। समाज एक तरफ विकास के पथ पर आगे बढ़ता है, पर दलितों की समस्या का समाधान नहीं होता है। वे आज भी शोषण के

ISSN 0975-735X

शिकार हैं। रेणु को लगता है कि उनका संपूर्ण लेखन ही व्यर्थ है। उन्हें लेखक के रूप में प्रशंसा अवश्य मिली, लेकिन उससे समाज का कोई फायदा नहीं हुआ। उन्होंने सड़े-गले बिहार के समाज का वर्णन किया, ताकि सड़ांध दूर करने के लिए बिहार के लोगों को जागरूक किया जा सके, पर वे अपने उद्देश्य में असफल रहे। यह असफलता एक साहित्यकार के रूप में उन्हें पीड़ा देती है। रेणु ने बिहार के संबंध में यह टिप्पणी कितने दुःख के साथ किया होगा। यह सर्वविदित है कि रेणु अपनी मिट्टी और अपने क्षेत्र से कितना प्रेम करते हैं।

रेणु का निबंध 'जनजागरण में साहित्यकार की भूमिका' राजनीतिक दृष्टि से अत्यंत महत्वपूर्ण है। वास्तव में साहित्यकारों को देश और जनता के प्रति अपने दायित्व को समझना होगा। रेणु ने भी इस बात को बहुत पहले ही महसूस किया था। उनका मानना था, राष्ट्र को बचाने और हर तरह से उसे तरक्की और विकास के रास्ते पर ले जाने की जिम्मेदारी जितनी एक सिपाही की है, उतनी साहित्यकार की भी है। रेणु अपने लेखन से संपूर्ण जीवन इसी बात को प्रमाणित करते रहे। उन्होंने 1942 ई॰ में जेल की सजा काटी, नेपाल की जनक्रांति में सिर्फ भाग ही नहीं लिया, वरन् राइफल भी उठाया। 1975 ई॰ के बिहार-आंदोलन में रेणु के साथ-साथ बिहार के अंदर और बाहर के हजारों युवा शामिल होते हैं और जेल जाते हैं। कुछ फरार भी हो जाते हैं। कुछ को गैर बिहारी कहकर राज्य से निष्कासित कर दिया जाता है। रेणु लिखते हैं–'एक ओर राष्ट्रीय एकता नेशनल इंटीग्रेशन की लंबी बातें और दूसरी ओर किसी भारतीय का अपने ही देश के किसी प्रांत से निष्कासन–कैसी विडंबना है? राज्य की ओर से यह अलगाव की भावना हमें आश्चर्य में ही नहीं डाल रही, बल्कि आशंकित करती है कि किसी दिन हमें, यानी हम बुद्धिजीवियों को अपने देश से ही निष्कासित करने का परवान न निकाल दें।'[10] रेणु ने जिस अलगाववाद की समस्या का उल्लेख किया है, वह आज पूरे देश में जोर पकड़ती जा रही है। आज सत्ता का विरोध करनेवाले बुद्धिजीवी स्वयं को असुरक्षित महसूस कर रहे हैं। 1975 ई॰ के बिहार-आंदोलन में भाग लेने के लिए रेणु ने अपने शारीरिक बीमारी की भी उपेक्षा की। डॉक्टरों ने सावधानी बरतने को कहा था, लेकिन रेणु ने उनकी एक भी सलाह को नहीं माना, यहाँ तक कि ऑपरेशन की तारीख को भी आगे करवाते गए जिसका परिणाम यह हुआ कि 11 अप्रैल 1977 की सुबह उनकी मौत हो गई, परंतु उनका पार्थिव शरीर मानो अब भी पुकार रहा है–'सिर्फ कलम से नहीं अपनी काया से भी कुछ लिखना जरूरी है। अपने ही कलेजा के रक्त में अपनी उँगली डुबाकर दीवार पर 'क्रांति अमर हो' लिख पाऊँ।'[11]

वही साहित्यकार जनता को अधिक प्रभावित कर पाए हैं, जो सर्वसाधारण की आवाज बनकर महान आंदोलनों के अगुआ बने। रेणु भी इस बात से सहमत हैं–'सच कहता हूँ, अगर इस जन-आंदोलन से अपने को किसी तरह अलग-थलग रख पाने में सफल हो पाता या तटस्थ हो पाता अथवा मौखिक सहानुभूति प्रकट कर रह जाता तो न प्रेमचंद ने मुझे माफ किया होता और न निराला ने।'[12] आजादी के बाद राष्ट्रनिर्माण सबसे चुनौतीपूर्ण कार्य था। रेणु अपने निबंधों में राष्ट्रनिर्माण के मार्ग में आनेवाली बाधाओं की चर्चा करते हैं। वे राष्ट्रनिर्माण में सामाजिक कार्यकर्ताओं और लेखकों से सहयोग की अपेक्षा करते हैं। वे जनजागरण पर बल देते हैं और जनजागृति में साहित्यकार की भूमिका को स्वीकार करते हैं। रेणु के निबंध आलोचना जगत् के साथ-साथ चलचित्र जगत के क्रूर चेहरे को समाज के सामने लाते हैं। साहित्यकार समाज का एक अंग है। वह भी समस्याओं से जूझता है। रेणु ने हमेशा साहित्यिकता को सृजन के साथ जोड़ा हैं। उनका मानना है कि एक साहित्यकार को कभी भी इसकी अवहेलना नहीं करनी चाहिए। साहित्यकार

ISSN 0975-735X

समाज का स्रष्टा है, निर्माता है वह चाहे तो अपनी वास्तविक शक्ति का प्रयोग कर समाज को एकता, ममता, प्रेम और विश्वबंधुत्व का पाठ पढ़ा सकता है। लेकिन साहित्यकारों को उनकी सही शक्ति और सामर्थ्य की पहचान कराने वाला आलोचक होता है। और उसे निष्पक्ष भाव से साहित्यकारों की सही आलोचना करनी होगी। आलोचकों पर भी उन्होंने अविश्वास प्रकट किया है। अधिकांश आलोचकों का पूर्वाग्रह से ग्रस्त होना रेणु को अप्रिय है। कवि एवं लेखकों को अपनी लेखनी किसी दबाव में आकर नहीं चलाना चाहिए। उन्हें राजनीतिज्ञ, एवं पूँजिपतियों का गुणगान करने के लिए लेखनी का दुरुपयोग नहीं करना चाहिए। रेणु ने अपनी लेखनी की निष्पक्षता की रक्षा के लिए पद्मश्री को लौटा दिया था।

निष्कर्षत: कहा जा सकता है कि उनके अधिकांश निबंध जीवन के प्रत्यक्ष अनुभवों की उपज हैं। उनके कई निबंध संस्मरणात्मक हैं और कई आत्मसंस्मरणात्मक। उनकी दृष्टि मूलत: मानवीय समस्याओं के विविध पहलुओं पर बार-बार चली जाती है। उन समस्याओं के समाधान के लिए वे कभी सामाजिक कार्यकर्त्ताओं से अपेक्षा करते हैं, कभी लेखकों से सहयोग की आशा करते हैं। वे जनता को शोषण के विरुद्ध आवाज उठाने के लिए प्रेरित करते हैं। वे जनजागरण में साहित्यकार की भूमिका को महत्त्वपूर्ण मानते हैं। साहित्य-जगत में साहित्यकार भी अपने लेखन के कारण अनेक समस्याओं का सामना करता है। प्रेमचंद, निराला और रेणु सबको आलोचना का सामना करना पड़ा था, लेकिन इन लोगों ने अपनी लेखनी को कभी विराम नहीं दिया। रेणु भी आलोचकों के समक्ष नतमस्तक नहीं हुए क्योंकि उनके लेखन के केंद्र में आम इंसान और उसकी समस्यायें रही हैं। रेणु का मानना है कि साहित्यकारों को चाहिए कि वह बंद कमरों से निकलकर समाज के जरूरतमंदों का साथ दें। उनके बारे में कोरे कागजों पर लिखना ही सबकुछ नहीं है। परिवर्तन, इनक्लाव क्रांति आदि का साक्षी बनकर ही उन्हें साहित्य में स्थान दिया जाना चाहिए–'बंद कमरे में बैठकर लिखने का जमाना लद चुका है। लेखक को परिवर्तन की प्रक्रिया का गवाह नहीं, भागीदार बनना है।'[13]

संदर्भ

1. भारत यायावर (संपादक), रेणु रचनावली (खंड-5), राजकमल प्रकाशन, नई दिल्ली, संस्करण 2007, पृ॰ 268
2. वही, पृ॰ 268
3. वही, पृ॰ 271
4. वही, पृ॰ 287
5. वही, पृ॰ 287
6. वही, पृ॰ 287
7. वही, पृ॰ 287
8. वही, पृ॰ 287
9. वही, पृ॰ 287
10. वही, पृ॰ 288
11. वही, पृ॰ 288
12. वही, पृ॰ 293
13. वही (खंड-4), राजकमल प्रकाशन, नई दिल्ली, संस्करण 2007, पृ॰ 479

Highland Garden , Tower-III, 6th Floor,
Bigbazar Complex, Purulia-723101, West Bengal
portiasarkar1@gmail.com

ISSN 0975-735X

देवानां भद्रा सुमतिर्ऋजूयताम्।। ऋ० १/८९/२

ISSN : 2395-7115
June 2022
Issue 15, Vol. 6(2)

Impact Factor
5.642

Bohal Shodh Manjusha

AN INTERNATIONAL PEER REVIEWED, REFEREED MULTIDISCIPLINARY
& MULTIPLE LANGUAGES RESEARCH JOURNAL

UGC Valid Journal (The Gazette of India, Extraordinary Part III, Section 4, Dated July 18, 2018)

विशेषांक सम्पादक :
डॉ. पायल लिल्हारे

सम्पादक :
डॉ. नरेश सिहाग, एडवोकेट

Publisher :

Gugan Ram Educational & Social Welfare Society (Regd.)
202, Old Housing Board, Bhiwani, Haryana-127021

जून 2022

www.bohalsm.blogspot.com
Impact Factor : 5.642

Bohal Shodh Manjusha ISSN : 2395-7115
June 2022 Page No. : 38-44

AN INTERNATIONAL PEER REVIEWED, REFEREED MULTIDISCIPLINARY
& MULTIPLE LANGUAGES RESEARCH JOURNAL

समकालीन हिंदी आदिवासी कवयित्री निर्मला पुतुल की कविताओं में स्त्री-प्रश्न

डॉ. पोर्शिया सरकार

सहायक अध्यापिका, हिंदी विभाग, निस्तारिणी कॉलेज पुरुलिया, पश्चिम बंगाल

साहित्य निरंतर बहती जल धारा है। इसकी गतिशीलता ही इसका प्राण है। सैकड़ों वादों एवं विमर्शों को संजोए यह आज भी मानवजाति के लिए संजीवनी का काम कर रही है। आज का दौर काफी विमर्शों का दौर है। जिनमें दलित विमर्श, स्त्री विमर्श और आदिवासी विमर्श काफी चर्चित है। परंतु ऐसा नहीं है कि आज से पहले ये विमर्श साहित्य की विषय वस्तु से बाहर थे। समय–समय पर बहुत से कवियों एवं लेखकों ने जातिवाद, रूढ़िवादी विचारधारा, पुरानी परम्परा, असपृश्यता, लैंगिक असमानता आदि पर अपनी लेखनी से प्रहार किया। परंतु आदिवासी समाज का जीवन–सत्य एवं संघर्ष का दौर उन्हीं की लेखनी से प्रकट होना यह समय और इस सदी की सबसे बड़ी उपलब्धि है अर्थात् समसामयिक जितने भी विमर्श है पहले भी साहित्य में क्षीण रूप से विद्यमान थी। परंतु इन सभी विमर्शों में सबसे महत्त्वपूर्ण विमर्श है जिसने आज एक आन्दोलन का रूप धारण कर लिया है वह है आदिवासी साहित्य में 'स्त्री लेखन'।

जैसा कि हम सभी जानते हैं कि कोई भी वाद या आन्दोलन ऐसे ही साहित्य और समाज का हिस्सा नहीं बन जाता। इसके पीछे सदियों का शोषण का इतिहास होता है। युग–युग से भारतीय स्त्रियों को क्षमा, दया, त्याग, प्रेम और सेवा का प्रतिरूप कहकर उनका शोषण किया जाता रहा। हमारी संस्कृति और सभ्यता ने स्त्रियों को देवी का दर्जा देकर भी उन्हें शोषण मुक्त होने नहीं दिया और अगर हम तथाकथित मुख्य धारा से हटकर इन आदिवासी महिलाओं का जीवन देखें तो उसमें शोषण, अपमान, असमर्थता और विद्रूपता के सिवा और कुछ नहीं मिलेगा। इस वजह से आदिवासी महिला लेखन वास्तव में आदिवासी महिलाओं की अस्तित्व की लडाई की पहली क्रांति है। चाहे स्त्री निम्न वर्ण की हो या उच्च वर्ण की उनकी परिस्थितियाँ और समस्याएँ समान है। उन पर होने वाला शोषण भी समान है। आदिवासी महिलाओं के जीवन का दर्द अकल्पनीय है। इन महिलाओं द्वारा लिखा गया साहित्य ने अभी तक पाठकों के समक्ष अपनी पहचान नहीं बना पाई। जितनी कि आदिवासी लेखकों और साहित्यकारों ने बनाई है। अभी भी आदिवासी महिला लेखन बहुत हद तक उपेक्षित ही है। परंतु वह समय दूर नहीं जब इन महिलाओं का स्वर सम्पूर्ण देश भर में गूँजने लगेगा।

अब तक हमने स्त्रियों के दुख, दर्द और पीड़ा को जितना भी साहित्य के द्वारा महसूस किया है। वे अधिकांशतः कवि या लेखकों की कल्पना की उपज थी। हिंदी साहित्य में भी विभिन्न युगों में अनगिनत कवियों एवं लेखकों ने स्त्रियों के जीवन से जुड़ी नाना समस्याओं, असमर्थताओं और विसंगतियों का वर्णन करने का प्रयास किया।

जिसमें प्रेमचंद, प्रसाद, निराला, महादेवी एवं मैथिलीशरण प्रमुख है। परन्तु अधिकांश कवि या लेखक पुरूष ही रहे जिन्होंने नारी हृदय के कोने–कोने को दर्शाया। परंतु आदिवासी महिलाओं के जीवन–सत्य अंधकार में ही रह गया है। कहने का अभिप्राय यह है कि आदिवासी स्त्रियाँ क्या सोचती है? क्या महसूस करती है, किन मूल्यों को धारण करती है? उनके विश्वास एवं आस्थाएँ क्या है? उन्हें समाज के किस रवैए पर क्षोभ है? कहाँ अपने अस्तित्व के मिटने के दर्द को सहती है? कब असमानता के दंश को अपने अंतरात्मा के बहुत भीतर चुभता हुआ महसूस करती है? आदि बातें युगों से ही अनसुनी रह गई है। आदिवासी महिलाएँ अक्सर जातिगत भेदभाव और पारिवारिक अत्याचार के रूप में दोहरे शोषण का शिकार होती है। उनकी सारी जिन्दगी शोषण और दमन का लेखा–जोखा होता है। आदिवासी समाज में सामाजिक, आर्थिक एवं शारीरिक रूप से महिलाएँ ही शोषण का शिकार होती है। अतः आदिवासी स्त्रियों का अपनी पीड़ा और तड़प को दुनिया से साझा करना ही अपने आप में एक इंकलाब है।

आदिवासी स्त्रियों का इस लेखन क्षेत्र में प्रत्यक्ष रूप से भाग लेना और अपने अधिकारों की माँग करना ही आदिवासी महिला लेखन आन्दोलन की सफलता की पहली सीढ़ी है। साहित्य में स्त्रियों का दुःख–दर्द, पीड़ा, अधिकार आदि की बात कहना कोई नई बात नहीं है। परन्तु अगर कुछ भी नया है तो वह है आदिवासी स्त्रियों की कहानी का उनकी जुबानी होना। ये स्त्रियाँ तमाम उम्र सामाजिक भेदभाव, जातिगत भेदभाव, लैंगिक शोषण का शिकार होती रही। साफ शब्दों कह सकते हैं कि वह एक ही चक्की में सैकड़ों बार पीसती है। इसलिए भी इन स्त्रियों का अपनी लेखनी के माध्यम से अपने विचारों को व्यक्त करना ही इनके अस्तित्व को दर्शाती है। किसी भी आन्दोलन में स्त्रियों का सक्रिय रूप से भाग लेना ही उन आन्दोलनों की सार्थकता है।

सम्पूर्ण आदिवासी साहित्य और भारतीय आदिवासी महिला लेखन को देखें तो हम पाएँगे कि दोनों एक दूसरे के बिना अधूरे है। आदिवासी महिला साहित्य लेखन एक साहित्यिक आन्दोलन का रूप ले चुका है। इस प्रसंग में अगर समकालीन आदिवासी कवयित्रियों एवं लेखिकाओं की बात करें तो एलिस एक्का, रोज केरकेट्टा, निर्मला पुतुल, सरोज केरकेट्टा, वंदना टेटे, दमयंती सिंकू, सावित्री बड़ाइक, रेशमा हासदा आदि काफी चर्चित हैं। जिनके सशक्त लेखन से होकर ही समकालीन आदिवासी महिला लेखन गुजर रहा है। यह विषय अपने आप में इसलिए और भी महत्त्वपूर्ण है क्योंकि इस आंदोलन में स्त्रियों की भागीदारी परोक्ष नहीं बल्कि प्रत्यक्ष है। स्त्री की अनुभूति को उसकी जुबानी सुनना ही एक बहुत बड़े आन्दोलन का आगाज़ है। जिसमें झारखंड के दुमका जिले के दुधनी कुरुवा गाँव के एक ग़रीब आदिवासी परिवार में जन्मी कवयित्री निर्मला पुतुल की कविताएँ बहुत महत्त्वपूर्ण है। जिनकी कविताओं का मूल स्वर है दलित और शोषित आदिवासी महिलाओं के भोगे हुए यथार्थ को दर्शाना। अब तक आदिवासी महिलाएँ जिस शोषण, उत्पीड़न और हिंसा का शिकार होती रही। उन सारी बातों का उनकी कविताएँ विरोध करती हुई मिलती है। उनकी कविताओं में पितृसत्तात्मकता के प्रति गहरा आक्रोश है। उनकी कविताओं में आदिवासी महिलाओं के जीवन का द्वंद्व, पीड़ा, अपमान, ग्लानि और असमर्थताओं की झाँकी जहाँ है, वहीं प्रतिवाद, विद्रोह और क्रांति का तीव्र स्वर भी।

वे एक ऐसी साहित्यकार है जिनके साहित्य में आदिवासी स्त्रियों का सम्पूर्ण जीवन झलकता है। उनकी कुछ प्रमुख कविताएँ है– 'मेरे एकांत का प्रवेश द्वार', 'क्या तुम जानते हो', 'उतने ही जनमेगी निर्मला पुतुल', 'अपने घर की तलाश में', आदिवासी स्त्रियाँ', अभी खूँटी में टाँगकर रख दो माँदल,' उतनी दूर मत ब्याहना बाबा'

आदि। उनकी तीन कविता संग्रह प्रकाशित हो चुकी है। पहली 'अपने घर की तलाश में' दूसरा 'नगाड़े की तरह बजते शब्द' और तीसरा 'बेघर सपने' इन कविता–संग्रहों से ही वे आदिवासी महिला लेखन आन्दोलन की अग्रणी बन गई। उनकी कविताओं की भावभूमि स्त्री–अस्तित्व की पहचान को लेकर आगे बढ़ती है। एक तरह से अपने कविताओं के माध्यम से उन्होंने सैकड़ों सवाल समाज के सामने रखा है। इनकी कविताएँ नारी की अंतस की तड़प और गहन वेदना को दर्शाती है। जिस वेदना एवं पीड़ा को सदियों से स्त्री कहने और प्रकट करने से हिचकती थी। परम्परावादी रूप में जिस परिवार में लड़की का जन्म होता है वहाँ भी उसे पूरी तरह से बोलने का हक नहीं होता है। कवयित्री का मानना है कि इस सड़ी गली सोच को मिटाकर ही समाज के लिए नया रास्ता तैयार करना होगा। लड़कियों को पैदा होने के बाद से ही अक्सर यह याद दिलाया जाता है कि एक दिन उसे अपने घर को छोड़कर पराया घर जाना पड़ेगा। उस पराए घर को भी वह 'अपना घर' अनगिनत शर्तों के बदले ही कह पाती है। निर्मला पुतुल अपनी कविता 'क्या तुम जानते हो' में ऐसे ही कुछ सवालों के जबाव ढूँढने की कोशिश करती है–

"घर प्रेम और जाति से अलग
एक स्त्री को उसकी जमीन के बारे में बता सकते हो।
बता सकते हो तुम?
बता सकते हो
सदियों से अपना घर तलाशती
एक बेचैन स्त्री को
उसके घर का पता?"[1]

उपर्युक्त पंक्तियों में छिपे दर्द का एहसास एक स्त्री ही बता सकती है। कवयित्री ने कितना सच ही कहा है। स्त्रियाँ उम्रभर अपना घर समझकर घरों को संवारती है पर उन घरों पर अक्सर उनका कोई अधिकार नहीं होता है। निर्मला पुतुल की कविताएँ बिना किसी आडम्बर और लाग लपेट के पूरी ईमानदारी के साथ सच्चाई को दर्शाती है। जिनके साहित्य के द्वारा सदियों से शोषण का शिकार होती आदिवासी महिलाओं को सही माईने में बोलने की आजादी मिली है। इनसे प्रेरित होकर कई आदिवासी स्त्रियाँ भी अपने हृदय के कोने में छिपे दर्द की परत खोलने का साहस कर रही है। अब ये हर तरह से वंचित होना अपना नसीब नहीं मानती। वह आज अनायास ही साहस कर अपने पिता से कहती है कि उसे किस तरह का घर और किस तरह के वर के हाथों सौंपे। कवयित्री की 'उतनी दूर मत ब्याहना' नामक कविता में इन भावों को अनायास देखा जा सकता है। जहाँ वे कह उठती है–

"बाबा!
मुझे उतनी दूर मत ब्याहना
जहाँ मुझसे मिलने जाने खातिर
घर की बकरियाँ बेचनी पड़े तुम्हें
मत ब्याहना उस देश में
जहाँ आदमी से ज्यादा

ईश्वर बसते हो।"[2]

यह कविता एक बहुत ही महत्त्वपूर्ण कविताओं में से एक है जहाँ एक आदिवासी लड़की अपने पिता से प्रार्थना करती है कि उसे ऐसी जगह न ब्याहे जहाँ आदमी से ज्यादा ईश्वर बसते हो। वह अपने पिता से आग्रह करती है कि उसे ऐसी जगह ब्याहे जहाँ जंगल हो, पहाड़ हो, नदी हो और जहाँ सूर्योदय एवं सूर्यास्त दिख दे। कवयित्री ऐसी बहुत सी इच्छाओं को अपनी कविता में कहती हुई मिलती है। इस कविता को मामूली कविता नहीं समझनी चाहिए क्योंकि लड़कियों को इस प्रकार से अपनी इच्छा और विचार जाहिर करने का हक नहीं था। युग-युग से नारी को प्रताड़ित हो कर भी उफ तक करने की आजादी नहीं थी। नई युग की नई ने युगों से शोषित एवं अवहेलित महिलाओं को बोलने की आजादी दी। निर्मला पुतुल की कविताओं में विरोध से लड़ने का स्वर जहाँ है वहीं सामाजिक दोगलेपन और जातिगत व्यवस्था के बंधनों पर प्रहार का स्वर भी है।

कितना सच ही कहा है विवाह के नाम पर लाखों लड़कियों को एक ऐसी खूँटी के साथ बाँध दिया जाता है जहाँ झटपटहट के सिवाय और कुछ नहीं मिलता। कवयित्री का मानना है कि एक लड़की सबसे पहला जुल्म माँ-बाप के घर में ही शोषित होना शुरू होती है। उन्हें शिक्षा तो दूर की बात सही माइने में पौष्टिक आहार भी नसीब नहीं होता। वे इतनी बदनसीब होती है जिन्हें विधवा होने पर और पति के छोड़ देने पर उनको किसी भी प्रकार की सम्पत्ति में हिस्सेदारी न के बराबर होती है। माता-पिता अक्सर विवाह के समय कुछ दान दहेज और बारातियों का आवभगत कर उससे हमेशा के लिए छुटकारा पा लेते हैं। ससुराल में उसकी स्थिति कठपुतली की भांति हो जाती है। वहाँ उसका सबसे जरूरी काम ससुराल की मर्यादा को सहेजकर रखना होती है। जहाँ उसके सिवाय हर कोई पर्फेक्ट है। जहाँ साँझ सवेरे अपमान के शब्द और लांछनाओं के तीर अंतरात्मा तक को लहुलूहान कर देते हैं तब उसे माँ बाप की याद हो आती है और उसे विलाप करने के लिए अंधेरे कोने को चुनने के सिवाय और कोई चारा नहीं होता है। अपने को कोसकर और दिल को कचोट कर वह रह जाती है। जो अत्यंत पीड़ादायक है। आदिवासी महिलाओं के जीवन का दुःख, पीड़ा और असमर्थताएं इससे कई गुना अधिक है। परन्तु आज की इस आदिवासी महिला साहित्यकारा ने मानो असमर्थताओं का चोला उतार फेंका है और सारी व्यवस्था के विरुद्ध विद्रोह छेड़ दिया है। वह अपने परिवार और समाज के सामने अपने वजुद को जताना चाहती है। वह चीख-चीख कर कहना चाहती है कि देखो मेरे शरीर के भीतर भी एक आत्मा है। मेरे भी कुछ जज्बात, ख्वाहिशें और सपने है। 'क्या तुम जानते हो' नामक कविता में निर्मला पुतुल कहती है-

'तन के भूगोल से परे
एक स्त्री के
मन की गाँठे खोल कर
कभी पढ़ा है तुमने
उसके भीतर का खौलता इतिहास?"[3]

पितृसत्ता के विद्रूप चेहरे ने ही असंख्य आदिवासी महिला साहित्यकारों को जन्म दिया है। इसी पितृसत्ता से उत्पन्न शोषण ने लाखों शोषिताओं को अपनी चुप्पी तोड़ने पर मजबूर किया। अति निम्न वर्ग और आदिवासी घरों में पैदा होने वाली महिलाओं के हाथों में कुदाल और फावड़े की जगह अब कलम ने ले लिया है। सदियों से शोषित, खेतों में काम करती और मजदूर महिलाओं को अब अपने अस्तित्व का एहसास होने लगा। उनको

अब लगने लगा है कि पाशविक दुर्व्यवहार सहना अब न उनकी मजबूरी है और न ही किस्मत। उन्हें भी सर उठाकर जीने का अधिकार है। अब वे जान चुकी है कि जीवन भर समझौता करने की बजाए अपनी इच्छाओं को प्रकट करने का भी समय आ गया है। आदिवासी महिला लेखन परम्परा को आगे बढ़ाने का काम निर्मला पुतुल की कविताओं में देखा एवं महसूस किया जा सकता है। इनकी कविताओं के जरिए भी आदिवासी महिला लेखन की दिशा और दशा को और भली–भांति समझा जा सकता है। उनकी कविताओं का मुख्य स्वर नारी की अस्मिता की पहचान है। अपनी अनुभूतियों को शब्दों में अभिव्यक्ति प्रदान करना यह भी एक बहुत बड़े आन्दोलन से कम नहीं है। सदियों से मूक और बधिर की कोटि में आने वाली ये आदिवासी महिला वर्ग की कविताओं में 'उसके भीतर का खौलता इतिहास?' कहना बहुत बड़ी बात है। निर्मला पुतुल ऐसी हिम्मतवाली कवयित्रियों में अग्रणी है। उनकी तरह असंख्य आदिवासी महिलायों को अब इस पुरुष तांत्रिक समाज पर आस्था नहीं रहीं। न समाज व्यवस्था पर वे विश्वास करती है और न ही किसी रिश्तों पर। अब वे जान चुकी है कि उनका हर हाल में शोषण होना तय हैं। चाहे कुछ भी हो जाए कुछ नहीं बदलने वाला। अगर कुछ बदलता है तो वह है शोषण के पैंतरे। उनकी कविता 'मैं वो नहीं हूँ जो तुम समझते' नामक कविता की कुछ पक्तियाँ यहाँ दृष्टव्य है–

"मैं चुप हूँ तो मत समझो कि गूँगी हूँ
या कि रखा है मैंने आजीवन मौन–व्रत
गहराती चुप्पी के अँधेरे में सुलग रही है भीतर
जो आक्रोश की आग
इसकी रोशनी में पढ़ रही हूँ
तुम्हारे खिलाफ अकेले लड़ने के खतरों का लेख।"[4]

उपर्युक्त पक्तियाँ 'इसकी रोशनी में पढ़ रही हूँ तुम्हारे खिलाफ अकेले लड़ने के खतरों का लेख' कहने के लिए काफी हिम्मत की जरूरत है। क्योंकि जो हमारी तथाकथित संस्कार के खिलाफ है। समकालीन आदिवासी महिला लेखन के जरिए अब महिला अपने मन और शरीर की बात कह देने में संकोच नहीं करती। अब वह मजबूर नहीं है अपनी बात कहने में। अब वह निःसंकोच अपने जज़्बातों को दूसरों को प्रकट करने लगी है। सदियों से होने वाला दमन चक्र को उसका मन, तन, विवेक और बुद्धि मानने से इंकार कर चुका है। अब वह शोषकों का विरोध ही नहीं बल्कि उनके खिलाफ लड़ने के लिए तैयार खड़ी है। कवयित्री मात्र पारिवारिक और सामाजिक शोषण पर ही प्रहार नहीं करती है वरन् देश की राजनैतिक काली करतूतों का भी पर्दाफाश करने से नहीं हिचकती है। 'चुड़का सोरेन' नामक कविता का मूल स्वर यही है। इस कविता में आदिवासी समाज में व्याप्त बहुत सी समस्याओं को कवयित्री ने उजागर किया हैं। उदाहरण के लिए इनका अशिक्षित और नशेबाज होना। आदिवासी समाज का हरेक वर्ग किसी न किसी नशे का शिकार होता है। परंतु इसके पीछे भी अधिकांशतः राजनैतिक सत्ताधारियों का ही हाथ है।

कवयित्री ने चुड़का सोरेन को इस नशेबाजी से दूर रहने की हिदायत दी। अक्सर आदिवासी लोग नशे के कारण घर–बार, खेत–खलिहान और अपनी सारी जमा पूँजी गिरवी रखने पर मजबूर हो जाते हैं। यहाँ तक चंद सिक्कों के बदले उन्हें अपनी माँ और बेटी तक को निलाम करना पड़ता है। दूसरी तरफ देश का सफेदपोश नेतावर्ग अपनी चिकनी चुपड़ी बातों में फाँसकर उन्हें बड़े–बड़े सपने दिखाकर उनकी जमीन, जंगल और खेतों

को अजाड़ कर कारखानों का निर्माण कर देता है और वे बेसहारे घर–बार हीन दर–दर की ठोकरें खाते हैं। अप
एक लेख 'झारखंडी महिलाओं का पलायन और उनका शोषण' में आदीवासी महिलाओं के भोगे हुए यथार्थ के बा
में निर्मला पुतुल लिखती है–"आदिवासी महिलाएँ जिनके पास भूख है, भूख में दूर तक पसरी उबड़–खाब
धरती है, सपने हैं, सपनों से दूर तक पीछा करती अधूरी इच्छाएँ हैं, जिसकी लिजलिजी दीवारों पर पाँव रखक
वे भागती हैं, बेतहाशा, कभी पूरब तो कभी पश्चिम की ओर....।"[5]

कवयित्री का मानना है कि इस सम्पूर्ण दमन चक्र में सबसे अधिक शोषण औरतों का ही होता है। चा
सामाजिक रूप से हो या शारीरिक रूप से इनमें ये आदिवासी औरतें ही अधिक पीसती है। कवयित्री ने चुड़
सोरेन के माध्यम से इन मासूम आदिवासी समाज को इन मुखौटा पहने लोगों से बचने को कहा। जि
निम्नलिखित पंक्तियों के माध्यम से अंदाज़ा लगाया जा सकता है–

"तुम्हारी भाषा में बोलता वह कौन है
जो तुम्हारे भीतर बैठा कुतर रहा है
तुम्हारे विश्वास की जड़े?
दिल्ली की गणतंत्र की झांकियों में
अपनी टोली के साथ नुमाइश बनकर कई–कई बार
पेश किए गए तुम
पर गणतंत्र नाम की कोई चिड़िया
कभी आकर बैठी तुम्हारे घर की मुंडेर पर?"[6]

इस कविता में कवयित्री ने व्यापक रूप से आदिवासी सामाज की समस्याओं का वर्णन किया है। पर
इन समस्याओं के मूल में राजनैतिक गतिविधियाँ ही काम करती है। इस बात को भली–भांति समझते हुए उन्हों
व्यापक रूप से आदिवासी समाज को जागरूक करने का प्रयत्न किया।

निष्कर्षतः कहा जा सकता है कि समकालीन हिंदी आदिवासी स्त्री लेखन सही माइने में आदिवासी समाज
का आईना है। निर्मला पुतुल की कविताएँ इस परिप्रेक्ष्य में काफी महत्त्वपूर्ण हैं। अनेक साहित्य के केन्द्र में स्त्रियों
की समस्याएँ, प्रश्न, शोषण, असमता, अशिक्षा, भूखमरी, विस्थापन, पलायन और स्त्री अस्मिता की लड़ाई है। वे
हिंदी की ऐसी आदिवासी साहित्यकार है जिनका साहित्य अपने आप में बेजोड़ है। जिन्हें घुट–घुटकर जीना
कतई स्वीकार नहीं। वे उन स्त्रियों में से एक है जिनका आत्म सम्मान बोध उनके जीवन से भी ऊँचा है। जो
सही माइने में आदिवासी विमर्श और आदिवासी महिला लेखन को एक आन्दोलन का रूप देने वाली क्रांतिकारी
से कम नहीं है। उनकी कविताएँ लाखों आदिवासी महिलाओं के लिए प्रेरणा का श्रोत है। इसे उन्होंने अपनी
कविता 'उतनी ही जनमेगी निर्मला पुतुल' में स्वीकार भी किया है –

"आज की तारीख के साथ
कि गिरेंगी जितनी बूँदे, लहू की धरती पर
उतनी ही जनमेगी निर्मला पुतुल
हवा में मुट्ठी बाँधे हाथ लहराते हुए।"[7]

संदर्भ सूची :-

1 'क्या तुम जानते हो' तिलक रजनी और अनुरागी रजनी (सं.), समकालीन भारतीय दलित महिला लेखन, स्वराज प्रकाशन, नई दिल्ली, प्रथम संस्करण, 2011 पृष्ठ संख्या–19

2. 'उतनी दूर मत ब्याहना', वही, पृष्ठ संख्या–24

3. 'क्या तुम जानते हो' वही, पृष्ठ संख्या–20

4. 'मैं वो नहीं हूँ जो तुम समझते' वही, पृष्ठ संख्या–28

5. 'झारखंडी महिलाओं का पलायन और उनका शोषण' –http./streekal.com 2017/06 rev (निर्मला पुतुल की कविताएँ : आदिवासी पीड़ा और प्रतिरोध का काव्य संसार–रेखा शेठी)

6. 'चुड़का सोरेन' वहीं, पृष्ठ संख्या–21

7. 'उतनी ही जनमेगी निर्मला पुतुल', पुतुल निर्मला, नगाड़े की तरह बजते शब्द, भारतीय ज्ञानपीठ, नई दिल्ली, संस्करण 2004 पृष्ठ संख्या–91

पता –हाईलैंड गार्डन, टावर - III
G-6, देशबंधु रोड,
पुरुलिया, पश्चिम बंगाल–723101
Phone -9832153804, 8250202978
email Id- portiasarkar1@gmail.com

Research and Reviews Journal of Agriculture and Allied Sciences

e-ISSN: E 2347-226X
p-ISSN: 2319-9857

Quantitative Estimation of Dust Fall in Monsoon and Winter Seasons in Purulia Town, West Bengal, India

Moumita Sinha[1]*, Indrani Chatterjee[2], Munmun De[3], Nafisa Khatoon[4], Susmita Mukherjee[5]

[1]Department of Environmental Science, Nistarini College (Under SKBU), Purulia, India
[2]Department of Environmental Science, University of Kalyani, India
[3]Department of Environmental Science, Visva Bharati, India
[4]Department of Environmental Science, Nistarini College, India
[5]Department of Environmental Science, Purnadisha Joychandi Teachers Training College, India

Research Article

Received date: 20/09/2021
Accepted date: 04/10/2021
Published date: 11/10/2021

***For Correspondence**
Moumita Sinha, Department of Environmental Science, Nistarini College, India.

E-mail: sinhanayek@gmail.com

Keywords:
Dust fall, Monsoon dust, Winter dust, Dust fall stream, Road dust

ABSTRACT

An investigation was carried out during two different seasons i.e., monsoon and winter to quantify the dust fall in ten different sites of Purulia Town of West Bengal, India. Enhancement (at 5% level of significance) in dust fall level was observed in all sample collection sites during winter than that of monsoon excluding the Bongabari area where no significant difference was recorded in dust deposition in between monsoon and winter. During monsoon highest dust fall was noticed in Bongabari area, whereas in winter period Zilla School More was found as maximum dust fall site.

INTRODUCTION

Air quality is becoming the most burning issue in present day situation. With rapid advancement of industrial operations, extension of agro fields as well as agricultural activities, expansion of roads, transportation, extension of urban areas, exploration of mining areas, industrial expansion and construction related activities are continuously causing severe degradation of air quality. Dust is one among various factors responsible for air quality deterioration. Dusts, particulate matters are generated due to not only by anthropogenic activities but also due to natural incidences like spread of pollen grains, emission of volcanic ashes and sandstorms. Profuse dust particles are felt in Indian atmosphere. The major sources of dust particles include suspension from land, agricultural activities, paved and unpaved roads; automobile emission, power plants emissions, activities related to construction, cements factories, brick furnace, mining area, stone crushing sites etc. Seasonal variation of Dust fall stream having the order winter>summer>monsoon was noticed by Gupta et al [1]. Dust may cause undesirable effects on human health, vegetation as well as other sectors of environment. Present study was conducted with an aim to measure quantitatively the dust fall, mostly along the paved road sides in certain areas of Purulia town. Kamble carried out a work to estimate dust fall in the Chandrapur industrial belt during winter period. He noticed that dust fall rate was comparatively higher in industrial cluster than that of the residential belts [2]. Giunta et al, estimated dust quantity generated during the period of a motorway construction; he noticed that PM10 was emitted mainly from the rupture of trucks on unpaved roads [3]. Road dusts become airborne from the abrasion of tires moving on dust burdened paved roads and unpaved dirt roads [4]. A work was undertaken by Naddafi et al to quantify dust fall as well as its relation with climate in Yazd. There was abundant amount of dust and particles in

e-ISSN: E 2347-226X
p-ISSN: 2319-9857

the atmosphere of Yazd city due to industrial activities besides sandstorms [5]. Pillai et al, collected dust fall at Pune and at rural area Sinhagad and he found comparatively higher quantity of dust at Pune [6].

MATERIALS AND METHODS

In present dissertation work, investigation was carried out on quantification of the dust fall in ten different places, in most of the cases along paved road sides during two different seasons of Purulia town of W.B., India. Dust samples were collected during the month of September, 2019 (monsoon) and January of 2020 (winter). Purulia is situated in the central west of West Bengal and normally known as the drought prone area. Sub-tropical type of climate of Purulia is characterized by high level of evaporation with little precipitation. It is placed just north of the Kasai River [7]. DMS longitude and latitude of Purulia Town area are 23° 20' 32.1252" N and 86° 21' 46.2204" E respectively. The sample collection sites in Purulia town were Nistarini College premises, Deshbandhu Road near Raghabpur More, Station para (near Maheswari lodge), Railway station and surrounding areas; Bus stand to Taxi stand, Goshala More, Bhatbandh, Gopal More, Zilla School More, Bongabari (near Bharat Super Cement factory and Purulia Metal Casting). To measure dust fall rate, Whatman 42 filter papers were used. Filter papers were initially dried then after cooling at desiccator, initial weight was taken, and then these were set on thick layer of card boards using pin. After that, these filter papers were placed in the balcony of road side houses or shops or waiting room for buses, in sampling sites in such a way so that trouble from birds were minimum and least rainfall might come. All the filter papers set up were collected when the observation period was over, then these were brought into laboratory and filter papers were further dried, cooled at dessicator and then weight was taken using digital balance and dust fall was quantified.

RESULT AND DISCUSSION

Atmospheric temperature in Purulia generally observed as maximum 30 °C and minimum 23 °C in the month of September while maximum 25 °C and minimum 12 °C temperatures are commonly observed in the month of January (Table 1).

Table 1: Meteorological Information of Purulia

Meteorological Parameters ↓	Months	
	September 2019	January 2020
Average rainfall (mm)	495.4	16.6
Total rain days	28	07
Maximum Temperature (°C)	29	25
Minimum Temperature (°C)	23	17
Average Temperature (°C)	27	22
Humidity (%)	81	46
Cloud (%)	48	18
Maximum Wind Speed (kmph)	15.8	12.5
Average Wind Speed (kmph)	11.9	8.4

Analytical results are represented by the respective Figure 1 and Tables 2 and 3. From Graph 1 it is obtained that highest dust fall rate was recorded from Bongabari followed by Nistarini College Campus, Bhatbandh, Goshala More and other sites in monsoon. Picture was slightly different in winter when highest dust fall rate was found in Zilla School More followed by Deshbandhu Road near Raghabpur More, Bongabari, Railway Station Area, Goshala More and other spots. Results obtained after quantification of dust during monsoon were compared with the results of winter and it is clearly revealed that (Graph 1) dust fall rates were higher at every sample collection spots during

e-ISSN: E 2347-226X
p-ISSN: 2319-9857

winter season than that of monsoon period excluding the Bongabari area where the reverse incidence was observed but analyzing the t-test results (Table 1) it is finally found that there was no significant difference in dust fall rate between two different sample collection periods in Bongabari area; whereas higher (at 5% level of significance) dust fall rates were noticed in D.B. Road near Raghabpur More, Station para near Maheswari Lodge, Railway Station surrounding area, Bhatbandh, Gopal More, Zilla School More and Goshala More during winter in comparison to the monsoon. Dusts pose serious threat to human health, produce significant adverse impact on plant health. Nazari et al, revealed that dust can produce negative impact on human health and causes a number of diseases like respiratory, cardiovascular, cerebral vascular, fever; allergies etc. Moreover, DNA of skin and lung cells gradually becomes damaged [8]. The higher rate of dust emission increases dust fall on vegetation, soil, structures, buildings etc. Supe et al, observed that effects of dust pollution on the plants and land can differ depending upon the density of falling dusts. Reduction in the plant leaves pigments, enhancement in stresses and reduction in plant productivity, decline in soil fertility occur while dust particles accumulate on green leaves and fall on land respectively [9]. Dust fall and its accumulation on leaves also may interact with crop yield. Regular monitoring to measure the level of dust fall especially in the human settlement areas must be performed. Appropriate strategies can be adopted to prevent dust fall related ill effects on human health and environment. Biological, chemical, mechanical methods or water sprays can be used to control dust storm. Among all, biological methods are the best one and this can be accomplished by creating road side vegetation cover, or ecological barriers like green belts surrounding urban areas [8].

Table 2: |t| test result (Dust fall Rate) between monsoon and winter

Sample collection sites	|t| test result (Dust fall Rate)	Comments
Within the Nistarini College premises	$\|t\|_6$=0.410, $\|t\|_{0.05,6}$=2.447, $\|t\|_{0.01,6}$=3.707	No significant difference
Deshbandhu Road near Raghabpurmore	$\|t\|_9$=3.07, $\|t\|_{0.05,9}$=2.262*, $\|t\|_{0.01,9}$=3.250	Significant difference*
Station Para (Near Maheshwari Lodge)	$\|t\|_8$=2.90, $\|t\|_{0.05,8}$=2.306*, $\|t\|_{0.01,8}$=3.355	Significant difference*
Railway Station	$\|t\|_7$=3.02, $\|t\|_{0.05,7}$=2.365*, $\|t\|_{0.01,7}$=3.499	Significant difference*
Bus Stand to Taxi Stand	$\|t\|_7$=0.94, $\|t\|_{0.05,7}$=2.365, $\|t\|_{0.01,7}$=3.499	No significant difference
Bhatbhandh	$\|t\|_7$=2.44, $\|t\|_{0.05,7}$=2.365*, $\|t\|_{0.01,7}$=3.499	Significant difference*
Gopal More	$\|t\|_9$=2.14, $\|t\|_{0.05,9}$=2.262*, $\|t\|_{0.01,9}$=3.250	Significant difference*
Zilla School More	$\|t\|_9$=3.14, $\|t\|_{0.05,9}$=2.262*, $\|t\|_{0.01,9}$=3.250	Significant difference*
Goshala More	$\|t\|_6$=2.64, $\|t\|_{0.05,6}$=2.447*, $\|t\|_{0.01,6}$=3.707	Significant difference*
Bongabari	$\|t\|_{12}$=1.11, $\|t\|_{0.05,12}$=2.179, $\|t\|_{0.01,12}$=3.055	No significant difference

Table 3: Dust fall rate in monsoon and winter

Sample collection site	Winter	SD winter	Monsoon	SD Monsoon
Within the Nistarini college premises	0.230	0.092	0.201	0.108
Deshbandhu Road near Raghabpur More	0.405	0.240	0.103	0.038
Station Para (Near Maheshwari Lodge)	0.221	0.082	0.102	0.040
Railway Station	0.294	0.101	0.111	0.075
Bus stand to Taxi Stand	0.258	0.101	0.111	0.187
Bhatbhandh	0.258	0.101	0.127	0.036
Gopal More	0.245	0.095	0.131	0.079
Zilla School More	0.421	0.205	0.089	0.036
Goshala More	0.276	0.106	0.128	0.037
Bongabari	0.368	0.282	0.791	0.967

e-ISSN: E 2347-226X
p-ISSN: 2319-9857

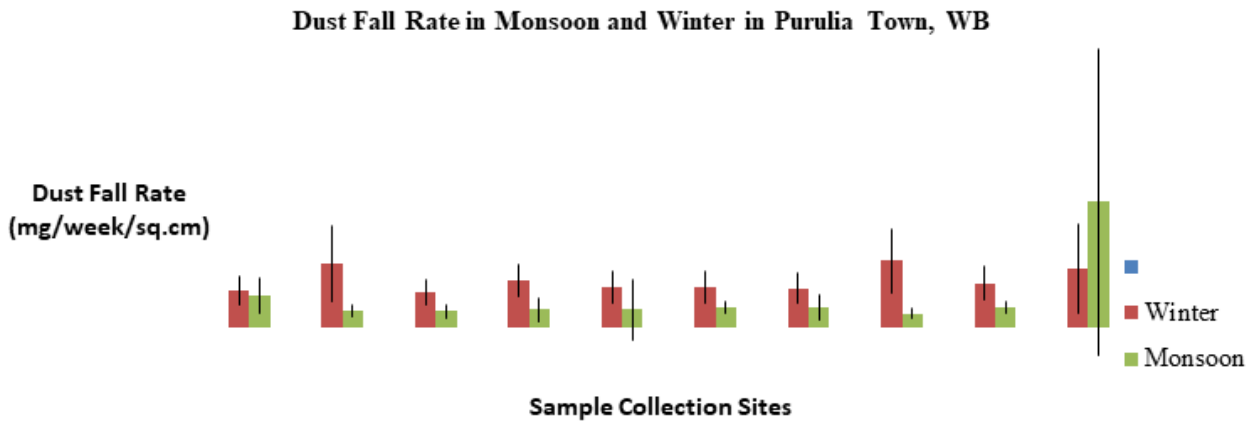

Figure 1: Dust fall rate in monsoon and winter

CONCLUSION

Dust fall in a particular area may depend on meteorological conditions, sandstorm as well as presence of other anthropogenic sources of that site. Present survey reveals that during monsoon higher level of dust deposition was observed in Bongabari, Nistarini College premises, Goshala More, Bhatbandh, Gopal More while in winter period, Zilla School More, Bongabari, Deshbandhu Road near Raghabpur More, Goshala More were found as highly dust fall areas. Naturally, vegetation cover can resist the spread of dust particles in atmosphere. Besides, other strategies like chemical, mechanical methods can be adopted. Personal protection should also be taken to minimise the generation of ill health due to inhalation of dust particles.

REFERENCES

1. Gupta GP, et al. Deposition and impact of urban atmosphere dust on two medicinal plants during different seasons in NCR, Delhi. Aerosol and Air Quality Research (AAQR). 2016;16: 2920-2932.
2. Kamble RK. Dust Fall rate and its composition in chandrapur industrial cluster, central India. Int J Environ (IJE). 2015;4(3): 96–110.
3. Giunta M, et al. Estimation of gas and dust emissions in construction sites of a motorway project. Sustainability. 2019;11:7218.
4. Khan RK, et al. Road dust and its effect on human health: A Literature Review. Epidemiol Health. 2018; 40.
5. Naddafi K, et al. Evaluation of dust fall in the air of Yazd. Iran. J Environ Health Sci Eng. 2016; 03(03): 161-168.
6. Pillai AG, et al. Studies of wet deposition and dustfall at Pune, India. Water Air and Soil Pollution. 2001;1309(1): 475-480.
7. District survey report, 2021 (For mining of minor minerals) as per Notification No. S.O.3611 (E) New Delhi dated 28th Of December 2020 Ministry of Environment, Forest and Climate Change (MoEFCC) prepared by: rsp green development and laboratories pvt. Ltd. Iso 9001:2015 and iso 14001:2015 certified company qci-nabet accredited february, 2021.
8. Nazari SH, et al. The origins and sources of dust particles, Their effects on environment and health and control strategies: A review. J Air Pollution and Health. 2016;1(2): 137-152.
9. Supe NG, et al. Effects of dust fall on vegetation. Int J Sci and Res. 2015;4(7).

Research Article

Journal of Scientific Enquiry
Vol: 1, Pages: 103-113

Analysis of Biochemical Parameters and APTI of Neem (*Azadirachta indica*) and Sajina (*Moringa oleifera*) Plants during Monsoon and Winter Seasons in Purulia Town, WB, India

Moumita Sinha[1*], Indrani Chatterjee[2], Munmun De[3], Nafisa Khatoon[4] and Susmita Mukherjee[5]

[1*] *Assistant Professor, Department of Environmental Science, Nistarini College (Under SKBU), Purulia, WB.*
[2] *PG Student, Department of Environmental Science, University of Kalyani, Kalyani, WB.*
[3] *PG Student, Department of Environmental Science, Visva-Bharati, Bolpur, WB.*
[4] *UG Student, Department of Environmental Science, Nistarini College, Purulia, WB.*
[5] *Student, Purnadisha Joychandi Teachers Training College, Purulia, WB.*

Received: 02.10.2021; accepted: 08.12.2021; published online: 30.12.2021

A survey was undertaken to evaluate the biochemical parameters like chlorophyll, carbohydrate, ascorbic acid, APTI of Neem *(Azadirachta indica)* and Sajina *(Moringa oleifera)* plants and sample leaves were collected during two different seasons like monsoon of 2019 and winter of 2020, from ten different sites of Purulia town like Nistarini College premises, Deshbandhu Road near Raghabpur more, Station para (near Maheswari lodge), Railway station and surrounding areas, Bus stand to Taxi stand, Gopal More, Zilla School More, Bhatbandh, Goshala More, Bongabari. All of these areas are either in the vicinity of heavily vehicle burdened roads or railway station. Neem *(Azadirachta indica)* and Sajina *(Moringa oleifera)* plants were selected as these plants are very commonly found in this area. Carbohydrate in Neem leaves were significantly higher during monsoon at all sites excluding Station Para, Gopal More and Bhatbandh where no significant differences were noticed. Carbohydrate levels were reduced during winter in Nistarini College Premises, Railway Station, Bus Stand to Taxi Stand, Bhatbandh and Goshala More but reverse results were observed during winter in leaves samples collected from Station Para and Zilla School More. Air Pollution Tolerance Index (APTI) indicates the tolerance capacity of plants species to air pollution and can be calculated to categorize sensitive, intermediate and tolerant species. Lowest and highest APTI value for Neem leaves during monsoon were recorded from Gopal More (13.88) and Goshala More (17.84) respectively while during winter season lowest APTI value of same species was observed in Deshbandhu Road (5.96) but highest value was experienced from Zilla School More (20.56). In case of Sajina leaves, during monsoon, maximum APTI was noticed in Nistarini College premises (15.97) and minimum value was recorded from Goshala More (12.72). In winter season lowest APTI was noticed in Bus stand to Taxi stand area (10.12) and highest value was from Station para near Maheswari Lodge (16.59).

Key words: APTI, Air Pollution, Green belt, Carbohydrate

1. Introduction

Air pollution now-a-days is one of the major global problems producing huge stress to health and environment [1]. Urbanization, increasing mining activities, expansion of agro-fields, road extension as well as transportation, construction activities, booming industrialisation and related other anthropogenic activities poses serious threat to air quality. Around 80% population residing in urban air quality is being exposed to emissions which exceed the standards guided by WHO [2]. A gradual increase in the global population in the modern decades have been observed from 7.4 billion in 2016 to 7.7 billion in 2019, 7.8 billion in 2020 to 7.9 billion in 2021. The world population is predicted to reach 9.9 billion by 2050 [3]. 800000 annual deaths as a result of urban air pollution have been reported by Researchers [4]. The gradual degradation of air quality urgently requires suitable techniques or policies to curb air pollution [5]. Vegetation covers or plants can be used as natural, cost effective way to reduce the problem of air pollution. Plants are susceptible to air pollutants. Deposition of pollutant particulates on soil indirectly affects plant growth. Au-

*Corresponding author Email id: sinhanayek@gmail.com

tomobile based pollutants deposit on leaves, block the stomata and eventually affect transpiration. These depositions obstruct absorption and eventually decrease photosynthesis and affect the growth of plants and their productivity [3]. Air Pollution Tolerance Index indicates the tolerance capacity of plant species to air pollution and APTI can be estimated by using the data of pH, ascorbic acid, total chlorophyll and relative water content. APTI of plants can be evaluated to identify sensitive, intermediate and tolerant species. Plants having APTI value ≤ 11 are considered as sensitive while plants having APTI value which falls in the range 12–16 is classified as intermediate plant while APTI value ≥ 17 is known as tolerant plant. The sensitive plant species can be used as bio indicator to detect the level of air pollution while tolerant species can be widely used to create green belt to combat with the difficulties of air pollution [6]. Panda *et al.*, 2018 observed that air pollution tolerance index is a natural feature of trees to reduce air pollution nuisance. The trees having higher APTI values are tolerant towards air pollution and these plants can be used to reduce the burden of air pollution whereas the trees having low APTI values can be used to detect the rate and intensity of air pollution [7]. Plants of Perumalmalai Hill situated at Salem district were surveyed to recognize the tolerance level to air pollution in the month of Feb, 2013. *Nerium oleander* was identified as intermediate tolerant species (APTI value 16.65) while *ficus benghalensis*, *Psidium guajava*, *Skothodea campanulata*, *Opunitaficus indica* (APTI 15.92, 15.41, 9.92, 9.74 respectively) was recognized as sensitive species [8]. APTI value of 69 plant species of herbs, shrubs, trees of urban industrial belt Lahartara of Varanasi were analysed and it was found that C. roseus etc. were observed as tolerant and D. sissoo, L. chinensis, C. carandus and C. rottleri were observed as sensitive to air pollution [9]. Present study was conducted with an aim to assess biochemical parameters like pH, RWC, ascorbic acid, carbohydrate and chlorophyll content as well as Air Pollution Tolerance Index (APTI) of Neem *(Azadirachta indica)* and Sajina *(Moringa oleifera)* leaves collected from ten different places of Purulia town of W.B., India.

2. Materials and Methods

Purulia is situated in the central-west of West Bengal and normally known as the drought prone area. Sub-tropical type of climate of Purulia is characterized by high level of evaporation with little precipitation. It is placed just north of the Kasai River [10]. DMS longitude and latitude of Purulia Town area are $23°20'32.1252''$ N and $86°21'46.2204''$ E respectively. The sample collection sites in Purulia town were Nistarini College premises, Deshbandhu Road near Raghabpur more, Station para (near Maheswari lodge), Railway Station and surrounding areas; Bus Stand to Taxi Stand, Gopal More, Goshala More, Bhatbandh, Zilla School More, Bongabari (in between Bharat Super Cement Factory and Metallurgical Factory). All of these areas are either in the vicinity of heavily vehicle burdened roads or railway station. Neem *(Azadirachta indica)* and Sajina *(Moringa oleifera)* plants were selected as these plants are very commonly found in this area. After collecting the leaves of Neem *(Azadirachta indica)* and Sajina *(Moringa oleifera)* plants from the sampling sites, these were brought into the laboratory and then pH [11], RWC [12], chlorophyll [13], carbohydrate [14] and ascorbic acid [15] were estimated as early as possible. Chlorophyll, carbohydrate and ascorbic acid were estimated from the plant materials using centrifuge machine and spectrophotometer. Data of analytical results of biochemical parameters and statistical calculations i.e., *t*-tests (SPSS 13) are presented by the respective graphs and tables. Air Pollution Tolerance Index (APTI) indicates the tolerance capacity of plants species to air pollution and can be calculated to categorize sensitive, intermediate and tolerant species and can be calculated as follows [16]:

$$APTI = [A(T + P)] + R/10$$

A = Ascorbic acid content of leaf (mg/g), T = Total chlorophyll content of leaf (mg/g), P = Leaf Extract pH, R = % Relative Water Content

3. Results and Discussion

Analytical results of biochemical parameters of Neem *(Azadirachta indica)* as well as Sajina *(Moringa oleifera)* are presented by the Fig. 1 to 5 and Fig. 6 to 10 respectively. No significant differences in pH level in Neem leaves were observed at Zilla School more and Bongabari in between two seasons. pH level of leaves samples collected from Nistarini College campus as well as Bongabari area were significantly higher during monsoon whereas pH level of same were significantly enhanced during winter in remaining six spots (Fig. 1). No significant differences in RWC of Neem leaves between two seasons were observed in case of samples collected from Station Para and Railway Station but significant reduction in RWC were observed during winter in the

spots like Nistarini College Premises, D. B. Road, Bus Stand to Taxi Stand, Gopal More, Goshala More, Bhatbandh and Bongabari while RWC increased during winter in case of Zilla School More only (Fig. 2). Chlorophyll levels in Neem leaves were significantly higher during monsoon period in most of the sample collection sites except Railway Station, Bhatbandh and Goshala More where no significant differences were observed (Fig. 3). Carbohydrate in Neem leaves were significantly higher during monsoon at all sites excluding Station Para, Gopal More and Bhatbandh where no significant differences were noticed (Fig. 4). Ascorbic acid level in Neem leaves were significantly elevated in winter season at the spots like Railway Station, Gopal More, Zilla School More, Bhatbandh and Bongabari (Fig. 5).

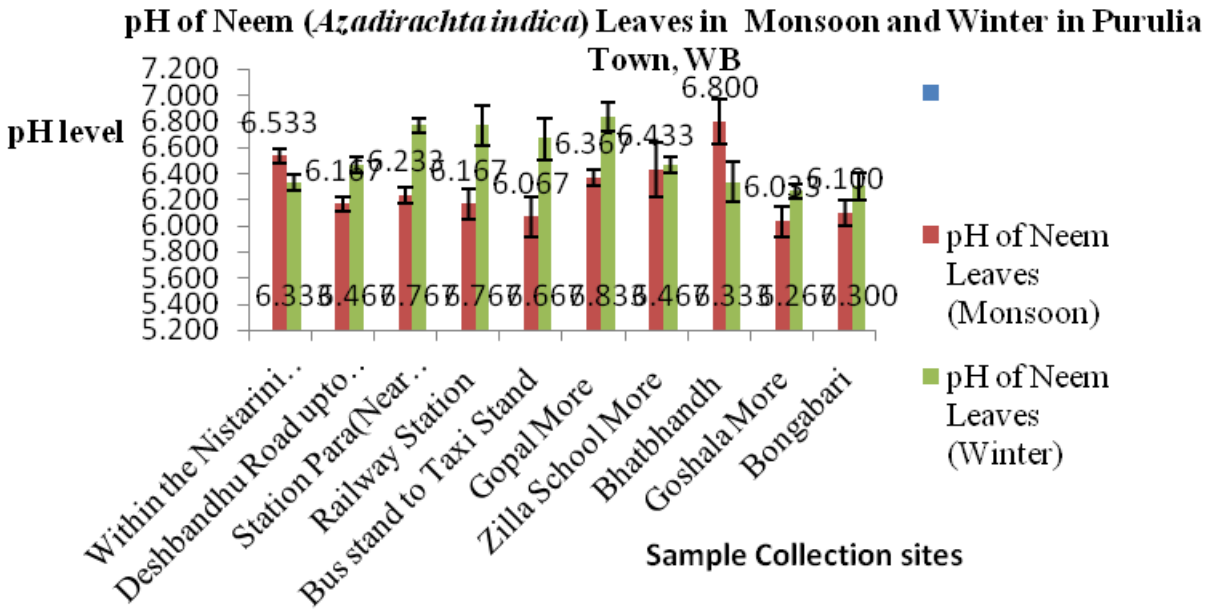

Fig. 1. pH of Neem leaves in monsoon and winter

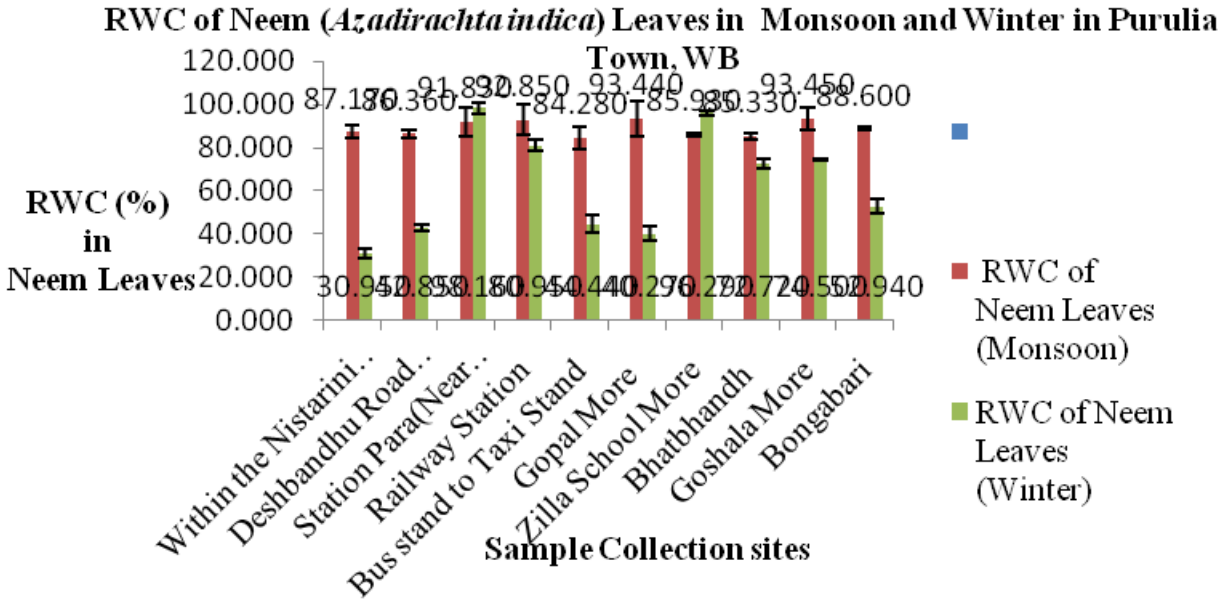

Fig. 2. RWC of Neem leaves in monsoon and winter

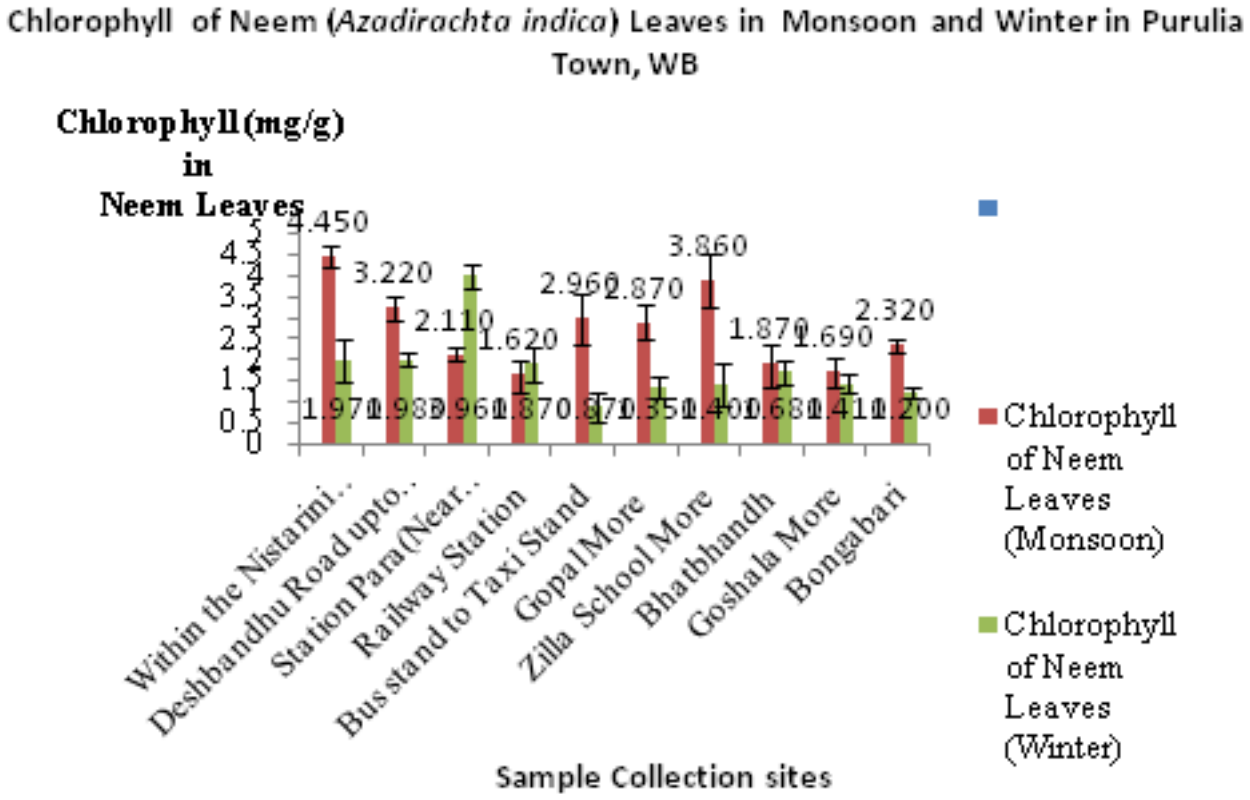

Fig. 3. Chlorophyll of Neem leaves in monsoon and winter

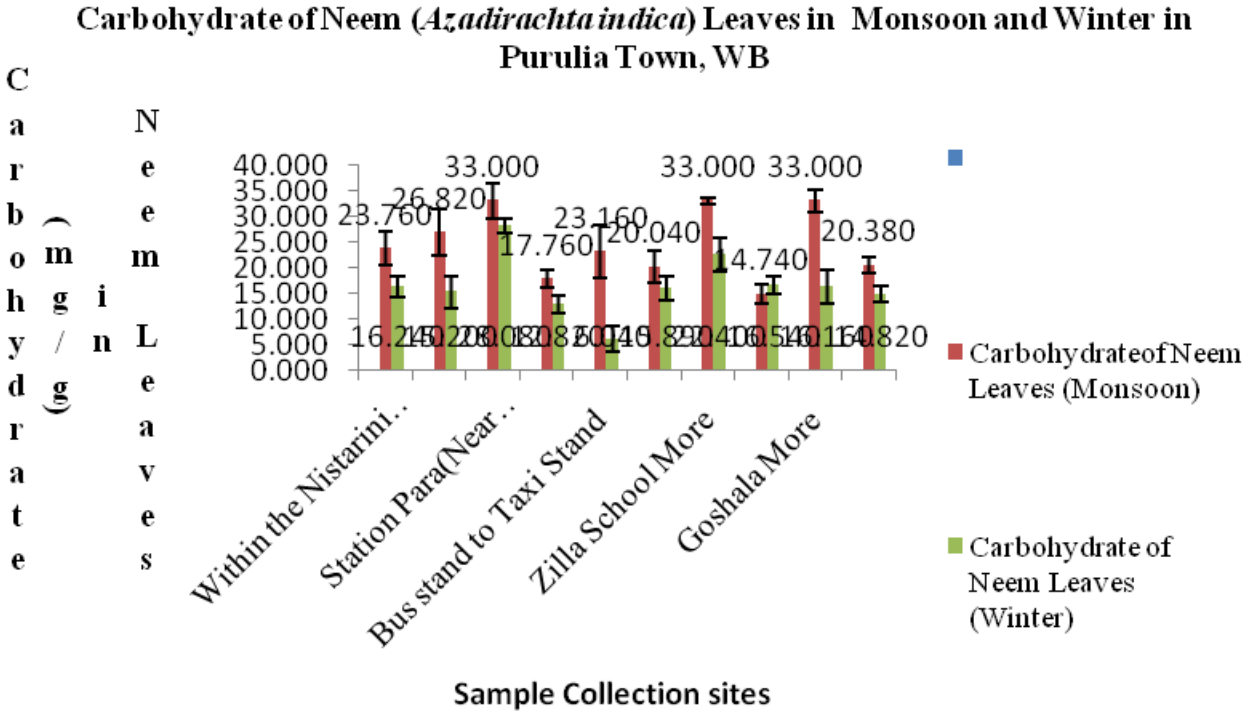

Fig. 4. Carbohydrate of Neem leaves in monsoon and winter

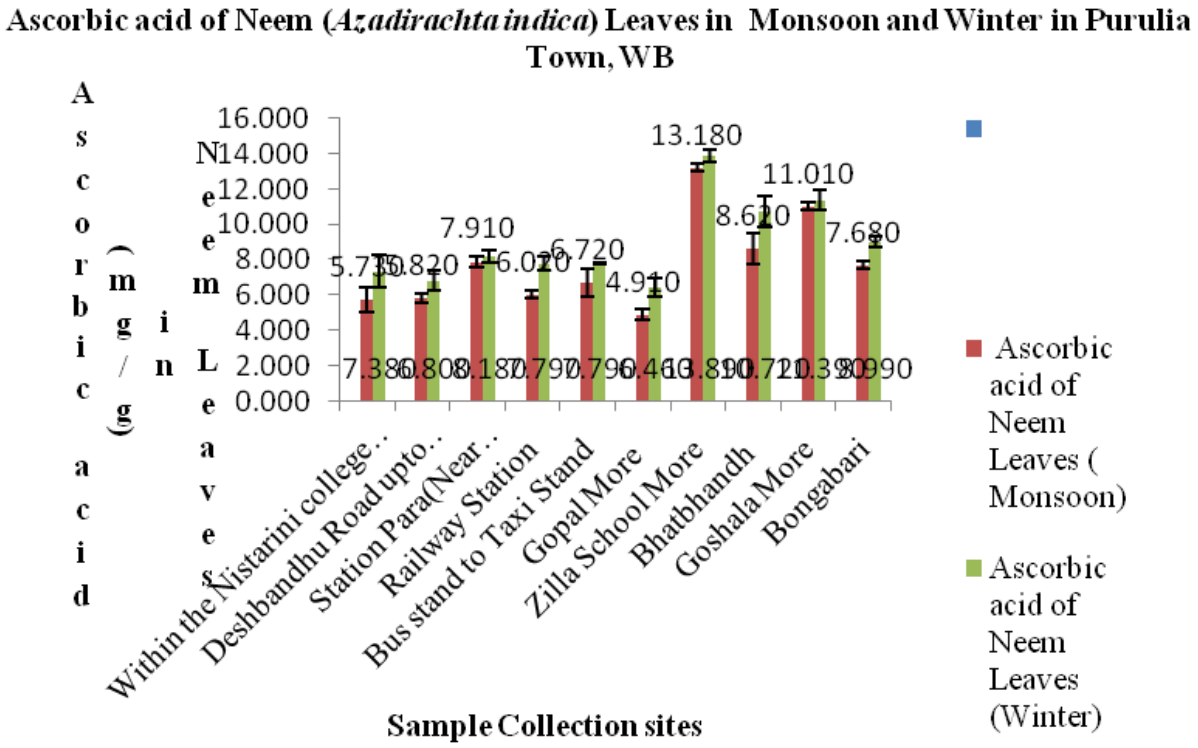

Fig. 5. Ascorbic acid of Neem leaves in monsoon and winter

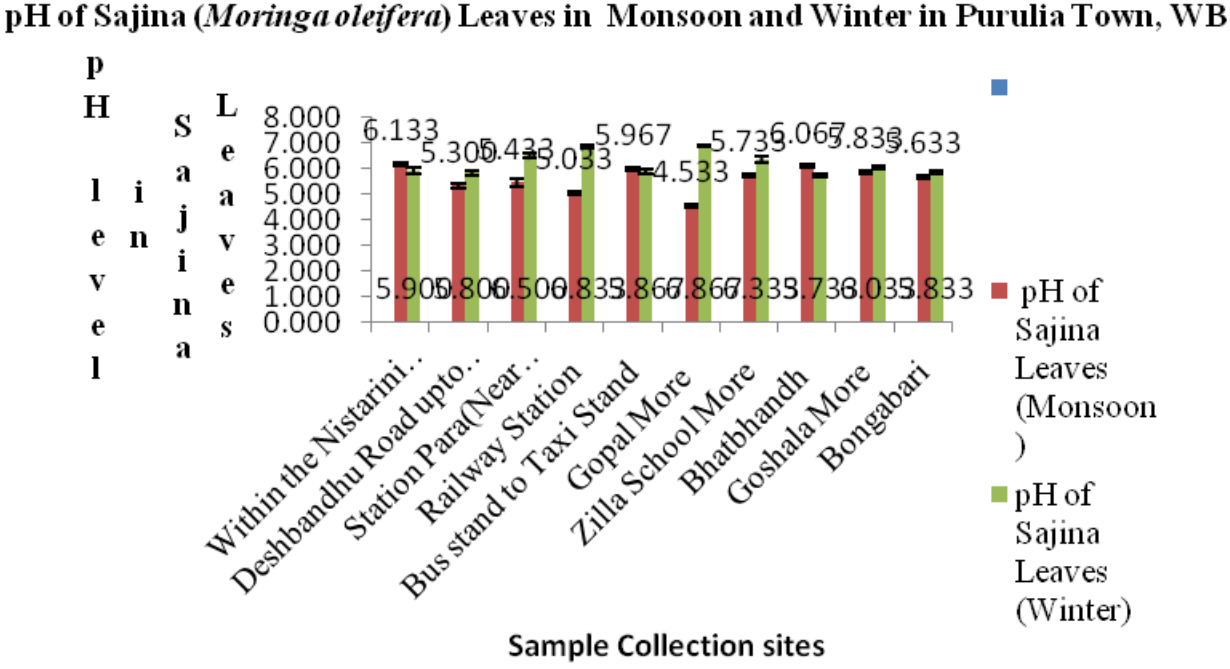

Fig. 6. pH of Sajina leaves in monsoon and winter

pH of Sajina leaves were significantly reduced in winter in the Nistarini College campus as well as in Bhatbandh area but elevated level of pH was observed in winter in Sajina leaves samples collected from other spots except the bus stand to taxi stand area only, where no significant differences were noticed in between two seasons (Fig. 6). No significant differences were found

in RWC level in Sajina leaves between two seasons in the places like Nistarini College Campus and Station para (surrounding area of Maheswari Lodge). RWC increased during winter in the samples collected from Zilla School More and Goshala More whereas samples collected from the rest of the sites showed increased level of RWC in monsoon time (Fig. 7). Chlorophyll level of Sajina leaves were significantly reduced in winter in the areas like Bus Stand to Taxi Stand, Gopal More, Bhatbandh, Goshala More and Bongabari (Fig. 8). Carbohydrate levels were reduced during winter in Nistarini College Premises, Railway Station, Bus Stand to Taxi Stand, Bhatbandh and Goshala More but reverse results were observed during winter in leaves samples collected from Station Para and Zilla School More (Fig. 9). Significant increases in Ascorbic acid level were noticed in Sajina leaves during winter in Station Para near Maheswari Lodge, Bus Stand to Taxi Stand, Zilla School More and Bhatbandh (Fig. 10). Air pollutants for instance O_3 and NO_x, influence the metabolic activity of plant leaves and hamper net carbon fixation by the plant shade. Air pollutants

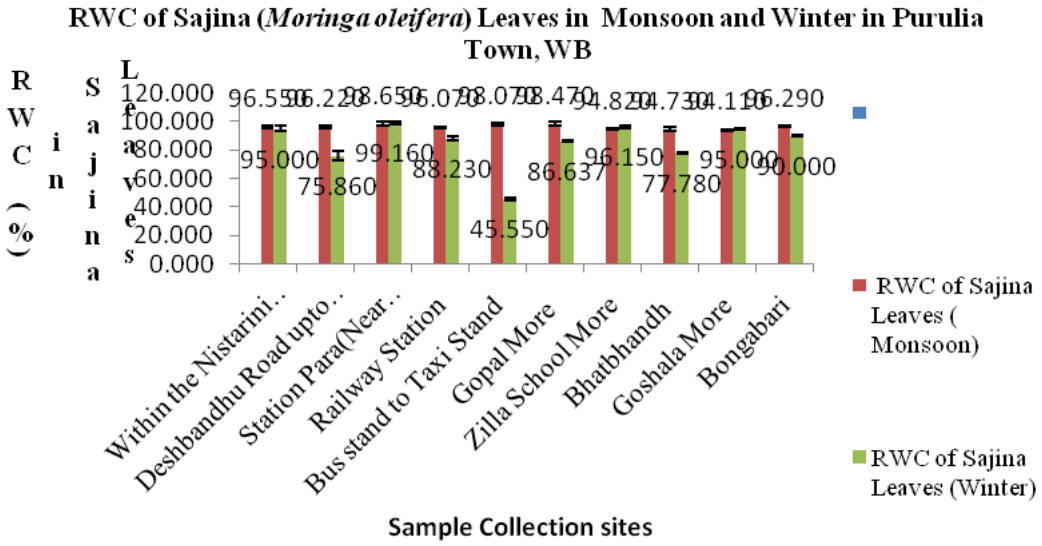

Fig. 7. RWC of Sajina leaves in monsoon and winter

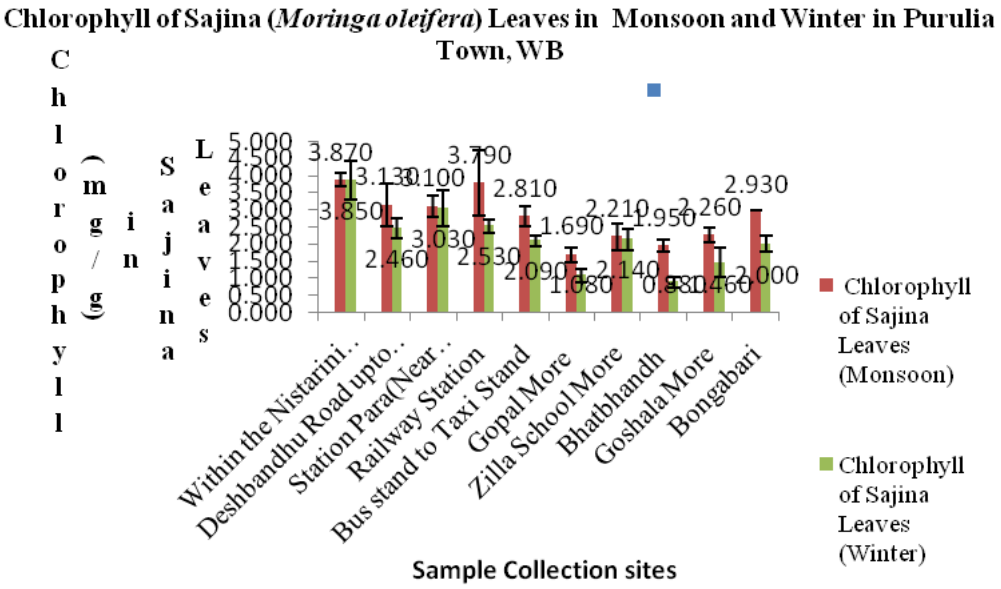

Fig. 8. Chlorophyll of Sajina leaves in monsoon and winter

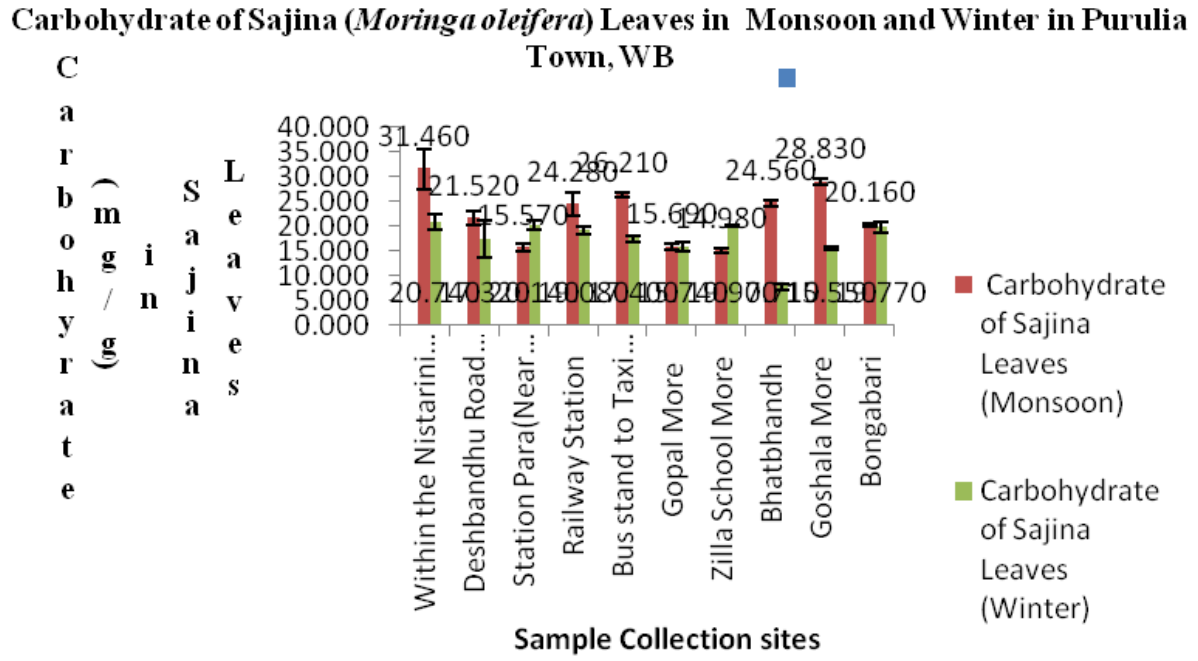

Fig. 9. Carbohydrate of Sajina leaves in monsoon and winter

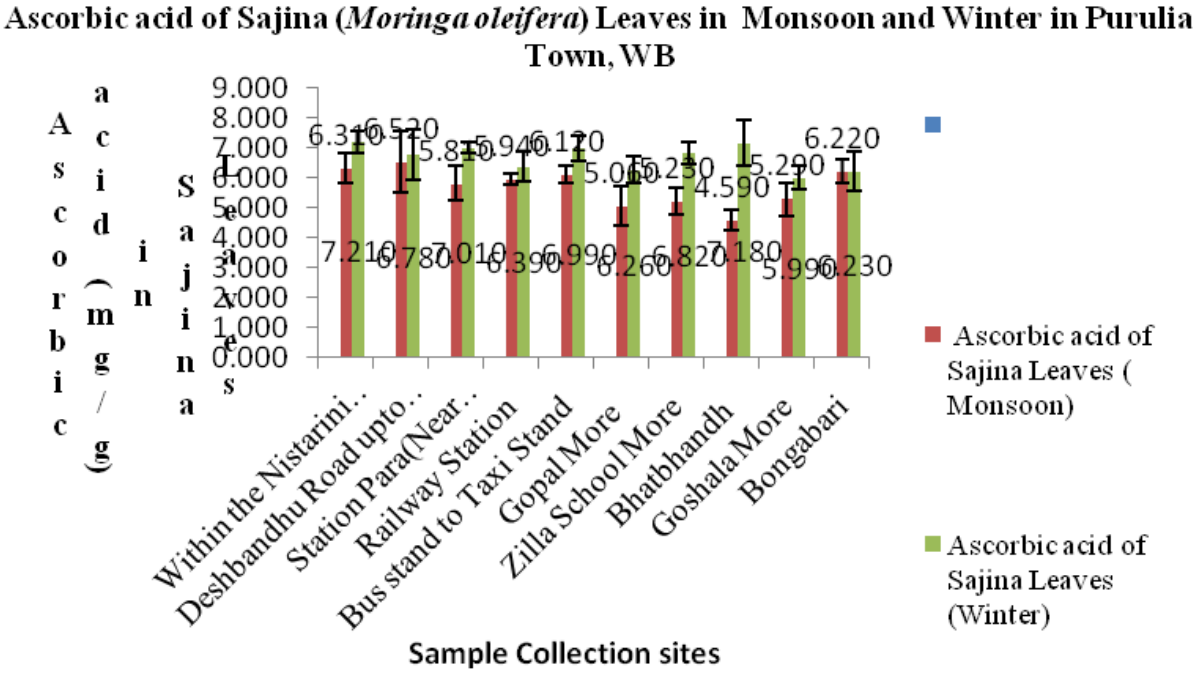

Fig. 10. Ascorbic acid of Sajina leaves in monsoon and winter

such as heavy metals deposited on the soil affect the performance of roots and hinder soil resource capture by the plant. This decline in resource capture will influence plant growth [17]. Plants when become incessantly exposed to pollutants, build up pollution incorporation capacity in to their own system and as a result of certain changes leaves turn out to be more sensitive towards pollution. During monsoon, accumulated dust particles are generally washed out from leaves while during winter and summer accumulation of dust is more. These dusts come into contact with cell sap and increase the pH level of plant leaves [18]. Chlorophyll is an index of productivity of plant which

indicates its photosynthetic activity as well as the growth. Jyothi and Jaya (2010) had the view that high levels of automobile emission lessen chlorophyll content in roadside plants [19]. Ascorbic acid acts as a strong reductant and helps to build up defence mechanisms in plants. It's reducing activity become more at increased pH levels. The efficacy of conversion of hexose form of sugar to ascorbic acid and the ability to tolerate the pollution may increase at high pH [20]. RWC of leaves helps in retaining the physiological balance under stressed circumstances. RWC level is reduced in plant species due to the effect of pollutants on rate of transpiration in leaves [21]. Bhattacharya *et al.* (2013) noticed higher level of Relative Water Content during monsoon [22]. Das and Prasad (2010) also found high RWC value in rainy season, low in winter and least in summer [23]. Analysis of biochemical parameters of leaves assess this alteration and also facilitates to estimate the APTI values [24]. Manjunath and Reddy, (2019) observed from their survey work that APTI level of plants in polluted area was ranged from 9.42 to 25.87 while APTI of plants in non-polluted area was ranged from 8.77 to 19.21. Lowest APTI value was estimated from *O. sanctum* both from both polluted and non-polluted area at 9.42 and 8.77, respectively. This plant is sensitive to air pollution [25]. Agbaire and Esiefarienrhe, (2009) experienced that plants in comparatively polluted environment have higher APTI value than that of the less polluted environment [11]. Lohe *et al.*, (2015) also observed higher level of APTI of plants in polluted sites than that of non-polluted sites [26].

3.1 APTI of Neem *(Azadirachta indica)* in monsoon in sample collection sites (Fig. 11)

Goshala More > Zilla School More > Bhatbandh > Station para (near Maheswari lodge) > Bongabari > Nistarini College premises > Bus stand to Taxi stand > Deshbandhu Road near Raghabpur more > Railway station and surrounding areas > Gopal More.

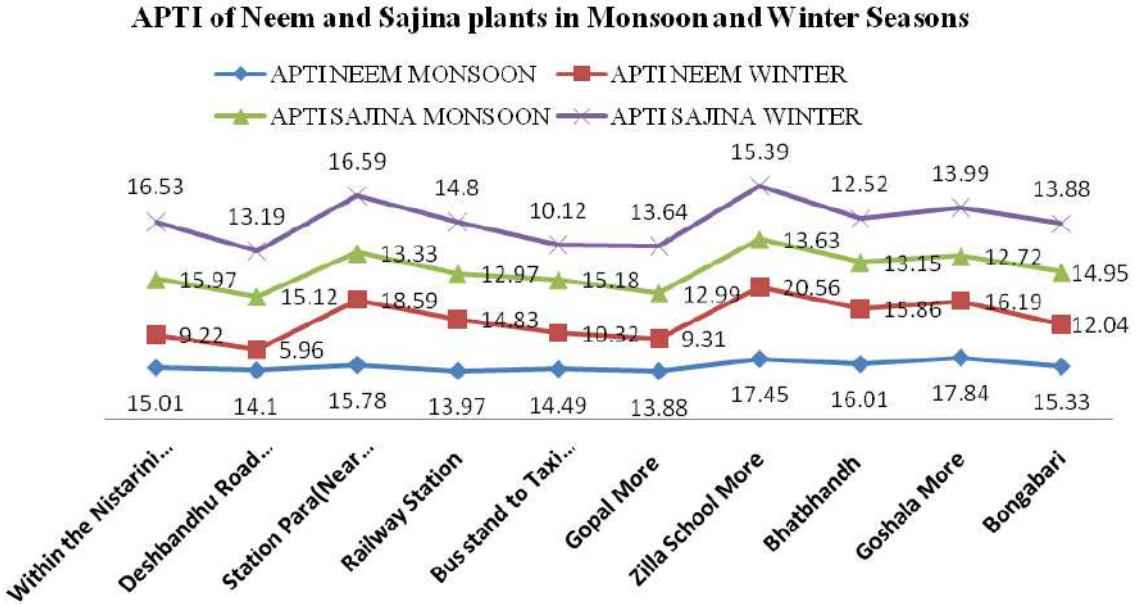

Fig. 11. APTI of Neem and Sajina plants in monsoon and winter

3.2 APTI of Neem *(Azadirachta indica)* in winter in sample collection sites (Fig. 11)

Zilla School More > Station para (near Maheswari lodge) > Goshala More > Bhatbandh > Railway station and surrounding areas > Bongabari > Bus stand to Taxi stand > Gopal More > Nistarini College premises > Deshbandhu Road near Raghabpur more.

3.3 APTI of Sajina *(Moringa oleifera)* in monsoon in sample collection sites (Fig. 11)

Nistarini College premises > Bus stand to Taxi stand > Deshbandhu Road near Raghabpur more > Bongabari > Zilla School More > Station para (near Maheswari lodge) > Bhatbandh Gopal More > Railway station and surrounding areas > Goshala More.

Table 1: $|t|$ test Result (biochemical parameters of *Azadirachta indica*) between Monsoon and Winter

Sample Collection Sites	pH	RWC	Chlorophyll	Carbohydrate	Ascorbic Acid
Within the Nistarini College Premises	4.24^{*}	27.44^{**}	7.74^{**}	3.26^{*}	2.50^{NSD}
Deshbandhu Road upto Raghabpur More	6.36^{**}	27.02^{**}	6.84^{**}	3.70^{*}	2.73^{NSD}
Station Para (Near Maheshwari Lodge)	11.31^{**}	1.61^{NSD}	9.94^{**}	2.33^{NSD}	0.95^{NSD}
Railway Station	5.43^{**}	2.69^{NSD}	0.80^{NSD}	3.43^{*}	6.76^{**}
Bus Stand to Taxi Stand	6.36^{**}	10.52^{**}	5.29^{**}	5.15^{**}	2.39^{NSD}
Gopal More	6.26^{**}	10.48^{**}	5.27^{**}	1.84^{NSD}	4.27^{*}
Zilla School More	0.27^{NSD}	13.37^{**}	5.12^{**}	5.49^{**}	3.11^{*}
Bhatbhandh	3.50^{*}	8.88^{**}	0.56^{NSD}	1.24^{NSD}	2.85^{*}
Goshala More	3.13^{*}	6.51^{**}	1.20^{NSD}	7.53^{**}	1.07^{NSD}
Bongabari	2.45^{NSD}	17.01^{**}	9.20^{**}	4.36^{*}	6.23^{**}

$|t|_{0.05,4} = 2.776^{*}$; $|t|_{0.01,4} = 4.604^{**}$; NSD-no significant difference

SD*-Significant Difference 95% level of confidence; SD**-Significant Difference 99% level of confidence

Table 2: $|t|$ test Result (biochemical parameters of *Moringa oleifera*) between Monsoon and Winter

Sample Collection Sites	pH	RWC	Chlorophyll	Carbohydrate	Ascorbic Acid
Within the Nistarini college premises	3.50^{*}	1.39^{NSD}	0.06^{NSD}	4.19^{*}	2.53^{NSD}
Deshbandhu Road upto Raghabpur More	6.12^{**}	10.51^{**}	1.67^{NSD}	1.88^{NSD}	0.34^{NSD}
Station Para (Near Maheshwari Lodge)	10.12^{**}	0.51^{NSD}	0.20^{NSD}	6.22^{**}	3.38^{*}
Railway Station	38.18^{**}	11.95^{**}	2.23^{NSD}	3.63^{*}	1.48^{NSD}
Bus stand to Taxi Stand	1.34^{NSD}	63.46^{**}	3.69^{*}	23.25^{**}	3.08^{*}
Gopal More	49.50^{**}	13.21^{**}	3.64^{*}	0.08^{NSD}	2.58^{NSD}
Zilla School More	8.05^{**}	3.02^{*}	0.25^{NSD}	21.57^{**}	4.88^{**}
Bhatbhandh	7.07^{**}	24.08^{**}	8.78^{**}	30.44^{**}	5.51^{**}
Goshala More	4.24^{*}	2.86^{*}	2.95^{*}	30.87^{**}	1.80^{NSD}
Bongabari	4.24^{*}	13.01^{**}	6.42^{**}	0.60^{NSD}	0.02^{NSD}

$|t|_{0.05,4} = 2.776^{*}$; $|t|_{0.01,4} = 4.604^{**}$; NSD-no significant difference

SD*-Significant Difference 95% level of confidence; SD**-Significant Difference 99% level of confidence

3.4 APTI of Sajina *(Moringa oleifera)* in winter in sample collection sites (Fig. 11)

Station para (near Maheswari lodge) > Nistarini College premises > Zilla School More > Railway station and surrounding areas > Goshala More > Bongabari > Gopal More > Deshbandhu Road near Raghabpur more > Bhatbandh > Bus stand to Taxi stand.

4. Conclusion

APTI estimation are of important use as with rapid increase of industries, factories, mining activities, construction activities, road extension, automobile emission, urban expansion and as a result of that deforestation enhance the danger of air pollution. With the help of APTI value, natural control method like green belt can be created especially in the threatened areas to re-

duce the ill effect of air pollution. The status of air quality of different sites of Purulia town was observed with the help of APTI level of Neem *(Azadirachta indica)* and Sajina *(Moringa oleifera)* plants and it was clearly established that Goshala More, Nistarini College premises were in comparatively stressed condition during monsoon while Zilla School More and Station para (near Maheswari lodge) were in worst air quality condition during winter.

Acknowledgements

Authors wish to express their thankfulness to Dr. Indrani Deb, Principal, Nistarini College, Purulia for her continuous support and co-operation. Authors wish to record their warmest gratitude to the teachers Sri Priyabrata Mukherjee, Dr. Sabyasachi Mukhopadhyay, Smt. Sayantika Dey and non-teaching staff Sri Debasish Das Karmakar of the Department of Environmental Science for their constant encouragement and valuable suggestions.

References

[1] A S Nagpure, B R Gurjar, V Kumar and P Kumar, Estimation of Exhaust and Non-exhaust Gaseous, Particulate Matter and Air Toxic Emissions from on-road Vehicles in Delhi, Atmospheric Environment, 127, 118–24 (2016).

[2] Ambient Air Pollution: A Global Assessment of Exposure and Burden of Disease, World Health Organization (WHO) (2016).

[3] M Muthu, J Gopal, D H Kim, I Sivanesan, Reviewing the Impact of Vehicular Pollution on Road side Plants—Future Perspectives, Sustainability, 13, 5114 (2021).

[4] The World Health Report 2002: Reducing Risks, Promoting Healthy Life, World Health Organization, Geneva, Sweden (2002).

[5] R G Bhola, Air Pollution in India: Major Issues and Challenges, The Energy Resources Institute (2021).

[6] S K Bharti, A Trivedi, N Kumar, Air Pollution Tolerance Index of Plants Growing Near an Industrial Site, Urban Climate, 24, 820–829 (2018).

[7] L R L Panda, R K Aggarwal, D R Bhardwaj, A Review on Air Pollution Tolerance Index (APTI) and Anticipated Performance Index (API), Current World Environment, 13(1), 55–65 (2018).

[8] M Krishnaveni, R Chandrasekhar, L Amsavalli, P Madhaiyan, S Durairaj, Air Pollution Tolerance Index of Plants at Perumalmalai Hills, Salem, Tamilnadu, India, International Journal of Pharmaceutical Science: Review and Research, 20(1), 234–239 (2013).

[9] S K Singh, D N Rao, A Agrawal, J Pandey, D Naryan, Air Pollution Tolerance Index of Plants, Journal of Environmental Management, 32(1), 45–55 (1991).

[10] District Survey Report, 2021 (For mining of minor minerals) As per Notification No. S.O. 3611 (E) New Delhi dated 28th of December 2020 Ministry of Environment, Forest and Climate Change (MoEFCC) Prepared By: Rsp Green Development & Laboratories Pvt. Ltd. ISO 9001: 2015 & ISO 14001: 2015 Certified Company QCI-NABET Accredited, February (2021).

[11] P O Agbaire and E Esiefarienrhe, Air Pollution Tolerance Indices of Some Plants Around Otogan Gas Plant in Delta State, Nigeria, J. Appl. Sci. Environ. Manage, 13(1), 11–14 (2009).

[12] A Singh, Practical Plant Physiology, Kalyari Publishers. New Delhi, (1977).

[13] D I Arnon, Copper Enzymes in Isolated Chloroplast Polyphenol Oxidase in Beta Vulgaris, Plant Physiol, 24, 1–15 (1949).

[14] R M Mc Cready, J Guggolz, V Silviera and H S Owens, Determination of Starch and Amylase in Vegetable, Analyt. Chem, 22, 1156–1158 (1950).

[15] S P Mukherjee and M A Choudhury, Implications of Water Stress Induced Changes in the Levels of Endogenous Ascorbic Acid and Hydrogen Peroxide in Vigna Seedlings, Physiol. Plant, 58, 166–170 (1983).

[16] S K Singh and D N Rao, Evaluation of the Plants for Their Tolerance to Air Pollution Proc. Symp on Air Pollution Control held at IIT, Delhi, 218–224 (1983).

[17] J Weber, D Tingey and C. Andersen, Plant Response to Air Pollution, U.S. Environmental Protection Agency, Washington, DC, (published 2002), (revised 2021).

[18] V Katiyar and P S Dubey, Sulphur Dioxide Sensitivity on Two Stage of Leaf Development in a Few Tropical Tree Species, Ind. J. Environ. Toxicol, 11, 78–81 (2001).

[19] J S Jyothi and D S Jaya, Evaluation of Air Pollution Tolerance Index of Selected Plant Species along Road Sides in Thiruvananthapuram, Kerala, J. Environ. Biol, 31, 379–386 (2010).

[20] Y J Liu and H Ding, Variation in Air Pollution Tolerance Index of Plants near a Steel Factory: Implication for Landscape-plant Species Selection for Industrial Areas, WSEAS. Trans. Environ. Dev., 4, 24–32 (2008).

[21] A Swami, D Bhatt, P C Joshi, Effects of Automobile Pollution on Sal (Shorea robusta) and Rohini (Mallotus phillipinensis) at Asarori, Dehradun, Himalayan J. Environ. Zool, 18(1), 57–61 (2004).

[22] T Bhattacharya, L Kriplani, S Chakraborty, Seasonal Variation in Air Pollution Tolerance Index

of Various Plant Species of Baroda City, Univer. J. Environ. Res. Tech., 3 (2): 199–208 (2013).

[23] S Das and P Prasad, Seasonal Variation in Air Pollution Tolerance Indices and Selection of Plant Species for Industrial Areas of Rourkela, IJEP, 30 (12), 978–988 (2010).

[24] M Krishnaveni and K Lavanya, Air Pollution Tolerance Index of Plants—A Comparative Study. International Journal of Pharmacy and Pharmaceutical Sciences, 6(5), 320–324 (2014).

[25] B T Manjunath and J Reddy. Comparative Evaluation of Air Pollution Tolerance of Plants from Polluted and Non-polluted Regions of Bengaluru, Journal of Applied Biology and Biotechnology, 7(03), 63–68 (2019).

[26] R N Lohe, V Tyagi, P Singh, T Kumar, D R Khanna, R Bhutiani, A Comparative Study for Air Pollution Tolerance Index of Some Terrestrial Plant Species, Global J. Environ. Sci. Manage., 1(4), 315–324 (2015).

Universe International Journal of Interdisciplinary Research
(Peer Reviewed Refereed Journal)

© UIJIR | ISSN (O) – 2582-6417
JUNE 2022 | Vol. 3 Issue 1
www.uijir.com

AIR POLLUTION TOLERANCE INDEX (APTI) OF SELECTED PLANTS AT SANTALDIH AREA UNDER PARA COMMUNITY DEVELOPMENT BLOCK, PURULIA DISTRICT, W.B. (INDIA)

Author's Name: [1]Sabyasachi Mukhopadhyay, [2]Moumita Sinha, [3]Susmita Sen, [4]Agnibina Mahato

Affiliation: [1]Department of Environmental Science, Nistarini College, Purulia, West Bengal, India

[2]Department of Environmental Science, Nistarini College, Purulia, West Bengal, India

[3]Department of Environmental Science, SKBU, Purulia, West Bengal, India

[4]Department of Environmental Science, Visva Bharati, Shantiniketan, West Bengal, India

E-Mail: sabyasachi.envs@gmail.com

DOI No. – **08.2020-25662434**

Abstract

Present study has been attempted to establish the effects of air pollutants on four dominant plant species i.e., *Plant species* Mangifera indica *(Aam),* Tagetes erecta *(Marigold),* Ocimum sanctum *(Tulsi), and* Azadiracta indica *(Neem) growing at Santaldih area under Para community Development Block, Purulia district, West Bengal (India) encompassing Dharmasthan para,* i.e., *Commercial area), Korgali (Residential area), Nabagram (control area, which is situated far away from the industries) and Washery (very near to cement industry) in 2019-20. The impact of air pollutants on the biochemical characters of the selected plant species from industrial and urban areas was studied by calculating ascorbic acid, total chlorophyll, leaf extract pH and relative water content from leaf tissues. From calculated APTI, it may be concluded that here all species at all locations are belonging to "intermediate species" group.*

Keywords*: Air pollution*, Mangifera indica, Tagetes erecta, Ocimum sanctum, Azadiracta indica, *biochemical characteristics*, *APTI.*

INTRODUCTION

In recent times pollution has become the prime menace for the survival of the biological species. There are various kinds of pollution *e.g.*, air, water, soil, sound and mental pollution. Most of the countries including India, the environment has reached its carrying capacity in terms of air pollutants. In recent times, in almost all cities, medium and small towns in India; there has been significant development activity in terms of industrialization and urbanization. Plants provide an enormous leaf area for impingement, absorption and accumulation of air pollutants to reduce the pollutants level in the environment, with a various extent (Lui and Ding, 2008). Plants can be effectively used as bio indicators of air pollutants, although their sensitivities could vary across the plant community with tolerant species showing no or minimal symptoms while sensitive ones showing symptoms even if the air pollutants increase in small amounts (Singh, 2003). Singh and Verma (2007) reported that, plants sensitivity and tolerance to air pollutants varies with change in Leaf extract pH, Relative water contents (RWC), ascorbic acid (AA) content and Total Chlorophyll content.

MATERIALS AND METHODS

Santaldih area is located at 23.36°N 86.28°E. Leaves were collected in triplicate for analysis from

Dharmasthan para, *i.e.,* Commercial area), Korgali (Residential area), Nabagram (control area, which is situated far away from the industries) and Washery (very near to cement industry). Plant species *Mangifera indica* (Aam), *Tagetes erecta* (Marigold), *Ocimum sanctum* (Tulsi), and *Azadiracta indica* (Neem) were studied. Samples were collected in early morning and brought to laboratory in polythene bag kept in ice box to nullify the adverse effect of high light intensity and temperature. The collected leaf samples were analyzed for the following biochemical estimations namely pH of leaf extract (Singh and Rao, 1983), Total chlorophyll (Yoshida *et al*., 1971), Ascorbic acid (Bajaj and Kaur,1981) and Relative water content (Singh and Rao,1983).The air pollution tolerance index (APTI) has been determined to find the tolerance levels of trees against the air pollutants. The APTI is calculated by the formula, APTI = (A (T=P)+R/10 (Singh and Rao, 1983) where, A= Ascorbic acid (mg/ g), T=Total chlorophyll (mg/g), P = pH of leaf extract and R=Relative water content of leaf extract.

RESULTS AND DISCUSSION

Table.1: Status of biochemical parameters of *Mangifera indica*

Sampling sites	*Mangifera indica* (Aam)				
	pH	Chlorophyll (mg/g)	Ascorbic acid (mg/g)	Relative Water Content (%)	APTI
Dharmasthan para	6.22	2.43	6.73	83.64	14.19
Korgali	6.45	2.38	6.71	79.65	13.89
Nabagram	6.59	2.49	6.42	88.12	14.64
Washery	6.19	2.25	6.89	71.32	12.95

Table.2: Status of biochemical parameters of *Azadiracta ind*ica

Sampling sites	*Azadiracta indica (Neem)*				
	pH	Chlorophyll (mg/g)	Ascorbic acid (mg/g)	Relative Water Content (%)	APTI
Dharmasthan para	6.93	2.86	5.93	70.33	12.84
Korgali	6.87	4.16	6.87	79.54	12.81
Nabagram	6.96	3.90	5.76	72.36	13.49
Washery	6.31	3.91	6.04	68.57	13.03

Table.3: Status of biochemical parameters of *Tagetes erecta*

Sampling sites	*Tagetes erecta* (Marigold)				
	pH	Chlorophyll (mg/g)	Ascorbic acid (mg/g)	Relative Water Content (%)	APTI
Dharmasthan para	7.12	3.48	5.73	83.64	14.44
Korgali	5.47	2.31	6.73	72.65	12.50
Nabagram	7.59	4.39	5.48	88.12	15.38
Washery	5.38	2.08	6.80	73.32	12.40

Table.4: Status of biochemical parameters of *Ocimum sanctum*

Sampling sites	*Ocimum sanctum* (Tulsi)				
	pH	Chlorophyll (mg/g)	Ascorbic acid (mg/g)	Relative Water Content (%)	APTI
Dharmasthan para	6.93	2.17	4.93	73.36	11.82
Korgali	6.06	4.19	5.81	69.54	12.91

Nabagram	6.23	3.96	5.77	79.36	13.82
Washery	6.28	3.91	6.04	67.57	12.91

pH of *Mangifera indica* (Aam) ranges between 6.19 and 6.59. pH of *Azadiracta indica* (Neem) ranges between 6.31 and 6.96. The pH of *Tagetes erecta,* and *Ocimum sanctum* leaves ranges between 5.38 and 7.59; and 6.06 and 6.93 respectively. Chlorophyll contents of leaves gradually decreased in both species from control to more polluted zones; minimum of Aam at Washery (2.25 mg/l), maximum at Nabagram (2.49 mg/l); whereas range of chlorophyll of Neem recorded between 2.86 and 4.16 mg/l. Chlorophyll contents of *Tagetes erecta,* and *Ocimum sanctum* leaves ranges from 2.08-4.39, and 2.17-4.19 respectively. Total chlorophyll (TCH) is related to Ascorbic Acid productivity and Ascorbic acid is concentrated mainly in chloroplast. Ascorbic acid content of all species was higher at industrial areas, moderate at commercial, and low at control area. Relative Water Content of all species found maximum at control zone and minimum at industrial area. So, here all species at all locations are belonging to "intermediate species" group.

CONCLUSION

These specieses are in stress condition. These are acting as indicator species in this area. Pollution status should be checked. Tolerant species should be planted.

REFERENCES

1. Bajaj, K.L. and Kaur, G. Spectrophoto-metric Determination of Ascorbic Acid in vegetables and Fruits. *Analyst*. 106 : 117-120 (1981).
2. Lui Y.J. and Ding H., Variation in air pollution tolerance index of plants near a steel factroy, Impication for landscape plants species selection for industrial areas, WSEAS Trans. *Environ. and Develop*, 4, 24-32 (2008).
3. Singh and Verma, Phytoremediation of Air Pollutants, A review, In, Environmental Bioremediation Technology, Singh, S.N. and R.D. Tripathi (Eds.), *Springer*, Berlin Heidelberg., 1, 293-314 (2007).
4. Singh S.K. and Rao D.N. Evaluation of plants for their tolerance to air pollution. In, *Proceedings Symposium on Air Pollution Control*, New Delhi India, 1, 218-224 (1983).
5. Singh, S.K.: Phytomonitoring of urban industrial pollution: A new approach. *Env. Moni.Assess*., 24, 27-34 (2003).
6. Yoshida, S. Azrapraveen and A.K.M. Ghouse. A Comparative study on the cuticular trails of Mangifera indica L. and Psidium gujava L. in relation to local smoke pollution. Environmental and Adaptive Biology of plants. 285-295 (1971).

ISSN : 0975-9468 Volume 27 • Issue 4 • Number 57

TABU EKALAVYA

তবু একলব্য

An International Peer-reviewed Refereed Research Journal on Arts & Humanities

সমাজ

সংস্কৃতি

সাহিত্য

The Village as a Representative of the Real India : A Comparative Study of Bibhutibhusan Bandyopadhyay's 'Pather Panchali' and Anita Desai's 'The Village by the Sea'

Indrajit Mukherjee

Many writers have shown that the true spirit of our motherland lies in its villages and small towns. Though Gandhiji praises the role of colonial Indian villages in the freedom struggle, Nehru describes postcolonial Indian villages as a kind of "naked, starving, crushed, and utterly miserable" entity (quoted in Misra 103). In this paper, I try to draw a striking contrast between Bibhutibhusan Bandyopadhyay's Pather Panchali (1929) and Anita Desai's The Village by the Sea (1982) to bring out "an original and authentic picture of India" (Gooptu 141). Though these two books appear to have little in common with one another at first glance, a close reading reveals close affinities between them, regarding the social and economic condition of rural life and the graphic pen picture of nature. Both novels provide a space where the novelists skilfully intertwine childhood hopes and fears with a powerful sense of place and a lush green arcadian landscape. Geoffrey Kain shows this kind of fictions creates a contrast between the country and city life in Indian literary oeuvre:

> They [...] foreground the fundamental connection of the villager to the natural world, and that tends to place them in contrast to their inverse depiction of the presumed darker aspects of urban life, most notably [...] alienation from nature, and a survivalist sophistication that expresses itself in deceit and exploitation. (Kain 179)[1]

The graphic pen pictures of rural milieu that both novelists draw for the reader are rich with the elements of serenity, intimacy and homeliness. We have gone via these novels to the villages of Nischindipur and Thul--- space

Rupkatha Journal on Interdisciplinary Studies in Humanities
Vol. 13, No. 3, 2021. 1-11
DOI: https://doi.org/10.21659/rupkatha.v13n3.35
First published on October 26, 2021

www.rupkatha.com

Who Remembers those "Undocumented Minors"? Locating the Genealogy of the Oppressed in Valeria Luiselli's *Tell Me How It Ends*

Indrajit Mukherjee
Assistant Professor, Dept. of English, Nistarini Women's College, Research Scholar, Vidyasagar University. Email ID: perfectindrajit.mukherjee@gmail.com

Abstract
We can always look upon the intersection of history and events as an exciting façade, full of deceptions, half-baked truths, and awkward reconciliations in the framework of cultural studies. The Mexican author Valeria Luiselli's *Tell Me How It Ends* (2017) attempts to trace the evolution of a set of social, political, and cultural circumstances that are pregnant with significance in the traumatic past of millions of Latin-American children refugees in the United States. First, the article will unpack how Luiselli's impalpable domain tries to connect the unresolved experiences of the violent wounds of those children's deportation and dislocation from Guatemala, Honduras, and Mexico with their unfortunate encounters in the foreign land. Second, it will attempt to dismantle, disrupt, and deconstruct the construction of America as a heteroglossic space around the challenges of those displaced children by displaying some questions addressed to them at the immigrant court. Finally, the proposed paper will critically scrutinise how this non-fictional work follows the creeping imperialist approaches of the United States through the hazes of childhood recollections, making a heartfelt appeal to everyone to halt discrimination, racial hatred, and poisonous ignorance. Applying Agamben's idea of the *homo sacer*, such a study will bring to the fore the dialectics of postcoloniality in the United States, where undocumented children's claims to identity formation and self-determination processes would be at odds with the more comprehensive national identity in contemporary times.

Keywords: History, Refugees, Heteroglossic, Imperialist, *Homo Sacer*, Identity.

Tell Me How It Ends (2017) talks about the writer's experiences as an interpreter for Central American child refugees, exploring one of the most complex and unequal cross-border relations in light of the rise of Donald Trump to the throne of power in 2016 (Raul Hinojosa-Ojeda and Edward Telles, 2021, p. 21). The genesis of the book traces back to the writer's problems as a Mexican lady in the United States, illustrating that the problematics of citizenship right in America is based "on the notion of being a serving citizen, rather than one who deserves rights" (Rudrappa, 2008, p. 308). The narrative demonstrates the politics of "the still ongoing refugee and migration crisis" (Nedoh, 2017, p. 1) through the microcosmic presentation of one of contemporary

water

MDPI

Article

Comparison between Deep Learning and Tree-Based Machine Learning Approaches for Landslide Susceptibility Mapping

Sunil Saha [1], Jagabandhu Roy [1], Tusar Kanti Hembram [2], Biswajeet Pradhan [3,4,*], Abhirup Dikshit [3], Khairul Nizam Abdul Maulud [4,5] and Abdullah M. Alamri [6]

1 Department of Geography, University of Gour Banga, Malda 732103, India; sunilgeo.88@gmail.com (S.S.); jagabandhuroy1991@gmail.com (J.R.)
2 Department of Geography, Nistarini College, Purulia 723101, India; tusarpurulia1991@gmail.com
3 Centre for Advanced Modelling and Geospatial Information Systems (CAMGIS), Faculty of Engineering and Information Technology, University of Technology Sydney, Sydney 2007, Australia; abhirup.dikshit@student.uts.edu.au
4 Earth Observation Centre, Institute of Climate Change, Universiti Kebangsaan Malaysia (UKM), Bangi 43600, Malaysia; knam@ukm.edu.my
5 Department of Civil Engineering, Faculty of Engineering and Built Environment, Universiti Kebangsaan Malaysia, Bangi 43600, Malaysia
6 Department of Geology & Geophysics, College of Science, King Saud University, P.O. Box 2455, Riyadh 145111, Saudi Arabia; alamri.geo@gmail.com
* Correspondence: Biswajeet.Pradhan@uts.edu.au or Biswajeet24@gmail.com

Abstract: The efficiency of deep learning and tree-based machine learning approaches has gained immense popularity in various fields. One deep learning model viz. convolution neural network (CNN), artificial neural network (ANN) and four tree-based machine learning models, namely, alternative decision tree (ADTree), classification and regression tree (CART), functional tree and logistic model tree (LMT), were used for landslide susceptibility mapping in the East Sikkim Himalaya region of India, and the results were compared. Landslide areas were delimited and mapped as landslide inventory (LIM) after gathering information from historical records and periodic field investigations. In LIM, 91 landslides were plotted and classified into training (64 landslides) and testing (27 landslides) subsets randomly to train and validate the models. A total of 21 landslides conditioning factors (LCFs) were considered as model inputs, and the results of each model were categorised under five susceptibility classes. The receiver operating characteristics curve and 21 statistical measures were used to evaluate and prioritise the models. The CNN deep learning model achieved the priority rank 1 with area under the curve of 0.918 and 0.933 by using the training and testing data, quantifying 23.02% and 14.40% area as very high and highly susceptible followed by ANN, ADtree, CART, FTree and LMT models. This research might be useful in landslide studies, especially in locations with comparable geophysical and climatological characteristics, to aid in decision making for land use planning.

Keywords: landslide; deep learning model; tree-based machine learning model; ridge regression; GIS; East Sikkim Himalaya

Citation: Saha, S.; Roy, J.; Hembram, T.K.; Pradhan, B.; Dikshit, A.; Abdul Maulud, K.N.; Alamri, A.M. Comparison between Deep Learning and Tree-Based Machine Learning Approaches for Landslide Susceptibility Mapping. *Water* **2021**, *13*, 2664. https://doi.org/10.3390/w13192664

Academic Editor: Francesco Fiorillo

Received: 20 August 2021
Accepted: 24 September 2021
Published: 27 September 2021

1. Introduction

In mountainous regions, landslides are regarded as one of the reoccurring natural hazards affecting human property and lives. Landside susceptibility (LS) indicates the spatial probability of landslides in an area [1]. Landslides are often triggered by earthquakes or heavy precipitations within certain geomorphological, geological and hydrological settings. However, other primary factors controlling landslide failure mechanisms, including in situ stresses, weathering and heave, play vital roles. In mountainous regions, the effect of landslides can change the topographic characteristic, forest, soil properties (consistence, structure, density, temperature, etc.), road and farming land, depending on the magnitude

Stochastic Environmental Research and Risk Assessment
https://doi.org/10.1007/s00477-022-02212-3

ORIGINAL PAPER

Prediction of spatial landslide susceptibility applying the novel ensembles of CNN, GLM and random forest in the Indian Himalayan region

Sunil Saha[1] · Anik Saha[1] · Tusar Kanti Hembram[2] · Kanu Mandal[1] · Raju Sarkar[3] · Dhruv Bhardwaj[3]

Accepted: 12 March 2022

Abstract
This research aims to generate a landslide susceptibility map (LSM) for the Bhagirathi river basin located in the Tehri Garhwal district of Uttarakhand state in India. For this study, we incorporated and utilized machine learning novel ensemble models, namely: Generalize Linear Model (GLM), Random Forest (RF), Convolutional Neural Network (CNN), GLM-RF, CNN-RF, CNN-GLM and CNN-GLM-RF. The above-specified ensemble models were incorporated for the preparation of LSM. A total of 171 landslide locations were chosen and studied for the preparation of landslide inventory. From the landslide inventory, 70% of landslides were utilized for the training purpose, whereas the rest, 30%, were used for the validation purpose. In the ongoing research study, a total of 17 landslide conditioning factors (LCFs) were utilized, and the analysis for multi-collinearity was performed by tolerance (TOL) as well as variance inflation factor (VIF) methods. These LSM were then validated through receiver operating characteristic curve (ROC), mean absolute error (MAE), root mean square error (RMSE) and Chi-Square methods. Finally, the outcomes of the analysis, as well as validation models, show that the CNN model proves to be the most effective for predicting landslide susceptibility in the study area. The study found that the methods incorporated for the area under consideration can be applied to the regions having similar geo-environmental factors globally.

Keywords Generalize linear model · Random forest · Convolutional neural network · Landslide susceptibility maps · Tehri region

1 Introduction

Landslides fall in the category of highly complex quasi-natural hazards that consequences in the lateral and downward movement in sloping components, which includes rock, soil, or their combination. It is occurred by natural triggering factors like rainfall, earthquake, volcanic eruption, marine erosion, and anthropogenic activities like modification of slope (construction of road, preparation of agricultural field, etc.), unplanned construction of houses in the hilly mountainous regions (Froude and Petley, 2018; Haque et al. 2019). The National Aeronautics and Space

✉ Raju Sarkar
rajusarkar@dce.ac.in

Sunil Saha
sunilgeo.88@gmail.com

Anik Saha
aniksahamalda@gmail.com

Tusar Kanti Hembram
tusarpurulia1991@gmail.com

Kanu Mandal
kanumandal666@gmail.com

Dhruv Bhardwaj
dhruv97bhardwaj@gmail.com

[1] Department of Geography, University of Gour Banga, Malda, West Bengal 732103, India

[2] Department of Geography, Nistarini Women's College, Purulia, West Bengal, India

[3] Department of Civil Engineering, Delhi Technological University, Delhi 110 042, India

Published online: 04 April 2022

GeoJournal
https://doi.org/10.1007/s10708-021-10528-w

Spatial analysis and modelling for primary healthcare site selection in Midnapore town, West Bengal

Bikash Dutta · Manas Das · Utpal Roy · Sutapa Das · Sutapa Rath

Accepted: 27 September 2021

Abstract Unprecedented and chaotic growth of cities results in reducing open spaces and water bodies, worsening infrastructure facilities and changes in ecological morphology. This unregulated growth of the urban population led to uneven distribution of urban amenities, facilities and healthcare services. Considering this, the study aimed to draw attention to the existing spatial pattern of healthcare facility centres as well as to find out the possible sites for the provision of healthcare facility centres in the municipal ward (micro-scale) of Midnapore town. This prototype study was conducted using Analytical Hierarchy Process (AHP) and Ordinary Least Square (OLS) evaluation model based on various criteria through Arc GIS environment. The findings indicate that the spatial distribution patterns of existing public healthcare centres were significantly dispersed. Weights based on a set of criteria were calculated by AHP and OLS algorithm and generated suitability evaluation maps classified from 1 (poor suitable) to 4 (most suitable). According to the employed criteria in this study unveil those existing hospitals and primary healthcare centres have not been located in the appropriate locations. The model is found to be valid for the given study area and there is no significant difference between AHP and OLS results. Further, it can be used for preparing the suitability map for the other areas with similar geo-environmental conditions for the proviso of healthcare services as well as will be most effective in preventing disease progression and reducing healthcare inequality on a large scale.

Keywords AHP · OLS · PHCs · Suitability map · Spatial analysis · Unequal distribution

Introduction

Healthcare facilities are important criteria and/or indicators for social well being as well as socio-

Supplementary Information The online version contains supplementary material available at https://doi.org/10.1007/s10708-021-10528-w.

B. Dutta (✉)
Department of Geography, Nistarini College, Purulia, West Bengal 723101, India
e-mail: bikashgeovu@gmail.com

M. Das
Department of Remote Sensing and G.I.S, Vidyasagar University, Midnapore, West Bengal 721102, India

U. Roy (✉)
Department of Geography, University of Calcutta, Kolkata, West Bengal 700073, India
e-mail: utpalgeovu@gmail.com

S. Das
Department of Economics, Vidyasagar University, Midnapore, West Bengal 721102, India

S. Rath
Department of Geography, Vidyasagar University, Midnapore, West Bengal 721102, India

PalArch's Journal of Archaeology of Egypt / Egyptology

QUALITY OF LIFE AND HEALTH SECURITY AMONG THE SLUM NEIGHBOURHOODS OF MIDNAPORE MUNICIPALITY, INDIA

Bikash Dutta*[1], Utpal Roy[2], Manas Das[3], Sutapa Das[4], Sutapa Rath[5]

[1]Assistant Professor, Dept. of Geography, Nistarini College, Purulia-723101, West Bengal, India And, Research scholar, Dept. of Geography, Vidyasagar University, Midnapore-721102, West Bengal, India.

[2]Associate Professor, Dept. of Geography, University of Calcutta, Kolkata-700073, West Bengal, India.

[3]Research scholar, Dept. Of Remote sensing and G.I.S, Vidyasagar University, Midnapore-721102, West Bengal, India.

[4]Research scholar, Dept. of Economics, Vidyasagar University, Midnapore-721102, West Bengal, India.

[5]Research scholar, Dept. of Geography, Vidyasagar University, Midnapore-721102, West Bengal, India.

Bikash Dutta , Utpal Roy , Manas Das , Sutapa Das , Sutapa Rath , Quality Of Life And Health Security Among The Slum Neighbourhoods Of Midnapore Municipality, India, Palarch's Journal Of Archaeology Of Egypt/Egyptology 18(10), 571-594. ISSN 1567-214x.

Keywords: Quality of life index (QoLI), Health security index (HSI), Ordinary least square (OLS), Inductive and deductive methods, Slum neighbourhoods, Midnapore municipality.

Abstract

The concept of quality of life and health security is multidimensional and dynamically varies across places with respect to physical, socio-economic and psychological environments. Health security can improve quality of life, health status, life expectancy and adaptive capabilities as

well as prevent disease progression. Slums are examples of the most vulnerable localized communities in the urban morphology that face a range of difficulties. This study aimed to examine the spatial distribution and correlation of and between the quality of life and health security among the slum neighbourhoods of Midnapore municipality as well as to find the similarity among the methods employed under study. The modified quality of life (QoLI) and health security index (HSI) was developed using inductive and deductive methods with the available datasets through a questionnaire survey. The results of the analysis show that slum neighbourhoods are more vulnerable with least prepared for their health security while living with decent to moderate quality of life. The ordinary least square (OLS) method was examined among the indicators of quality of life and health security showing a statistically significant correlation. This prototype study may help the researcher for further study at a local scale with the specific method whenever needed. Moreover, it is suggested to the local authority, policymakers, NGOs and district planning commission that more community participation, awareness creation and planning interventions can improve the place inequalities of the quality of life and health security among the slum neighbourhoods.

1. **Introduction**

The World Health Organization (WHO, 2020) defines the quality of life as "an individual's perception of their position in life in the context of the culture and value systems in which they live and concerning their goals, expectations, standards and concerns". Quality of life is the degree to which human beings can live within a healthy, comfortable environment and can take pleasure in their livelihoods. Quality of life is multidimensional and has become more holistic which includes socio-economic, emotional, physical and mental health, recreation and leisure time, material, built environment, employment, education, safety, security and freedom and overall healthcare accessibility and social well-being. However, perception of quality of life is highly subjective because it varies from place to place even person to person. For example, rural households with standard income may perceive the standard quality of life as the households living in urban areas. In contrast, health security is a recent concern in the Covid-19 pandemic. According to the World Health Organisation (WHO, 2020), health security encompasses the "activities required to minimise the danger and impact of acute public health events that endanger the collective health of populations living across geographical regions and international boundaries". Public health security is defined as the activities and measures across geographical regions that reduce vulnerability to infectious diseases and the impact of acute public health incidents caused by overpopulation growth, rapid urbanization, environmental degradation, and the misuse of antimicrobials (Stoeva 2020; Paranjape and Franz 2015). The spread of diseases, pandemics, and epidemics have become a recent global issue, requiring essential resources for rapid and effective healthcare services to the vulnerable groups especially in the developing world (Feldbaum et al. 2006; Chiu et al. 2009). The Global Health Security Agenda advocates health security, aiming to improve detection, prevention, and response to infectious diseases through the initiatives of public health surveillance among the states in the world (Blazes et al. 2016). The shifting nature of human society and severe natural disasters may cause emerging infectious diseases with pandemic potential which demand equal distribution of resources and healthcare facilities and services (Ganapathy et.al 2016). Therefore, every state has a liability to preventing health insecurity and ensures the wellbeing of their populations (Aldis 2008). India has been initiatives to protect health insecurities by launching the Nation Health Protection Scheme (NHPS) 2018 as a part of the Ayushman Bharat Programme, which aiming of covering

Vol. 5 No. 2 (2021)

ARTICLES

Analysing social vulnerability to health shocks among the slum neighbourhoods of Midnapore municipality, India: a new approach

PDF

Bikash Dutta, Utpal Roy, Manas Das, Sutapa Das, Sutapa Rath

Published 2021-08-19

Abstract

A measure of social vulnerability is a critical issue in developing countries due to place inequalities of the level of impacts, damage and recovery from the natural and man-made disasters. Identification of socially vulnerable populations can reduce disaster risk through preparedness, response and recovery. Evidences from the literature shows that the slum neighbourhoods of Midnapore municipality have been facing socio-economic inequity and health shocks. However, we did not find any significant measures on social vulnerability in the study area. In this regard, we have developed susceptibility mapping of social vulnerability using GIS and statistical models. We have selected forty variables in the context of slum neighbourhoods. Using Principal component analysis (PCA), forty variables were reduced to seventeen components with a total explained variance of 70.832%. Component scores are combined to construct a modified Social vulnerability index (SoVI). The results from the analysis reveal that 10.25 % of are slum neighbourhoods with high levels of socially vulnerable and 30.15% slum neighbourhoods characterised with moderate to high levels of socially vulnerable, while only 3.20% slum neighbourhoods are less socially vulnerable. The findings of this small scale analysis have the potential to assist urban authorities, medical and health policymakers, district planning commission and authorities under disaster management in the development of more effective and geographically targeted urban health mission and healthcare management programs.

Nano-Structures & Nano-Objects 26 (2021) 100756

Contents lists available at ScienceDirect

Nano-Structures & Nano-Objects

journal homepage: www.elsevier.com/locate/nanoso

Design of π-conjugated flexible semiconductive 2D MOF and MOF derived CuO nano-spheres for solvent free C-X (S, O) hetero-coupling catalysis with enhanced conductivity

Maxcimilan Patra [a,1], Soumen Kumar Dubey [a,1], Bibhas Mondal [a], Kajal Gupta [a], Angshuman Ghosh [b], Subhankar Mandal [c], Satyajit Hazra [c], Ajit Kumar Meikap [d,*], Ujjal Kanti Roy [a,*], Subham Bhattacharjee [a,*], Rajat Saha [a,*]

[a] Department of Chemistry, Kazi Nazrul University, Asansol-713340, India
[b] TCG Lifescience, Block BN, Sector V, Saltlake, Kolkata-700156, India
[c] Saha Institute of Nuclear Physics, HBNI, 1/AF Bidhannagar, Kolkata 700064, India
[d] Department of Physics, NIT Durgapur, Durgapur-713209, India

ARTICLE INFO

Article history:
Received 1 January 2021
Received in revised form 15 April 2021
Accepted 28 April 2021

Keywords:
2D MOF
$\pi \cdots \pi$ Interaction
Flexible MOF
MOF derived CuO-NPs
Green catalysis
Electrical conductivity

ABSTRACT

A flexible, 2-fold interpenetrated 3D supramolecular structure $[Cu(ndc^{2-})(1,10\text{-phen})]_n$ (where ndc^{2-} = 2,6-napthalenedicarboxylate and 1,10-phen = 1,10-phenanthroline) comprising neutral 2D metal–organic layers as the basic building block was prepared. Structural study reveals that metal ions are bridged by ndc^{2-} ligands to form 2D coordination layers and the coordinated 1,10-phen moieties are hanging from the layers in the interlamellar spaces. The gliding motion of $\pi \cdots \pi$ stacked layers through 1,10-phen moieties was found to be responsible for the flexibility of MOF and the consequent extended conjugation also rendered semiconducting behaviour in the material. Thermal stability studies revealed that the framework was pretty stable below 260°C. Additionally, the MOF was characterized by performing BET adsorption and photoluminescence studies. Further, the MOF was calcinated at 650°C to prepare well defined, nearly uniform and spherical shaped CuO nanoparticles (CuO-NPs) with an average size of ~25 nm. Interestingly, CuO-NPs showed around 16 times more conductivity (4.8×10^{-2} S/cm) in relative to the parent MOF (3×10^{-3} S/cm). CuO-NPs induced cross-coupling reactions of alcohols and thiols with arylhalides have been reported. A simple, general, ligand-free and solvent-free procedure for the efficient synthesis of the cross-coupled products in high yield was successfully demonstrated.

1. Introduction

In last three decades, metal–organic frameworks (MOFs) are appeared as one of the most promising functional material due to their inherent porous structure and modular behaviour [1]. Initially, the inception was that the implication of inert metal ions and insulating bridging ligands makes MOFs weakly conducting or insulating in nature [2]. But, from last decade, design of conducting MOFs has gained much attention due to their several applications in energy storage, sensing, electrocatalysis, etc. [3]. Researchers have developed two different types of conductive MOFs: (a) intrinsically conductive MOFs: electrically conducting organic building blocks, such as 2,3-pyrazinedithiolate [4], dihydroxybenzoquinone [5] etc. have been used to induce conductivity in the designed framework, and (b) extrinsically conductive MOFs: electrically conducting guests, both neutral I_2, [6] (TCNQ) [7], and charged (BF_4^-) [8], are incorporated in the void space of MOFs to enhance conductivity. Intrinsically conducting MOFs have gained much attention over its extrinsic counterpart due to low cost production and easy synthesis [2a], [9]. Several types of design principles have been adopted by scientists to build intrinsically conducting MOFs: (a) use of metal ions and bridging ligands having equivalent band structure which will help to transport electrons through the framework [10], (b) use of radical generating ligands that will boost the conductivity of the designed framework [5c,10b] (c), use of extended $\pi \ldots \pi$ conjugation between 2D coordination polymer [5b], [11]. In organic electronics, π-interaction is used to develop conducting materials [12] and, in similar way, several research groups have developed conducting MOFs based on extended $\pi \ldots \pi$ conjugation using different

* Corresponding authors.
E-mail addresses: meikapnitd@yahoo.com (A.K. Meikap), uroccu@gmail.com (U.K. Roy), sbpb2012@gmail.com (S. Bhattacharjee), rajat.saha@knu.ac.in (R. Saha).

[1] Both have equal contributions.

https://doi.org/10.1016/j.nanoso.2021.100756
2352-507X/

organic ligands e.g. napthalenediimide, [9b] tetrathiofulvalene [13], anthracene [14], etc. Formation of continuous π-conjugation throughout the framework is the primary condition to design such materials. Herein, we have used 1,10-phen, highly potential to participate in $\pi \ldots \pi$ interaction, as the building block to develop conducting material and found that the synthesized 3D supramolecular framework showed semiconducting behaviour.

Recently, syntheses of various nano-materials using MOFs as sacrificial scaffolds are of great interest [15]. The regular periodic arrangement of metal nodes within the MOF architecture provides an excellent platform to design nano-particles of uniform size distribution as well as their intriguing porosity. The structure, composition, phase and size of the nano-particles can be controlled by optimizing the synthetic conditions: chemical environment (O_2, N_2 etc.), temperature and synthetic methods [16]. Several research groups have synthesized metal, [16a] metal–oxide, [16b,16c,16d,16e,16f,16g] mixed metal–oxide, [16h] metal carbide [16i] NPs, etc, and explored their enormous applications in gas adsorption, [16j] catalysis, [16b] and so on. Besides, these MOF derived NPs have been used for several types of electronic applications like electrocatalysis, [17] battery, [18] etc. based on their versatile conducting properties from insulating to metallic behaviour [17–19]. In this work, we have used our synthesized semiconductive MOF to develop NPs and interestingly found that the MOF-derived NPs showed higher conductivity than the parent MOF.

C–O and C–S bonds are prevalent in numerous compounds that are of biological, pharmaceutical, and material interest [20]. Specially, a large variety of aryl sulfides are in use for diverse clinical applications [21]. One of the most common synthetic methods for their preparation is the copper-assisted classic Ullmann reaction. However, these reactions often require harsh conditions such as high temperature (>200 °C), stoichiometrically higher amount of copper reagent and thus produce a lot of wastes [22]. Currently, to follow strict environmental laws, chemical based industries are desperate in reducing various harmful chemical wastes by designing intelligent catalysts those perform in mild or environment benign conditions with high yield, large selectivity and good efficacy [23]. Palladium and copper complexes containing electron-rich ligands have been studied considerably for the cross-couplings of oxygen and sulphur nucleophiles with aryl halides [24]. Subsequently, few studies have focused on the use of iron and nickel-based catalytic systems for this purpose also [25]. Unlike homogeneous catalyst, use of heterogeneous catalyst is much more advantageous in terms of their easy separation, recyclability, high thermal stability and longer lifetime. In this respect, we have focused on CuO-NPs induced heterogeneous C(aryl)-S and C(aryl)-O hetero-coupling reactions with the following advantages: (a) the reaction proceeds under solvent free condition, (b) easy separation of catalysts and products from the reaction mixture after completion, (c) high selectivity of the catalysts for the substrate, (d) high catalysis rate and e) re-usability.

In this endeavour, we have synthesized a 2-fold interpenetrated, flexible, 3D supramolecular framework: **[Cu(2,6-ndc)(1,10-phen)]$_n$**, by solvothermal method and characterized by SCXRD analysis. Structural analysis revealed that each Cu centres are connected by 2,6-ndc ligands to form 2D coordination layers with hanging coordinated 1,10-phen moieties and these 2D metal–organic coordination layers are assembled by 1,10-phen mediated $\pi \ldots \pi$ interactions to form the overall 3D supramolecular structure. The presence of $\pi \ldots \pi$ interactions help to: (i) induce flexibility and (ii) create electronic conducting pathway within the framework. The resultant flexible framework showed semiconducting nature in association with micro-porosity. TGA analysis revealed that the framework decomposes at 350 °C. The MOF was decomposed by heating at 650 °C to produce CuO-NPs which were characterized by PXRD, SEM and EDAX analyses. Four probe electrical conductivity experiments revealed that the synthesized CuO-NPs have 16 times higher conductivity than parent MOF. Further, we have successfully demonstrated solvent free C–S and C–O heterocouplings in excellent yields in bulk utilizing the CuO-NPs. Product analysis revealed exclusive formation of the desired products with minimum amounts of wastes; hence, we would be able to make the process green and highly applicable for industrial scale synthesis.

2. Experimental section

Materials and Methods: Copper (II) nitrate, monohydrate; 2,6-napthalene dicarboxylic acid and 1,10-phenanthroline were purchased from Merck chemical company. All other chemicals used were AR grade. Elemental analysis (C, H, N) was carried out using a Perkin-Elmer 240C elemental analyzer. The thermal analysis was carried out using a Mettler Toledo TG-DTA 85 thermal analyzer under a flow of N_2 (30 ml/min). The sample was heated at a rate of 10 °C/min with inert alumina as a reference. IR spectroscopy was measured on Nicolet Impact 410 spectrometer between 400 and 4000 cm^{-1}, using the KBr pellet method. Photoluminescence spectra were collected on a Shimadzu RF-5301PC spectrophotometer. Powder XRD patterns were recorded by using Cu-Kα radiation (Bruker D8; 40 kV, 40 mA). The elemental analysis for CuO-NPs was performed by BRUKER energy dispersive X-ray spectrometer (EDS) attached with the FEI, INSPECT F50 field emission scanning electron microscope (FESEM). ^{1}H-NMR studies were carried out by using 300 MHz Bruker NMR spectrometer. The XPS measurements of the sample was carried out in an ultrahigh vacuum (UHV) multiprobe setup (Omicron Nanotechnology) at a base pressure of $\sim 2.0 \times 10^{-9}$ mbar, which was equipped with an EA125 hemispherical energy analyzer and an X-ray source [26]. For the XPS measurements, monochromatic Al Kα X-ray of 1486.6 eV photon energy was used as a source and the corresponding spectrometer energy resolution was $\sim$ 0.8 eV. C 1s level (binding energy of 284.8 eV) was chosen as the reference level to calibrate the other core-level spectra.

Synthesis of Complex 1 {[Cu(O-phen)(ndc)]$_n$: A mixture of $Cu(NO_3)_2$ (0.5 mmol, 0.1214 g), ndc (0.5 mmol, 0.1092 g), 1,10-phen (0.25 mmol, 0.0502 g) and 1 mL Et_3N in 6 mL DMF was stirred for 15 min. Then the mixture was transferred into a 15 ml Teflon-lined stainless-steel vessel and heated for 24 h at 120 °C. Afterwards, it was cooled to room temperature for another 24 h. After 48 h, green coloured single crystals (Figure S1) suitable for X-ray structure determination were isolated by filtration. Yield: 70%. Anal. Calcd. for $C_{24}H_{14}CuN_2O_4$ indicates C: 62.85% (62.88% theo), H: 3.10% (3.12% theo) and N: 6.10 (6.08% theo). IR (KBr pellet, cm^{-1}): 1606(s), 1560(s), 1544(w), 1426(w), 1394(s), 1357(s), 1221(w) and 1191(w) (Figure S2).

Electrical conductivity measurement: The resistance of the sample is measured by means of a four terminal direct current technique with resolution of $\delta R/R = 10^{-5}$ using a pressed pellet (10 ton pressure) of the samples. The four terminal connections are made using fine copper wire with pure silver paste. As a confirmatory test towards ensuring good electrical contact using silver paste, the continuity of the samples was checked before placing it within the sample holder. Contribution of conductivity of silver of the paste is ignored as it is used for all cases. All these measurements were performed by the following equipments, (i) A constant current source (KEITHLEY INSTRUMENT, Model 220), (ii) A nanovoltmeter (KEITHLEY INSTRUMENT, Model 181), (iii) Hewlett Packard 3458 A, 81/2 digit multi-metre.

General Procedure for C-X (X = S and O) Hetero-coupling Reactions: The catalytic reactions were carried out in a glass batch reactor. To a stirred solution of the phenol or thiophenol

(25 mmol), aryl halide (5 mmol), KOH (5 mmol) and CuO (2.5 mol%) were added, and the reaction mixture was stirred at 100 °C for 17 h under inert atmosphere and monitored continuously by TLC (hexane/ethyl acetate = 9:1 v/v). After completion of the C–O or C–S cross-coupling of phenol/thiophenol with aryl halide, (i.e. after complete consumption of the aryl iodide which takes near about 17 h), the reaction mixture was treated with diethyl ether. The solution was centrifuged and then catalyst was isolated, washed water and ether. After complete drying, the catalyst can be reused for the next cycle. The remaining mixture was diluted with water and extracted with diethyl ether thrice. The combined organic layer was dried over anhydrous Na_2SO_4, filtered, and concentrated to afford the crude material. The crude material was then purified by column chromatography (silica 100–200 mesh, ethyl acetate-hexane 5%–10%) to afford the desired C–O or C–S cross coupling product (yield = 95%–99%).

Crystallographic Data Collection and Refinement: Suitable single crystal of the complex was mounted on a Bruker SMART diffractometer equipped with a graphite monochromator and Mo-K_α(λ = 0.71073 Å) radiation. Unit cell parameters were determined by using the APEX2 [27] program. Data reduction was carried out by the SAINT [27] program and correction or absorption was performed using the SADABS [27] program. The structure was solved using Patterson method by using the SHELXS-2018/3 [28] embedded in WINGX software package [29]. Subsequent difference Fourier synthesis and least-square refinement revealed the positions of the remaining non hydrogen atoms. Non-hydrogen atoms were refined with independent anisotropic displacement parameters. Hydrogen atoms were placed in idealized positions and their displacement parameters were fixed to be 1.2 times larger than those of the attached non-hydrogen atom. All Figures were drawn by using PLATON [30] and ORTEP [31]. Data collection and structure refinement parameters and crystallographic data for complex 1 are given in Table S1. The structure was previously reported in literature [32] and, herein, we have described from a different perspective. Some selected coordination bond lengths, bond angles and non-covalent interaction parameters are summarized in Table S2-S3.

Indexing of the PXRD data: The indexing of the XRPD pattern was carried out using NTREOR and McMaille programs of EXPO 2009. Indexing reveals that the complex is still crystalline with a monoclinic system with a = 13.5426 Å, b = 13.9326 Å, c = 12.0862 Å, β = 100.1023° and V = 2245.11 Å^3. The space group was obtained from statistical analysis of the powder pattern with the help of find space module of the EXPO 2009 software package. Statistical analysis shows that the most probable space group is $P2_1/n$. For this unit cell and space group, full pattern decompositions were performed using Le Bail method giving good fit between calculated and experimental powder X-ray patterns. This result was corroborated from the indexing and Pawley refinement of the PXRD pattern of the complex by the reflex module of the Material studio program. Unit cell, peak profiles, zero-shift, background were refined simultaneously. Peak profiles were refined by the Pseudo-Voight function with Berar–Baldinozzi asymmetry correction parameters. The background was refined using a 4th order polynomial.

3. Result and discussions

Structural description of Complex 1: X-ray crystal structure analysis revealed **1** as a neutral 3D supramolecular framework (formula $[C_{24}H_{14}CuN_2O_4]_n$). The asymmetric unit contains one Cu(II) ion, two halves two ndc^{2-} ligands and one 1,10-phen (Figure S3). Each Cu(II) atom shows distorted square pyramidal geometry (τ = 0·07) with CuN_2O_3 chromophore (Figure S4). ndc^{2-} ligands show two different types of bridging modes: μ4-*bis*-bridging and μ2-*bis*-bridging. Coordination of two different types of ndc^{2-} with the Cu^{2+} ions forms 2D coordination sheet in the ***bc***-plane with 1,10-phen ligands hanging into the interlamellar spaces from the metal centres, Figure S5. These 1,10-phen moieties between two 2D layers are connected through are interacted by $\pi \ldots \pi$ interactions between aromatic rings present within the 1,10-phen molecules. Such $\pi \ldots \pi$ interactions further assemble these 2D layers along *a*-axis to generate a spongy 3D supramolecular framework, as shown in Fig. 1a. The dimensions of all $\pi \ldots \pi$ interactions are listed in Table S4. It is to be noted that 1D channel of dimension 12.071 × 13.294 Å is formed along ***a***-axis (Figure S6). The channel is filled by two-fold self impregnation in order to achieve an efficient packing (Fig. 1b and S7).

Framework Stability and PXRD: Thermo-gravimetric analysis of the compound was performed in the temperature range of 25–500 °C under N_2 atmosphere (Fig. 2). The TG analysis indicated that complex **1** is stable up to 260 °C and undergoes decomposition in two consecutive steps above this temperature. In the first step, 1,10-phen moieties undergo dissociation within 260 and 300 °C and above this temperature it degrades in another step at about ∼325 °C.

To know about framework flexibility, the PXRD analyses with complex **1** were done at room temperature and at 150 °C temperature. The PXRD pattern of the as synthesized complex **1** is matched very well with the simulated pattern which indicated the phase purity of the sample. The PXRD (Fig. 3) pattern at higher temperature has peaks at slightly lower angle. The indexing of the PXRD pattern was carried out using NTREOR and McMaille programs of EXPO 2009 (supporting information, Figure S8). This reveals that the complex is still crystalline with monoclinic system (***a*** = 13.5426, ***b*** = 13.9326, ***c*** = 12.0862 Å, ***β*** = 100.1073° with a larger cell volume of 2245.11 Å^3, Table S4). So, the length of the ***a***-axis, along which 2D layers are stacked through $\pi \ldots \pi$ interactions, increases in large amount compared to ***b***- and ***c***-axes and this corresponds to the expansion of layer gap assisted by the gliding motion of the π-stacked layers [33], which is feasible for 1,10-phen ligand. So, both the increase in bond length and expansion of layer gap along ***a***-axis contribute to the overall 15% increase in the overall cell volume. Upon cooling to room temperature, the PXRD pattern reverts back to the original pattern. This proves the π-induced flexibility of the framework.

Adsorption study: Though PLATON study indicates the non-porous nature the framework at ambient condition but the variable temperature PXRD study showed that there is a chance to create porous channel along crystallographic ***c***-axis by thermally stimulated π-induced flexibility — and thus we have attempted to analyse sorption behaviour of the sample. N_2 adsorption study at 77 K revealed the non-porosity of the material while the solvent sorption studies at 298 K indicated micro-porosity. Water adsorption isotherm (at 298 K) of complex showed type **III** behaviour. The volume uptake of water is 15.6 cm^3/g (Fig. 4). Complex **1** also adsorbs 12.9 cm^3/g methanol and 6.24 cm^3/g ethanol (Fig. 4). Small amount of adsorption may be interpreted as that due to interpenetration very narrow channels were created within the framework or surface adsorption [34]. Desorption curve does not coincide with the adsorption curve in all cases, showing a hysteresis loop and incomplete desorption. A very little amount of water, methanol and ethanol remains within the framework. Small hysteresis in the water adsorption isotherm is probably because of trapping by the coordinatively unsaturated metal sites.

Photoluminescence: Photoluminescence property of complex **1** was performed at room temperature in solid state. The emission spectra of both 1,10-phen ligand and complex **1** are shown in

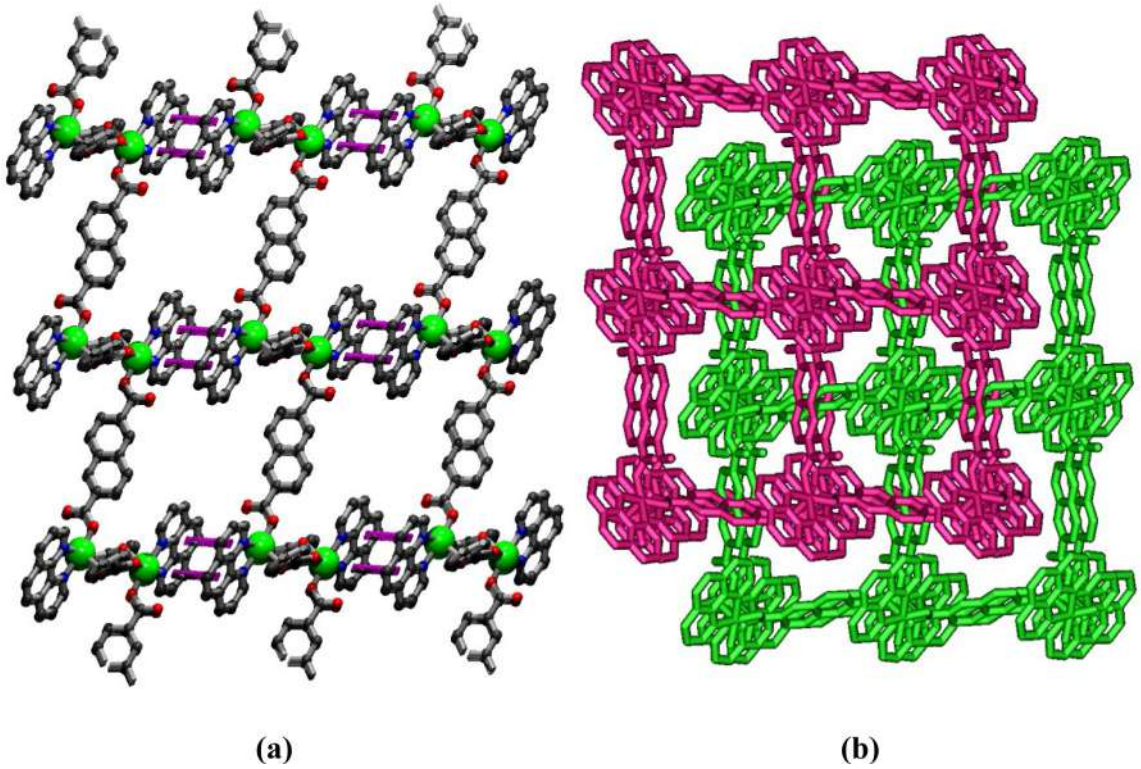

Fig. 1. $\pi \ldots \pi$ (magenta) conjugated 3D supramolecular structure (a) and 2-fold interpenetration (b) of complex **1**. (For interpretation of the references to colour in this figure legend, the reader is referred to the web version of this article.)

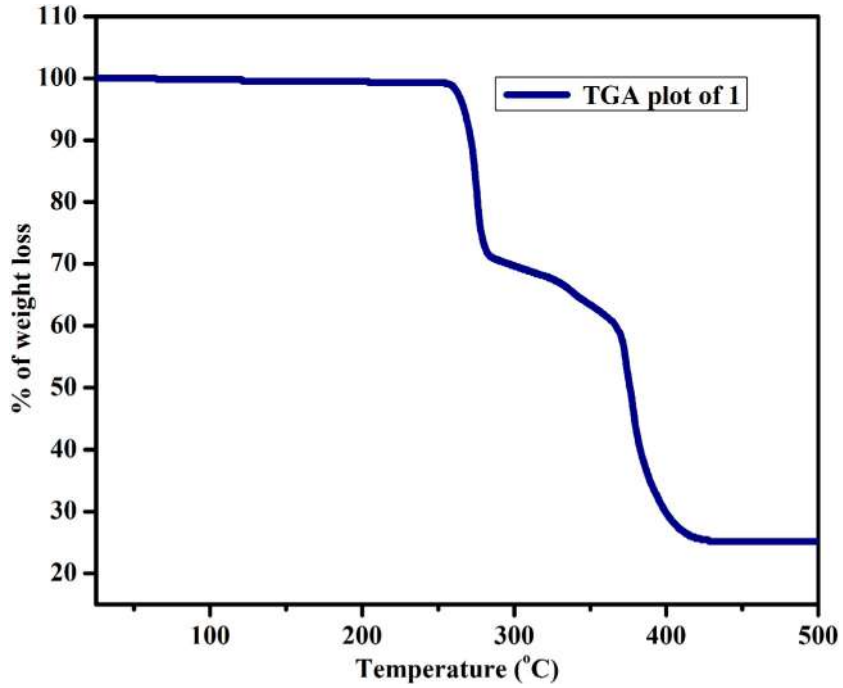

Fig. 2. The thermal plot of complex **1**.

Figure S9. The luminescence spectra of 1,10-phen ligand show two peaks at 412 nm and 434 nm with a shoulder at 461 nm. The spectra arise due to π-π^* transition. The luminescence spectra of complex 1 show similar pattern — the spectra contain two peaks at 414 nm and 434 nm with three different shoulders at 458 nm, 464 nm and 468 nm. The spectra arise due to both intra-ligand π-π^* transition and M-L charge transfer transition. So due to metal complex formation, a small red shift occurs.

Synthesis and Characterization of CuO-NPs: Nano-particles are highly interesting as their properties are critically dependent on synthetic condition, size distribution, morphology and shape.

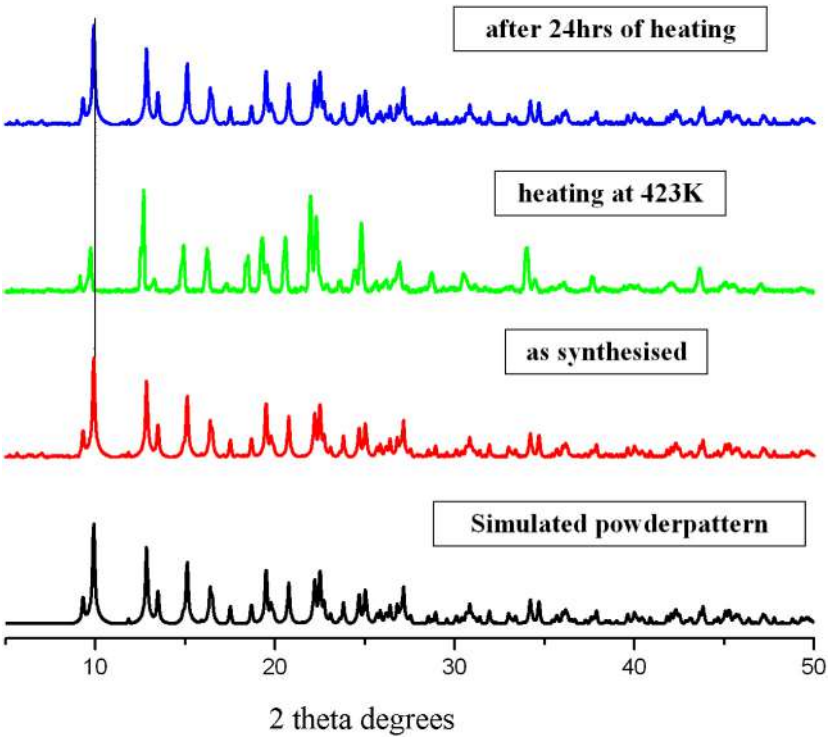

Fig. 3. Variable temperature PXRD pattern of **complex 1**.

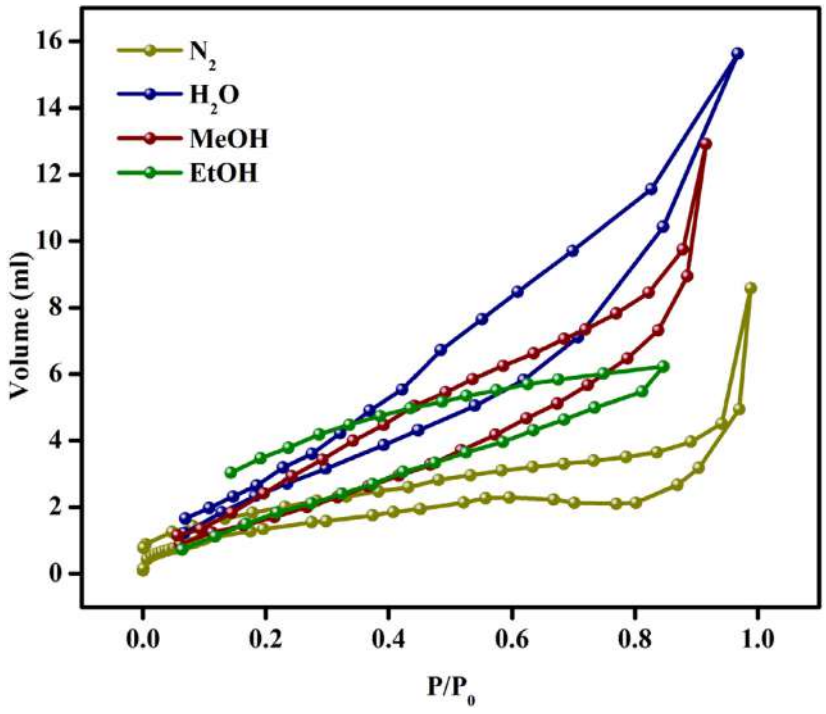

Fig. 4. Gas and solvent sorption behaviour of complex **1**.

CuO-NPs have great potential for their applications in electrochemical cells, magnetic storage media, photovoltaic cells, etc. Here, the 2D-MOF is used as a template to synthesize CuO-NPs by calcinations. The bulk material of the MOF was heated at 650 °C for 4 h at normal condition. Upon heating, the green coloured compound turned in black powder, which was characterized by PXRD, EDS, IR, TEM and SEM analyses. IR spectra of the CuO-Nps are presented in Figure S10. The PXRD pattern matches with the reported PXRD pattern of CuO with JCPDS No. 08-0234 (Fig. 5a). The TEM micrograph indicated the spherical morphology of the synthesized NPs (Fig. 5b) with average size of ∼25 nm and this corroborates with the PXRD data. EDS study indicated the presence of characteristic peaks for the constituents (Cu and O) (Figure S11). The Cu $2p_{3/2}$ core-level spectra (Fig. 6) have been studied to know the oxidation state of Cu present in the copper oxide nanoparticles. The binding energy position of the

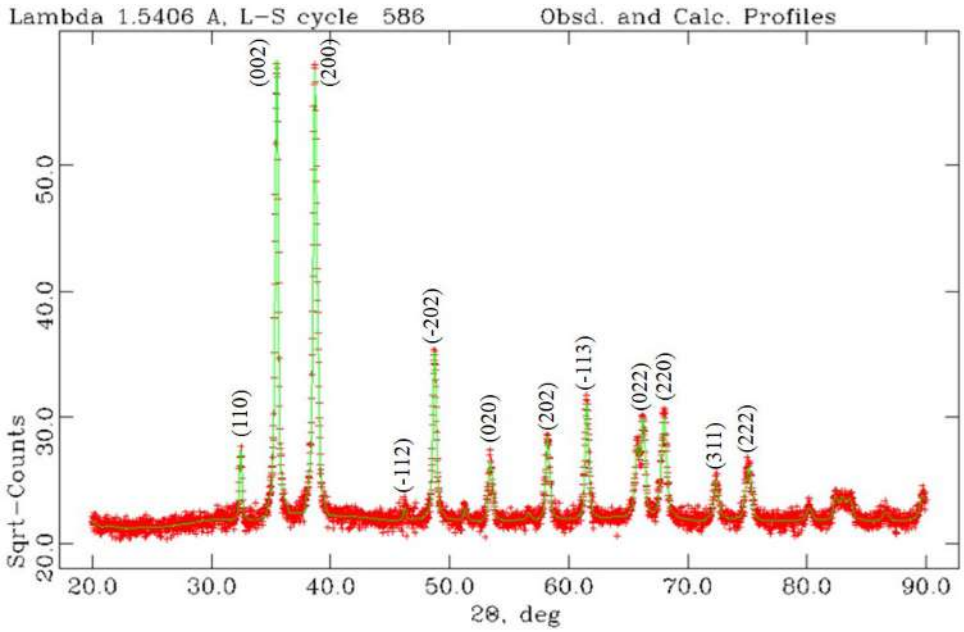

(a)

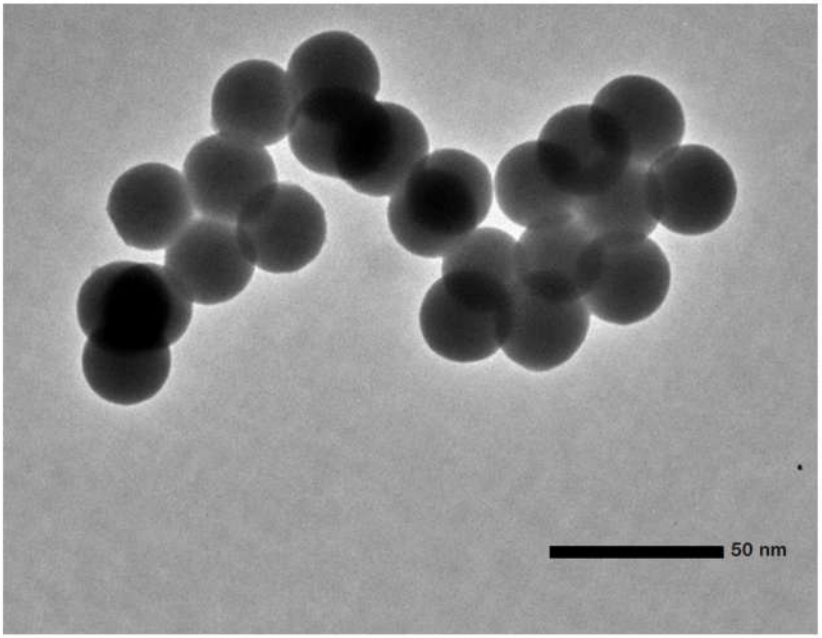

(b)

Fig. 5. PXRD pattern (a) and TEM image (b) of the synthesized CuO-NPs.

main peak in the spectra was observed at around 933.7 eV that informs about the presence of Cu^{2+} species, which was observed previously by many people [35]. The strong shake-up satellite observed in these spectra is also an indication of the presence of Cu^{2+} species that was mentioned by many authors previously [35]. So, the Cu $2p_{3/2}$ core-level spectra confirm that the Cu present in this copper nanoparticles sample is mostly in the Cu^{2+} oxidation state.

Green Catalytic C-X Hetero-coupling Reactions: In the present work, the synthesized spherical shaped CuO-NPs are used for the catalytic cross-coupling (C–O and C–S) reactions of alcohols and thiols with arylhalides. Generally, for such C–O and C–S cross-coupling reactions, high boiling solvents like DMSO, DMF, NMP, etc. are required in both homogeneous and heterogeneous conditions. And consequently, separation of products from these solvents becomes very difficult and tedious. Here, we are going to report a solvent free, neat reaction protocol for such hetero-coupling reactions of phenol, thiophenol, alcohol, and thiols with aryl halides.

Literature review indicates that in previous studies of copper-catalyzed hetero-coupling reactions, *N*-methylpyrrolidinone (NMP), dimethylformamide (DMF), dimethylsulfoxide (DMSO)

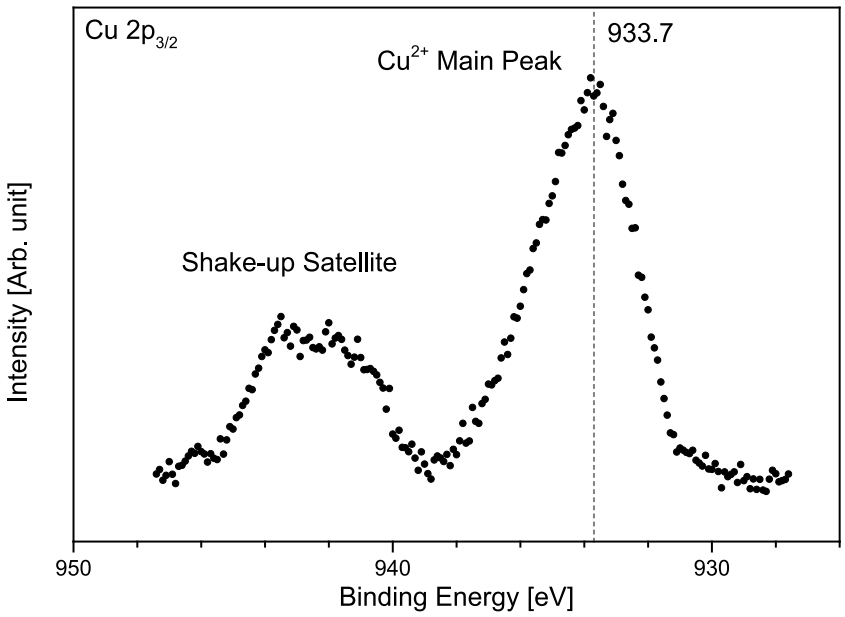

Fig. 6. XPS data of CuO-NPs reveals the presence of only Cu^{2+} ions.

etc. are used as solvent with KOH and K_2CO_3 as base [36] and, thus here, we have also followed the same protocol initially. Punniyamurthi et al. have carried out the C-X (X = S, N and O) hetero-coupling catalytic reactions using CuO-NPs in DMSO [36d]. Here, catalytic activity of the synthesized CuO-NPs was first investigated for the cross-coupling of iodobenzene with phenol and latter with thiophenol. The reactions of chlorobenzene, bromobenzene, phenyltosylate, and phenylboronic acid are studied, but those are found to be inferior to that of aryl iodides. Catalytic tests were also performed with CuCl, CuBr and CuI, freshly prepared before use, provided the same results as obtained with synthesized CuO-NPs. Other Cu(II) salts tested ($CuBr_2$, $CuSO_4 \cdot 5H_2O$, $CuCl_2$) were found to be less efficient catalysts (yields 55%–69%) than the CuO-NPs. A low amount of 2.5 mol % of CuO-NPs was employed in these initial standardization reactions. Our first goal was to optimize reaction conditions and to achieve information about the role of additives and solvent polarity. It appeared that, by applying KOH as base in DMF, diphenylether was obtained in quantitative yield in presence of 20 mol% CuO-NPs catalyst without the use of added ligands. Solvent polarity has significant impact on the yield of the reactions (Table S5) – high polarity solvents like DMF, DMA and NMP show better yield than toluene (entries 3–5). It is noteworthy that very low yield (40%) was obtained for using water as solvent (Table S5, entry 6). Now, difficulty in separation of these solvents from the product prompted us to choose the neat reaction conditions (Table S5, entry 7). And interestingly, we have found that the yield of neat reaction conditions are similar to that in DMF, DMA and NMP and then we decided to go further with the neat reaction conditions.

Similarly, a series of bases were also screened. Among inorganic bases, KOH gave almost quantitative results for the coupling reaction to diphenylethers (Table S6), while, among organic bases, triethylamine and Hunig's base (DIPEA) gave also good results (Table S6, entries 2 and 3) in heterogeneous reaction mixture. Notably, in our case the required amount for the base is only one equiv. (based on the aryl halide), while in common reports this is usually in between 1.5 and 2.5 equiv. Further experiments were performed to find the optimal reaction temperature and reaction time. Both Tables S5 and S6 refer to around 17 h reaction with temperature of 100 °C. It was noted that a small decrease in temperature of only 10 °C caused a significant decrease in diaryl thioether yield (85%). Lowering the time of the reaction in the present conditions also decreases the yield of the desired products. Accordingly, at 100 °C, the reaction of iodobenzene with phenol is relatively fast (65 and 95% after 2 and 6 h, respectively). It also appeared that fluoro-, chloro-, and bromobenzene are very less reactive under the optimized conditions, giving extremely lower yields (4%–55%) of the C–O coupling products (Table S7). Aryltosylate and boronic acids are also very less effective compared to that of iodide (Table S7, entries 5 & 6). Finally, the effect of the copper catalyst and its loading amount was evaluated. As discussed earlier and shown in Table S8, Cu(II) catalysts performed badly (Table S8, entries 1–4, yields 55%–69%). Only a minor difference in yields were observed when catalytic activity of CuO-NPs was compared with Cu(I) salts (Table S8, entries 5–8). The desired products are purified by column chromatography, identified by NMR spectra and then the isolated yield was calculated.

Table 1
Reaction of Aryl Iodides with Phenol and Thiophenol (conditions: phenol or thiophenol (25 mmol), aryl iodide (5 mmol), KOH (5 mmol), CuO (2.5 mol%), 100 °C, 17 h.

Entry	Aryl iodide	Alcohol or thiol	Product	Yield (%)
1	PhI	PhOH	Ph-O-Ph	99
2	PhI	PhSH	Ph-S-Ph	99
3	PhI	$PhCH_2OH$	$PhCH_2$-O-Ph	95
4	PhI	$PhCH_2SH$	$PhCH_2$-S-Ph	95

To determine the scope of the catalytic system, the present protocol was further applied to reactions of a variety of commercially available aryl iodides and phenols or thiophenols (Table 1). As shown in Table 1, the coupling of phenol and thiophenol with iodobenzene was successful, leading to the desired products in good yields. The protocol is equally efficient for aromatic and aliphatic phenols and thiophenols. The catalyst system is highly efficient providing the corresponding diaryl ethers and thioethers in good to excellent yields. Iodobenzene was maintained as arylating substrate. The present optimized catalytic process provides the arylation of phenols and thiophenols with aryl iodides, in the presence of KOH as a base under neat conditions. To the best of our knowledge, this is the first report about aryl-sulphur and aryl-oxygen bond formation in which a MOF derived CuO-NPs catalyst

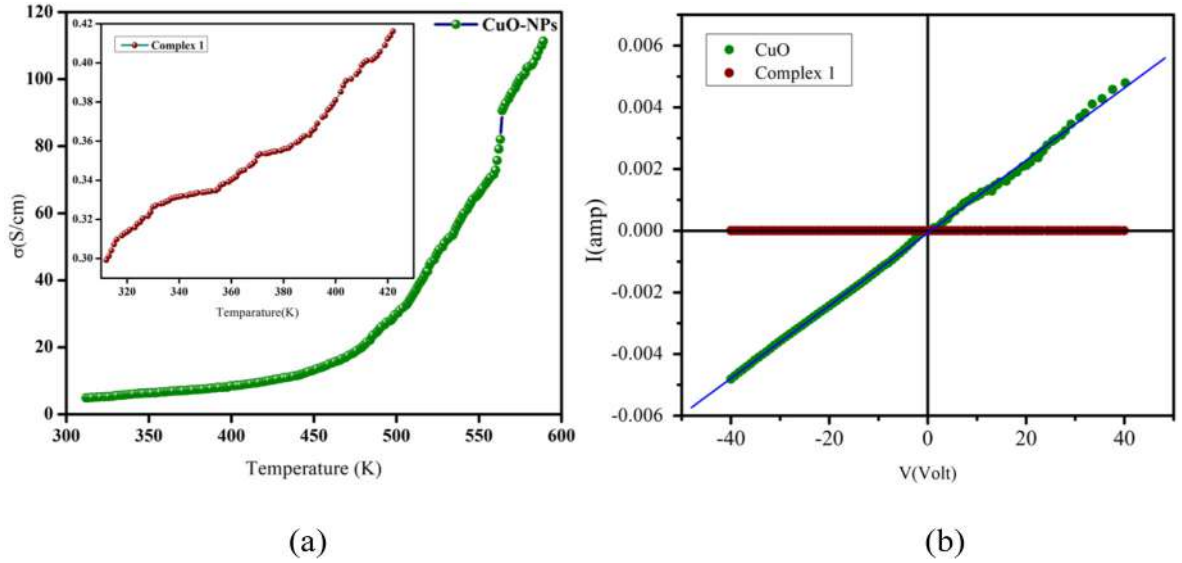

Fig. 7. Variable temperature electrical conductivity and corresponding I–V curve of the both complex **1** and MOF derived NPs.

is used without addition of any ligand and solvent. In the present study diphenylether and diphenylthioether was formed in 99% yield in the reaction of iodobenzene with phenol and thiophenol in solvent free neat conditions.

The CuO nanoparticles are recyclable upto 5th cycle without loss of significant reactivity (Table S9). After completion of the C–O cross-coupling of phenol with iodobenzene, the reaction mixture was treated with diethyl ether. Then, the overall mixture was centrifuged to isolate the catalyst. After isolation, it was washed with water and ether repeatedly and then dried for further use (Figure S13). The reusability tests indicate high yield. A comparative study with the bulk CuO synthesized by precipitation method was also studied – a lower amount of yield (∼40%–55%) was obtained for CuO bulk.

The catalytic activity of our synthesized CuO-NPs was investigated for the cross-coupling of iodobenzene with phenol and compared with similar heterogeneous catalysts (Table S10). Unlike homogeneous catalyst, use of heterogeneous catalyst is much more advantageous in terms of their easy separation, recyclability, high thermal stability and longer lifetime. In this respect, based on literature and availability of the heterogeneous catalysts, the reactivity of ZnO, SnO, SnO_2, CuO, Cu_2O and CuO NPs/SiO_2 [37] has been judged and compared with respect to C–O coupling reaction of phenol and iodobenzene. Our synthesized CuO is found to be most effective with respect to yield of the desired coupling product. Heterogeneous catalysts other than CuO and Cu_2O found to be completely ineffective giving no yield of the desired C–O coupling product (entries 1–3).

A suitable mechanistic pathway for the above-mentioned catalysis reactions was proposed (Scheme S1). These results suggest that the reaction may occur by oxidative addition followed by reductive elimination. The oxidative addition of the aryl halide with catalyst can give intermediate **A**, which can undergo reaction with an alcohol or thiol to afford intermediate **B**. Intermediate **B** can provide the C–O or C–S cross coupling product by reductive elimination. According to Sambiagio et al. the mechanism of such reactions is still unclear and it is considered that the mechanism actually varies depending on the substrate, ligand and reaction conditions [22b]. It is believed that the most active catalyst is Cu(I)-species which may form from the initial copper source.

Electrical Conductivity of MOF and MOF derived CuO-NPs: In complex **1**, the coordination between the metal centres and ndc^{2-} ligands forms 2D coordination layers and coordinated 1,10-phen moieties are hanging from the layers to connect next to neighbouring layers through $\pi \ldots \pi$ interaction to form 3D supramolecular structure. Due to the presence of extended $\pi \ldots \pi$ conjugation within the structure of **1**, we hope that the framework may show electrical conductivity. Bulk electrical conductivity of complex **1** has been measured by four probe contact using Ag wire on the pressed pellets. The conductivity of complex **1** is 3 x 10^{-3} S/cm at 312 K with Ohomic behaviour within the range of ± 40 V, Fig. 7(a and b). Variable temperature conductivity measurement within the temperature range of 312 K to 423 K indicates that with increasing temperature, conductivity of the framework increases — the framework is semiconducting in nature. The conductivity value is 4.2 × 10^{-3} S/cm at 423 K. With increasing temperature, delocalization of π-electrons increases and this may be a reason behind the linear rise in conductivity value electrical conductivity. The calculated activation energy of the framework is 0.077 eV.

Koo et al. have reported a semiconductive metal–organic framework having 2,5,8-tri(4-pyridyl)1,3-diazaphenalene as the π-conjugated ligand. Single crystal electrical conductivity measurement gives a value of ∼1 x 10^{-6} S/cm [12a]. Kuang et al. have reported single crystal conductivity value of ∼1.2 × 10^{-5} S/cm of a framework having napthalenediimide [12b]. Haider et al. have measured conductivity on the single crystal of a framework containing 1,4,5,8-naphthalenetetracarboxylate and the framework shows conductivity of ∼10^{-4} S/cm [12c]. Chen et al. have reported the semiconducting behaviour of mixed metal MOF in which 4,4′-(anthracene-9,10-diylbis(ethyne-2,1-diyl))dibenzoate is used to induce $\pi \ldots \pi$ interaction within the framework at separation distance of 3.4 Å [12d]. Electrical conductivity measurement on single crystals gives a conductivity value of 1.3 × 10^{-3} S/cm. Qu et al. have measured electrical conductivity of a metal–organic framework containing N,N′-di(4-pyridyl)-1,4,5,8-naphthalenetetracarbox-diimide on both single crystal and pressed pellets [12e]. Single crystal conductivity measurement showed 10^3 times higher conductivity (3.3 × 10^{-3} S/cm) than measured on the pressed pellets (7.6 × 10^{-6} S/cm). In our case, four probe electrical conductivity measurement on the pressed pellet of complex **1** gives a value of 3 x 10^{-3} S/cm at 312 K.

We have also studied the electrical conductivity of the MOF derived CuO-NPs in a similar manner. CuO is a p-type semiconductor but the bandgap and electrical conductivity vary with

the size and morphology of the nano-particles [38]. In most cases, the bandgap of CuO-NPs varies in the range of 1.2 to 2.0 eV and, based on its narrow bandgap, CuO-NPs have significant applications in electronic and opto-electronics. The conductivity of the MOF derived CuO-NPs is 4.85 $\times$ 10^{-2} S/cm with similar Ohomic behaviour at 312 K and this conductivity value is 16 times higher than the parent MOF, Fig. 7a and b. Combustion of the organic moieties within the MOF leads to the occurrence of charge transfer interaction between the copper and oxygen atoms within the framework and this may be the reason behind this enhanced conductivity. The variable temperature conductivity of the NPs is measured within the range of 312 to 588 K and the CuO-NPs also show semiconducting behaviour. The conductivity value rises smoothly up to 430 K (11 x 10^{-2} S/cm) and afterwards increases very rapidly to 1.11 S/cm at 588 K. A plot of $\ln(\sigma)$ vs. 1000/T for CuO-NPs shows two linear portions intersecting each other (Figure S14). This indicates the presence of two activation energy of CuO and values are 73 and 370 meV respectively, with a crossover at 430 K. The comparatively small activation energy indicates that Cu(I) and Cu(0) in association with oxygen vacancies may be present in CuO-Nps [16a]. Change of activation energy with temperature may be due to the presence of any metastable state in the sample.

4. Conclusions

Single crystal X-ray analysis of complex 1 revealed two types of binding modes (μ2- and μ4-) of ndc^{2-} ligands to the central Cu(II) ions, which, in turn, resulted in the formation of 2D coordination sheet. While the hanging 1,10-phenanthroline ligands in the interlamellar space assembled together by π-π interactions, which led to the formation of spongy 3D supramolecular metal–organic framework (MOF). Careful analysis of the MOF, which was stable up to 260 °C, depicted the presence of interpenetrated network topology. Reversible structural transformation of the framework by gliding motion of π-π stacked 1,10-phenanthroline ligands along the crystallographic *a*-axis and hence reversible expansion and contraction among the layer gap of 2D coordination sheets was confirmed by variable temperature PXRD measurements. Adsorption studies of the MOF with water, methanol and ethanol depicted a hysteresis loop in adsorption/desorption cycle. After thorough characterization of the MOF, it was calcinated at 650 °C for 4 h to fabricate CuO-NPs. The PXRD patterns confirmed the formation of CuO-NPs. While microscopic images showed formation of nearly uniform CuO-NPs with an average size of ~25 nm. Electrical conductivity measurements of the MOF and MOF derived CuO-NPs suggested both of them are semiconducting nature. However, CuO-NPs were found to be far more conducting compared to the parent MOF. Further, selective and efficient CuO-NPs catalyzed C–O and C–S bond-forming reaction of aryl iodides and various thiophenols is developed. This catalytic procedure offers general applicability and simplicity, avoiding the expensive and time-consuming preparation of suitable ligands and activated substrates. Based on controlled experiments and green chemistry rules, we proposed a solvent free, neat reaction conditions. Because of these advantages, we strongly believe that the protocol demonstrated in this work could find large application. And, we hope that such MOF derived nano-particle synthesis technique may be used for the synthesis of different types of metal–oxide nano-materials like ZnO, Cr_2O_3, VO_2, rare earth oxides.

CRediT authorship contribution statement

Maxcimilan Patra: Synthesized the materials and carried out most of the experiments, Writing manuscript. **Soumen Kumar Dubey:** Synthesized the materials and carried out most of the experiments, Writing manuscript. **Bibhas Mondal:** Carried out all the catalysis experiments, Written the manuscript. **Kajal Gupta:** Carried out all the electrical conductivity measurements, Written the manuscript. **Angshuman Ghosh:** Carried out several characterizations like NMR, IR, Manuscript preparation. **Subhankar Mandal:** Carried out the XPS measurement, Manuscript preparation. **Satyajit Hazra:** Carried out the XPS measurement, Manuscript preparation. **Ajit Kumar Meikap:** Carried out all the electrical conductivity measurements, Written the manuscript. **Ujjal Kanti Roy:** Carried out all the catalysis experiments, Written the manuscript. **Subham Bhattacharjee:** Idea of this research project was drawn, Manuscript preparation. **Rajat Saha:** Idea of this research project was drawn, Manuscript preparation.

Declaration of competing interest

The authors declare that they have no known competing financial interests or personal relationships that could have appeared to influence the work reported in this paper.

Acknowledgements

This work was supported by funding from TARE, SERB to R. S. (TAR/2018/000744) and DST Inspire Faculty Research Grant to S.B. (Faculty Registration No.: IFA18-CH304, DST/INSPIRE/04/2018/000329). U.K.R. acknowledges financial support of this work by SERB New Delhi, SR/FT/CS-137/2011 dated 12.07.2012, and Science and Technology and Biotechnology-WB, 50 (Sanc.)/ST/P/S&T/15G-10/2018 dated 30.01.2019 to UKR is gratefully acknowledged. M. P. and S. K. D. thank DST Inspire Faculty Research Grant for financial assistance. The authors thank Goutam Sarkar for his technical support in XPS measurements. S. M. acknowledges the Council of Scientific & Industrial Research (CSIR), India for providing a research fellowship.

Appendix A. Supplementary data

Supplementary material related to this article can be found online at https://doi.org/10.1016/j.nanoso.2021.100756. The CCDC number is 2013885 for complex 1. Figure S1–S9, Table S1–S8, NMR spectra and catalytic mechanism scheme are given in Supporting information file.

References

[1] (a) H. Furukawa, K.E. Cordova, M. O'Keeffe, O.M. Yaghi, The chemistry and applications of metal-organic frameworks, Science 341 (2013) 1230444.
(b) R. Chakraborty, P.S. Mukherjee, P.J. Stang, Supramolecular coordination: self-assembly of finite two- and three-dimensional ensembles, Chem. Rev. 111 (2011) 6810.
(c) T.K. Maji, R. Matsuda, S. Kitagawa, A flexible interpenetrating coordination framework with a bimodal porous functionality, Nat. Mater. 6 (2007) 142.
(d) J.A. Mason, M. Veenstra, J.R. Long, Evaluating metal-organic frameworks for natural gas storage, Chem. Sci. 5 (2014) 32.
(e) J.-R. Li, R.J. Kuppler, H.-C. Zhou, Selective gas adsorption and separation in metal-organic frameworks, Chem. Soc. Rev. 38 (2009) 1477.
(f) A. Corma, H. García, F.X.L. Xamena, Engineering metal organic frameworks for heterogeneous catalysis, Chem. Rev. 110 (2010) 4606.
(g) J.L.C. Rowsell, O.M. Yaghi, Metal-organic frameworks: a new class of porous materials, Microporous Mesoporous Mater. 73 (2004) 3.
(h) S. Kitagawa, R. Kitaura, S. Noro, Functional porous coordination polymers, Angew. Chem. Int. Ed. 43 (2004) 2334.

(i) W.P. Lustig, S. Mukherjee, N.D. Rudd, A.V. Desai, J. Li, S.K. Ghosh, Metal–organic frameworks: functional luminescent and photonic materials for sensing applications, Chem. Soc. Rev. 46 (2017) 3242.
(j) A.M. Al-Enizi, J. Ahmed, M. Ubaidullah, S.F. Shaikh, T. Ahamad, M. Naushad, G. Zheng, Utilization of waste polyethylene terephthalate bottles to develop metal–organic frameworks for energy applications: A clean and feasible approach, J. Clean. Prod. 248 (2020) 119251.
(k) A.M. Al-Enizi, M. Ubaidullah, J. Ahmed, T. Ahamad, T. Ahmad, S.F. Shaikh, M. Naushad, Synthesis of niox@ npc composite for high-performance supercapacitor via waste pet plastic-derived ni-mof, Compos. B. Eng. 183 (2020) 107655.
(l) M. Ubaidullah, J. Ahmed, T. Ahamad, S.F. Shaikh, S.M. Alshehri, A.M. Al-Enizi, Hydrothermal synthesis of novel nickel oxide@ nitrogenous mesoporous carbon nanocomposite using costless smoked cigarette filter for high performance supercapacitor, Mater. Lett. 266 (2020) 127492.
(m) N. Bakhtiari, S. Azizian, S.M. Alshehri, N.L. Torad, V. Malgras, Y. Yamauchi, Study on adsorption of copper ion from aqueous solution by mof-derived nanoporous carbon, Microporous Mesoporous Mater. 217 (2015) 173–177.
(n) H. Zhang, M. Zhang, M.V. Lin Ping, J. Tang, S.M. Alshehri, Y. Yusuke, D. Shaowu, J. Zhang, A highly energetic n-rich metal-organic framework as a new high-energy-density, Material. Chem. Eur. J. 22 (2015) 1141–1145.

[2] (a) N. Nidamanuri, K. Maity, S. Saha, Electrically conductive metal-organic frameworks, in: Book Chapter, World Scientific Publishing, 2017.
(b) V. Stavila, A.A. Talin, M.D. Allendorf, Mof based electronic and opto-electronic devices, Chem. Soc. Rev. 43 (2014) 5994.

[3] (a) E.M. Miner, T. Fukushima, D. Sheberla, L. Sun, Y. Surendranath, M. Dincă, Electrochemical oxygen reduction catalysed by Ni_3(Hexaiminotriphenylene)$_2$, Nature Commun. 7 (2016) 10942.
(b) M.G. Campbell, D. Sheberla, S.F. Liu, T.M. Swager, M. Dincă, Cu_3(Hexaiminotriphenylene)$_2$: An electrically conductive 2D metal-organic framework for chemiresistive sensing, Angew. Chem. Int. Ed. 54 (2015) 4349.
(c) J. Park, M. Lee, D. Feng, Z. Huang, A.C. Hinckley, A. Yakovenko, X. Zou, Y. Cui, Z. Bao, Stabilization of hexaaminobenzene in a 2D conductive metal-organic framework for high power sodium storage, J. Am. Chem. Soc. 140 (2018) 10315.
(d) S. Roy, M. Das, A. Bandyopadhyay, S.K. Pati, P.P. Ray, T.K. Maji, Colossal increase in electric current and high rectification ratio in a photoconducting, self-cleaning, and luminescent schottky barrier nmof diode, J. Phys. Chem. C 121 (2017) 23803.
(e) S.S. Shinde, C.H. Lee, J.-Y. Jung, N.K. Wagh, S.-H. Kim, D.-H. Kim, C. Lin, S.U. Lee, J.-H. Lee, Unveiling Dual-Linkage 3D Hexaiminobenzene Metal-Organic Frameworks towards Long-Lasting Advanced Reversible Zn-Air Batteries. Energy Environ. Sci. 12 (2019) 727.
(f) D. Feng, T. Lei, M.R. Lukatskaya, J. Park, Z. Huang, M. Lee, L. Shaw, S. Chen, A.A. Yakovenko, A. Kulkarni, J. Xiao, K. Fredrickson, J.B. Tok, X. Zou, Y. Cui, Z. Bao, Robust and conductive two-dimensional metal-organic frameworks with exceptionally high volumetric and areal capacitance, Nat. Energy 3 (2018) 30.
(g) D. Sheberla, J.C. Bachman, J.S. Elias, C.-J. Sun, Y. Shao-Horn, M. Dinca, Conductive MOF electrodes for stable supercapacitors with high areal capacitance, Nat. Mater. 16 (2017) 220.
(h) X. Huang, S. Zhang, L. Liu, L. Yu, G. Chen, W. Xu, D. Zhu, Superconductivity in a copper(ii) based coordination polymer with perfect kagome structure, Angew. Chem. Int. Ed. 57 (2018) 146.

[4] (a) S. Takaishi, M. Hosoda, T. Kajiwara, H. Miyasaka, M. Yamashita, Y. Nakanishi, Y. Kitagawa, K. Yamaguchi, A. Kobayashi, H. Kitagawa, Electroconductive porous coordination polymer Cu[Cu(Pdt)$_2$] composed of donor and acceptor building units, Inorg. Chem. 48 (2009) 9048.
(b) Y. Kobayashi, B. Jacobs, M.D. Allendorf, J.R. Long, Conductivity, doping, and redox chemistry of a microporous dithiolene-based metal-organic framework, Chem. Mater. 22 (2010) 4120.

[5] (a) M.E. Ziebel, L.E. Darago, J.R. Long, Control of electronic structure and conductivity in two-dimensional metal-semiquinoid frameworks of titanium, vanadium, and chromium, J. Am. Chem. Soc. 140 (2018) 3040.
(b) S. Benmansour, A. Abhervé, P. Gómez-Claramunt, C. Vallés- García, C.J. Gómez-García, Nanosheets of two-dimensional magnetic and conducting Fe(II)/Fe(III) mixed-valence metal-organic frameworks, ACS Appl. Mater. Interfaces 9 (2017) 26210.
(c) J.A. DeGayner, I.-R. Jeon, L. Sun, M. Dincă, T.D. Harris, 2D conductive iron-quinoid magnets ordering up to T_c = 105 K via heterogenous redox chemistry, J. Am. Chem. Soc. 139 (2017) 4175.

[6] (a) M.-H. Zeng, Q.-X. Wang, Y.-X. Tan, S. Hu, H.-X. Zhao, L.-S. Long, M. Kurmoo, Rigid pillars and double walls in a porous metal-organic framework: Single-crystal to single-crystal, controlled uptake and release of iodine and electrical conductivity, J. Am. Chem. Soc. 132 (2010) 2561.
(b) X. Zhang, I. da Silva, R. Fazzi, A.M. Sheveleva, X. Han, B.F. Spencer, S.A. Sapchenko, F. Tuna, E.J.L. McInnes, M. Li, S. Yang, M. Schröder, Iodine adsorption in a redox-active metal-organic framework: electrical conductivity induced by host-guest charge-transfer, Inorg. Chem. 58 (2019) 14145.

[7] (a) A.A. Talin, A. Centrone, A.C. Ford, M.E. Foster, V. Stavila, P. Haney, R.A. Kinney, V. Szalai, F.E. Gabaly, H.P. Yoon, F. Léonard, M.D. Allendorf, Tunable electrical conductivity in metal-organic framework thin-film devices, Science 343 (2014) 66.
(b) C. Schneider, D. Ukaj, R. Koerver, A.A. Talin, G. Kieslich, S.P. Pujari, H. Zuilhof, J. Janek, M.D. Allendorf, R.A. Fischer, High electrical conductivity and high porosity in a Guest@MOF Material: Evidence of TCNQ Ordering within Cu_3BTC_2, Micropores. Chem. Sci. 9 (2018) 7405.

[8] J.G. Park, M.L. Aubrey, J. Oktawiec, K. Chakarawet, L.E. Darago, F. Grandjean, G.J. Long, J.R. Long, Charge delocalization and bulk electronic conductivity in the mixed- valence metal-organic framework Fe(1, 2, 3-Triazolate)$_2$(BF_4)$_x$, J. Am. Chem. Soc. 140 (2018) 8526.

[9] (a) L.S. Xie, G. Skorupskii, M. Dinca, Electrically conductive metal-organic frameworks, Chem. Rev. 120 (2020) 8536–8580.
(b) X. Kuang, S. Chen, L. Meng, J. Chen, X. Wu, G. Zhang, G. Zhong, T. Hu, Y. Li, C.-Z. Lu, Chem. Commun. 55 (2019) 1643–1646.

[10] (a) L. Sun, T. Miyakai, S. Seki, M. Dincă, Mn_2(2, 5-disulfhydrylbenzene-1, 4-dicarboxylate): A microporous metal-organic framework with infinite (-Mn-S-)∞ chains and high intrinsic charge mobility, J. Am. Chem. Soc. 135 (2013) 8185.
(b) F. Gándara, F.J. Uribe-Romo, D.K. Britt, H. Furukawa, L. Lei, R. Cheng, X. Duan, M. O'Keeffe, O.M. Yaghi, Porous, conductive metal-triazolates and their structural elucidation by the charge-flipping method, Chem. Eur. J. 18 (2012) 10595.

[11] L. Liu, J.A. DeGayner, L. Sun, D.Z. Zee, T.D. Harris, Reversible redox switching of magnetic order and electrical conductivity in a 2D manganese benzoquinoid framework, Chem. Sci. 10 (2019) 4652.

[12] (a) J.Y. Koo, Y. Yakiyama, G.R. Lee, J. Lee, H.C. Choi, Y. Morita, M. Kawano, Selective formation of conductive network by radical-induced oxidation, J. Am. Chem. Soc. 138 (2016) 1776.
(b) X. Kuang, S. Chen, L. Meng, J. Chen, X. Wu, G. Zhang, G. Zhong, T. Hu, Y. Li, C.-Z. Lu, Supramolecular aggregation of a redox-active copper-naphthalenediimide network with intrinsic electron conduction, Chem. Commun. 55 (2019) 1643.
(c) G. Haider, M. Usman, T.-P. Chen, P. Perumal, K.-L. Lu, Y.-F. Chen, Electrically driven white light emission from intrinsic metal-organic framework, ACS Nano 10 (2016) 8366.
(d) D. Chen, H. Xing, Z. Su, C. Wang, Electrical conductivity and electroluminescence of a new anthracene-based metal-organic framework with π-conjugated zigzag chains, Chem. Commun. 52 (2016) 2019.
(e) L. Qu, H. Iguchi, S. Takaishi, F. Habib, C.F. Leong, D.M. D'Alessandro, T. Yoshida, H. Abe, E. Nishibori, M. Yamashita, Porous molecular conductor: electrochemical fabrication of through-space conduction pathways among linear coordination polymers, J. Am. Chem. Soc. 141 (2019) 6802.

[13] S.S. Park, E.R. Hontz, L. Sun, C.H. Hendon, A. Walsh, T. Van Voorhis, M. Dincă, Cation-dependent intrinsic electrical conductivity in isostructural tetrathiafulvalene-based microporous metal-organic frameworks, J. Am. Chem. Soc. 137 (2015) 1774.

[14] P.I. Scheurle, A. Mähringer, A.C. Jakowetz, P. Hosseini, A.F. Richter, G. Wittstock, D.D. Medina, T. Bein, A highly crystalline anthracene-based MOF-74 series featuring electrical conductivity and luminescence, Nanoscale 11 (2019) 20949.

[15] J.K. Sun, Q. Xu, Functional materials derived from open framework templates/precusros: Synthesis and applications, Energy Environ. Sci. 7 (2014) 2071.

[16] (a) R. Das, P. Pachfule, R. Banerjee, P. Poddar, Metal and metal oxide nanoparticles synthesis from metal organic frameworks (MOFs): finding the border of metal and metal oxides, Nanoscale 4 (2012) 591.
(b) S. Singha, A. Saha, S. Goswami, S.K. Dey, S. Payra, S. Banerjee, S. Kumar, R. Saha, A metal organic framework to CuO nanospheres of uniform morphologyfor synthesis of α-aminonitriles under solvent-free conditions along with crystal structure of the MOF, Cry. Growth Des. 18 (2018) 189.
(c) S. Ekambaram, K.C. Patil, M. Maaza, Synthesis of lamp phosphors: facile combustion approach, J. Alloys Compd. 393 (2005) 81-92.
(d) B.T. Sone, E. Manikandan, A. Gurib-Fakim, M. Maaza, Sm_2o_3 nanoparticles green synthesis via callistemon viminalis' extract, J. Alloys Compd. 650 (2015) 357-362.
(e) S. Khamlich, E. Manikandan, B.D. Ngom, J. Sithole, O. Nemraoui, I. Zorkani, Synthesis, characterization, and growth mechanism of α-cr_2o_3 monodispersed particles, J. Phys. Chem. Solids. 72 (2011) 714-718.
(f) S. Karthik, P. Siva, K.S. Balu, R. Suriyaprabha, V. Rajendran, M. Maaza, Acalypha indica-mediated green synthesis of ZnO nanostructures under differential thermal treatment: effect on textile coating, hydrophobicity, uv resistance, and antibacterial, Adv. Powder Technol. 28 (2017) 3184-3194.

(g) N. Mayedwa, N. Mongwaketsi, S. Khamlich, K. Kaviyarasu, N. Matinise, Green synthesis of nickel oxide, palladium and palladium oxide synthesized via aspalathus linearis natural extracts: physical properties & mechanism of formation, Appl Surf Sci. 446 (2018) 266-272.
(h) H. Guo, T.T. Li, W.W. Chen, L.X. Liu, J.L. Qiao, J. Zhang, Self-assembly formation of hollow Ni-Fe-O nanocage architectures by metal–organic frameworks with high-performance lithium storage, Sci. Rep. 5 (2015) 13310, 5.
(i) H.B. Wu, B.Y. Xia, L. Yu, X.-Y. Yu, X.W. Lou, Porous molybdenum carbide nano-octahedrons synthesized via confined carburization in metal–organic frameworks for efficient hydrogen production, Nature Comm. 6 (2015) 6512, 1.
(j) P. Panchfule, X. Yang, Q. Zhu, N. Tsumori, T. Uchida, Q. Xu, From Ru nanoparticle-encapsulated metal–organic frameworks to highly catalytically active Cu/Ru nanoparticles-embedded porous carbon, J. Mater. Chem. A 5 (2017) 4835.
(k) Z. Liang, C. Qu, D. Xia, R. Zou, Q. Xu, Atomically dispersed metal sites in MOF-based materials for electrocatalytic and photocatalytic energy conversion, Angew. Chem. Int. Ed. 57 (2018) 9604.

[17] (a) R. Dai, W. Sun, Y. Wang, Ultrasmall tin nanodots embedded in nitrogen-doped mesoporous carbon: Metal-organic-framework derivation and electrochemical application as highly stable anode for lithium ion batteries, Electrochim. Acta 217 (2016) 123.
(b) A.C. Nwanya, D. Obi, K.I. Ozoemena, R.U. Osuji, C. Awada, A. Ruediger, M. Maaza, F. Rosei, F.I. Ezema, Facile synthesis of nanosheet-like CuO film and its potential application as a high-performance pseudocapacitor electrode, Electrochimica Acta 198 (2016) 220-230.
(c) B.T. Sone, A. Diallo, X.G. Fuku, A. Gurib-Fakim, M. Maaza, Biosynthesized CuO nano-platelets: physical properties & enhanced thermal conductivity nanofluidics, Arab. J. Chem. 13 (2020) 160-170.
(d) A.C. Nwanya, M.M. Ndipingwi, N. Mayedwa, L.C. Razanamahandry, C.O. Ikpo, Maize (zea mays l.) fresh husk mediated biosynthesis of copper oxides: potentials for pseudo capacitive energy storage, Electrochimica Acta 301 (2019) 436-448.

[18] H. Pang, B. Guan, W. Sun, Y. Wang, Metal-organic-frameworks derivation of mesoporous nio nanorod for high-performance lithium ion batteries, Electrochim. Acta. 213 (2016) 351.

[19] (a) J. Wu, Y. Song, R. Zhou, S. Chen, L. Zuo, H. Hou, L. Wang, Zn–Fe–ZIF-derived porous $ZnFe_2o_4$/C@NCNT nanocomposites as anodes for lithium-ion batteries, J. Mater. Chem. A. 3 (2015) 7793.
(b) W.J. Meng, W. Chen, L. Zhao, Y. Huang, M.S. Zhu, Y. Huang, Y.Q. Fu, F.X. Geng, J. Yu, X.F. Chen, Porous Fe_3O_4/carbon composite electrode material prepared from metal–organic framework template and effect of temperature on its capacitance, Nano Energy 8 (2014) 133.

[20] C.F. Lee, Y.C. Liu, S.S. Badsara, Transition-metal-catalyzed C-S bond coupling reaction, Chem. Asian J. 9 (2014) 706.

[21] (a) S.F. Nielsen, E.O. Nielsen, G.M. Olsen, T. Liljefors, D. Peters, Novel potent ligands for the central nicotinic acetylcholine receptor: Synthesis, receptor binding, and 3D-QSAR analysis, J. Med. Chem. 43 (2000) 2217.
(b) G. De Martino, M.C. Edler, G. La Regina, A. Cosuccia, M.C. Barbera, D. Barrow, R.I. Nicholson, G. Chiosis, A. Brancale, E. Hamel, M. Artico, R. Silvestri, New arylthioindoles: potent inhibitors of tubulin polymerization. 2. structure-activity relationships and molecular modeling studies, J. Med. Chem. 49 (2006) 947.

[22] (a) S.V. Ley, A.W. Thomas, Modern synthetic methods for copper-mediated C(aryl)-O, C(aryl)-N, and C(aryl)-S Bond Formation, Angew. Chem. Int. Ed. 43 (2003) 5400.
(b) C. Sambiagio, S.P. Marsden, A.J. Blacker, P.C. McGowan, Chem. Soc. Rev. 43 (2014) 3525-3550.

[23] T. Punniyamurthy, L. Rout, Recent advances in copper-catalyzed oxidation of organic compounds, Coord. Chem. Rev. 252 (2008) 134.

[24] (a) K.E. Torraca, X. Huang, C.A. Parrish, S.L. Buchwald, An efficient intermolecular palladium-catalyzed synthesis of aryl ethers, J. Am. Chem. Soc. 123 (2001) 10770.
(b) J. Mondal, A. Modak, A. Dutta, A. Bhaumik, Facile C–S coupling reaction of aryl iodide and thiophenol catalyzed by cu-grafted furfural functionalized mesoporous organosilica, Dalton Trans. 40 (2011) 5228.
(c) G.B.B. Varadwaj, S. Rana, K.M. Parida, Stable amine functionalized montmorillonite supported Cu, Ni catalyst showing synergistic and cooperative effectiveness towards C-S coupling reactions, RSC Adv. 3 (2013) 7570.
(d) E. Sperotto, G.P.M. van Klink, J.G. de Vries, G. van Koten, Ligand-free copper-catalyzed C-S coupling of aryl iodides and thiols, J. Org. Chem. 73 (2008) 5625.

[25] (a) G.T. Venkanna, H.D. Arman, Z.J. Tonzetich, Catalytic C-S cross-coupling reactions employing Ni complexes of pyrrole-based pincer ligands, ACS Catal. 4 (2014) 2941.
(b) X. Xu, J. Liu, J.J. Zhang, Y.W. Wang, Y. Peng, Nickel-mediated inter- and intramolecular C-S coupling of thiols and thioacetates with aryl iodides at room temperature, Org. Lett. 15 (2013) 3, 550.
(c) O. Bistri, A. Correa, C. Bolm, Iron-catalyzed C-O cross-couplings of phenols with aryl iodides, Angew. Chem. Int. Ed. 47 (2008) 586.

[26] S. Mandal, M. Mukherjee, S. Hazra, Evolution of electronic structures of polar phthalocyanine substrate interfaces, ACS Appl. Mater. Interfaces 12 (2020) 45564–45573.

[27] Bruker, APEX2, SAINT and SADABS, BRUKER AXS, Inc., Madison, Wisconsin, USA, 2008.

[28] G.M. Sheldrick, Crytal structure refinement with SHELX, Acta Cryst. C71 (2015) 3–8.

[29] L.J. Farrugia, Wingx and ORTEP for windows, an update, J. Appl. Crystallogr. 45 (2012) 849–854.

[30] A.L. Spek, Structure validation in chemical crystallography, Acta Cryst. D65 (2009) 148–155.

[31] L.J. Farrugia, ORTEP-3 for windows - a version of ORTEP-III with a graphical user interface (GUI), J. Appl. Crystallogr. 30 (1997) 565.

[32] X. He, C. Lu, D. Yuan, L. Chen, Q. Zhang, C. Wu, Hydrothermal synthesis, crystal structures, and properties of a class of 2D coordination polymers, Eur. J. Inorg. Chem. (2005) 4598.

[33] (a) R. Kitaura, K. Seki, G. Akiyama, S. Kitagawa, Porous coordination-polymer crystals with gated channels specific for supercritical gases, Angew. Chem. Int. Ed. 42 (2003) 428.
(b) J. Zhang, S. Kitagawa, Supramolecular isomerism, framework flexibility, unsaturated metal center, and porous property of Ag(I)/Cu(I) 3, 3', 5, 5'-tetrametyl-4, 4'-bipyrazolate, J. Am. Chem. Soc. 130 (2008) 907.

[34] T.K. Maji, M. Ohba, S. Kitagawa, Transformation from a 2D stacked layer to 3D interpenetrated framework by changing the spacer functionality: Synthesis, structure, adsorption, and magnetic properties, Inorg. Chem. 44 (2005) 9225.

[35] M.C. Biesinger, Advanced analysis of copper X-ray photoelectron spectra, Surf. Interface Anal. 49 (2017) 1325–1334.

[36] (a) X. Lv, W. Bao, J. Org. Chem. 72 (2007) 3863.
(b) D. Ma, Q. Cai, N, N-dimethyl glycine-promoted ullmann coupling reaction of phenols and aryl halides, Org. Lett. 5 (2003) 3799.
(c) H.-J. Cristau, P.P. Cellier, S. Hamada, J.-F. Spindler, M. Taillefer, A general and mild ullmann-type synthesis of diaryl ethers, Org. Lett. 6 (2004) 913.
(d) S. Jammi, S. Sakthivel, L. Rout, T. Mukherjee, S. Mandal, R. Mitra, P. Saha, T. Punniyamurthi, Cuo nanoparticles catalyzed c-n, c-o and c-s cross coupling reaction: scope and mechanism, J. Org. Chem. 74 (2009) 1971-1976.

[37] A.R. Hajipour, F. Dordahan, F. Rafiee, M. Mahdavi, C–n cross-coupling reaction catalysed by efficient and reusable cuo/sio2 nanoparticles under ligand-free conditions, Appl. Organ. Chem. 28 (2014) 809–813.

[38] S. Sagadevan, P. Murugasen, Electrical properties of copper oxide nanoparticles, J. Nano Res. 30 (2015) 1.

CrystEngComm

ROYAL SOCIETY OF CHEMISTRY

PAPER

View Article Online
View Journal | View Issue

Cite this: *CrystEngComm*, 2021, **23**, 3510

Photo-responsive Schottky diode behavior of a donor–acceptor co-crystal with violet blue light emission†

Soumen Singha,[a] Rajkumar Jana,[ab] Rituparna Mondal,[ac] Partha Pratim Ray,[a] Partha Pratim Bag,[d] Kajal Gupta,[e] Nandan Pakhira,[e] Corrado Rizzoli,[f] Arabinda Mallick,[e] Sanjay Kumar *[a] and Rajat Saha *[ae]

Herein, we report the crystal structure, supramolecular structure, electronic transport properties and optoelectronic behaviour of a co-crystal made of tetrabromoterephthalic acid (TBTA) and quinoxaline (QUIN) (1 : 1). The sample has been characterized using thermogravimetric analysis and spectral techniques. Moreover, theoretical analyses of noncovalent interactions, optical properties and the band structure of the co-crystal have been performed. The co-crystal has been crystallized in an orthorhombic system with the *Pnma* space group and the constituent molecules assemble in the solid state by using O–H···N hydrogen bonding, π···π, Br···π and Br···O interactions. The ground state geometry optimization over the hydrogen bonded dimer by DFT method indicates that TBTA acts as the donor and QUIN as the acceptor within the self-assembled co-crystal. According to UV-vis spectroscopic study the bandgap of the co-crystal is ~3.18 eV. In the solid state it exhibits a broad emission band with a maximum at 405 nm while in aqueous medium its photoluminescence emission peaks are obtained at 350 and 403 nm. The values of the average fluorescence lifetime of the sample in aqueous medium are 3.38 ns at 352 nm and 4.94 ns at 403 nm. Under UV-irradiation, the co-crystal emits violet-blue light. The emission spectrum in solution phase shows a relative quantum yield of 0.018. Band structure calculation indicates that the co-crystal is a p-type semiconductor with a bandgap of 2.835 eV. Due to its semiconducting character, the ITO/co-crystal/Al sandwiched structured device acts as a Schottky barrier diode with rectification ratio, ideality factor, barrier height and series resistance of 41, 1.36, 0.70 eV, and 26.97 kΩ, respectively. The current through the device increases substantially under visible light exposure. Upon visible light illumination the values of electrical conductivity, mobility and carrier concentration increase by 35 (±0.5), 54 (±0.5) and 6 (±0.5)%, respectively, with respect to dark conditions. It has been shown that π···π and hydrogen bonding interactions can play a crucial role in producing the donor–acceptor (D–A) type co-crystal, semiconducting behaviour can be incorporated in the organic co-crystal utilizing π···π and hydrogen bonding interactions and weak intermolecular π···π, Br···π and Br···O interactions can act as the pathway for electrical conduction.

Received 5th January 2021,
Accepted 2nd March 2021

DOI: 10.1039/d1ce00020a

rsc.li/crystengcomm

Introduction

In recent times, photo-responsive organic semiconductors[1] have attracted enormous attention because of their significant application potential in photodetectors,[2] optical switches,[3] LED[4] and photovoltaic cells.[5] In this context, donor–acceptor molecular co-crystals connected by charge transfer and weak intermolecular interactions like hydrogen bonding[6] and π-interactions[7] which also have success in crystal engineering have emerged as the most promising material of this category.[8–11] The physicochemical properties of co-crystals are poles apart from the sum of their components. These properties can be tuned rationally by altering intermolecular interactions through judicious selection of the constituents. Recently, study of the semiconducting and optoelectronic

[a] *Department of Physics, Jadavpur University, Jadavpur, Kolkata-700032, WB, India. E-mail: kumars@phys.jdvu.ac.in, rajatinorg1@gmail.com*
[b] *Department of Physics, Techno India University, EM-4, Sector-V, Salt lake, Kolkata-700091, India*
[c] *Department of Electronics, Barrackpore Rastraguru Surendranath College, Barrackpore, West Bengal 700120, India*
[d] *Dumka Engineering College, Dumka, Jharkhand-814101, India*
[e] *Department of Chemistry, Kazi Nazrul University, Asansol-713340, WB, India*
[f] *Dipartimento SCVSA, Università di Parma, Parco Area delle Scienze 17/A, Parma, Italy*

† Electronic supplementary information (ESI) available: Experimental procedures, tables, relevant figures and other related documents. CCDC 1841621. For ESI and crystallographic data in CIF or other electronic format see DOI: 10.1039/d1ce00020a

behaviour of organic co-crystals/salts has attracted paramount attention due to their enormous application possibilities in next generation environment friendly electronic and optoelectronic devices in place of the Si-based devices used nowadays.[12–36] However, very few co-crystals exhibit photo-responsive properties.[15–36] Thorough investigation of the electronic and optoelectronic properties of a number of organic co-crystal based devices fabricated in laboratory conditions yielded very promising results in respect to their application possibilities in the area of light emitting diodes,[17] light emitting transistors,[18,19] lasers,[20] photoconductors,[21,22] and photovoltaic cells.[23]

Tsutsumi *et al.*, have reported the photovoltaic behaviour of a device fabricated by using DBTTF–TCNQ (dibenzotetrathiofulvalene–tetracyanoquinodimethane) co-crystal with narrow bandgap (0.7 eV).[24] The thin film solar cell made of tetracene-doped anthracene co-crystal exhibits an optical efficiency of 23.72%.[25] The highest power conversion efficiency achieved in fullerene and squarine co-crystal based heterojunction solar cells is 10%.[26] The organic p–n junction photovoltaic cell made from contorted hexabenzocoronene (donor) and spherical fullerene (acceptor) exhibits a good response but large scale production of the device has not yet been taken up due to lack of proper structural characterization of the co-crystal used.[27] W. Hu and co-workers have assessed the optoelectronic performance of several D–A type charge transfer co-crystals.[28–32] They have examined morphology dependant photo-responsive behaviour of two different co-crystals of perylene (P) and TCNQ (T) and shown that the on–off photocurrent ratios of the devices made of 1 : 1 and 3 : 1 P–T co-crystals under visible light illumination are 5.4 and 4.4, respectively.[30] In another article, they have shown that the bipyridylethylene (BPE)–1,2,4,5-tetracyanobenzene (TCNB) co-crystal can be used as an optical waveguide.[31] They have also designed photonic logic gate properties of an organic co-crystal composed of 4-(1-naphthylvinyl)pyridine and 1,2,4,5-tetracyanobenzene.[32] The field effect transistor (FET) fabricated by using the co-crystal of C_{60} and 5,10,15,20-tetrakis(3,5-dimethoxyphenyl)porphyrin (3,5-TPP) responds to NIR radiation.[33] The heterojunction device made from the acridine–trimesic acid co-crystal exhibits an ultrahigh on–off photocurrent ratio of the order of 10^4.[34] The electrical conductivity of co-crystal of 1,3,6,8-pyrenetetrasulfonic acid tetrasodium salt as donor and 1,1′-bibutyl-4,4′-bipyridinium dibromide as acceptor increases upon illumination with laser beam of wavelength 405 nm.[35] However, this co-crystal has low conductivity.[35]

Earlier we have reported the role of weak intermolecular interactions (like hydrogen bonding, π–π, Br···π and Br···O interactions) in the electrical response of tetrabromoterephthalic acid (TBTA) based multi-component semiconducting co-crystals through formation of Schottky barriers.[36] Recently, we have reported the photo-responsive behaviour of some organic co-crystal/salts based Schottky barrier diodes.[15] It is noteworthy that the weak intermolecular interactions between the donor and acceptor molecules of co-crystals can be utilized for generation of photocarriers.[1,5,15–23] Thus, from a fundamental view point of crystal engineering it appears that the possibility of forming a co-crystal utilizing charge transfer/π···π stacking between TBTA and quinoxaline (QUIN) molecules and having the supramolecular network formed by weak hydrogen bonding, π–π, Br···π and Br···O interactions can be explored in order to examine the role of such weak noncovalent interactions in the electronic transport properties and optoelectronic behaviour through a comprehensive study of the photo-responsive properties of a TBTA–QUIN based Schottky barrier diode.

Herein, we have designed a semiconducting-luminescent co-crystal of the poly-bromo organic molecule TBTA as donor and QUIN as acceptor (Fig. S1†) using the solvent evaporation method, characterized it using single crystal X-ray diffraction (SCXRD), UV-vis, luminescence lifetime measurements and fluorescence microscopic imaging techniques. Its photo-responsive properties have also been examined. Structural study reveals that this TBTA–QUIN co-crystal has been formed by the self-assembly of its constituents TBTA and QUIN through hydrogen bonding and π–π interactions and it has assembled in the solid state through supramolecular O–H···N hydrogen bonding, Br···O, Br···π and π–π interactions. Theoretical inspection of the energy levels of frontier molecular orbitals of the hydrogen bonded dimer shows that TBTA acts as donor while QUIN acts as acceptor. Band structure calculations show that the bandgap of the co-crystal is 2.835 eV and this value agrees well with the optical bandgap (3.18 eV) obtained from solid state UV-vis spectra. Under UV-irradiation the co-crystal emits violet-blue light. To examine the electrical response, thin film of the co-crystal is fabricated on an ITO surface and the ITO/co-crystal/Al sandwich structure exhibits "Schottky diode" behaviour with a rectification ratio of 45 in dark conditions. The conductivity of the co-crystal made device increases by 35 (±0.5)% upon visible light exposure and it exhibits "Schottky diode" behaviour with a rectification ratio of ~56.

Experimental section

This study includes the solvent evaporation synthesis of TBTA–QUIN co-crystal, X-ray single crystal structural characterization, density functional theory (DFT) based calculation of the binding energy and non-covalent interactions within the components, Hirshfeld surface analysis, spectroscopic study and its theoretical verification by DFT and periodic DFT calculations (details are provided in the ESI†). The *I–V* measurements in dark and under visible light illumination have been performed on an Al/co-crystal/ITO sandwich structure fabricated by using an SCU 2700 spin coating system. Aluminium (Al) electrode is deposited on the active thin film by a vacuum coating unit (12A4D of HINDHIVAC) using a shadow mask. The *I–V* characteristics, in dark and under visible light irradiation, of the co-crystal have been recorded using the two probe method using a

Keithley 2400 sourcemeter interfaced with a PC at applied bias voltage in the range of −2 to +2 V. The *I–V* measurements have been carried out in a dark box. The photo-responsive behaviour of the device has been investigated under AM 1.5 G photo-irradiation. Details of the *I–V* measurements are provided in the ESI.†

Results and discussion

Molecular and supramolecular structure of the co-crystal

Upon mixing equimolar ethanolic solutions of TBTA and QUIN (Fig. 1) the co-crystal was grown *via* the solvent evaporation method. Rhombohedral shaped (Fig. S1†) colourless single crystals were collected and characterized using the single crystal X-ray crystallographic technique (ESI†). Structural analysis reveals that the co-crystal crystallizes in the orthorhombic system with *Pnma* space group (Tables 1 and S1†). The asymmetric unit of the co-crystal contains half of each of the TBTA and QUIN molecules (Fig. S2†). In the molecule of TBTA, the carboxylic groups are almost perpendicular (angle between the plane of the phenyl ring and the plane of carboxylic acid group is 87.23°, Fig. S3†) to the plane of the phenyl ring. The C–O bond lengths (O1–C5 = 1.302(3) Å, O2–C5 = 1.192(3) Å) confirm the presence of the carboxylic acid group. The QUIN moiety is completely planar and is co-planar to the phenyl ring of the TBTA moiety.

Interestingly, the TBTA and QUIN molecules are connected by O–H···N hydrogen bonds to form the 1D supramolecular chains along the *b*-axis (Fig. 2, S4 and Table S2†). Two parallel 1D chains are connected by π···π interactions (Fig. S5 and Table S3†) between the TBTA and QUIN molecules to form a double layer which is further connected by Br···O interactions (Fig. S6 and Table S4†) to form a 2D supramolecular structure within the *ab*-plane (Fig. 2). These 2D sheets are further bridged by Br···π interactions (Table S5†) to form a 3D supramolecular network (Fig. S7†).

PXRD, thermal and IR analyses

The phase purity of the bulk material was characterized by PXRD analysis (Fig. S8†). Thermal analysis reveals two-step degradation of the co-crystal. The sample is stable up to 140 °C, and then for the 1st step of decomposition within the temperature range 140–220 °C the weight loss of the sample is nearly 24.5% indicating the removal of the QUIN moiety from the structure. In the next step the remaining part of the sample gets completely degraded in the temperature interval of 270–360 °C (Fig. S9†). The vibrational spectra recorded in ATR mode (Fig. S10†) show shifts in the frequency band positions corresponding to C═O and O–H vibrations in the co-crystal with respect to TBTA towards lower frequencies. This may be attributed to the weakening of C═O and O–H vibrations due to intermolecular hydrogen bonding interactions between TBTA and QUIN in the co-crystal.

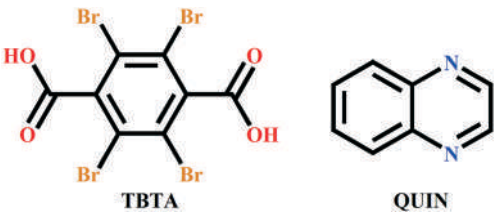

Fig. 1 Molecular structures of co-crystallizing components.

Table 1 Crystallographic data of the TBTA–QUIN co-crystal

Structure	Crystal form
System	Orthorhombic
Space group	*Pnma*
a (Å)	9.4972(18)
b (Å)	14.745(3)
c (Å)	13.181(2)
α (°)	90
V (Å^3)	1845.8(6)
Z, density	4, 2.202
CCDC no.	1841621

Inspection of noncovalent interactions within the co-crystal

Hirshfeld surface analysis

The Hirshfeld surface analysis provides more detailed information regarding the intermolecular interactions and the 2D fingerprint plot quantifies these interactions within the crystal structure (details are provided in the ESI†). The Hirshfeld surfaces were calculated over TBTA molecules (Fig. 3) and the 2D fingerprint plots (Fig. S11†) were analysed accordingly. The d_{norm} surface of TBTA was mapped over the fixed colour scale of −0.751 to 1.417 Å. It displays some bright circular red spots, which correspond to the short intermolecular O···H and N···H interactions. The light red spots correspond to the long intermolecular Br···O, Br···π, C···H and H···H interactions. The 2D fingerprint plots reveal that the O···H interactions comprise 17.0% of the total Hirshfeld surface and appear as a blunt spike with the lowest contact distance $d_i \approx 1.5$ Å and $d_e \approx 1.3$ Å. The N···H

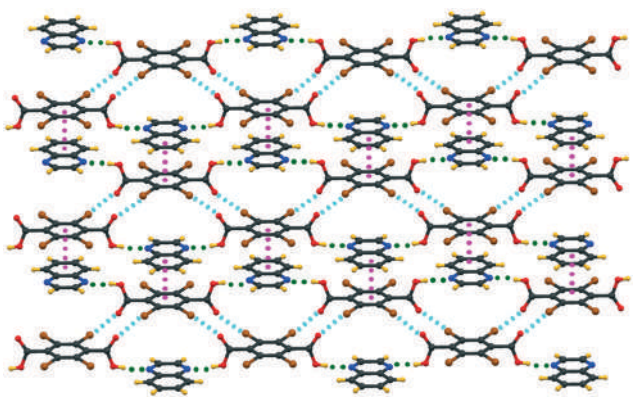

Fig. 2 2D supramolecular structure formed by hydrogen bonds (green), halogen bonds (cyan) and π···π interactions (magenta).

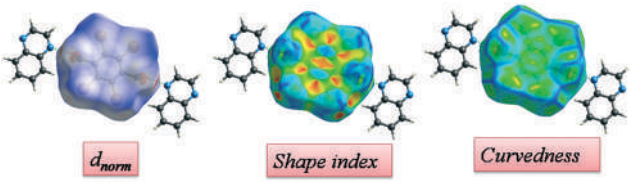

Fig. 3 Hirshfeld d_{norm}, shape index and curvedness surfaces of TBTA–QUIN around TBTA.

interactions cover 4.3% of the total surface and emerge as a sharp spike with contact distance $d_i \approx 0.6$ Å and $d_e \approx 1.0$ Å. The Br···C interaction corresponding to Br···π comprises 13.5% of the surface and appears as two spikes with average contact distance $d_e + d_i \approx 3.4$ Å. The C···H, Br···O, H···H and Br···H interactions are found in the 2D fingerprint plot with relative surface areas 2.3%, 18.4%, 7.1% and 27.4%, respectively as shown in Fig. S10.†

Intermolecular interaction energies

The quantitative view of the topology of the distribution of overall interaction energies sustaining the molecular components within the crystal structure have been calculated by two ways. Firstly on the basis of pair-wise interaction energies by summing up four energy components *viz.*, electrostatic (E_{el}), polarization (E_{pol}), dispersion (E_{dis}) and exchange repulsion (E_{rep}) on a structure-cluster mapped within 6 Å in the neighbourhood of each component (TBTA and QUIN) of the co-crystal to include long-range interactions. Secondly the binding energies of the four kinds of self-assembled dimeric model geometries focussing different kinds of intermolecular interactions (Fig. 4) were calculated from the difference of the energy of the system and the sum of individual components in the framework of DFT with counterpoise correction.

For a cluster of molecules within the 2 × 2 × 2 unit cell, graphical representation of the individual energy components has been simulated in the energy framework and is depicted in Fig. S12.† The interactions for different kinds of orientations of the component molecules within the crystals have been explored in the energy framework and are presented in Fig. S13–S15.† The electrostatic and dispersion energies coexisting together provide the total interaction energy for the self-assembly of the co-crystal. Signatures of electrostatic force due to the strong O–H···N hydrogen bonded arrays and dispersion force due to π-stacking interactions, Br···O halogen bonding with Br···π and C–H···π interactions within the constituents of the heterodimers have been detected in the interaction energy plots (Fig. S13 and S14†). The Br···O halogen bonding interactions between the TBTA homodimer have been detected to form a 2D-planar geometry made of a $R_2^2(10)$ network between the TBTA molecules (Fig. S15†).

On the other hand Fig. 4(a) describes the binding energy of the first model dimer considering only the O–H···N hydrogen bonding interactions, the second model (Fig. 4(b)) gives the binding energy of the weakly interacting π stacked dimer, the third and fourth models diagnose the intermolecular interactions between the homo-dimers, Br···O and Br···π interactions between two TBTA moieties (Fig. 4(c)) and C–H···π interactions between two QUIN moieties (Fig. 4(d)). The calculated values of these interactions as listed in Table 2 show comparable results.

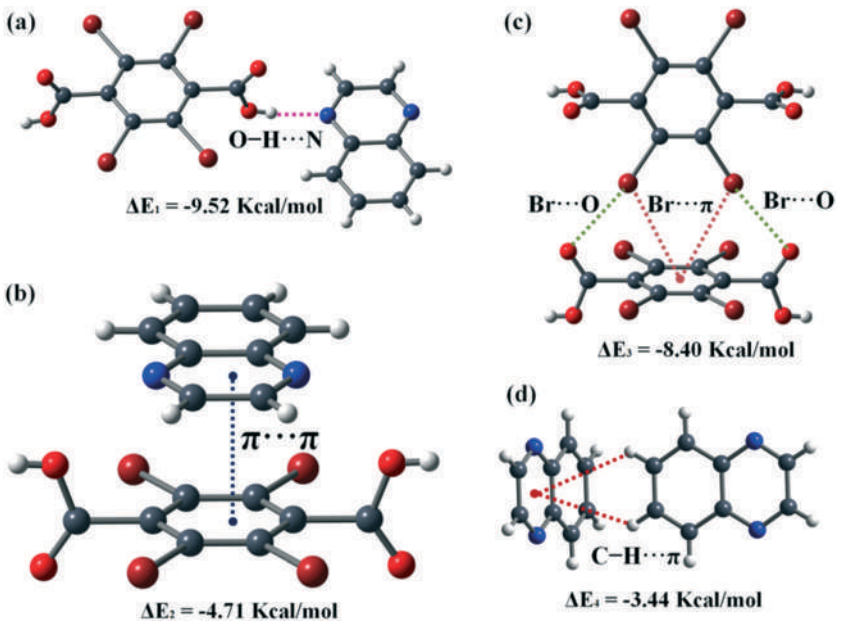

Fig. 4 Theoretical model geometries with the synthon energies describing (a) O–H···N hydrogen bonding interaction, (b) π···π interaction for the TBTA-QUIN hetero-dimer model structures, (c) Br···O and Br···π interactions within the TBTA homo-dimer and (d) C–H···π interactions between the QUIN homo-dimer model structure.

Table 2 Comparison between interaction energies calculated from the energy framework and binding energies from DFT computation

Pair	Interaction	Interaction energy	Binding energy
TBTA–QUIN heterodimer	O–H···N hydrogen bonding interactions	−50.5 kJ mol^{-1}	−9.52 kcal mol^{-1}
	π··· stacking interactions	−36.5 kJ mol^{-1}	−4.71 kcal mol^{-1}
TBTA homodimer	Br···O halogen bonding with Br···π	−31.4 kJ mol^{-1}	−8.40 kcal mol^{-1}
QUIN homodimer	C–H···π interactions	−11.6 kJ mol^{-1}	−3.44 kcal mol^{-1}
TBTA homodimers with $R_2^2(10)$ network forming a 2D-planar geometry	Br···O halogen bonding interaction between the TBTA homodimers	−19.0 kJ mol^{-1}	

QTAIM and NCI plot analysis

A qualitative analysis of the topological properties of the noncovalent interactions prevailing within the dimer geometries based on the electron density has been performed using the quantum theory of atoms in molecules (QTAIM). In the QTAIM distribution of critical points (CPs) and bond paths each noncovalent interaction is characterized by a bond CP (yellow sphere) and bond path interconnecting the atoms of two different molecular units and to visualize the nature of the non-covalent interactions (NCI), the reduced density gradient (RDG) has been represented by iso-density surfaces over the interacting dimers (Fig. 5). The nature of the interaction between the molecules within the dimer can be traced through a red–blue–green colour scheme on the calculated iso-surface where blue colour usually highlights strong attractive interaction whereas red points towards strong repulsive interaction. Weak interactions (attractive) are indicated by green colour.

Fig. 5(a) shows the QTAIM representation of the heterodimer, where the O–H···N hydrogen bond is portrayed by the bond critical point (BCP) represented by a yellow sphere and the bond path shown by a pink line interconnecting the H and N atoms. The small blue iso-surface located between the H and N atoms shows the NCI plot representation which confirms the presence of strong O–H···N hydrogen bonding interactions. Fig. 5(b) displays several BCPs connecting the π-systems of both the QUIN rings and the TBTA molecule, characterizing the π-stacking interaction. The extended green iso-surface between the π-stacked hetero-dimers indicates the weakly attractive nature of the interactions between the participating residues.

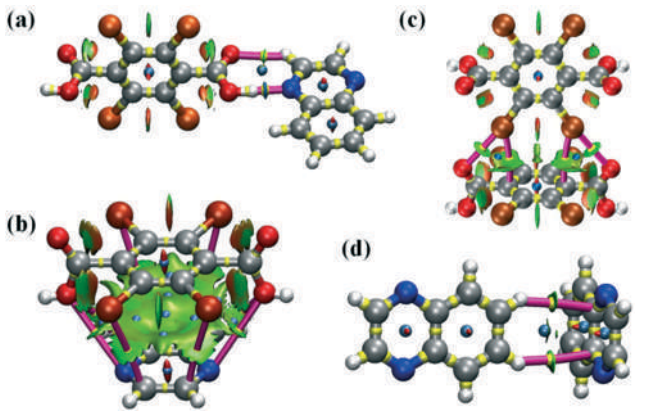

Fig. 5 AIM distribution of bond and ring critical points (yellow and tan spheres respectively), bond paths (magenta lines) and the nature of non-covalent interactions for the model dimeric geometries revealing (a) O–H···N strong H-bonding interaction, (b) π-stacking interaction, (c) Br···O and Br···π interactions and (d) C–H···π short contacts.

It can be observed that for the self-assembled homo-dimer (Fig. 5(c)) the distribution of bond critical points (CPs) and bond paths reveals two different types of interaction, one corresponds to the XB, where the Br and O atoms are interconnected by a bond CP and bond path and the other contact can be defined as a Br···π interaction that is characterized by a bond CP and bond path connecting the Br atom to one C-atom of the π-aromatic ring. The natures of weakly interacting Br···O and Br···π interactions are characterized by three separate green iso-surfaces between them. On the other hand Fig. 5(d) presents the similar distribution of bond critical points (CPs) and bond paths, revealing the C–H···π short contacts by a bond CP and bond path interconnecting the H atom to one C-atom of the π ring of QUIN. The strength of the interaction can be observed by four discrete green iso-surfaces between the QUIN homo-dimer and was found to be weak in nature.

Optical, electronic and electrical transport properties

Spectroscopic and light emitting behaviour

The optical properties of the co-crystal have been examined in both solid state and aqueous medium (Fig. 6). The solid state absorption spectrum of the co-crystal shows a broad band in the UV region while in the aqueous medium multiple peaks appear (Fig. 6(a)). The peaks obtained at lower wavelength can be attributed to π–π* transition while higher wavelength peaks are due to inter-ligand charge transfer (ILCT) between different moieties of the co-crystal. Usually, in the UV-vis reflectance spectra the band for the co-crystal formed by the charge transfer (CT) interaction appears at lower energy with respect to its individual components.[12] However, in the present case no such shifting of the band for the co-crystal has been observed, which discards the possibility of the presence of CT interaction between TBTA and QUIN moieties in the co-crystal (Fig. S16(a)†). The absorption spectra of the co-crystal in both solid state and solution phase show two major bands. The solution phase spectrum is blue shifted with respect to the solid state spectrum. The peaks in solution phase absorption spectrum are clearly resolved whereas for the solid state spectrum the

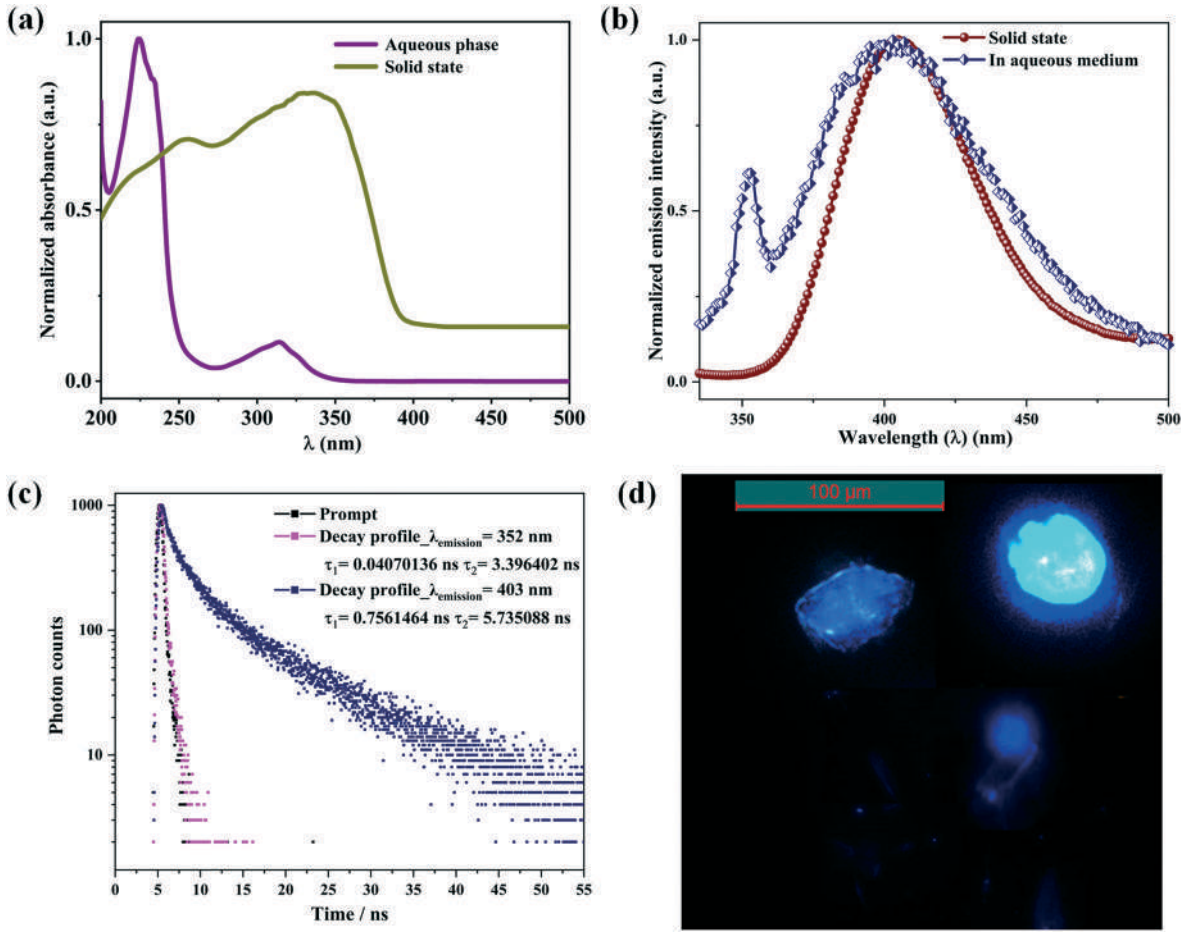

Fig. 6 (a) UV-vis absorption spectra of the sample in both solid state and aqueous medium, (b) steady state emission spectra of the sample in both solid state and aqueous medium (λ_{ex} = 313 nm, conc. = 10^{-4} mol l^{-1}), (c) lifetime profile of the sample in solution phase and (d) fluorescence image of the co-crystal. The spectra of the sample in solid state and in solution phase as shown in Fig. 6(a) and (b) are normalized to illustrate their differences.

band nature can be observed, which mainly arises due to the aggregation effect. Fig. S16(b)† depicts the absorption behaviour of the sample and its components in solution phase. By correlating the experimental and simulated absorption spectra of the sample in solution phase it has been shown that the co-crystal retains its supramolecular assembly in the aqueous medium (see ESI†).

The solid state emission spectrum of the co-crystal shows a broad band with a maximum at 405 nm while in aqueous medium it has two peaks with maxima at 350 nm and 403 nm (Fig. 6(b)). Such behaviour is due to the solid state aggregation effect within the multi-component material. Concentration dependent absorption and emission spectra of the sample have also been studied in solution phase (Fig. S17(a) and (b)†). With increasing concentration, the intensity of the peaks in the absorption spectra increases continuously; while in the emission spectra, the intensity of the peak at 350 nm decreases and it increases for the peak at 403 nm. Most probably self-assembled aggregation is responsible for the decrement and the incessant increase in the propensity of the inter-ligand charge transfer interaction with increasing concentration causes the significant enhancement in the intensity of the second peak.

Fluorescence lifetime is a very effective tool for probing the local environment around a fluorescent molecule and excited state interactions. The decay profiles of the sample recorded in aqueous environment have been fitted with a double-exponent (Fig. 6(c)) and the respective lifetime values τ_1 and τ_2 are provided in Table 3. The average lifetime values of the material in aqueous medium for those emission maxima were determined from the results of the time-resolved fluorescence spectroscopy using the equation: $\langle\tau_{av}\rangle = (a_1\tau_1^2 + a_2\tau_2^2)/(a_1\tau_1 + a_2\tau_2)$, where a_1, a_2 are the percentage contributions for these two lifetime values and are presented in Table 3.

The relative quantum yield (Φ_F) calculation from the luminescence measurement carried out in solution phase (considering only the area under the emission spectrum with maximum at 403 nm) using quinine sulfate (QS) in 0.1 M H_2SO_4 as the standard reference shows that the sample is minimally radiative with Φ_F = 0.018. The consequential radiative and non-radiative transition rate constants for this

Table 3 Lifetime values of the sample in aqueous environment

Monitoring wavelength (λ_{em})	a_1	τ_1 (ns)	a_2	τ_2 (ns)	$\langle\tau_{av}\rangle$ (ns)
352	0.17	0.04	0.83	3.39	3.38
403	0.59	0.75	0.41	5.73	4.94

a_1, a_2: percentage contributions for lifetime values; τ_1, τ_2: lifetime; and $\langle\tau_{av}\rangle$: average lifetime.

emission peak were extracted from the relations $k_r = \varphi_F/\tau_{av}$ and $k_{ir} = (1 - \varphi_F)/\tau_{av}$, respectively, and these values are found to be $k_r = 3.64 \times 10^6$ s^{-1} and $k_{ir} = 9.96 \times 10^8$ s^{-1}. The fluorescence microscopic image of the co-crystal under UV irradiation has been recorded (Fig. 6(d)). The co-crystal shows violet-blue emission from its edges as expected from the coordinate (0.151, 0.056) of the CIE chromaticity diagram ((Fig. S18(c)†) drawn from the solid state PL spectra.

Ground state structural and electronic properties

The molecular structure of the co-crystal has been optimized in the electronic ground state (S_0) in both the gaseous phase and in water medium employing the DFT method with the 6-311++G(d,p) basis set. The gas phase and solution phase optimized geometries of the co-crystal are presented in Fig. S18† and the coordinates are reported in Tables S6 and S7.† As the present sample is not a CT type co-crystal and the hydrogen bonding interaction is the strongest interaction between the components of the co-crystal, the hydrogen bonded heterodimer was chosen as the molecular unit of the co-crystal for all molecular level calculations. In the starting solid state geometry derived from the crystal structure a molecular unit of the co-crystal contains a TBTA and a QUIN moiety where the carboxylic groups of TBTA are perpendicular to the aromatic ring of TBTA and the aromatic ring of TBTA is coplanar with the QUIN ring. The relative orientations of the different fragments of the optimized geometry in the aqueous phase is almost the same as the solid state molecular structure. The slight difference between these conformations is because of the presence of solvent interactions in the aqueous phase. On the other hand, for the optimized geometry in the gaseous phase the aromatic ring of the TBTA molecule becomes perpendicular with respect to the QUIN moiety and the carboxylic groups turn coplanar with the QUIN moiety. Due to the absence of crystalline packing force the optimized geometry of the molecule in the gaseous phase exhibits such a substantially different conformation from the solid state molecular geometry. Except for the bonds with H atoms all the optimized bond lengths are within the appreciable limit of ~0.02 Å. In the solution phase optimized geometry the increment of the O–H bond dimension is more than the gaseous phase optimized geometry. Some of the selected bond lengths of the co-crystal are listed in Table S8.†

The isodensity surface plots (isodensity = 0.02 e Bohr^{-3}) of some of the selected frontier molecular orbitals (FMO) of both the optimized structures of the co-crystal along with their orbital energies are depicted in Fig. 7. For the FMOs the contributions coming from different parts of the co-crystal in terms of atomic contribution are obtained by the fragment analysis method, and energies of the FMOs along with the HOMO–LUMO energy differences are provided in Table S9.† It can be clearly seen that the FMOs for the geometries optimized in the gaseous phase and in water medium have different energies and the electron density distributions of the FMOs (Fig. 7) show different distribution of the isodensities over different parts of the molecules.

In the hydrogen bonded dimer the HOMO e-density is found over TBTA and the LUMO e-density is on QUIN for both the phases. Therefore for the ground state of the TBTA–QUIN self-assembly, TBTA will act as donor, whereas QUIN will act as acceptor. This observation is further supported by the calculation of the Mulliken charges over the atoms of the hydrogen bonded dimer geometry (Tables S10 and S11†). It may be noted that for both the phases all virtual orbitals subsequent to the LUMO are composed of contributions from a single entity. For both the phases, LUMO+1 to LUMO+3 are composed of the contribution from the TBTA moiety and LUMO+4 is composed of the sole contribution from the QUIN moiety. The HOMO−2 and HOMO−4 orbitals in the gaseous phase optimized structure and the HOMO−1 orbital in the aqueous medium optimized geometry are composed of sole contributions from the QUIN moiety. For all other occupied orbitals both the TBTA and QUIN moieties contribute in different ratios. All the % contributions are listed in Table S9.†

Singlet excited states and calculated absorption spectra

We have computed the theoretical UV-vis spectra of the co-crystal in both the gaseous state and aqueous medium using the ground state optimized geometries in the respective phases, with the help of the non-equilibrium approach of the time dependent density functional (TD-DFT) method. The energy of each excited state (S_n) represents the vertical excitation energy in electron volts (eV) from the ground state (S_0).

The theoretically (both in the gaseous and solution phases) and experimentally obtained UV-vis spectra of the co-crystal in aqueous medium are presented in Fig. 8. The absorption spectra of the co-crystal show multiple transitions and these excitations are primarily attributed to charge transfer transition between different moieties within the molecular unit of the co-crystals. The peaks in the experimental spectrum have been assigned by visual inspection. The values of theoretically calculated excitation wavelengths matching with experimental result, excitation energies, oscillator strengths and CI coefficients along with the corresponding most relevant transitions involved are presented in Tables S12 and S13.† Both the experimental and calculated spectral features of the co-crystal are more or less similar and lie in the UV region of the spectrum, except the fact that in the theoretical spectra there is a slight bathochromic shift relative to the experimental spectrum in the lower wavelength region.

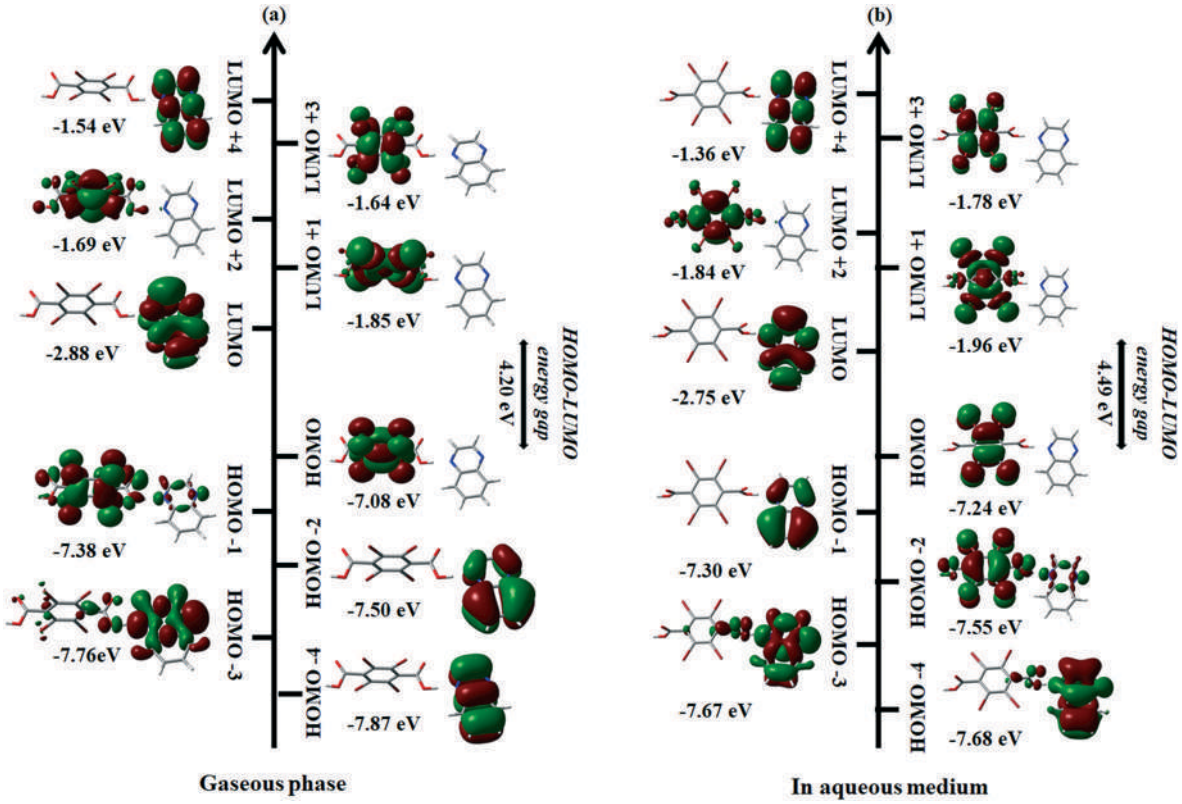

Fig. 7 Schematic representations of the selective FMOs of the co-crystal (a) in gaseous phase and (b) water medium.

The natural transition orbital (NTO) analysis based on the calculated transition density matrices allows us to identify and visualize the electronic transitions in terms of excitation from hole to electron of the singlet excitons. Further, the transition orbitals provide a graphical real-space representation of the transition densities associated with the molecular electronic excitations computed within the framework of TD-DFT. The NTOs of the co-crystal for the gaseous phase and water medium excitations are depicted in Fig. S19 and S20.† The experimental transition wavelength, most appropriate theoretical transitions and corresponding hole and electron NTOs involved along with the weights of the respective configuration λ ($\lambda \leq 1$, where the parameter λ actually refers to the fraction of the NTO pair contribution to a given electronic excitation) have been pictorially provided in Fig. S19 and S20.† These calculated NTOs corresponding to the main absorption band clearly indicate the π–π^* character of these transitions. Both the hole and electron orbitals are spread over the different parts of the co-crystal, establishing a generalised characteristic π (for holes) and π^* (for electrons) nature of orbitals.

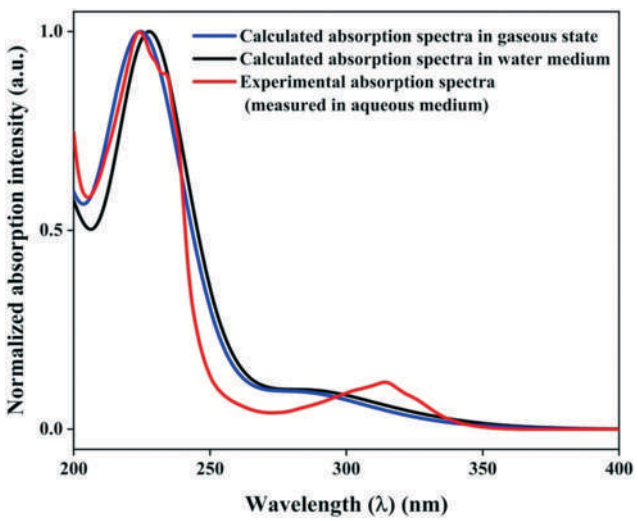

Fig. 8 Experimental absorption spectrum in aqueous medium along with the calculated absorption spectra in gaseous phase and water medium for the co-crystal at room temperature.

In Fig. S19† the lowest energy transition observed around 315 nm is found at *ca.* 308.49 nm (4.02 eV, $f = 0.0349$), which can be described by one set of NTOs (each with $\lambda = 0.98$) and is exclusively attributed to the π (QUIN) → π^* (QUIN) ILCT transition. The next UV transition observed near 294 nm is computed at 282.18 nm (4.39 eV, $f = 0.0861$) and can be ascribed to π (QUIN) → π^* (QUIN) ILCT transition. The most intense transition obtained ~237 nm is calculated at 232.75 nm (5.33 eV, $f = 0.2717$). This transition is due to n(N-QUIN) + π (TBTA) → π^* (TBTA) ILCT transition in association with a slight LLCT nature. The most appropriate calculated transition near the experimentally observed transition at 225 nm is found at 218.82 nm (5.67 eV, $f = 0.2295$). This transition has both LLCT and ILCT characters and can be

represented by π (TBTA + QUIN) → π* (TBTA) LLCT/ILCT transition. The experimentally observed UV-vis transitions of the co-crystal in water medium are theoretically interpreted in a similar manner and the results are summarized in Fig. S20.† So, the TD-DFT with NTO analysis establishes the excitations occurring due to inter/intra-molecular charge transfer interactions between TBTA and QUIN.

Electronic band structure and comparison with optical bandgap

The calculated band structure of the co-crystal along the high symmetry points of the 1st Brillouin zone is represented in Fig. 9(a) (and S21†). It shows that the bandgap of the co-crystal is 2.835 eV, which is close to the value of the optical bandgap (~3.179 eV) calculated from the absorption band edge of the solid state UV-vis spectra (Fig. 9(b)). The dispersions in the valence and conduction bands are clearly described in Fig. 9(a). The parameters corresponding to the band structure are given in Table S14.† The lowest energy (2.835 eV) of the CBs is located at the *G* point (CBM), whereas, the highest energy (0.000 eV) of the VBs is localized at the *Z* point (VBM). This indicates that this co-crystal is an indirect bandgap semiconductor. The calculated band gap shows a slightly smaller value compared to the experimental optical bandgap which is again a general flaw of DFT calculations with the GGA functional. So it can be said without ambiguity that the co-crystal is an indirect band p-type semiconductor with a wide bandgap.

Now, the bands can be assigned according to total and partial densities of states (DOS) as depicted in Fig. S22.† The resonance of C-2s, O-2s, N-2s and Br-4s states in conjunction with a partial amount of H-1s, C-2p, N-2p and O-2p states construct the VB located in the range −24.2 eV to −10.5 eV. The bottom portion of the VB is mainly dominated by the contribution from O-2p (21.4 electrons per eV) and N-2p (7.8 electrons per eV) orbitals. The next region above it is formed by C-2s (18.27 electrons per eV) and Br-4s (12.5 electrons per eV) orbitals. The top of the VB just below the Fermi level between the energy range −10.2 eV to the Fermi level (0.0 eV) are formed by the superposition of C-2p (35.8 electrons per eV) and Br-4p (30.70 electrons per eV) states in association with a considerable amount of contribution from N-2p (8.90 electrons per eV), O-2p (24.90 electrons per eV) and H-1s states. The topmost level of the VB (VBM ~ −1.02 eV ~ 0 eV) is formed due to the resonance of C-2p, N-2p and Br-4p orbitals. The conduction band (CB) just above the Fermi level ranging from 2.83 eV to 5.7 eV is formed due to the superposition of C-2p, N-2p and Br-4p orbitals mixing with a slight amount of O-2p orbitals where the states C-2p (8.35 electrons per eV) and N-2p (6.87 electrons per eV) dominate the bottom of the CB. The states C-2p and Br-4s mixing with a small amount of C-2s and H-1s have created the region ranging from 5.8 eV to 18.9 eV in the CB.

The partial density of state (PDOS) contribution of the two molecular units TBTA and QUIN in the total density of states for the co-crystal is depicted in Fig. S23.† In the PDOS, some peaks appearing at the same energy level (hybridization) for different atomic orbitals (Fig. S22†) and for different molecular fragments (Fig. S23†) clearly show the evidence of strong intermolecular interactions between the moieties of the co-crystal and intramolecular interactions within the moieties. The N-2p orbits hybridize with H-1s due to the resonance in peak positions from −13.5 eV to 0 eV implying partial charge transfer from H atoms to N atoms. So, the presence of strong H bonds between H atoms and N atoms is ensured. Again, a strong resonance is observed between the O-2p and Br-4p peaks within the range −7.9 eV to 0.0 eV. This can be argued to be the evidence of the presence of strong Br···O halogen interaction between the non-bonded atoms.

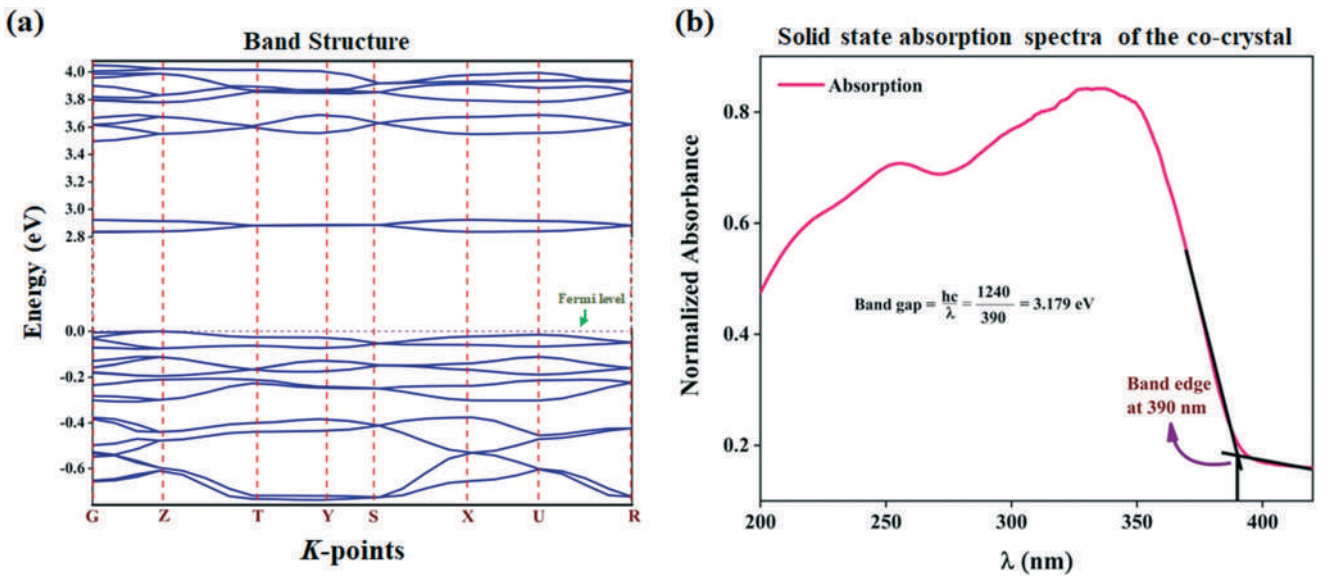

Fig. 9 (a) Calculated band structure zoomed in over the top of the VBs and bottom of CBs and (b) solid state UV-DRS spectrum of the co-crystal in the wavelength range 200 to 420 nm.

Optical properties from the electronic band structure

The electronic band structure calculation can provide insight regarding the optical response. The salient features of the parameters: real ($\varepsilon'(\omega)$) and imaginary ($\varepsilon''(\omega)$) parts of dielectric permittivity, reflectivity ($R(\omega)$), refractive index ($n(\omega)$), extinction coefficient ($k(\omega)$), optical conductivity ($\sigma(\omega)$), absorption coefficient ($\alpha(\omega)$) and energy-loss function ($L(\omega)$) as a function of frequency of the incident photon are displayed in Fig. 10 in the energy range 0–45 eV.

The plots of $\varepsilon''(\omega)$ and $\varepsilon'(\omega)$ against photon energy are shown in Fig. 10(a). The characteristic spectra for the $\varepsilon''(\omega)$ of the co-crystal comprise mainly four sharp peaks at 2.97, 7.12, 11.61 and 14.26 eV together with some shoulder peaks near 17.40 eV and beyond. At low frequency, the imaginary part $\varepsilon''(\omega)$ is zero and the threshold energy for the $\varepsilon''(\omega)$ is consistent with the bandgap of the material at equilibrium. At higher frequency (>35 eV), the $\varepsilon''(\omega)$ approaches to zero. The value of the static dielectric constant ($\varepsilon_s = \varepsilon'(0)$) is 2.98. The $\varepsilon'(\omega)$ fluctuates with increasing frequency and shows four peaks at 2.37, 6.11, 10.76 and 13.16 eV and afterward it starts decreasing, becoming negative in the energy range 19.20–24.32 eV which may be due to the metallic character of the sample in this energy range. At higher energy, the value of $\varepsilon'(\omega)$ again turns positive and is almost independent of energy ($\varepsilon'(\infty) \sim 0.80$).

The reflectivity spectrum of the sample as displayed in Fig. 10(b) shows two distinct peaks: one sharp and strong peak at 6.92 eV and another weak peak at 2.46 eV. A broad band appears in the energy range 9 to 29 eV due to the superposition of several peaks located at 11.66, 14.78, 19.74 and 23.42 eV (accompanied by a shoulder). The reflectivity of the material approaches to zero when the frequency reaches near 45 eV. The zero energy value of reflectivity (*i.e.*, $R(0)$) is 7% and up to 4.83 eV the value of the reflectivity remains within 8.8%. Due to such a low value of reflectivity, the compound is nearly transparent in the infrared and visible energy range. Now, materials with a low refractive index are suitable for application in optoelectronic devices such as LEDs and solar cells. In the entire frequency range, the calculated value of the reflectivity of the co-crystal is lower than that in inorganic compounds like the metal oxides and thus it can be used for fabricating optoelectronic devices. The highest value of reflectivity (21.08%) is observed at 23.42 eV. It has been observed that the reflectivity value attains maximum when the value of $\varepsilon'(\omega)$ becomes negative (Fig. 10(a) and (b)).

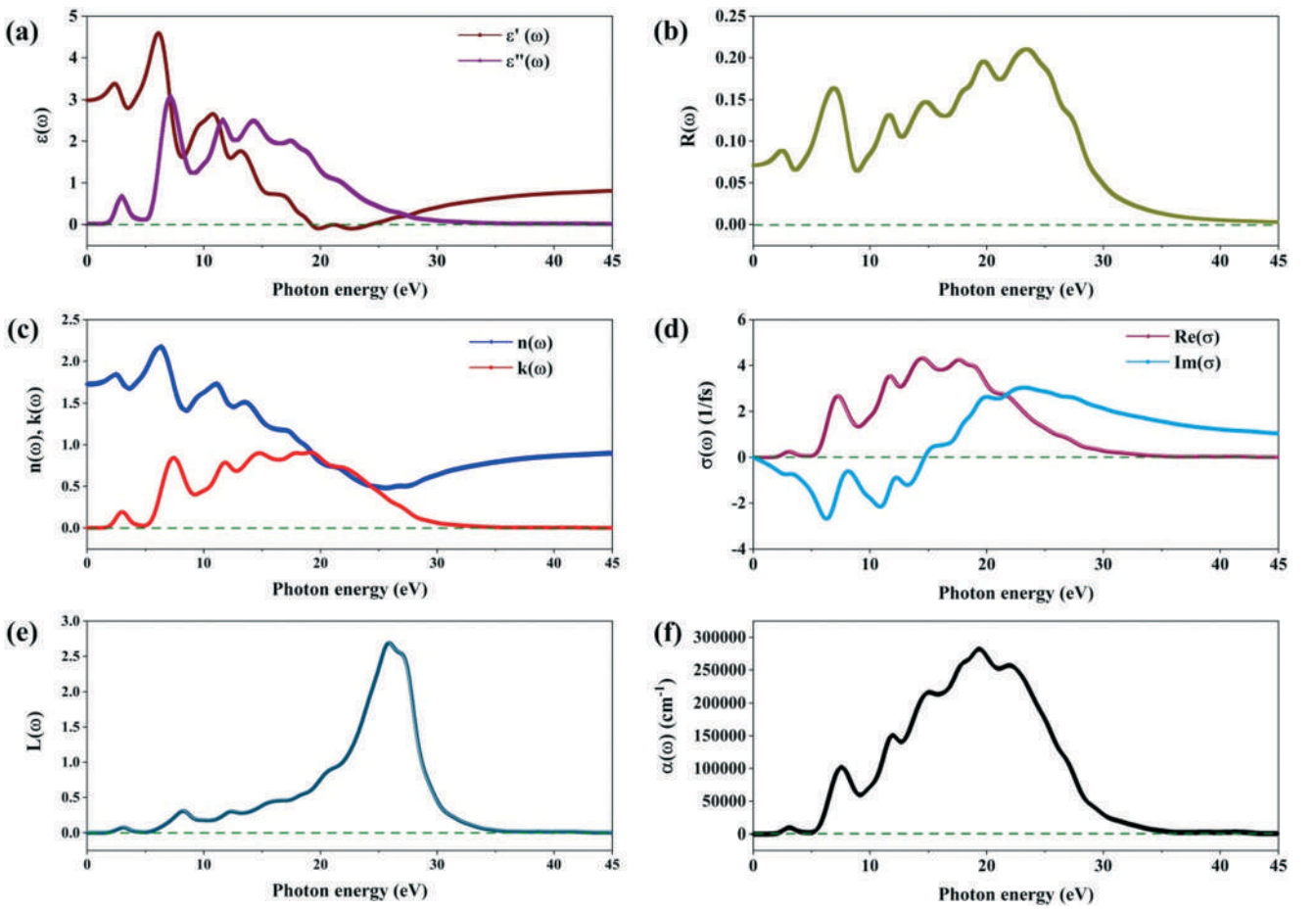

Fig. 10 The plot for (a) dielectric permittivity $\varepsilon(\omega)$; (b) reflectivity $R(\omega)$; (c) refractive index $n(\omega)$ and extinction coefficient $k(\omega)$; (d) optical conductivity $\sigma(\omega)$; (e) energy loss function $L(\omega)$ and (f) absorption coefficient $\alpha(\omega)$ of the co-crystal as a function of photon energy.

The co-crystal shows a non-zero value of refractive index $n(\omega)$ up to 45 eV (Fig. 10(c)). The value of $\varepsilon'(\omega)$ at zero energy ($\varepsilon'(0) = 2.98$) could be used to estimate the refractive index $n(\omega)$ at zero energy using the relationship $n(0) = [\varepsilon'(0)]^{1/2}$ and the estimated value of the static refractive index $n(0)$ for the co-crystal is found to be 1.73. From its zero energy value, the refractive index increases with frequency, reaching the maximum value of 2.17 at 6.23 eV. A value for the refractive index of more than one signifies that when the photons traverse through the material they get slowed down due to their interactions with the electrons. The extinction coefficient $k(\omega)$ (the imaginary part of the complex refractive index) shows two sharp peaks at 3.02 and 7.42 eV and satellite peaks at 11.84, 14.76, 17.94 and 19.13 eV to form a broad band. The $\varepsilon''(\omega)$ and $k(\omega)$ spectra display similar trends (Fig. 10(a) and (c)). The optical conductivity $\sigma(\omega)$ spectrum of the co-crystal is shown in Fig. 10(d). The real part of the complex conductivity exhibits peaks at 3.06, 7.24, 11.70 and 14.46 eV along with shallow shoulders located in the high energy region (~17.60 eV). The maximum value of the conductivity of the co-crystal was achieved at 14.46 eV with a magnitude of 4.32 1/fs.

The energy-loss function $L(\omega)$ (Fig. 10(e)) is an important optical parameter describing the energy loss of a fast moving photon traversing through a material. The peaks in the $L(\omega)$ spectrum represent the characteristics associated with the plasma resonance and the corresponding frequency is called the plasma frequency above which the material is a dielectric insulator [$\varepsilon'(\omega) > 0$] and below which the material behaves as a metal [$\varepsilon'(\omega) < 0$]. For this material the resonant energy loss is manifested by a strong band situated in the energy region 22 to 28 eV composed of peaks located at 20.84 (low intensity), 25.86 (intense peak) and 26.83 eV (shoulder). This region of plasma resonance corresponds to the region in which $\varepsilon'(\omega)$ is negative. Again, the peak for the plasma resonance associated with the $L(\omega)$ spectrum coincides with the trailing edges in the reflectivity spectra. The $\alpha(\omega)$ and $R(\omega)$ spectra are similar in the energy range 2.84 to 45 eV (Fig. 10(f)). In the low energy region distinct sharp peaks are observed at 3.10 and 7.55 eV followed by a strong broad band in the high energy region consisting of peaks located at 11.93 and 15.07 eV with the largest peak at 19.38 eV accompanied by two shoulder peaks at about 18.16 and 21.94 eV.

Electrical transport properties

According to UV-vis spectroscopic study and band structure calculation the co-crystal is a p-type semiconductor. So, to assess the electrical transport properties of the sample we have measured the current–voltage (*I–V*) characteristics of a device made of an ITO/co-crystal/Al sandwich structure (Fig. 11(a)) at room temperature. The *I–V* measurements have been performed in the applied bias voltage range from −2 to +2 V using the two-probe technique with the help of a Keithley 2400 source meter. The SEM micrograph of the active thin film of the co-crystal cast on the ITO surface is shown in Fig. 11(b). The *I–V* characteristic curves of the device in the dark and under visible light illumination are presented in Fig. 11(c). The forward current of the device rises rapidly in a nonlinear fashion while it is very low and remains almost constant in the reversed bias region. The device is displaying rectifying behaviour with on/off ratios of 41 and 56 at ±2 V in the dark and under visible light exposure, respectively. Thus, it is acting like a Schottky barrier diode due to the presence of the semiconducting co-crystal between the electrodes. Further, in the voltage range 0 to 0.8 V (region I) the *I–V* curves of the device under dark conditions and visible light illumination obey the equation $I = C_1 \exp(-C_2)[\exp(C_3V) - 1]$, where C_1, C_2 and C_3 are constants that depend on different parameters of the device, portraying the thermionic emission behaviour of a Schottky barrier diode whereas in the voltage range 0.8 to 2 V (region II) they follow the power law behaviour ($I \propto V^n$, with $n = 2$), manifesting that the space charge limited current (SCLC) controls the electrical transport mechanism of the device in this region (Fig. S25†). This clearly indicates that the device is a Schottky barrier diode.[36] Accordingly, we have analyzed region I using thermionic emission theory to determine the different parameters of the device while in region II, SCLC theory has been employed to estimate the electrical transport parameters of the device.

The values of the ideality factor (η), series resistance (R_s) and barrier height (ϕ_b) of the device have been calculated by analyzing the *I–V* curve of the device in region I in the framework of the model proposed by S. K. Cheung and N. W. Cheung[37] following the methodology reported earlier (details are provided in the ESI†). The effective charge carrier mobility (μ_{eff}), transit time (τ) and carrier concentration (n) of the device have been estimated using the Mott–Gurney law in the SCLC region (region II) following the standard approach described in the literature (details are provided in the ESI†) and utilizing the capacitance *versus* frequency plot of the device (Fig. S26†).[38–40] The values of all the parameters of the device are listed in Table 4. The value of η deviates from its ideal value of unity due to the presence of the series resistance, existence of the interface states and the barrier inhomogeneities.[41,42] Under light exposure, the values of μ_{eff} and n are increased by 54 (±0.5)% and 6 (±0.5)%, respectively, compared to those under dark conditions.

In dark conditions the value of electrical conductivity of the device is found to be 0.56×10^{-5} S m^{-1} and it increases to 0.76×10^{-5} S m^{-1} under light illumination (Table 4). The photo-responsive behaviour of the device has been verified by measuring the transient photocurrent of the device at 2 V under an illumination of 100 mW cm^{-2}. Fig. 11(d) represents the photocurrent (dark currents subtracted) *versus* time graph of the device. The device shows fast and reproducible photo-switching behaviour with light on and off (Fig. 11(d)). Photosensitivity (S) is an important parameter of photosensitive electronic devices and it is calculated with the help of the relationship, $S = (I_L - I_D)/I_D$ (ref. 43) where I_D and I_L are the dark current and photocurrent at +2 V, respectively. The value of S is calculated as 0.45.

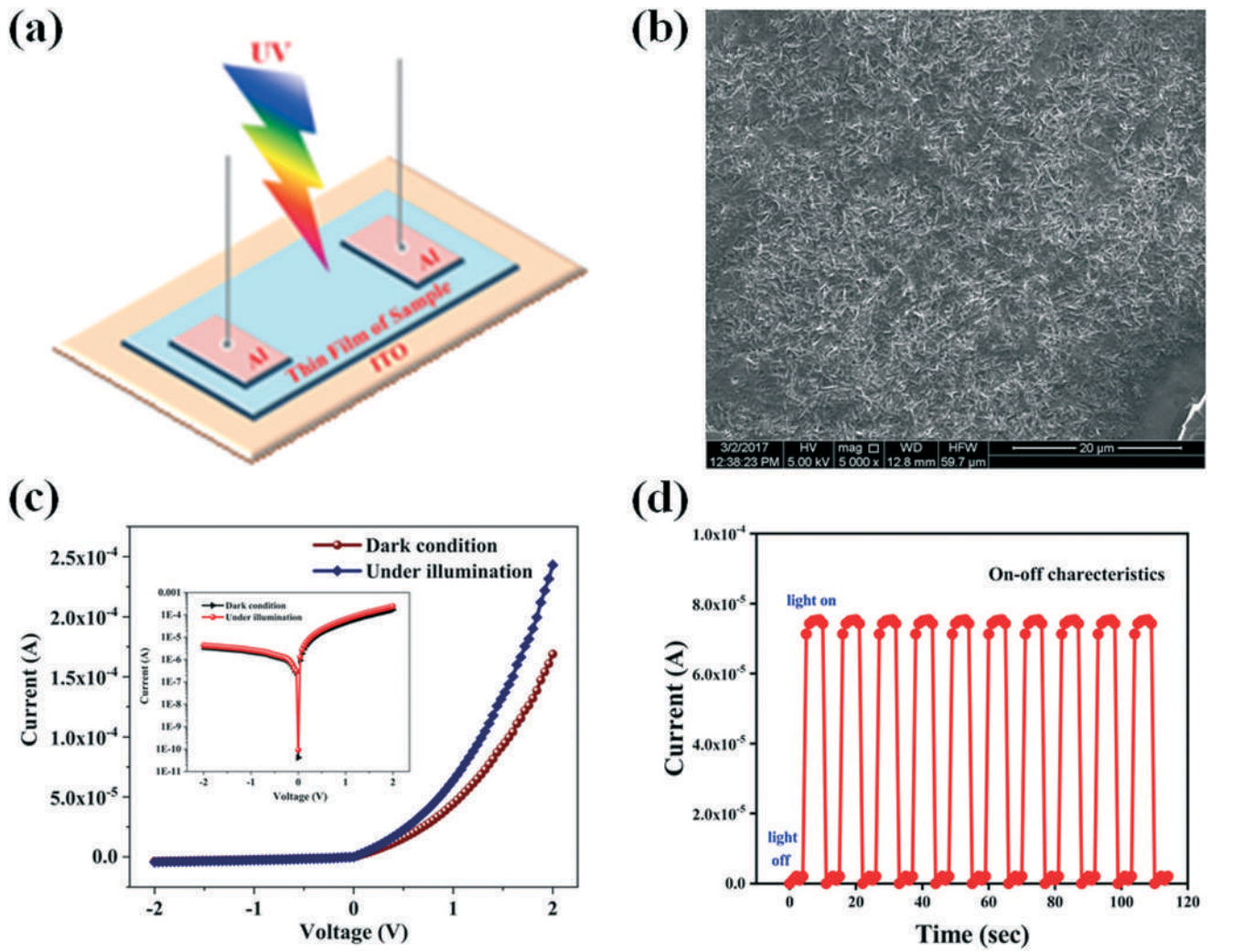

Fig. 11 (a) Schematic representation of the device, (b) SEM micrograph of the semiconducting layer, (c) photoconductive behaviour of the co-crystal, (d) on–off characteristics of the device.

Table 4 Important electrical and charge transport parameters of the Al/co-crystal/ITO device

Condition	On/off	S	η	R_s (kΩ)		Φ_b (eV)	$\sigma \times 10^{-5}$ (s m^{-1})	$\mu_{eff} \times 10^{-7}$ (m^2 V^{-1} S^{-1})	$\tau \times 10^{-7}$ (S)	$n \times 10^{20}$ (eV m^{-3})
				$dV/d\ln I$ *vs.* I	$H(I)$ *vs.* I					
Dark	41	0.45	1.36	26.97	26.50	0.70	0.56	4.44	3.9	3.57
Light	56		1.19	19.72	18.77	0.65	0.76	6.86	2.7	3.79

S: photosensitivity, η: ideality factor, R_s: series resistance, Φ_b: barrier height, σ: conductivity, μ_{eff}: mobility, τ: transit time, n: carrier concentration.

To the best of our knowledge, this is a unique report of a donor–acceptor co-crystal based photo-responsive Schottky barrier diode. The co-crystal acts as a semiconductor because of the presence of weak intermolecular interactions, more specifically π–π interactions, between the donor and acceptor molecules of the co-crystal, which helps in generation of carriers. It may be noted that the conductivity, mobility and carrier concentration of the device increase substantially under visible light illumination compared to the dark condition. This indicates that the co-crystal responds toward the visible light by generating photo carriers.

Theoretical investigation of the ground state energy levels of the frontier molecular orbitals of the hydrogen bonded dimer geometry of the co-crystal reveals that in the self-assembled co-crystal TBTA acts as donor whereas QUIN acts as acceptor when they interact through hydrogen bonding interactions. The Mulliken charge distribution analysis of the hydrogen bonded dimer (Table S11†) clearly indicates that an appreciable amount of charge has been transferred from donor TBTA to acceptor QUIN. Moreover, the MEP analysis has revealed that in the co-crystal the aromatic ring of the QUIN molecule is electron rich (π-e) while the aromatic ring

of TBTA is positively charged and acts as an electron deficient π-hole (π-h) (Fig. S24†). Thus, in the solid state, holes are created in the VB and the co-crystal acts as a p-type semiconductor as the concentration of holes in the VB is greater than the concentration of electrons in the CB. It may therefore be concluded that the π···π and hydrogen bonding interactions together play the key role in assembling the co-crystal and introducing the semiconducting behaviour in it. The weak intermolecular π–π, Br···π and Br···O interactions provide the pathway for electrical conduction.

Optoelectronic behaviour of a material can be understood by correlating the results of optical property analysis and the study of the electrical transport properties under light illumination. The absorption coefficient *versus* photon energy plot indicates the wavelengths prone to photon absorption whereas the optical conductivity *versus* photon energy plot provides the information regarding the change in conductivity due to photon absorption. From the theoretical calculations it has been found that when the co-crystal is exposed to a photon beam, the real part of the complex conductivity exhibits a peak at 3.06 eV and an absorption peak has been observed at 3.10 eV. Further the optical bandgap of the co-crystal is 3.17 eV and the calculated electronic bandgap is 2.835 eV. All these results together indicate that when the co-crystal is exposed to visible light it absorbs photons with energy ∼3 eV (the blue-violet region of visible light) and its conductivity increases in consequence of the photon absorption. It may be inferred that the bandgap energy is appropriate for transferring the electrons from the valence band to conduction band by absorbing the photons in the blue-violet region of the visible beam of light. Thus, holes are generated in the valence band and electron concentration in the conduction band increases. Therefore while performing the *I–V* measurements under visible light illumination, carriers have been generated due to the photo-responsive behaviour of the co-crystal. This leads to an increase in carrier concentration and subsequently the conductivity of the sample. Further NTO analysis reveals the presence of excitons in the sample. Thus there is another possibility that under visible light illumination the excitons in the co-crystal absorb energy from the incident photon beam and it breaks into electrons and holes and as a result the carrier concentration increases.

Conclusion

We have thoroughly examined the crystal structure, supramolecular structure, noncovalent interactions, band structure, optical properties, electronic transport mechanism and photo-responsive behaviour of a donor–acceptor co-crystal assembled by mainly π···π stacking and hydrogen bonding interactions along with minute contribution from halogen interactions. In conclusion, it has been shown that (i) apart from CT interaction, π···π and hydrogen bonding interactions can play a crucial role in formation of D–A type co-crystals, (ii) the co-crystal emits blue light under UV irradiation, (iii) a device fabricated with the co-crystal exhibits Schottky barrier diode behaviour and photo-responsive properties, (iv) the conductivity, mobility and carrier concentration of the co-crystal increase significantly upon visible light illumination, (v) π···π and hydrogen bonding interactions together can incorporate semiconducting behaviour, (vi) weak intermolecular π···π, Br···π and Br···O interactions provide the pathway for electrical conduction and (vii) in this sample carriers have been generated by transfer of electrons from the valence band to the conduction band or formation of electron/hole pairs by disintegration of excitons upon photon absorption.

Conflicts of interest

The authors declare no competing financial interest.

Acknowledgements

SS gratefully acknowledges DST, Govt. of India for providing a fellowship under the DST INSPIRE program. The PURSE and FIST programs of DST, Govt. of India are also acknowledged. Financial support from the UGC, New Delhi, DST, Govt. of India, through DRS (SAP-I) and FIST programs to Department of Physics, Jadavpur University are also acknowledged. RS also acknowledges SERB, Government of India for SERB-TARE project (File No: TAR/2018/000744).

References

1 C. Wang, H. Dong, L. Jiang and W. Hu, *Chem. Soc. Rev.*, 2018, **47**, 422–500.
2 D. Yang and D. Ma, *Adv. Opt. Mater.*, 2019, **7**, 1800522.
3 E. Orgiu, N. Crivillers, M. Herder, L. Grubert, M. Patzel, J. Frisch, E. Pavlica, D. C. Duong, G. Bratina, A. Salleo, N. Koch, S. Hecht and P. Samori, *Nat. Chem.*, 2012, **4**, 675–679.
4 M. Chaudhry, K. Muhieddine, R. Wawrzinek, J. Li, S. Lo and E. Namdas, *ACS Photonics*, 2018, **5**, 2137–2144.
5 Y. Yamamoto, G. Zhang, W. Jin, T. Fukushima, N. Ishii, A. Saeki, S. Seki, S. Tagawa, T. Minari, K. Tsukagoshi and T. Aida, *Proc. Natl. Acad. Sci. U. S. A.*, 2009, **106**, 21051–21056.
6 G. R. Desiraju, *Crystallogr. Rev.*, 2020, **26**, 64–65.
7 R. Thakuria, N. K. Nath and B. K. Saha, *Cryst. Growth Des.*, 2019, **19**, 523–528.
8 Y. Liu, Q. Zeng, B. Zou, Y. Liu, B. Xu and W. Tian, *Angew. Chem., Int. Ed.*, 2018, **57**, 15670–15674.
9 X. D. Wang, Z. Z. Li, M. P. Zhuo, Y. Wu, S. Chen, J. N. Yao and H. B. Fu, *Adv. Funct. Mater.*, 2017, **27**, 1703470.
10 M. Zhuo, Y. Tao, X. Wang, Y. Wu, S. Chen, L. Liao and L. Jiang, *Angew. Chem.*, 2018, **130**, 11470–11474.
11 S. J. Kang, S. Ahn, J. B. Kim, C. Schenck, A. M. Hiszpanski, S. Oh, T. Schiros, Y. Loo and C. Nuckolls, *J. Am. Chem. Soc.*, 2013, **135**, 2207–2212.
12 A. Mandal, A. Choudhury, P. K. Iyer and P. Mal, *J. Phys. Chem. C*, 2019, **123**, 18198–18206.
13 N. Yee, A. Dadvand and D. F. Perepichka, *Mater. Chem. Front.*, 2020, **4**, 3669–3677.

14 K. K. Ray, G. Campillo-Alvarado, H. Morales-Rojas, H. Höpfl, L. R. MacGillivray and A. V. Tivanski, *Cryst. Growth Des.*, 2020, **20**, 3–8.
15 S. Singha, S. Goswami, S. K. Dey, R. Jana, P. P. Ray, I. Saha, C. Rizzoli, P. Bag, S. Kumar and R. Saha, *CrystEngComm*, 2020, **22**, 8197–8207.
16 Z. Wang, F. Yu, J. Xie, J. Zhao, Y. Zou, Z. Wang and Q. Zhang, *Chem. – Eur. J.*, 2020, **26**, 3578–3585.
17 S. K. Park, J. H. Kim, T. Ohto, R. Yamada, A. O. F. Jones, D. R. Whang, I. Cho, S. Oh, S. H. Hong, J. E. Kwon, J. H. Kim, Y. Olivier, R. Fischer, R. Resel, J. Gierschner, H. Tada and S. Y. Park, *Adv. Mater.*, 2017, **29**, 1701346.
18 F. Cicoira and C. Santato, *Adv. Funct. Mater.*, 2007, **17**, 3421.
19 D. Liu, J. De, H. Gao, S. Ma, Q. Ou, S. Li, Z. Qin, H. Dong, Q. Liao, B. Xu, Q. Peng, Z. Shuai, W. Tian, H. Fu, X. Zhang, Y. Zhen and W. Hu, *J. Am. Chem. Soc.*, 2020, **142**, 6332–6339.
20 X. D. Wang, Z. Z. Li, M. P. Zhuo, Y. Wu, S. Chen, J. N. Yao and H. B. Fu, *Adv. Funct. Mater.*, 2017, **27**, 1703470.
21 W. Yu, X. Wang, J. Li, Z. Li, Y. Yan, W. Wang and J. Pei, *Chem. Commun.*, 2013, **49**, 54–56.
22 C.-H. Liu, M. R. Niazi and D. F. Perepichka, *Am. Ethnol.*, 2019, **131**, 2–11.
23 H. Zhang, L. Jiang, Y. Zhen, J. Zhang, G. Han, X. Zhang, X. Fu, Y. Yi, W. Xu, H. Dong, W. Chen, W. Hu and D. Zhu, *Adv. Electron. Mater.*, 2016, **2**, 1500423.
24 J. Tsutsumi, T. Yamada, H. Matsui, S. Haas and T. Hasegawa, *Phys. Rev. Lett.*, 2010, **105**, 226601.
25 G. Griffini, L. Brambilla, M. Levi, C. Castiglioni, M. Del Zoppo and S. Turri, *RSC Adv.*, 2014, **4**, 9893–9897.
26 T. Goh, J.-S. Huang, K. G. Yager, M. Y. Sfeir, C.-Y. Nam, X. Tong, L. M. Guard, P. R. Melvin, F. Antonio, B. G. Bartolome, M. L. Lee, N. Hazari and A. D. Taylor, *Adv. Energy Mater.*, 2016, **6**, 1600660.
27 S. J. Kang, S. Ahn, J. B. Kim, C. Schenck, A. M. Hiszpanski, S. Oh, T. Schiros, Y. Loo and C. Nuckolls, *J. Am. Chem. Soc.*, 2013, **135**, 2207.
28 L. Sun, W. Zhu, F. Yang, B. Li, X. Ren, X. Zhang and W. Hu, *Phys. Chem. Chem. Phys.*, 2018, **20**, 6009–6023.
29 W. Zhu, X. Zhang and W. Hu, *Sci. Bull.*, 2021, **66**, 512–520.
30 W. Zhu, Y. Yi, Y. Zhen and W. Hu, *Small*, 2015, **11**, 2150–2156.
31 W. Zhu, R. Zheng, X. Fu, H. Fu, Q. Shi, Y. Zhen, H. Dong and W. Hu, *Angew. Chem., Int. Ed.*, 2015, **54**, 6785–6789.
32 W. Zhu, L. Zhu, Y. Zou, Y. Wu, Y. Zhen, H. Dong, H. Fu, Z. Wei, Q. Shi and W. Hu, *Adv. Mater.*, 2016, **28**, 5954–5962.
33 T. Wakahara, K. Nagaoka, A. Nakagawa, C. Hirata, Y. Matsushita, K. Miyazawa, O. Ito, Y. Wada, M. Takagi, T. Ishimoto, M. Tachikawac and K. Tsukagoshi, *ACS Appl. Mater. Interfaces*, 2020, **12**(2), 2878–2883.
34 X.-G. Yang, Z.-M. Zhai, X.-M. Lu, L.-F. Ma and D. Yan, *ACS Cent. Sci.*, 2020, **6**, 1169–1178.
35 W. Yu, X. Wang, J. Li, Z. Li, Y. Yan, W. Wang and J. Pei, *Chem. Commun.*, 2013, **49**, 54.
36 S. K. Dey, R. Saha, S. Biswas, A. Layek, S. Middya, I. M. Steele, M. Fleck, P. P. Ray and S. Kumar, *Cryst. Growth Des.*, 2014, **14**, 207–221.
37 S. K. Cheung and N. W. Cheung, *Appl. Phys. Lett.*, 1986, **49**, 85–87.
38 N. F. Mott and R. W. Gurney, *Electronic Processes in Ionic Crystals*, Clarendon Press, Oxford, 1940.
39 J. A. Röhr, D. Moia, S. A. Haque, T. Kirchartz and J. Nelson, *J. Phys.: Condens. Matter*, 2018, **30**, 105901.
40 A. Dey, A. Layek, A. Roychowdhury, M. Das, J. Datta, S. Middya, D. Das and P. P. Ray, *RSC Adv.*, 2015, **5**, 36560–36567.
41 R. K. Gupta and F. Yakuphanoglu, *Sol. Energy*, 2012, **86**, 1539–1545.
42 M. Das, J. Datta, A. Dey, R. Jana, A. Layek, S. Middya and P. P. Ray, *RSC Adv.*, 2015, **5**, 101582–101592.
43 R. Jana, A. Dey, M. Das, J. Datta, P. Das and P. P. Ray, *Appl. Surf. Sci.*, 2018, **452**, 155–164.

Message of Indian Philosophy to the World Today

By Anita Shaw, Asst. Professor, Dept. of Philosophy, Nistarini College, Purulia.

Indian civilization is more than five thousand years old. During this long period, it produced a unique type of highly advanced and variegated culture. In spite of the innumerable regional, social and linguistic diversities of the country, there has always been a basic unity in Indian culture. Moreover, this culture maintained unbroken continuity from Vedic times to the present day, in spite of countless wars within the country, invasions from outside and two centuries of subjugation by the British. This indestructible unity and unbroken continuity of Indian culture are derived from its deep spiritual foundations.

Swami Vivekananda has pointed out that every civilization or culture has a particular life-centre, a dominant characteristic or trend. According to him the life-centre of Indian culture is spirituality. By spirituality is meant a way of life oriented to the ultimate purpose or goal of life which is the realization of the Supreme Spirit or God. Indian spirituality is deeply rooted in the ancient philosophical and religious traditions of the land. Philosophy arose in India as an enquiry into the mystery of life and existence. A parallel situation arose in ancient Greece also. But, as Swami Vivekananda pointed out, the Greek philosophers confined their enquiries to the external world, and the method they employed was only speculation, whereas in India philosophical enquiries were carried out in the inner world. Indian sages, called *Rishis* or 'seers', developed special techniques of transcending the senses and the ordinary mind, collectively called Yoga. With the help of these techniques they dived deep into the depths of consciousness and discovered important truths about the true nature of man and the universe.

The sages found that man's true nature is not the body or the mind, which are ever changing and perishable, but the spirit which is unchanging, immortal, pure consciousness. They called it the Atman. The Atman is man's true Self, the true knower, the true source of man's knowledge, happiness and power. The *Rishis* further found that all individual selves are parts of infinite Consciousness which they called Brahman. Brahman is the ultimate Reality, the ultimate cause of the universe. Ignorance of man's true nature is the main cause of human suffering and bondage. By gaining correct knowledge of *Jivatman* and Brahman it is possible to become free from suffering and bondage and attain a state of immortality, everlasting peace and fulfilment known as *Mukti* or liberation. Religion in ancient India meant a way of life which enabled man to realize his true nature and attain *Mukti***.**

Thus, philosophy provided a correct view of Reality, while religion showed the correct way of life; philosophy provided the vision, while religion brought about the fulfilment; philosophy was the theory, and religion was the practice. Thus, in ancient India, philosophy and religion complemented each other. In fact, they together constituted a single endeavour, an integral discipline. This integral religious philosophy or philosophical religion was called *Vedanta*. The term *Vedanta* comes from the fact that its basic principles constitute the last part or culmination of the ancient scriptures known as the *Vedas*. The *Vedas* are the oldest and most authoritative scriptures of Hinduism. All other scriptures are subordinate to them. They were not composed by anybody but were 'revealed' to the *Rishis*; hence they are also called '*Shruti*', 'that which is heard'. The earlier part of the *Vedas* may have been composed between 2000 B.C. and 1000 B.C. There are four *Vedas*: *Rig-veda, Yajur-veda*, *Sama-veda* and *Atharva-veda*. Each of these has four divisions**:** *Samhita***,** *Brahmana***,** *Aranyaka* and *Upanishads***.** *Samhita* is the collection of hymns addressed to various deities. Many of these hymns have deep mystical significance. *Brahmana* deals with various rituals and also with moral principles. *Aranyaka* contains various meditations. Some of these meditations are mental recreations of external rituals. *Upanishads* are the records of the transcendental experiences gained by *Rishis* by following different contemplative techniques. These experiences are actually revelations about *Atman, Brahman* and other eternal, universal truths regarding the ultimate Reality. These eternal truths and principles of the spiritual world, lying scattered in the Upanishads, were brought together and codified by Badarayana in the form of *sutras* or aphorisms in the 5^{th} century B.C. These *sutras* known as *Brahmasutras* form the foundation of the system of philosophy known as *Vedanta-Darshana*.

In this connection it should be pointed out that five more systems of philosophy arose in India in the early centuries of the Christian era. These are:

1) *Sankhya*, founded by Kapila
2) *Yoga*, founded by Patanjali
3) *Nyaya*, founded by Gautama
4) *Vaisheshika*, founded by Kanada
5) *Mimamsa*, founded by Jaimini

Vedanta alone remained the main philosophy of India from the *Vedic* period, and *Vedanta* alone got identified with the religion of the land. *Vedanta* is understood as both philosophy and religion. This combined religious and philosophical tradition of India came to be called ***Sanatana Dharma*****, "**Eternal Religion**"** and, still later, as Hinduism.

Although the Upanishads constitute the original and most authoritative source of *Vedanta*, they are not the only scripture of *Vedanta*. Several other books also came to be accepted as authoritative. Among these, the most important one is *Bhagavad-Gita*. It introduced several new concepts into *Vedanta* such as God incarnating Himself as the *Avatara* age after age, devotion to personal God as means to *Mukti*, discharging one's duties of life in a spirit of selflessness and self-surrender to God as a spiritual path, and so on. Over the centuries great teachers like Shankara, Ramanuja, and great saints of medieval period enriched *Vedanta* with philosophical concepts and devotional songs.

The Indian sages of antiquity believed that philosophy was an essential and practical element necessary to lead an optimised life. Therefore, philosophy had to be explained in terms of how it served the purpose of living. At the same time, Indian philosophy applies enormous analytical rigour to solving metaphysical problems, and goes into details regarding the function of the human mind and its relationship with 'reality'. These analyses were also tempered by the underlying belief that there was a fundamental and unitary order in the universe—all pervasive and omniscient. Most of the Indian philosophical schools concentrated on explaining the existence of such an order and the extraordinary entity at the centre of it that was the sole source that created the universe.

The Indian approach to philosophy illustrates an inherent dichotomy in the overall socio-religious system that was has been prevalent in the country from *Vedic* times. This system, while being reorganized through social experiments in modern India, still holds firm in the Indian psyche, manifesting itself in myriad subtle and not so subtle ways in the daily life of the modern nation. On the one hand, the Indian social structure is essentially communal with the society subsuming the individual as part of a group, the basic unity of the system being the joint family. The joint family system was designed to ensure that the weak and incompetent members, including the sick and the aged, were looked after and therefore inherently favored the weak. The corollary was that it hindered the strong from forging ahead since any chain is only as strong as its weakest link. This situation inhibited adventurous Endeavour and brought about a gradual acceptance and subsequent entrenchment of mediocrity across all levels of society. Even the much-maligned caste system was an off-shoot of this group dynamics. On the other hand, Indian philosophy is highly individualistic and deals mainly with the growth of an individual's personality towards inner perfection. Philosophy provided the outlet to a person for free thinking and development of ideas, essentially the freedom to believe. In a paradoxical manner this process was also required to confirm to the societal norms, although the more renowned thinkers, mainly sages and seers, broke free of these restrictive chains. The third phase of *Vedanta* was inaugurated by Sri Ramakrishna and Swami Vivekananda in the 19th century. During this period *Vedanta* was transformed from an ethnic religious philosophy into a universal philosophy of life.

Sri Ramakrishna is the real link between ancient India and modern India. Through stupendous spiritual efforts Sri Ramakrishna revealed the entire range of spiritual experiences of the sages and saints of the past from *Vedic* times to his times. He thereby re-established the truths of *Vedanta*. He traversed the paths of *Vedic*, Shaiva, *Shakta* and *Vaishnava* traditions, including obscure and forgotten paths. He brought about the purification of spiritual life by emphasizing its moral foundation, and rejecting occultism, mysticism and miracle-mongering. He made God realization possible for all even in the midst of the distractions of the modern world. He imparted tremendous encouragement to the efforts to realize God. All this has resulted in a thorough rejuvenation of *Vedanta* in modern times.

Another modern sage, Swami Vivekananda's great work was to make ancient *Vedantic* concepts acceptable to modern minds by interpreting the eternal truths in the light of modern rational thought and science. This modernized version is what most of the present-day educated Hindus understand by *Vedanta*. *Vedanta* had split into different schools in the Middle Ages. Swami Vivekananda brought about the reintegration of these schools. He did this by stressing the common ground of different schools, especially the principle of *Atman*, and by showing that the different schools represent different stages of realization of the ultimate Reality.

Sri Ramakrishna taught, from his realization, that all spiritual paths lead to the same ultimate goal, *Yato mat tato path*. "As many views, so many paths to God". This principle, which forms the basis of his doctrine of *dharma-samanvaya* or Harmony of Religions, came to be applied within Hinduism itself in due course. This has given rise to a sense of unity among Hindu sects in modern times, in spite of many differences in customs and traditions. Till the eleventh century A.D. the only challenges *Vedanta* had to face were internal; these came mainly from Buddhism and Jainism and from dissensions of different schools of *Vedanta* and sects of Hinduism each of which claimed superiority over the others. From the thirteenth century Islam began to exert its influence on Indian society in a big way. Many great saints then arose in different parts of India and responded to the Islamic challenge by spreading the ideas of oneness of God, brotherhood of man and social equality among the common people.
However, the greatest challenge Indian society ever faced came from Western culture in the eighteenth and nineteenth centuries. Western culture brought three major challenges to Indian society, which were: (1) modern rational thought and science puzzled the Indian culture, (2) an open society which values freedom and social justice, and (3) the idea of a saviour God who identifies himself with the poor, the sick and the fallen.

Sri Ramakrishna and Swami Vivekananda met these Western challenges by revitalizing *Vedantic* spirituality, by interpreting the eternal truths of *Vedanta*, discovered by the ancient sages, in the light of modern rational thought, and by introducing a new gospel of social service based on the practical application of *Vedantic* principles in day-to-day life. By "Practical Vedanta" is meant the practical application of the basic principles of *Vedanta* in solving the problems of day-to-day life. For centuries *Vedantic* principles were intended only to help people to attain *Mukti* or liberation. Swami Vivekananda, however, showed that the highest principles of *Vedanta* can be applied even in ordinary life to solve the day-to-day problems of life. *Vedantic* principles can be applied not only in individual life but also in social life. In fact, Swamiji held that India's downfall took place mainly because the eternal spiritual principles were not applied in collective life.

For many centuries the essential, basic truths of *Vedanta* remained bound up with innumerable beliefs, myths, customs, castes, etc. Moreover, the higher truths of *Vedanta* were available only to a small group of privileged people, and it was believed that to follow the principles of *Vedanta* one had to be born in a certain Hindu caste. Sri Ramakrishna and Swami Vivekananda separated the essential truths of *Vedanta* from the non-essentials. Swamiji showed that the essential truths of *Vedanta* constitute the eternal, universal truths of the spiritual world which form the rationale and basis of all the religions of the world. As a matter of fact, the eternal principles of *Vedanta* themselves constitute the Universal Religion of all mankind, and the different religions of the world are only manifestations of this Universal Religion in different places and times. Furthermore, through his lectures and books and through the *Vedanta* Centres which he founded, Swamiji made the life-giving principles of *Vedanta* available to all people without any distinction of caste, creed or race.

In this way, through the pioneering efforts of Swami Vivekananda, *Vedanta* has crossed the boundaries of India and has now become the common property of all mankind. The work started by Swamiji is now being carried on by many teachers and organizations around the world
Swami Vivekananda that, "Education is the manifestation of perfection already in man". He said that education which does not enable a person to stand on his own feet, does not teach him self-confidence and self-respect, is useless. Education should be man-making, life giving and character-building. He also said that children should be given "positive education", i.e they should be encouraged to learn new things till they gain self-confidence and self-respect. Since a country's future depends on the character of its people, Vivekananda stressed on character building education, he called it "man-making". According to Vivekananda, *Jiva* is *Shiva* or every man is potentially Divine. To become divine (or great), man must give

up suspicion, jealousy, conceit and learn to work unitedly for the common good. Courage, faith in oneself and in God, patience and steady work, according to Swami Vivekananda, is the way to success. He told that purity, patience and perseverance overcome all obstacles.

Swami Vivekananda said that since the a*tman* (soul) has neither sex nor caste, it is wrong to discriminate between sexes. He suggested not thinking of people as men and women, but as human beings. According to Vivekananda, there is no chance for welfare in the world unless the condition of woman is improved. He felt that it was impossible to get back India's lost pride and honour unless the condition of women was improved. According to Vivekananda, the ideal of womanhood in India is motherhood and that Sita was the ideal of Indian womanhood. Vivekananda lived at a time when India was quite backward and that many improvements have taken place since that time. Let us now look at what has changed and how much has changed in Indiain society. Consider the following statistics of the present-day:

Education: -- It is estimated that, 60 million children out of around 200 million children in the 6-14 years age group, in India, are not in school, and that, even of those children enrolled in school, only 47 out of 100 children enrolled in class I reach class VIII, putting the dropout rate at 52.78%. The figures for female literacy, male literacy, youth literacy and adult literacy are respectively, 65.46%, 82.14%, 82%, 74.04%. The stated figures are only for Primary Education (10th Std. and below), with the figures for Senior Secondary Education, Degree Education and higher being much worse (in single digits!). State wise, Kerala is the most literate state in India (almost 100% literacy), while Bihar is the least literate (63%).

Health: -- India's fares quite poorly in Health, by world standards. Indian children make up one-third of the world's malnourished children. 75% of Indian women suffer from Anaemia. Every year, HIV/AIDS, Malaria, TB, Polio, Diarrhoea, Respiratory infections, Pneumonia and other diseases claim thousands of lives. Infant mortality, maternal health and issues related to child protection, including trafficking and child labour are other serious health concerns.

Water crisis: -- As per the 2010 UN estimates, 626 million people in India (>60%) has practice of open defecation which leads to a very high risk of microbial contamination (bacteria, viruses, amoeba) of water that cause water-borne diseases. India has one of the highest numbers of people in the world without continuous access to water. According to Water Aid, an international NGO, by 2015, 29% of the rural population or 244 million people, and 23% of the urban population or 90 million people, would lack access to adequate safe, sustainable water. Even major cities and urban areas face shortage of continuous water supply. It is said that 13% of Delhi's citizens do not get water supply every day and 40% of households in Madhya Pradesh are not supplied even 40 litres per person per day.

Corruption: -- Corruption, in the form of bribes, evasion of tax, embezzlement, need of paying bribe or peddling influence to get a job done in a public office, is widespread in India. India is ranked 95 out of 179 countries in Transparency International's Corruption survey.

Violence: -- Women and children in India today leave under deplorable conditions. Trust Law, a news service run by Thomson Reuters, has ranked India as the worst G20 country in which to be a woman. Female foeticide, domestic violence, sexual harassment, emotional abuse, inadequate healthcare, inequality, dowry deaths, rape and other forms of gender-based violence constitute the reality of most girls' and women's lives in India. Rape is one of the most common crimes against women and is seen as a "national problem" in India. With more than 24,000 reported cases in 2011 alone, the number of rape cases in India has doubled between 1990 and 2008. Deep-rooted social attitudes, deeply entrenched patriarchy, widespread misogyny and a strong preference for sons over daughters are believed to be at the root of bad treatment of women in India.

Although India is constitutionally a secular state, incidents of large-scale communal and caste-based violence occur from time to time. Major religious violent incidents include the Kashmir insurgency, Punjab insurgency, Delhi serial blasts and anti-Sikh riots, Ayodhya violence (1996), Bombay Riots and bombings (1992/1993), Gujarat violence (2002), Amarnath piligrimage massacre (2000), attacks against Christians in Orissa and Karnataka, Naxal violence in West Bengal, Chhatisgarh, Andhra Pradesh, violence against Dalits & other minorities etc.

What inference can we draw from above figures for our country? Let us ask ourselves: Are the problems of our country related only to poverty, population and inadequate natural resources? What really is our understanding of the core human values viz. respect for women, social equality, individual freedom and justice for all citizens, tolerance towards other castes and religions, basic hygiene, purpose of education? Have we really understood Vivekananda? How much has changed at the basic levels of society during the last 150 years? Are we indeed on the path of improvement?

Let us reconsider once more the most important problems that we, as a nation, are facing. Water and sanitation, Literacy, Equitable distribution of food, Unemployment, Violence, slowly degrading Environment, Population growth, Pseudo-democracy, Corruption in most public systems, very limited opportunities for youth to pursue Higher Education or Research, highly inefficient or inadequate Public Health system, need to pay high price even for essential commodities and so on. Let us now try to develop a template for solving above problems based on Vivekananda's teachings. To solve the problems, we need to not only look at them from the National perspective, but also consider how they have to be implemented at the grass-roots level i.e., what needs to happen at the level of villages if it concerns a Taluk, at the level of localities if it is a city, at the level of families/households, at the level of ordinary people.

Consider a grass-roots level project such as the building of a hospital or the implementation of a modern curriculum for children in a remote village. Its implementation will involve the following phases:

(1) A satisfactory and feasible solution has to be designed considering all details.
(2) Moral values should be included in the syllabus from the very beginning of the educational life of the students.
(2) The Government must frame policies that are fair to all. Then, it must authorize the project and then, it must promptly dispatch money, raw material, resources and expertise to the work-spot.
(3) The ordinary people and community involved in the project have to play their role by following Vivekananda's teachings i.e., display the spirit of service, show due regard for divinity of fellow Atman, perform an unselfish action, etc.

The project will be implemented if all phases proceed quickly and smoothly. Hence, it should be clear from the above template that any grass-roots level project can be successfully implemented if everyone thinks pure thoughts and plan and discharge all their duties with a pure heart. Indeed, this is what all our leaders – Ishwara Chandra Vidyasagar, Rabindranath Tagore, Pt. Madan Mohan Malaviya, Sarojini Naidu, Mahatma Gandhi, Maulana Abul Kalam Azad, Jawaharlal Nehru, Lal Bahadur Shastri, – strived to achieve. They worked for the eradication of caste barriers, spread of education, socioeconomic development, emancipation of the weak and suffering, the nurturing of public works and industries and for the building of a strong, vibrant nation. Why are we then a "developing nation" even today? Are all of us working selflessly and unitedly for the common good, performing only pure actions with the spirit of service, with compassion and with due regard for the divinity of fellow *atmans*, as taught by Swami Vivekananda?

I said before that our country is near ruins. I'd like to conclude this essay by suggesting how things can be turned round. I will mention two recent examples that highlight the power of public rallies, Satyagraha and Social movements. Anna Hazare's call for "Anti-corruption Satyagraha" received widespread support from thousands of people all across India, forcing the Government of India to table the Lokpal Bill (Anti-corruption Bill) in Rajya Sabha. International reaction and nationwide protests demanding justice and more protection for women in the wake of the death of Damini, the Delhi gang-rape victim, prompted Central and several State Governments to immediately announce several steps to ensure more safety of women. In India today, Public rallies and Satyagrahas are the most effective ways of raising awareness and mobilizing support for social causes. Hence, more such social movements, public demonstrations and Satyagrahas are needed to create awakening among people on the basic issues or problems that we are facing. More and more Indian youth must enthusiastically organize and participate in Satyagrahas. More and more youth must volunteer to work in NGOs. The present time is the time for action for all Indians! In Swami Vivekananda's words: "Go, all of you, wherever there is an outbreak of plague or famine, or wherever the people are in distress, and mitigate their sufferings…… Die you must, but have a great ideal to die for and, it is better to die with a great ideal in life…. On you lies the future hope of our country. Set yourselves to work – to work!" There is a lot of work to do and the ball is squarely in the court of India's young men and women. If

all we were to follow Vivekananda's teachings, if all were to serve the country in this time of its need, we will achieve the ultimate goal that is Shiva or Brahman or liberation in true sense.

Bibliography

1. Eight Upanisads, Vol. 1, trans. Swami Gambhirananda Calcutta: Advaita Ashram, 1952.
2. Joshi, Kireet, The Veda and Indian Culture, New Delhi, Rashtriya Veda Vidya Pratisthan, 1992.
3. Krishnamurti, J, Education and the Significance of Life, San Francisco: Harper & Row, 1981.
4. Altekar, A.S., Education in Ancient India, New Delhi, Motilal Banarsidas Pub.1943.
5. "Complete Works of Swami Vivekananda", in 9 Volumes
6. "The Legacy of Vivekananda", Frontline February 2013 issue.
7. Data from websites of following Organizations: UNICEF, UNESCO, WHO and Wikipedia.

Intuition includes Experience—an explanation after S. Radhakrishnan

By Dr. Anita Shaw, Asst. Professor, Dept. of Philosophy, Nistarini College, Purulia.

Email ID – anitashaw1973@gmail.com

Sarvapalli Radhakrishnan is a versatile genius, universally recognised as teacher, scholar, and administrator, as philosopher, statesman, and India's cultural ambassador throughout the world. His deep learning and his absolute tolerance have brought him recognition not only as the greatest interpreter of Indian philosophy, religion, and culture, but also as an original and creative thinker of the first order. Radhakrishnan located his metaphysics within the Advaita (non-dual) Vedanta tradition (*sampradaya*). And like other Vedantins before him, Radhakrishnan wrote commentaries on the *Prasthanatraya* (that is, main primary texts of Vedanta): the *Upanisads* (1953), *Brahma Sutra* (1959), and the *Bhagavadgita* (1948).

I like to focus on Radhakrishnan's understanding of intuition and his interpretations of experience. It begins with a general survey of the variety of terms as well as the characteristics Radhakrishnan associates with intuition. For Radhakrishnan, intuition is an "integral experience". Radhakrishnan uses the term "integral" in at least three ways. First, intuition is integral in the sense that it coordinates and synthesizes all other experiences. It integrates all other experiences into a more unified whole. Second, intuition is integral as it forms the basis of all other experiences. In other words, Radhakrishnan holds that all experiences are at beginning intuitional. Third, intuition is integral in the sense that the results of the experience are integrated into the life of the individual. For Radhakrishnan, intuition finds expression in the world of action and social relations.

For Radhakrishnan, intuition is a distinct form of experience. Intuition is self-established (*svataḥsiddha*), self-evidencing (*svāsaṃvedya*), and self-luminous (*svayaṃ-prakās*). Intuition entails pure comprehension, entire significance, and complete validity. It is both truth-filled and truth-bearing. Intuition is its own cause and its own explanation. It is a positive feeling of calm and confidence, joy and strength and above all it is sovereign. For Radhakrishnan intuition is the ultimate form of experience. It is ultimate in the sense that intuition constitutes the fullest and therefore the most authentic realization of the Ultimate Reality (*Brahman*). According to Radhakrishnan, the ultimacy of intuition is also accounted because it is the ground of all other forms of experience.

Finally, intuition, according to Radhakrishnan, is inexpressible. It escapes the limits of language and logic, and there is "no conception by which we can define it". While the experience itself transcends expression. The provocation of expression is, for Radhakrishnan, testimony to the creative impulse of intuition. All creativity and indeed all progress in the various spheres of life is the inevitable result of intuition.

1) Cognitive Experience

According to Radhakrishnan the other forms of experiences are cognitive, psychic, aesthetic, ethical and religious. Radhakrishnan recognizes three categories of cognitive experience: sense experience, discursive reasoning, and intuitive apprehension. For Radhakrishnan all of these forms of experience

contribute, in varying degrees, to a knowledge of the real (*Brahman*), and as such have their basis in intuition.

- ***Sense Experience***

Of the cognitive forms of knowledge, Radhakrishnan suggests that sensory knowledge is in one respect closest to intuition, for it is in the act of sensing that one is in "direct contact" with the object. Sense experience "helps us to know the outer characters of the external world. By means of it we acquire an acquaintance with the sensible qualities of the objects". "Intuitions," Radhakrishnan believes, "are convictions arising out of a fullness of life in a spontaneous way, more akin to sense than to imagination or intellect and more inevitable than either". In this sense, sense perception may be considered intuitive, though Radhakrishnan does not explicitly describe it as such.

- ***Discursive Reasoning***

Discursive reasoning, and the logical knowledge it produces, is subsequent to sensory experience (perception). Logical knowledge is obtained by the processes of analysis and synthesis. For Radhakrishnan, discursive reasoning and the logical systems they construct possess an element of intuition. For Radhakrishnan, "In any concrete act of thinking the mind's active experience is both intuitive and intellectual".

- ***Intuitive Apprehension***

While logic deals with facts already known, intuition goes beyond logic to reveal previously unseen connections between facts. Radhakrishnan holds that, "The art of discovery is confused with the logic of proof and an artificial simplification of the deeper movements of thought results. We forget that we invent by intuition though we prove by logic". Intuition not only clarifies the relations between facts and seemingly discordant systems, but lends itself to the discovery of new knowledge which then becomes an appropriate subject of philosophical inquiry and logical analysis.

Radhakrishnan offers three explanations to account for the tendency to overlook the presence of intuition in discursive reasoning. First, Radhakrishnan claims, intuition presupposes a rational knowledge of facts. "The insight does not arise if we are not familiar with the facts of the case…. The successful practice of intuition requires previous study and assimilation of a multitude of facts and laws. We may take it that great intuitions arise out of a matrix of rationality". Second, the intuitive element is often obscured in discursive reasoning because facts known prior to the intuition are retained, though they are synthesized, and perhaps reinterpreted, in light of the intuitive insight. Finally, intuition in discursive reasoning is often overlooked, disguised as it is in the language of logic. In short, the intuitive is mistaken for the logical. "Knowledge when acquired must be thrown into logical form and we are obliged to adopt the language of logic since only logic has a communicable language."

Intuition is not the end, but part of an ever-developing and ever-dynamic process of realization. Cognitive intuitions "are not substitutes for thought, they are challenges to intelligence. Mere intuitions are blind while intellectual work is empty. All processes are partly intuitive and partly intellectual. There is no gulf between the two".

2) Psychic Experience

Radhakrishnan accounts for psychic experiences in terms of a highly developed sensitivity to intuition. "The mind of man," Radhakrishnan explains, "has the three aspects of subconscious, the conscious, and the superconscious, and the 'abnormal' psychic phenomena, called by the different names of ecstasy, genius, inspiration, madness, are the workings of the superconscious mind". Such experiences are not "abnormal" according to Radhakrishnan, nor are they unscientific. Rather, they are the products of carefully controlled mental experiments. In the Indian past, "The psychic experiences, such as telepathy and clairvoyance, were considered to be neither abnormal nor miraculous. They are not the products of diseased minds or

inspiration from the gods, but powers which the human mind can exhibit under carefully ascertained conditions".

For Radhakrishnan, psychic intuitions are suprasensory: "We can see objects without the medium of the senses and discern relations spontaneously without building them up laboriously. In other words, we can discern every kind of reality directly". In a bold declaration, Radhakrishnan believes that the "facts of telepathy prove that one mind can communicate with another directly".

3) Aesthetic Experience

"All art," Radhakrishnan declares, "is the expression of experience in some medium". However, the artistic experience should not be confused with its expression. While the experience itself is ineffable, the challenge for the artist is to give the experience concrete expression. "The success of art is measured by the extent to which it is able to render experiences of one dimension into terms of another."

In Radhakrishnan's view, without the intuitive experience, art becomes mechanical and a rehearsal of old themes. Such "art" is an exercise in reproduction rather than a communication of the artist's intuitive encounter with reality. It is not simply a difference of quality but a "difference of kind in the source itself". For Radhakrishnan, true art is an expression of the whole personality, seized as it was with the creative impulse of the universe. For Radhakrishnan, artistic expression is dynamic. Having the experience, the artist attempts to recall it. Radhakrishnan believes that, the recollection of the intuition is not a plodding reconstruction, nor one of dispassionate analysis. Rather, there is an emotional vibrancy: "The experience is recollected not in tranquillity… but in excitement".

4) Ethical Experience

Not surprisingly, intuition finds a place in Radhakrishnan's ethics. For Radhakrishnan, ethical experiences are profoundly transformative. By definition, moral actions are socially rooted. As such the effects of ethical intuitions are played out on the social stage. While the intuition itself is an individual achievement, Radhakrishnan's view is that the intuition must be not only translated into positive and creative action but shared with others. The impulse to share the moral insight provides an opportunity to test the validity of the intuition against reason. The moral hero does not live by intuition alone. The intuitive experience, while it is the creative guiding impulse behind all moral progress, must be checked and tested against reason. There is a 'scientific' and 'experimental' dimension to Radhakrishnan's understanding of ethical behaviour. Those whose lives are profoundly transformed and who are guided by the ethical experience are moral heroes. To Radhakrishnan's mind, the moral hero, guided as he or she is by the ethical experience, who carves out an adventurous path is akin to the discoverer who brings order into the scattered elements of a science or the artist who composes a piece of music or designs buildings.

According to Radhakrishnan "Feeling the unity of himself and the universe, the man who lives in spirit is no more a separate and self-centred individual but a vehicle of the universal spirit". Like the artist, the moral hero does not turn his back on the world. Instead, "He throws himself on the world and lives for its redemption, possessed as he is with an unshakable sense of optimism and an unlimited faith in the powers of the soul". The moral hero is no longer guided by external moral codes, but by an 'inner rhythm' of harmony between self and the universe revealed to him in the intuitive experience. For Radhakrishnan "By following his deeper nature, he may seem to be either unwise or unmoral to those of us who adopt conventional standards. But for him the spiritual obligation is more of a consequence than social tradition".

5) Religious Experience

For the sake of clarity, we must make a tentative distinction between religious experience on the one hand and integral experience on the other. Religions, for Radhakrishnan, represent the various interpretations of experience, while integral experience is the essence of all religions. "If experience is the soul of religion, expression is the body through which it fulfils its destiny. We have the spiritual facts and their interpretations by which they are communicated to others". "The idea of God," Radhakrishnan affirms, "is an interpretation of experience". It follows here that religious experiences are, for Radhakrishnan, context relative and therefore imperfect. They are experienced through specific cultural, historical, linguistic and religious lenses. Because of their contextualisation and subsequent intellectualization, experiences in the religious sphere are limited. Radhakrishnan spends little time dealing with "religious experiences" as they occur in specific religious traditions. However, "religious experiences" have value for Radhakrishnan insofar as they offer the possibility of heightening one's religious consciousness and bringing one into ever closer proximity to "religious intuition".

Throughout his life, Radhakrishnan interpreted the Upaniṣadic *mahavakya*, *tattvamasi*, as a declaration of the non-duality (*advaita*) of Atman and Brahman. Radhakrishnan readily appropriates his acceptance of the non-dual experience to his interpretation of religious intuition. Radhakrishnan not only claimed to find support for his views in the Upaniṣads, but believed that the ancient sages expounded his interpretation of religious intuition. As the ultimate realization, religious intuition must not only account for and bring together all other forms of experience, but must overcome the distinctions between them. Radhakrishnan goes so far as to claim that intuition of this sort is the essence of religion.

With this, the present discussion of intuition and the varieties of experience has come full circle. Radhakrishnan identifies intuition — in all its contextual varieties — with integral experience. According to Radhakrishnan, the two expressions are synonymous. Integral experience coordinates and synthesizes the range of life's experiences. It furnishes the individual with an ever-deepening awareness of and appreciation for the unity of Reality. As an intuition, integral experience is not only the basis of all experience but the source of all creative ingenuity, whether such innovation is philosophical, scientific, moral, artistic, or religious. Moreover, not only does integral experience find expression in these various spheres of life, but such expression, Radhakrishnan believes, quickens the intuitive and creative impulse among those it touches.

Bibliografy:

Radhakrishnan, S., The Hindu View of Life. George Allen & Unwin Ltd., London, 1927.

Radhakrishnan, S., An Idealist View of Life. George Allen & Unwin Ltd., London, 1929.

Radhakrishnan, S., *East and West in Religion*. London: George Allen & Unwin, Ltd., 1933.

Radhakrishnan, S., *Religion and Society*. London: George Allen & Unwin Ltd., 1947.

Radhakrishnan, S., *Eastern Religions and Western Thought*, Oxford University Press, Second edition, 1940.

Journal Homepage: www.katwacollegejournal.com

New Directions in Research on Prostitution from Some Philosophical Aspects

Prakash Mondal, Philosophy, Katwa College, W.B., India

Asma Parbhin Khatun, Philosophy, Nistarini College, W.B., India

Article Record: Received Sep 28 2020, Revised Paper Received Dec 3 2020, Final Acceptance Dec 12 2020
Available Online Dec 13 2020

Abstract

Prostitution is the crudest manifestation of societies where women have been driven to sell their bodies as means of survival. Such women are expected to satisfy the uncontainable vice of male sexuality. Prostitution has been a part of our society since time immemorial. The article goes back into history of prostitution in India. The paper further examines the meaning of the term "prostitution" and the laws that define and deal with prostitution in India. Here the main aim of this article is to examine the countries where prostitution is legalized and determine the actual cause of prostitution, types of prostitution and a moral conclusion about prostitution.

Keywords: *Prostitution, Devadasi, Legalization, Moral Responsibility, and brothels.*

1. Introduction

The history of prostitution is perhaps as old as the male-female relationships. But it was born definitely along with the institution of marriage. In ancient India prostitution was firmly established as an institution. It had been prevalent in Buddhist and Mauryan period. The institution of Devadasi among the temples of south India is fairly ancient. In British period prostitution prospered in the form of glamour girls.

In contemporary India the greatest cause of increase in prostitution is industrialization and consequent rapid urbanization. These girls are known by several names such as dancing girls, massage girls, call girls and the ordinary prostitutes. Now a day, while most of the call girls are rich and educated, the ordinary prostitutes are generally poor and uneducated. Nevertheless, the causes of this most ancient profession in India are not much different from those in other countries but poverty is here a more important causative factor. In this connection I would like to discuss a new trend about prostitution in India as well as world. Of late, call boys like call girls have become popular in the society.

2. Objectives of the Study

The objectives of the proposed study are as follows:

1. To identify the main cause of prostitution and,
2. To make a moral conclusion about legalization of prostitution.

3. What is Moral Prostitution?

For practical, law-enforcement purposes, the definition of prostitution has usually not been too difficult. A prostitute defines herself when she "agrees to have sexual intercourse with a person (not her husband) who offers his money for engaging in the intercourse" (Benjamin, 1964).

In the august 1951 issue of the *International Journal of Sexology,* Albert Ellis wrote, "commercialized prostitutes would certainly be included – whether they accepted many or a chosen few paying partners. But also included would be girls who trade their sexual favours for food, entertainment, or other gifts and wives who , having no love and no sex desire for their husbands, continue to have sex relations in order to maintain the socio-economic benefits of marriage" (Ellis, 1951).

4. Types of Prostitutes

According to H. Benjamin, writing in *The Prostitute in Society,* the following are the important types of prostitutes found in modern societies:

a) The Call Girl: while the dictionary defines the call girl as independently operating prostitute, I am using the term in the special way in which I know it. The call girls are the aristocrats of prostitution. They live in the most expensive residential sections! They dress in rich, good taste.
b) The Streetwalker: streetwalking is probably one of the most ancient methods of prostitution. In the nineteenth and early twentieth century, prostitutes were sometimes permitted to work in bawdy houses specifically with the aim of getting them off the streets, where they would not be able to solicit, or even have to be seen by, 'decent people'. Her fees have traditionally been lower than those received by most other types of prostitutes.
c) Bar Prostitutes: R. E. K. Masters talked over the past 15 years with hundreds of young bar prostitutes in most parts of the United States. Most of them are not full-time whores, but are girls supplementing incomes earned as barmaids.
d) Child Prostitutes: Child prostitution is as ancient as civilization. Temple prostitutes were sometimes no older than 7 years, as in Babylonia. In ancient Egypt, also, the prostitution of young girls was a religious practice, so that, according to Strabo, some of the most beautiful and highest born Egyptian were forced into prostitution, and they continued as prostitutes until their first menstruation.

Apart from the above types of prostitution, there are many other types of prostitution in India which are not discussed here.

5. Causes of Prostitution in India

The social researchers made so far into the causes of prostitution in India reveal that females are drawn into it for a variety of reasons. A study of Kanpur prostitutes has revealed that though a majority of prostitutes have taken to their profession due to extreme poverty and hunger, there are many who have willingly adopted it after a series of love explores. Though the economic factor is quite important it is liable to be over-emphasized. Nevertheless, the main causes of prostitution can be classified in the following categories:

i) Economic causes: Though economic compulsions constitute the major factor in the causation of prostitution it is by no means the only and exclusive cause of the phenomenon. It is not the cause that every prostitute accepts money for her services or that all prostitutes hail from indigent homes. There are many prostitutes who hail from well-to-do families. In India, of course, there are many prostitutes who are compelled to adopt prostitution to feed themselves and their dependants. However, poverty is not the only economic factor, there are many other factors

which are economic. Economic factors comprise of: (1) poverty (2) under age employment (3) unhealthy working conditions (4) immoral traffic in women and children.

ii) Social causes: following are the social causes of prostitution.
   A. Family factors: a study of London prostitutes published as *Women of the Street* reveals that most of the prostitutes are connected with family troubles. Their parents were either living separately or their family relations were so strained that as children they were left to their own machinations and received no love. If the mother is of bad character and has to carry on with her clandestine liaisons, she rarely escapes the eager eyes of her daughter.
   B. Bad neighbourhood: children living near brothels become so used to seeing sex trade that they come to accept it as normal. The brothel keepers usually haunt these areas for their prey. The children who get exposed to sex business want to have these exhilarating experiences at the first available opportunity.
   C. Illegitimate motherhood: the women who become pregnant as a result of their liaisons and who cannot get abortion get exposed in society. Nobody wants to marry them but everybody wants to enjoy them sexually. Desperately such women prefer to become regular prostitutes.
   D. Psychological causes: there are some psychological factors which tend a person towards prostitution. A woman who is frigid becomes desperate. She tries one man after another. Because of frigidity she is unable to experience pleasure and becomes a prostitute by trial and error.

iii) Biological factors: the persons born with defective sex organs or overactive glands may feel compelled to seek sex gratification in a bizarre manner.

iv) Religious and cultural factors: In India there has been religious sanction to prostitution. In the south, certain selected families were supposed to offer one daughter each to the temple where apparently she was supposed to serve gods with total dedication. They were known as Devadasis – god-slaves. But in actual practice they lived a life of prostitution.

All causes listed above contribute more or less to prostitution. Prostitution has a very long and varied history. As a matter of fact it is considered to be the oldest profession in the world. In modern times it is becoming fashionable to consider prostitution a necessary part of society.

6. Prostitution and Legality in India

According to the Indian Penal Code, certain activities related to sex are not considered illegal per se and contradict laws that are in place. However, activities as enumerated below if found to be true, one is entitled to be punished in accordance with laws of the legal arena in place:

- Soliciting services of prostitution at public places
- Carrying out prostitution activities in hotels
- Being the owner of a brothel
- Indulge in prostitution by arranging a sex worker
- Arrangement of a sex act with a customer

Now the situation is such that the activities mentioned above are very much real and exist alongside. So by outlawing them does the Indian legal system make prostitution illegal? Because in most cases, government officials tend to ignore this fact that illegal trafficking of women and children is the root cause of growing prostitution as a business.

7. Conclusion

While prostitution is legal in the India, there is a lively debate as to whether this is acceptable. Prostitution is often viewed as morally impermissible, and therefore, wrong. However, as John Stuart Mill states in *On Liberty*, it is not clear that the government is or should be in the process of regulating morals based in paternalistic reasons. Something should not be regulated for someone's 'own good.' Acts that are primarily self-regarding that do not harm or affect the interests of others should never be regulated for someone's own good. Things should only be regulated if they harm others. Whether an act is moral or immoral is beside the point. So, laws against prostitution, which is primarily a self-regarding action, which affects others only with their consent, should not be illegal.

Further, it is not at all clear from this point that prostitution is in fact immoral. Theories that condemn it as wrong and impermissible tend to call upon various ideas of impropriety and unnaturalness to show why it is immoral. St. Thomas and socio-biologists claim that the only proper function of sex is for procreation, and thus prostitution is morally impermissible on this account. Similarly, Roger Scruton claims that the only proper function of sex is to express love because of the interpersonal nature of the act. However, among other issues, the primary problem with these two theories is the failure to connect the morally improper with a failure to fulfill the function of sex. The morally proper and the natural or proper function of sex are never shown to be the equivalent. Additionally, it is not at all clear that there is only a single function for everything. The radical feminist view that any heterosexual form of sex is immoral because of the power differential between men and women present in society makes it such that women can never properly consent to sex because women are always in a state of subjugation has many problems as well, not the least of which is universalization of the position of women that does not account for individual experiences of women. To claim that women as a group are suppressed by men as a group is a common feminist claim that is accepted by many. However, to claim as Pateman and other radical feminists that because of this every woman is therefore coerced or forced or subjugated by every man is simply untrue. This fails to account for an interaction between a successful woman CEO and a poor man, or any woman in a place of power interacting with men. To say as Pateman does that this does not matter that she is still a victim of subjugation, is simply unfounded. To universalize such a general claim is a huge fault in such a theory. These theories simply fail to provide adequate reason to suppose that an act such as prostitution is immoral. The theories are weak in many senses because they insist that any act that does not fit within the parameters of the theory, which are already on shaky ground, is morally impermissible. If the theories instead represented the ideal situation, there would be little problem with accepting one or the other as a personal preference attempting to live up to the ideal. In which case, failing to live up to the ideal, which is less than good, is not immoral. So, not only should prostitution not be illegal whether it is moral or not, it does not even appear to be immoral.

By looking at theories of consent that are based on a concept of autonomy, one is able to understand that prostitution, when performed under certain parameters, is morally permissible. The idea of personal autonomy or sovereignty is a part of what it means to be a human. Everyone has a sense of self and self-rule that allows for one to act and make choices based on their own decisions. When one acts is a way that does not infringe another's autonomy or significantly harm their interests, then they should be free to do so. If one does want to act in a way that does affect the interests of others, they are permitted to do so only with the permission, authorization, or consent of the other. This consent that is obtained must be valid. In other words, it cannot be gotten through coercion or deception. It must be gotten from a freely (unforced), informed consenting adult who is competent to make such a decision. If the agent is underage, under the influence of alcohol, or mentally deficient or disturbed, then the consent obtained is not valid. Additionally, if the agent is forced or coerced in any way either physically or through lying and withholding relevant information, then the consent is invalid and the act is wrong. However, if the consent is validly obtained, not only is the act allowable, but it is morally permissible. Indeed, not only should prostitution not be illegal based on its moral impermissibility, it is not even morally impermissible to begin with.

To conclude, prostitution, as such, is not coercive or immoral, so long as valid consent is obtained. Indeed any sex act that occurs between freely, informed consenting adults is morally acceptable. Prostitution is a combination of consenting sex and contractual exchange. Any governing set of rules or morals that govern prostitution are based on this dual aspect of the act. If the act is between such validly consenting adults, who agree to the terms of the contract and fulfill the terms, there should be no immoral issue with prostitution at all.

References

Aquinas, T. (1956). *Summa Contra Gentiles.* New York: Doubleday. pp. 13-14.

Benjamin, H. (1964). *The Prostitute in Society.* London: Mayflower Books. pp. 24.

E, Albert. (1951). *International Journal of Sexology.* New York: University Books. pp. 127.

Fernando, H. (1962). *Prostitution and Society.* London: MacGibbon & Kee. pp. 17-18.

Maryse, C. (1950). *A Month among the Girls.* New York: Pyramid. pp. 31.

Mill, J.S. (1956). *On Liberty.* Indianapolis: Bobbs-Merrill Educational Publishing. pp. 71-72.

Pateman, C. (1988). *Defending Prostitution: Charges against Ericsson.* Standford: Standford University Press. pp. 123-127.

Rovert, V. S. (1949). *Sex and the Statutory Law.* New York: Oceana. pp.7.

Nano-Structures & Nano-Objects 26 (2021) 100756

Contents lists available at ScienceDirect

Nano-Structures & Nano-Objects

journal homepage: www.elsevier.com/locate/nanoso

Design of π-conjugated flexible semiconductive 2D MOF and MOF derived CuO nano-spheres for solvent free C-X (S, O) hetero-coupling catalysis with enhanced conductivity

Maxcimilan Patra [a,1], Soumen Kumar Dubey [a,1], Bibhas Mondal [a], Kajal Gupta [a], Angshuman Ghosh [b], Subhankar Mandal [c], Satyajit Hazra [c], Ajit Kumar Meikap [d,*], Ujjal Kanti Roy [a,*], Subham Bhattacharjee [a,*], Rajat Saha [a,*]

[a] Department of Chemistry, Kazi Nazrul University, Asansol-713340, India
[b] TCG Lifescience, Block BN, Sector V, Saltlake, Kolkata-700156, India
[c] Saha Institute of Nuclear Physics, HBNI, 1/AF Bidhannagar, Kolkata 700064, India
[d] Department of Physics, NIT Durgapur, Durgapur-713209, India

ARTICLE INFO

Article history:
Received 1 January 2021
Received in revised form 15 April 2021
Accepted 28 April 2021

Keywords:
2D MOF
$\pi \cdots \pi$ Interaction
Flexible MOF
MOF derived CuO-NPs
Green catalysis
Electrical conductivity

ABSTRACT

A flexible, 2-fold interpenetrated 3D supramolecular structure $[Cu(ndc^{2-})(1,10\text{-phen})]_n$ (where ndc^{2-} = 2,6-napthalenedicarboxylate and 1,10-phen = 1,10-phenanthroline) comprising neutral 2D metal–organic layers as the basic building block was prepared. Structural study reveals that metal ions are bridged by ndc^{2-} ligands to form 2D coordination layers and the coordinated 1,10-phen moieties are hanging from the layers in the interlamellar spaces. The gliding motion of $\pi \cdots \pi$ stacked layers through 1,10-phen moieties was found to be responsible for the flexibility of MOF and the consequent extended conjugation also rendered semiconducting behaviour in the material. Thermal stability studies revealed that the framework was pretty stable below 260°C. Additionally, the MOF was characterized by performing BET adsorption and photoluminescence studies. Further, the MOF was calcinated at 650°C to prepare well defined, nearly uniform and spherical shaped CuO nanoparticles (CuO-NPs) with an average size of ~25 nm. Interestingly, CuO-NPs showed around 16 times more conductivity (4.8×10^{-2} S/cm) in relative to the parent MOF (3×10^{-3} S/cm). CuO-NPs induced cross-coupling reactions of alcohols and thiols with arylhalides have been reported. A simple, general, ligand-free and solvent-free procedure for the efficient synthesis of the cross-coupled products in high yield was successfully demonstrated.

1. Introduction

In last three decades, metal–organic frameworks (MOFs) are appeared as one of the most promising functional material due to their inherent porous structure and modular behaviour [1]. Initially, the inception was that the implication of inert metal ions and insulating bridging ligands makes MOFs weakly conducting or insulating in nature [2]. But, from last decade, design of conducting MOFs has gained much attention due to their several applications in energy storage, sensing, electrocatalysis, etc. [3]. Researchers have developed two different types of conductive MOFs: (a) intrinsically conductive MOFs: electrically conducting organic building blocks, such as 2,3-pyrazinedithiolate [4], dihydroxybenzoquinone [5] etc. have been used to induce conductivity in the designed framework, and (b) extrinsically conductive MOFs: electrically conducting guests, both neutral I_2, [6] (TCNQ) [7], and charged (BF_4^-) [8], are incorporated in the void space of MOFs to enhance conductivity. Intrinsically conducting MOFs have gained much attention over its extrinsic counterpart due to low cost production and easy synthesis [2a], [9]. Several types of design principles have been adopted by scientists to build intrinsically conducting MOFs: (a) use of metal ions and bridging ligands having equivalent band structure which will help to transport electrons through the framework [10], (b) use of radical generating ligands that will boost the conductivity of the designed framework [5c,10b] (c), use of extended $\pi \ldots \pi$ conjugation between 2D coordination polymer [5b], [11]. In organic electronics, π-interaction is used to develop conducting materials [12] and, in similar way, several research groups have developed conducting MOFs based on extended $\pi \ldots \pi$ conjugation using different

* Corresponding authors.
E-mail addresses: meikapnitd@yahoo.com (A.K. Meikap), uroccu@gmail.com (U.K. Roy), sbpb2012@gmail.com (S. Bhattacharjee), rajat.saha@knu.ac.in (R. Saha).

[1] Both have equal contributions.

https://doi.org/10.1016/j.nanoso.2021.100756
2352-507X/

organic ligands e.g. napthalenediimide, [9b] tetrathiofulvalene [13], anthracene [14], etc. Formation of continuous π-conjugation throughout the framework is the primary condition to design such materials. Herein, we have used 1,10-phen, highly potential to participate in $\pi \ldots \pi$ interaction, as the building block to develop conducting material and found that the synthesized 3D supramolecular framework showed semiconducting behaviour.

Recently, syntheses of various nano-materials using MOFs as sacrificial scaffolds are of great interest [15]. The regular periodic arrangement of metal nodes within the MOF architecture provides an excellent platform to design nano-particles of uniform size distribution as well as their intriguing porosity. The structure, composition, phase and size of the nano-particles can be controlled by optimizing the synthetic conditions: chemical environment (O_2, N_2 etc.), temperature and synthetic methods [16]. Several research groups have synthesized metal, [16a] metal–oxide, [16b,16c,16d,16e,16f,16g] mixed metal–oxide, [16h] metal carbide [16i] NPs, etc, and explored their enormous applications in gas adsorption, [16j] catalysis, [16b] and so on. Besides, these MOF derived NPs have been used for several types of electronic applications like electrocatalysis, [17] battery, [18] etc. based on their versatile conducting properties from insulating to metallic behaviour [17–19]. In this work, we have used our synthesized semiconductive MOF to develop NPs and interestingly found that the MOF-derived NPs showed higher conductivity than the parent MOF.

C–O and C–S bonds are prevalent in numerous compounds that are of biological, pharmaceutical, and material interest [20]. Specially, a large variety of aryl sulfides are in use for diverse clinical applications [21]. One of the most common synthetic methods for their preparation is the copper-assisted classic Ullmann reaction. However, these reactions often require harsh conditions such as high temperature (>200 °C), stoichiometrically higher amount of copper reagent and thus produce a lot of wastes [22]. Currently, to follow strict environmental laws, chemical based industries are desperate in reducing various harmful chemical wastes by designing intelligent catalysts those perform in mild or environment benign conditions with high yield, large selectivity and good efficacy [23]. Palladium and copper complexes containing electron-rich ligands have been studied considerably for the cross-couplings of oxygen and sulphur nucleophiles with aryl halides [24]. Subsequently, few studies have focused on the use of iron and nickel-based catalytic systems for this purpose also [25]. Unlike homogeneous catalyst, use of heterogeneous catalyst is much more advantageous in terms of their easy separation, recyclability, high thermal stability and longer lifetime. In this respect, we have focused on CuO-NPs induced heterogeneous C(aryl)-S and C(aryl)-O hetero-coupling reactions with the following advantages: (a) the reaction proceeds under solvent free condition, (b) easy separation of catalysts and products from the reaction mixture after completion, (c) high selectivity of the catalysts for the substrate, (d) high catalysis rate and e) re-usability.

In this endeavour, we have synthesized a 2-fold interpenetrated, flexible, 3D supramolecular framework: **[Cu(2,6-ndc)(1,10-phen)]$_n$**, by solvothermal method and characterized by SCXRD analysis. Structural analysis revealed that each Cu centres are connected by 2,6-ndc ligands to form 2D coordination layers with hanging coordinated 1,10-phen moieties and these 2D metal–organic coordination layers are assembled by 1,10-phen mediated $\pi \ldots \pi$ interactions to form the overall 3D supramolecular structure. The presence of $\pi \ldots \pi$ interactions help to: (i) induce flexibility and (ii) create electronic conducting pathway within the framework. The resultant flexible framework showed semiconducting nature in association with micro-porosity. TGA analysis revealed that the framework decomposes at 350 °C. The MOF was decomposed by heating at 650 °C to produce CuO-NPs which were characterized by PXRD, SEM and EDAX analyses. Four probe electrical conductivity experiments revealed that the synthesized CuO-NPs have 16 times higher conductivity than parent MOF. Further, we have successfully demonstrated solvent free C–S and C–O heterocouplings in excellent yields in bulk utilizing the CuO-NPs. Product analysis revealed exclusive formation of the desired products with minimum amounts of wastes; hence, we would be able to make the process green and highly applicable for industrial scale synthesis.

2. Experimental section

Materials and Methods: Copper (II) nitrate, monohydrate; 2,6-napthalene dicarboxylic acid and 1,10-phenanthroline were purchased from Merck chemical company. All other chemicals used were AR grade. Elemental analysis (C, H, N) was carried out using a Perkin-Elmer 240C elemental analyzer. The thermal analysis was carried out using a Mettler Toledo TG-DTA 85 thermal analyzer under a flow of N_2 (30 ml/min). The sample was heated at a rate of 10 °C/min with inert alumina as a reference. IR spectroscopy was measured on Nicolet Impact 410 spectrometer between 400 and 4000 cm^{-1}, using the KBr pellet method. Photoluminescence spectra were collected on a Shimadzu RF-5301PC spectrophotometer. Powder XRD patterns were recorded by using Cu-Kα radiation (Bruker D8; 40 kV, 40 mA). The elemental analysis for CuO-NPs was performed by BRUKER energy dispersive X-ray spectrometer (EDS) attached with the FEI, INSPECT F50 field emission scanning electron microscope (FESEM). ^{1}H-NMR studies were carried out by using 300 MHz Bruker NMR spectrometer. The XPS measurements of the sample was carried out in an ultrahigh vacuum (UHV) multiprobe setup (Omicron Nanotechnology) at a base pressure of $\sim 2.0 \times 10^{-9}$ mbar, which was equipped with an EA125 hemispherical energy analyzer and an X-ray source [26]. For the XPS measurements, monochromatic Al Kα X-ray of 1486.6 eV photon energy was used as a source and the corresponding spectrometer energy resolution was $\sim$ 0.8 eV. C 1s level (binding energy of 284.8 eV) was chosen as the reference level to calibrate the other core-level spectra.

Synthesis of Complex 1 {[Cu(O-phen)(ndc)]$_n$: A mixture of $Cu(NO_3)_2$ (0.5 mmol, 0.1214 g), ndc (0.5 mmol, 0.1092 g), 1,10-phen (0.25 mmol, 0.0502 g) and 1 mL Et_3N in 6 mL DMF was stirred for 15 min. Then the mixture was transferred into a 15 ml Teflon-lined stainless-steel vessel and heated for 24 h at 120 °C. Afterwards, it was cooled to room temperature for another 24 h. After 48 h, green coloured single crystals (Figure S1) suitable for X-ray structure determination were isolated by filtration. Yield: 70%. Anal. Calcd. for $C_{24}H_{14}CuN_2O_4$ indicates C: 62.85% (62.88% theo), H: 3.10% (3.12% theo) and N: 6.10 (6.08% theo). IR (KBr pellet, cm^{-1}): 1606(s), 1560(s), 1544(w), 1426(w), 1394(s), 1357(s), 1221(w) and 1191(w) (Figure S2).

Electrical conductivity measurement: The resistance of the sample is measured by means of a four terminal direct current technique with resolution of $\delta R/R = 10^{-5}$ using a pressed pellet (10 ton pressure) of the samples. The four terminal connections are made using fine copper wire with pure silver paste. As a confirmatory test towards ensuring good electrical contact using silver paste, the continuity of the samples was checked before placing it within the sample holder. Contribution of conductivity of silver of the paste is ignored as it is used for all cases. All these measurements were performed by the following equipments, (i) A constant current source (KEITHLEY INSTRUMENT, Model 220), (ii) A nanovoltmeter (KEITHLEY INSTRUMENT, Model 181), (iii) Hewlett Packard 3458 A, 81/2 digit multi-metre.

General Procedure for C-X (X = S and O) Hetero-coupling Reactions: The catalytic reactions were carried out in a glass batch reactor. To a stirred solution of the phenol or thiophenol

(25 mmol), aryl halide (5 mmol), KOH (5 mmol) and CuO (2.5 mol%) were added, and the reaction mixture was stirred at 100 °C for 17 h under inert atmosphere and monitored continuously by TLC (hexane/ethyl acetate = 9:1 v/v). After completion of the C–O or C–S cross-coupling of phenol/thiophenol with aryl halide, (i.e. after complete consumption of the aryl iodide which takes near about 17 h), the reaction mixture was treated with diethyl ether. The solution was centrifuged and then catalyst was isolated, washed water and ether. After complete drying, the catalyst can be reused for the next cycle. The remaining mixture was diluted with water and extracted with diethyl ether thrice. The combined organic layer was dried over anhydrous Na_2SO_4, filtered, and concentrated to afford the crude material. The crude material was then purified by column chromatography (silica 100–200 mesh, ethyl acetate-hexane 5%–10%) to afford the desired C–O or C–S cross coupling product (yield = 95%–99%).

Crystallographic Data Collection and Refinement: Suitable single crystal of the complex was mounted on a Bruker SMART diffractometer equipped with a graphite monochromator and Mo-K_α(λ = 0.71073 Å) radiation. Unit cell parameters were determined by using the APEX2 [27] program. Data reduction was carried out by the SAINT [27] program and correction or absorption was performed using the SADABS [27] program. The structure was solved using Patterson method by using the SHELXS-2018/3 [28] embedded in WINGX software package [29]. Subsequent difference Fourier synthesis and least-square refinement revealed the positions of the remaining non hydrogen atoms. Non-hydrogen atoms were refined with independent anisotropic displacement parameters. Hydrogen atoms were placed in idealized positions and their displacement parameters were fixed to be 1.2 times larger than those of the attached non-hydrogen atom. All Figures were drawn by using PLATON [30] and ORTEP [31]. Data collection and structure refinement parameters and crystallographic data for complex 1 are given in Table S1. The structure was previously reported in literature [32] and, herein, we have described from a different perspective. Some selected coordination bond lengths, bond angles and non-covalent interaction parameters are summarized in Table S2-S3.

Indexing of the PXRD data: The indexing of the XRPD pattern was carried out using NTREOR and McMaille programs of EXPO 2009. Indexing reveals that the complex is still crystalline with a monoclinic system with a = 13.5426 Å, b = 13.9326 Å, c = 12.0862 Å, β = 100.1023° and V = 2245.11 Å^3. The space group was obtained from statistical analysis of the powder pattern with the help of find space module of the EXPO 2009 software package. Statistical analysis shows that the most probable space group is $P2_1/n$. For this unit cell and space group, full pattern decompositions were performed using Le Bail method giving good fit between calculated and experimental powder X-ray patterns. This result was corroborated from the indexing and Pawley refinement of the PXRD pattern of the complex by the reflex module of the Material studio program. Unit cell, peak profiles, zero-shift, background were refined simultaneously. Peak profiles were refined by the Pseudo-Voight function with Berar–Baldinozzi asymmetry correction parameters. The background was refined using a 4th order polynomial.

3. Result and discussions

Structural description of Complex 1: X-ray crystal structure analysis revealed **1** as a neutral 3D supramolecular framework (formula $[C_{24}H_{14}CuN_2O_4]_n$). The asymmetric unit contains one Cu(II) ion, two halves two ndc^{2-} ligands and one 1,10-phen (Figure S3). Each Cu(II) atom shows distorted square pyramidal geometry (τ = 0·07) with CuN_2O_3 chromophore (Figure S4). ndc^{2-} ligands show two different types of bridging modes: μ4-*bis*-bridging and μ2-*bis*-bridging. Coordination of two different types of ndc^{2-} with the Cu^{2+} ions forms 2D coordination sheet in the ***bc***-plane with 1,10-phen ligands hanging into the interlamellar spaces from the metal centres, Figure S5. These 1,10-phen moieties between two 2D layers are connected through are interacted by $\pi \ldots \pi$ interactions between aromatic rings present within the 1,10-phen molecules. Such $\pi \ldots \pi$ interactions further assemble these 2D layers along *a*-axis to generate a spongy 3D supramolecular framework, as shown in Fig. 1a. The dimensions of all $\pi \ldots \pi$ interactions are listed in Table S4. It is to be noted that 1D channel of dimension 12.071 × 13.294 Å is formed along ***a***-axis (Figure S6). The channel is filled by two-fold self impregnation in order to achieve an efficient packing (Fig. 1b and S7).

Framework Stability and PXRD: Thermo-gravimetric analysis of the compound was performed in the temperature range of 25–500 °C under N_2 atmosphere (Fig. 2). The TG analysis indicated that complex **1** is stable up to 260 °C and undergoes decomposition in two consecutive steps above this temperature. In the first step, 1,10-phen moieties undergo dissociation within 260 and 300 °C and above this temperature it degrades in another step at about ∼325 °C.

To know about framework flexibility, the PXRD analyses with complex **1** were done at room temperature and at 150 °C temperature. The PXRD pattern of the as synthesized complex **1** is matched very well with the simulated pattern which indicated the phase purity of the sample. The PXRD (Fig. 3) pattern at higher temperature has peaks at slightly lower angle. The indexing of the PXRD pattern was carried out using NTREOR and McMaille programs of EXPO 2009 (supporting information, Figure S8). This reveals that the complex is still crystalline with monoclinic system (***a*** = 13.5426, ***b*** = 13.9326, ***c*** = 12.0862 Å, ***β*** = 100.1073° with a larger cell volume of 2245.11 Å^3, Table S4). So, the length of the ***a***-axis, along which 2D layers are stacked through $\pi \ldots \pi$ interactions, increases in large amount compared to ***b***- and ***c***-axes and this corresponds to the expansion of layer gap assisted by the gliding motion of the π-stacked layers [33], which is feasible for 1,10-phen ligand. So, both the increase in bond length and expansion of layer gap along ***a***-axis contribute to the overall 15% increase in the overall cell volume. Upon cooling to room temperature, the PXRD pattern reverts back to the original pattern. This proves the π-induced flexibility of the framework.

Adsorption study: Though PLATON study indicates the non-porous nature the framework at ambient condition but the variable temperature PXRD study showed that there is a chance to create porous channel along crystallographic ***c***-axis by thermally stimulated π-induced flexibility — and thus we have attempted to analyse sorption behaviour of the sample. N_2 adsorption study at 77 K revealed the non-porosity of the material while the solvent sorption studies at 298 K indicated micro-porosity. Water adsorption isotherm (at 298 K) of complex showed type **III** behaviour. The volume uptake of water is 15.6 cm^3/g (Fig. 4). Complex **1** also adsorbs 12.9 cm^3/g methanol and 6.24 cm^3/g ethanol (Fig. 4). Small amount of adsorption may be interpreted as that due to interpenetration very narrow channels were created within the framework or surface adsorption [34]. Desorption curve does not coincide with the adsorption curve in all cases, showing a hysteresis loop and incomplete desorption. A very little amount of water, methanol and ethanol remains within the framework. Small hysteresis in the water adsorption isotherm is probably because of trapping by the coordinatively unsaturated metal sites.

Photoluminescence: Photoluminescence property of complex **1** was performed at room temperature in solid state. The emission spectra of both 1,10-phen ligand and complex **1** are shown in

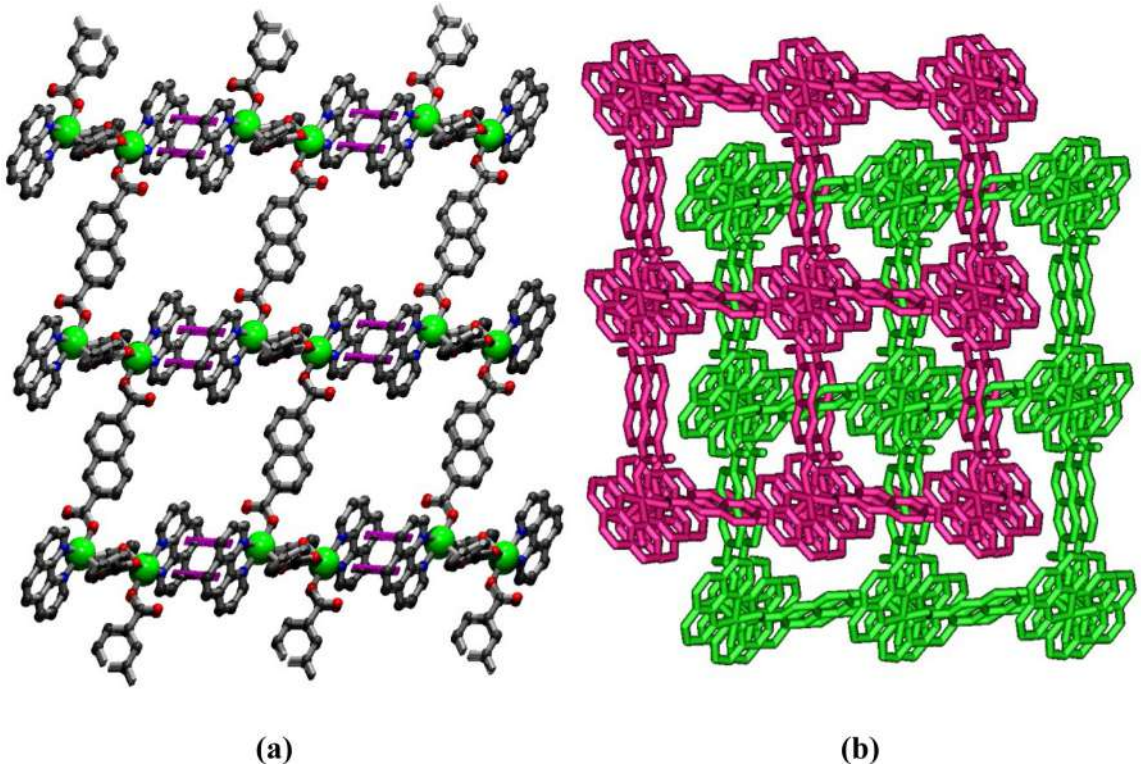

Fig. 1. $\pi \ldots \pi$ (magenta) conjugated 3D supramolecular structure (a) and 2-fold interpenetration (b) of complex **1**. (For interpretation of the references to colour in this figure legend, the reader is referred to the web version of this article.)

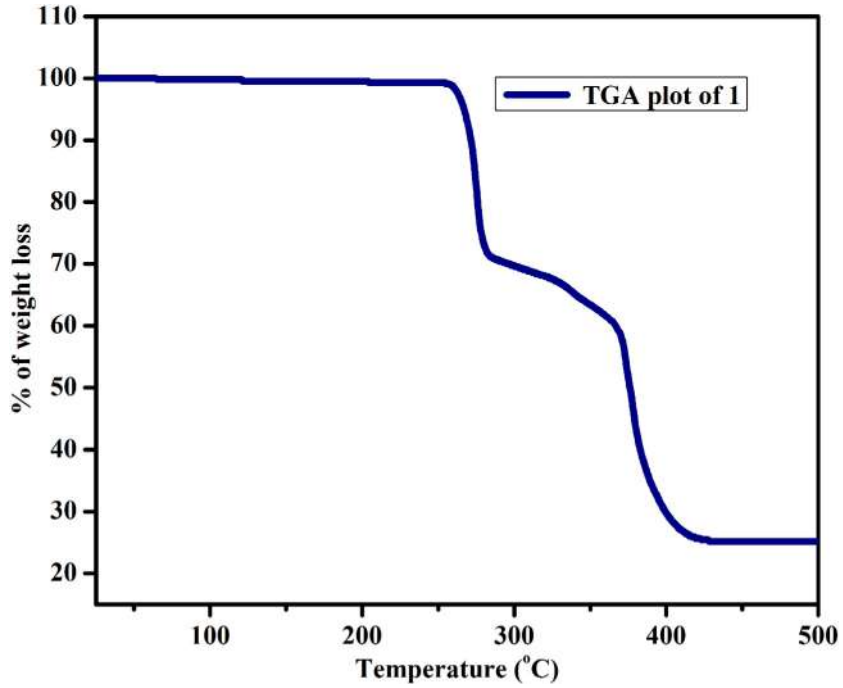

Fig. 2. The thermal plot of complex **1**.

Figure S9. The luminescence spectra of 1,10-phen ligand show two peaks at 412 nm and 434 nm with a shoulder at 461 nm. The spectra arise due to π-π^* transition. The luminescence spectra of complex 1 show similar pattern — the spectra contain two peaks at 414 nm and 434 nm with three different shoulders at 458 nm, 464 nm and 468 nm. The spectra arise due to both intra-ligand π-π^* transition and M-L charge transfer transition. So due to metal complex formation, a small red shift occurs.

Synthesis and Characterization of CuO-NPs: Nano-particles are highly interesting as their properties are critically dependent on synthetic condition, size distribution, morphology and shape.

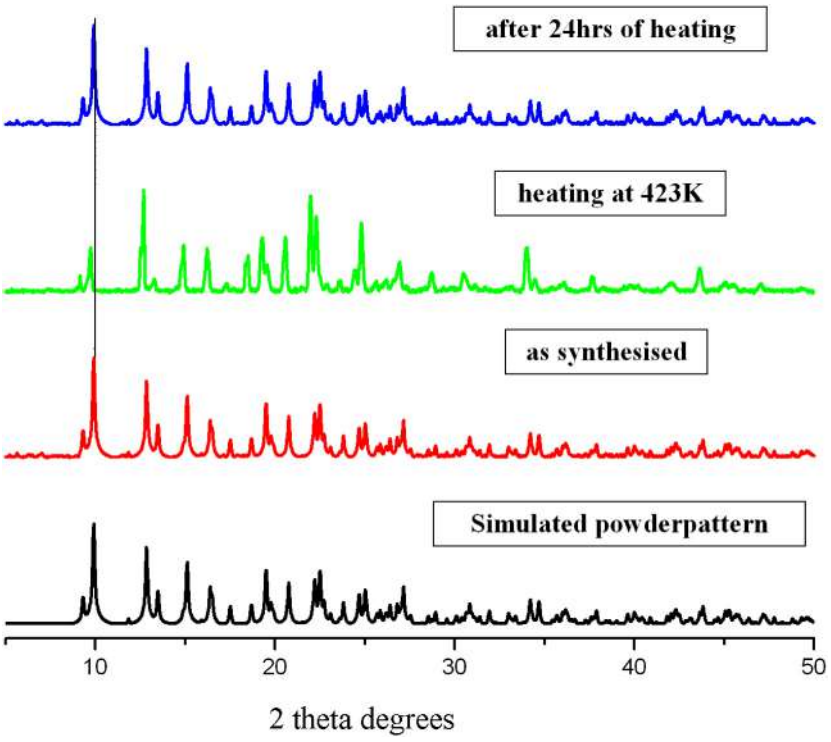

Fig. 3. Variable temperature PXRD pattern of **complex 1**.

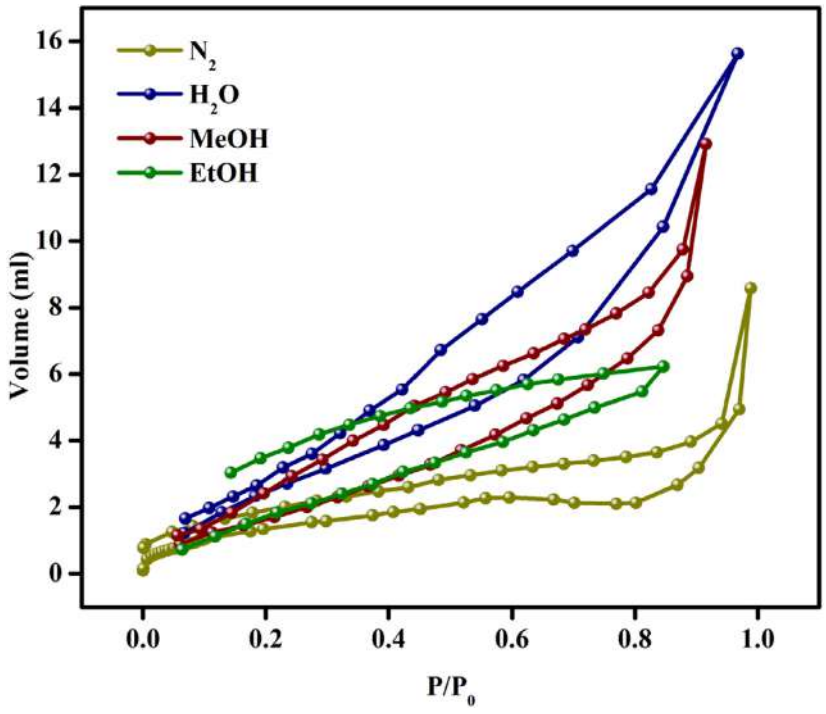

Fig. 4. Gas and solvent sorption behaviour of complex **1**.

CuO-NPs have great potential for their applications in electrochemical cells, magnetic storage media, photovoltaic cells, etc. Here, the 2D-MOF is used as a template to synthesize CuO-NPs by calcinations. The bulk material of the MOF was heated at 650 °C for 4 h at normal condition. Upon heating, the green coloured compound turned in black powder, which was characterized by PXRD, EDS, IR, TEM and SEM analyses. IR spectra of the CuO-Nps are presented in Figure S10. The PXRD pattern matches with the reported PXRD pattern of CuO with JCPDS No. 08-0234 (Fig. 5a). The TEM micrograph indicated the spherical morphology of the synthesized NPs (Fig. 5b) with average size of ∼25 nm and this corroborates with the PXRD data. EDS study indicated the presence of characteristic peaks for the constituents (Cu and O) (Figure S11). The Cu $2p_{3/2}$ core-level spectra (Fig. 6) have been studied to know the oxidation state of Cu present in the copper oxide nanoparticles. The binding energy position of the

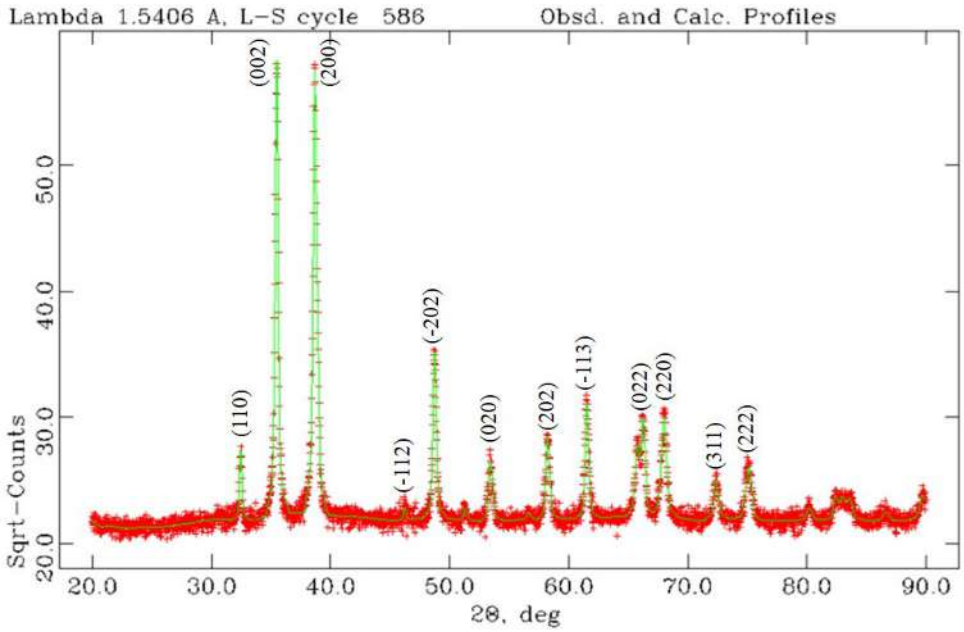

(a)

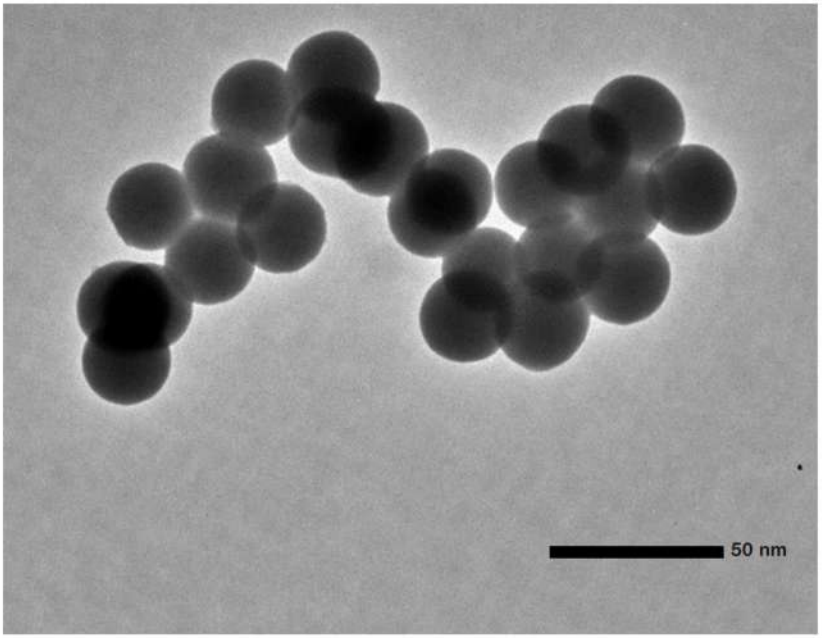

(b)

Fig. 5. PXRD pattern (a) and TEM image (b) of the synthesized CuO-NPs.

main peak in the spectra was observed at around 933.7 eV that informs about the presence of Cu^{2+} species, which was observed previously by many people [35]. The strong shake-up satellite observed in these spectra is also an indication of the presence of Cu^{2+} species that was mentioned by many authors previously [35]. So, the Cu $2p_{3/2}$ core-level spectra confirm that the Cu present in this copper nanoparticles sample is mostly in the Cu^{2+} oxidation state.

Green Catalytic C-X Hetero-coupling Reactions: In the present work, the synthesized spherical shaped CuO-NPs are used for the catalytic cross-coupling (C–O and C–S) reactions of alcohols and thiols with arylhalides. Generally, for such C–O and C–S cross-coupling reactions, high boiling solvents like DMSO, DMF, NMP, etc. are required in both homogeneous and heterogeneous conditions. And consequently, separation of products from these solvents becomes very difficult and tedious. Here, we are going to report a solvent free, neat reaction protocol for such hetero-coupling reactions of phenol, thiophenol, alcohol, and thiols with aryl halides.

Literature review indicates that in previous studies of copper-catalyzed hetero-coupling reactions, *N*-methylpyrrolidinone (NMP), dimethylformamide (DMF), dimethylsulfoxide (DMSO)

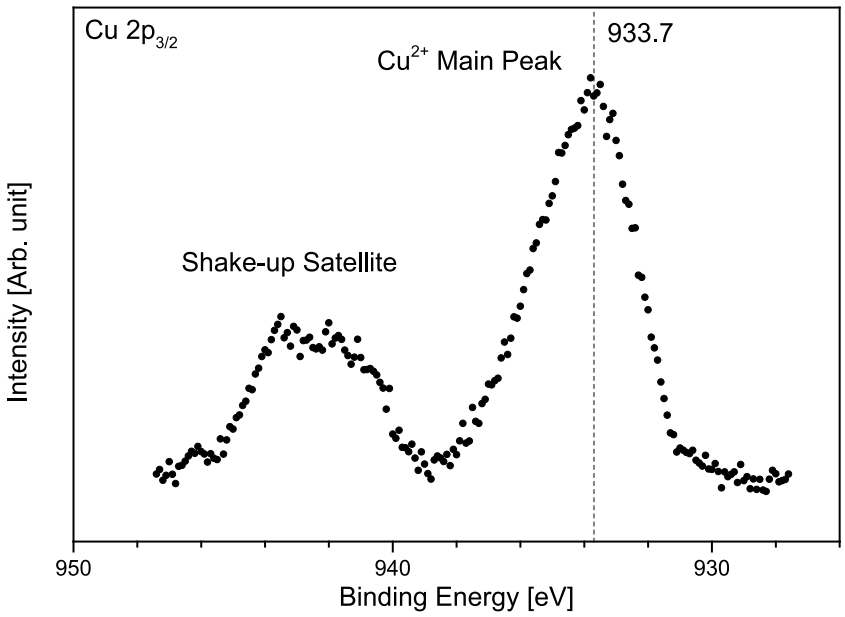

Fig. 6. XPS data of CuO-NPs reveals the presence of only Cu^{2+} ions.

etc. are used as solvent with KOH and K_2CO_3 as base [36] and, thus here, we have also followed the same protocol initially. Punniyamurthi et al. have carried out the C-X (X = S, N and O) hetero-coupling catalytic reactions using CuO-NPs in DMSO [36d]. Here, catalytic activity of the synthesized CuO-NPs was first investigated for the cross-coupling of iodobenzene with phenol and latter with thiophenol. The reactions of chlorobenzene, bromobenzene, phenyltosylate, and phenylboronic acid are studied, but those are found to be inferior to that of aryl iodides. Catalytic tests were also performed with CuCl, CuBr and CuI, freshly prepared before use, provided the same results as obtained with synthesized CuO-NPs. Other Cu(II) salts tested ($CuBr_2$, $CuSO_4 \cdot 5H_2O$, $CuCl_2$) were found to be less efficient catalysts (yields 55%–69%) than the CuO-NPs. A low amount of 2.5 mol % of CuO-NPs was employed in these initial standardization reactions. Our first goal was to optimize reaction conditions and to achieve information about the role of additives and solvent polarity. It appeared that, by applying KOH as base in DMF, diphenylether was obtained in quantitative yield in presence of 20 mol% CuO-NPs catalyst without the use of added ligands. Solvent polarity has significant impact on the yield of the reactions (Table S5) – high polarity solvents like DMF, DMA and NMP show better yield than toluene (entries 3–5). It is noteworthy that very low yield (40%) was obtained for using water as solvent (Table S5, entry 6). Now, difficulty in separation of these solvents from the product prompted us to choose the neat reaction conditions (Table S5, entry 7). And interestingly, we have found that the yield of neat reaction conditions are similar to that in DMF, DMA and NMP and then we decided to go further with the neat reaction conditions.

Similarly, a series of bases were also screened. Among inorganic bases, KOH gave almost quantitative results for the coupling reaction to diphenylethers (Table S6), while, among organic bases, triethylamine and Hunig's base (DIPEA) gave also good results (Table S6, entries 2 and 3) in heterogeneous reaction mixture. Notably, in our case the required amount for the base is only one equiv. (based on the aryl halide), while in common reports this is usually in between 1.5 and 2.5 equiv. Further experiments were performed to find the optimal reaction temperature and reaction time. Both Tables S5 and S6 refer to around 17 h reaction with temperature of 100 °C. It was noted that a small decrease in temperature of only 10 °C caused a significant decrease in diaryl thioether yield (85%). Lowering the time of the reaction in the present conditions also decreases the yield of the desired products. Accordingly, at 100 °C, the reaction of iodobenzene with phenol is relatively fast (65 and 95% after 2 and 6 h, respectively). It also appeared that fluoro-, chloro-, and bromobenzene are very less reactive under the optimized conditions, giving extremely lower yields (4%–55%) of the C–O coupling products (Table S7). Aryltosylate and boronic acids are also very less effective compared to that of iodide (Table S7, entries 5 & 6). Finally, the effect of the copper catalyst and its loading amount was evaluated. As discussed earlier and shown in Table S8, Cu(II) catalysts performed badly (Table S8, entries 1–4, yields 55%–69%). Only a minor difference in yields were observed when catalytic activity of CuO-NPs was compared with Cu(I) salts (Table S8, entries 5–8). The desired products are purified by column chromatography, identified by NMR spectra and then the isolated yield was calculated.

Table 1
Reaction of Aryl Iodides with Phenol and Thiophenol (conditions: phenol or thiophenol (25 mmol), aryl iodide (5 mmol), KOH (5 mmol), CuO (2.5 mol%), 100 °C, 17 h.

Entry	Aryl iodide	Alcohol or thiol	Product	Yield (%)
1	PhI	PhOH	Ph-O-Ph	99
2	PhI	PhSH	Ph-S-Ph	99
3	PhI	$PhCH_2OH$	$PhCH_2$-O-Ph	95
4	PhI	$PhCH_2SH$	$PhCH_2$-S-Ph	95

To determine the scope of the catalytic system, the present protocol was further applied to reactions of a variety of commercially available aryl iodides and phenols or thiophenols (Table 1). As shown in Table 1, the coupling of phenol and thiophenol with iodobenzene was successful, leading to the desired products in good yields. The protocol is equally efficient for aromatic and aliphatic phenols and thiophenols. The catalyst system is highly efficient providing the corresponding diaryl ethers and thioethers in good to excellent yields. Iodobenzene was maintained as arylating substrate. The present optimized catalytic process provides the arylation of phenols and thiophenols with aryl iodides, in the presence of KOH as a base under neat conditions. To the best of our knowledge, this is the first report about aryl-sulphur and aryl-oxygen bond formation in which a MOF derived CuO-NPs catalyst

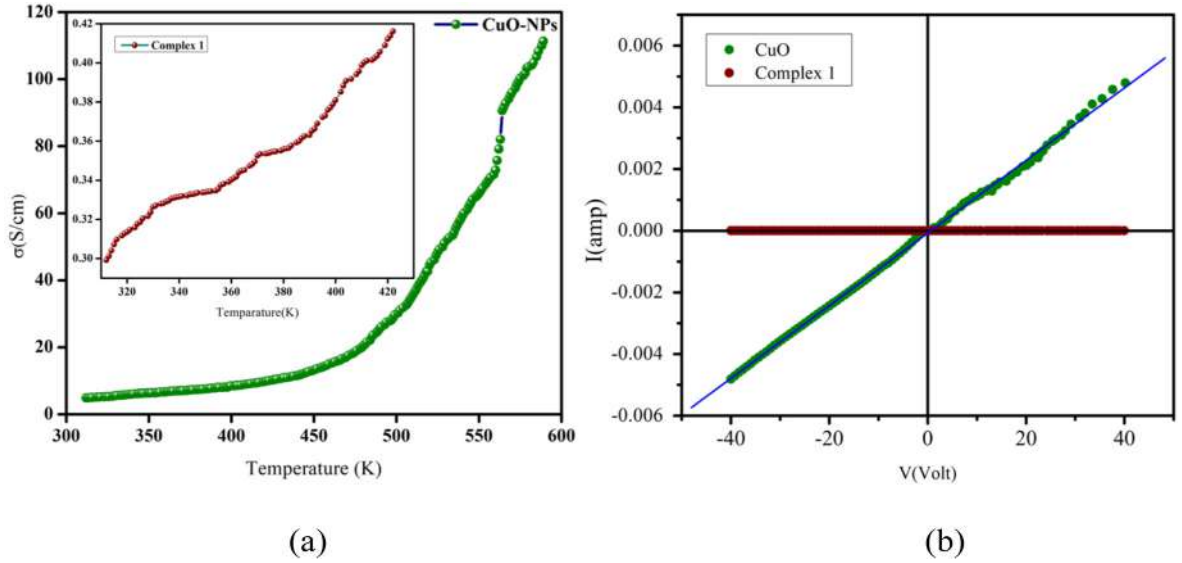

Fig. 7. Variable temperature electrical conductivity and corresponding I–V curve of the both complex **1** and MOF derived NPs.

is used without addition of any ligand and solvent. In the present study diphenylether and diphenylthioether was formed in 99% yield in the reaction of iodobenzene with phenol and thiophenol in solvent free neat conditions.

The CuO nanoparticles are recyclable upto 5th cycle without loss of significant reactivity (Table S9). After completion of the C–O cross-coupling of phenol with iodobenzene, the reaction mixture was treated with diethyl ether. Then, the overall mixture was centrifuged to isolate the catalyst. After isolation, it was washed with water and ether repeatedly and then dried for further use (Figure S13). The reusability tests indicate high yield. A comparative study with the bulk CuO synthesized by precipitation method was also studied – a lower amount of yield (∼40%–55%) was obtained for CuO bulk.

The catalytic activity of our synthesized CuO-NPs was investigated for the cross-coupling of iodobenzene with phenol and compared with similar heterogeneous catalysts (Table S10). Unlike homogeneous catalyst, use of heterogeneous catalyst is much more advantageous in terms of their easy separation, recyclability, high thermal stability and longer lifetime. In this respect, based on literature and availability of the heterogeneous catalysts, the reactivity of ZnO, SnO, SnO_2, CuO, Cu_2O and CuO NPs/SiO_2 [37] has been judged and compared with respect to C–O coupling reaction of phenol and iodobenzene. Our synthesized CuO is found to be most effective with respect to yield of the desired coupling product. Heterogeneous catalysts other than CuO and Cu_2O found to be completely ineffective giving no yield of the desired C–O coupling product (entries 1–3).

A suitable mechanistic pathway for the above-mentioned catalysis reactions was proposed (Scheme S1). These results suggest that the reaction may occur by oxidative addition followed by reductive elimination. The oxidative addition of the aryl halide with catalyst can give intermediate **A**, which can undergo reaction with an alcohol or thiol to afford intermediate **B**. Intermediate **B** can provide the C–O or C–S cross coupling product by reductive elimination. According to Sambiagio et al. the mechanism of such reactions is still unclear and it is considered that the mechanism actually varies depending on the substrate, ligand and reaction conditions [22b]. It is believed that the most active catalyst is Cu(I)-species which may form from the initial copper source.

Electrical Conductivity of MOF and MOF derived CuO-NPs: In complex **1**, the coordination between the metal centres and ndc^{2-} ligands forms 2D coordination layers and coordinated 1,10-phen moieties are hanging from the layers to connect next to neighbouring layers through $\pi \ldots \pi$ interaction to form 3D supramolecular structure. Due to the presence of extended $\pi \ldots \pi$ conjugation within the structure of **1**, we hope that the framework may show electrical conductivity. Bulk electrical conductivity of complex **1** has been measured by four probe contact using Ag wire on the pressed pellets. The conductivity of complex **1** is 3 x 10^{-3} S/cm at 312 K with Ohomic behaviour within the range of ± 40 V, Fig. 7(a and b). Variable temperature conductivity measurement within the temperature range of 312 K to 423 K indicates that with increasing temperature, conductivity of the framework increases — the framework is semiconducting in nature. The conductivity value is 4.2 × 10^{-3} S/cm at 423 K. With increasing temperature, delocalization of π-electrons increases and this may be a reason behind the linear rise in conductivity value electrical conductivity. The calculated activation energy of the framework is 0.077 eV.

Koo et al. have reported a semiconductive metal–organic framework having 2,5,8-tri(4-pyridyl)1,3-diazaphenalene as the π-conjugated ligand. Single crystal electrical conductivity measurement gives a value of ∼1 x 10^{-6} S/cm [12a]. Kuang et al. have reported single crystal conductivity value of ∼1.2 × 10^{-5} S/cm of a framework having napthalenediimide [12b]. Haider et al. have measured conductivity on the single crystal of a framework containing 1,4,5,8-naphthalenetetracarboxylate and the framework shows conductivity of ∼10^{-4} S/cm [12c]. Chen et al. have reported the semiconducting behaviour of mixed metal MOF in which 4,4′-(anthracene-9,10-diylbis(ethyne-2,1-diyl))dibenzoate is used to induce $\pi \ldots \pi$ interaction within the framework at separation distance of 3.4 Å [12d]. Electrical conductivity measurement on single crystals gives a conductivity value of 1.3 × 10^{-3} S/cm. Qu et al. have measured electrical conductivity of a metal–organic framework containing N,N′-di(4-pyridyl)-1,4,5,8-naphthalenetetracarbox-diimide on both single crystal and pressed pellets [12e]. Single crystal conductivity measurement showed 10^3 times higher conductivity (3.3 × 10^{-3} S/cm) than measured on the pressed pellets (7.6 × 10^{-6} S/cm). In our case, four probe electrical conductivity measurement on the pressed pellet of complex **1** gives a value of 3 x 10^{-3} S/cm at 312 K.

We have also studied the electrical conductivity of the MOF derived CuO-NPs in a similar manner. CuO is a p-type semiconductor but the bandgap and electrical conductivity vary with

the size and morphology of the nano-particles [38]. In most cases, the bandgap of CuO-NPs varies in the range of 1.2 to 2.0 eV and, based on its narrow bandgap, CuO-NPs have significant applications in electronic and opto-electronics. The conductivity of the MOF derived CuO-NPs is 4.85 $\times$ 10^{-2} S/cm with similar Ohomic behaviour at 312 K and this conductivity value is 16 times higher than the parent MOF, Fig. 7a and b. Combustion of the organic moieties within the MOF leads to the occurrence of charge transfer interaction between the copper and oxygen atoms within the framework and this may be the reason behind this enhanced conductivity. The variable temperature conductivity of the NPs is measured within the range of 312 to 588 K and the CuO-NPs also show semiconducting behaviour. The conductivity value rises smoothly up to 430 K (11 x 10^{-2} S/cm) and afterwards increases very rapidly to 1.11 S/cm at 588 K. A plot of $\ln(\sigma)$ vs. 1000/T for CuO-NPs shows two linear portions intersecting each other (Figure S14). This indicates the presence of two activation energy of CuO and values are 73 and 370 meV respectively, with a crossover at 430 K. The comparatively small activation energy indicates that Cu(I) and Cu(0) in association with oxygen vacancies may be present in CuO-Nps [16a]. Change of activation energy with temperature may be due to the presence of any metastable state in the sample.

4. Conclusions

Single crystal X-ray analysis of complex 1 revealed two types of binding modes (μ2- and μ4-) of ndc^{2-} ligands to the central Cu(II) ions, which, in turn, resulted in the formation of 2D coordination sheet. While the hanging 1,10-phenanthroline ligands in the interlamellar space assembled together by π-π interactions, which led to the formation of spongy 3D supramolecular metal–organic framework (MOF). Careful analysis of the MOF, which was stable up to 260 °C, depicted the presence of interpenetrated network topology. Reversible structural transformation of the framework by gliding motion of π-π stacked 1,10-phenanthroline ligands along the crystallographic *a*-axis and hence reversible expansion and contraction among the layer gap of 2D coordination sheets was confirmed by variable temperature PXRD measurements. Adsorption studies of the MOF with water, methanol and ethanol depicted a hysteresis loop in adsorption/desorption cycle. After thorough characterization of the MOF, it was calcinated at 650 °C for 4 h to fabricate CuO-NPs. The PXRD patterns confirmed the formation of CuO-NPs. While microscopic images showed formation of nearly uniform CuO-NPs with an average size of ~25 nm. Electrical conductivity measurements of the MOF and MOF derived CuO-NPs suggested both of them are semiconducting nature. However, CuO-NPs were found to be far more conducting compared to the parent MOF. Further, selective and efficient CuO-NPs catalyzed C–O and C–S bond-forming reaction of aryl iodides and various thiophenols is developed. This catalytic procedure offers general applicability and simplicity, avoiding the expensive and time-consuming preparation of suitable ligands and activated substrates. Based on controlled experiments and green chemistry rules, we proposed a solvent free, neat reaction conditions. Because of these advantages, we strongly believe that the protocol demonstrated in this work could find large application. And, we hope that such MOF derived nano-particle synthesis technique may be used for the synthesis of different types of metal–oxide nano-materials like ZnO, Cr_2O_3, VO_2, rare earth oxides.

CRediT authorship contribution statement

Maxcimilan Patra: Synthesized the materials and carried out most of the experiments, Writing manuscript. **Soumen Kumar Dubey:** Synthesized the materials and carried out most of the experiments, Writing manuscript. **Bibhas Mondal:** Carried out all the catalysis experiments, Written the manuscript. **Kajal Gupta:** Carried out all the electrical conductivity measurements, Written the manuscript. **Angshuman Ghosh:** Carried out several characterizations like NMR, IR, Manuscript preparation. **Subhankar Mandal:** Carried out the XPS measurement, Manuscript preparation. **Satyajit Hazra:** Carried out the XPS measurement, Manuscript preparation. **Ajit Kumar Meikap:** Carried out all the electrical conductivity measurements, Written the manuscript. **Ujjal Kanti Roy:** Carried out all the catalysis experiments, Written the manuscript. **Subham Bhattacharjee:** Idea of this research project was drawn, Manuscript preparation. **Rajat Saha:** Idea of this research project was drawn, Manuscript preparation.

Declaration of competing interest

The authors declare that they have no known competing financial interests or personal relationships that could have appeared to influence the work reported in this paper.

Acknowledgements

This work was supported by funding from TARE, SERB to R. S. (TAR/2018/000744) and DST Inspire Faculty Research Grant to S.B. (Faculty Registration No.: IFA18-CH304, DST/INSPIRE/04/2018/000329). U.K.R. acknowledges financial support of this work by SERB New Delhi, SR/FT/CS-137/2011 dated 12.07.2012, and Science and Technology and Biotechnology-WB, 50 (Sanc.)/ST/P/S&T/15G-10/2018 dated 30.01.2019 to UKR is gratefully acknowledged. M. P. and S. K. D. thank DST Inspire Faculty Research Grant for financial assistance. The authors thank Goutam Sarkar for his technical support in XPS measurements. S. M. acknowledges the Council of Scientific & Industrial Research (CSIR), India for providing a research fellowship.

Appendix A. Supplementary data

Supplementary material related to this article can be found online at https://doi.org/10.1016/j.nanoso.2021.100756. The CCDC number is 2013885 for complex 1. Figure S1–S9, Table S1–S8, NMR spectra and catalytic mechanism scheme are given in Supporting information file.

References

[1] (a) H. Furukawa, K.E. Cordova, M. O'Keeffe, O.M. Yaghi, The chemistry and applications of metal-organic frameworks, Science 341 (2013) 1230444.
(b) R. Chakraborty, P.S. Mukherjee, P.J. Stang, Supramolecular coordination: self-assembly of finite two- and three-dimensional ensembles, Chem. Rev. 111 (2011) 6810.
(c) T.K. Maji, R. Matsuda, S. Kitagawa, A flexible interpenetrating coordination framework with a bimodal porous functionality, Nat. Mater. 6 (2007) 142.
(d) J.A. Mason, M. Veenstra, J.R. Long, Evaluating metal-organic frameworks for natural gas storage, Chem. Sci. 5 (2014) 32.
(e) J.-R. Li, R.J. Kuppler, H.-C. Zhou, Selective gas adsorption and separation in metal-organic frameworks, Chem. Soc. Rev. 38 (2009) 1477.
(f) A. Corma, H. García, F.X.L. Xamena, Engineering metal organic frameworks for heterogeneous catalysis, Chem. Rev. 110 (2010) 4606.
(g) J.L.C. Rowsell, O.M. Yaghi, Metal-organic frameworks: a new class of porous materials, Microporous Mesoporous Mater. 73 (2004) 3.
(h) S. Kitagawa, R. Kitaura, S. Noro, Functional porous coordination polymers, Angew. Chem. Int. Ed. 43 (2004) 2334.

(i) W.P. Lustig, S. Mukherjee, N.D. Rudd, A.V. Desai, J. Li, S.K. Ghosh, Metal–organic frameworks: functional luminescent and photonic materials for sensing applications, Chem. Soc. Rev. 46 (2017) 3242.
(j) A.M. Al-Enizi, J. Ahmed, M. Ubaidullah, S.F. Shaikh, T. Ahamad, M. Naushad, G. Zheng, Utilization of waste polyethylene terephthalate bottles to develop metal–organic frameworks for energy applications: A clean and feasible approach, J. Clean. Prod. 248 (2020) 119251.
(k) A.M. Al-Enizi, M. Ubaidullah, J. Ahmed, T. Ahamad, T. Ahmad, S.F. Shaikh, M. Naushad, Synthesis of niox@ npc composite for high-performance supercapacitor via waste pet plastic-derived ni-mof, Compos. B. Eng. 183 (2020) 107655.
(l) M. Ubaidullah, J. Ahmed, T. Ahamad, S.F. Shaikh, S.M. Alshehri, A.M. Al-Enizi, Hydrothermal synthesis of novel nickel oxide@ nitrogenous mesoporous carbon nanocomposite using costless smoked cigarette filter for high performance supercapacitor, Mater. Lett. 266 (2020) 127492.
(m) N. Bakhtiari, S. Azizian, S.M. Alshehri, N.L. Torad, V. Malgras, Y. Yamauchi, Study on adsorption of copper ion from aqueous solution by mof-derived nanoporous carbon, Microporous Mesoporous Mater. 217 (2015) 173–177.
(n) H. Zhang, M. Zhang, M.V. Lin Ping, J. Tang, S.M. Alshehri, Y. Yusuke, D. Shaowu, J. Zhang, A highly energetic n-rich metal-organic framework as a new high-energy-density, Material. Chem. Eur. J. 22 (2015) 1141–1145.

[2] (a) N. Nidamanuri, K. Maity, S. Saha, Electrically conductive metal-organic frameworks, in: Book Chapter, World Scientific Publishing, 2017.
(b) V. Stavila, A.A. Talin, M.D. Allendorf, Mof based electronic and opto-electronic devices, Chem. Soc. Rev. 43 (2014) 5994.

[3] (a) E.M. Miner, T. Fukushima, D. Sheberla, L. Sun, Y. Surendranath, M. Dincă, Electrochemical oxygen reduction catalysed by Ni_3(Hexaiminotriphenylene)$_2$, Nature Commun. 7 (2016) 10942.
(b) M.G. Campbell, D. Sheberla, S.F. Liu, T.M. Swager, M. Dincă, Cu_3(Hexaiminotriphenylene)$_2$: An electrically conductive 2D metal-organic framework for chemiresistive sensing, Angew. Chem. Int. Ed. 54 (2015) 4349.
(c) J. Park, M. Lee, D. Feng, Z. Huang, A.C. Hinckley, A. Yakovenko, X. Zou, Y. Cui, Z. Bao, Stabilization of hexaaminobenzene in a 2D conductive metal-organic framework for high power sodium storage, J. Am. Chem. Soc. 140 (2018) 10315.
(d) S. Roy, M. Das, A. Bandyopadhyay, S.K. Pati, P.P. Ray, T.K. Maji, Colossal increase in electric current and high rectification ratio in a photoconducting, self-cleaning, and luminescent schottky barrier nmof diode, J. Phys. Chem. C 121 (2017) 23803.
(e) S.S. Shinde, C.H. Lee, J.-Y. Jung, N.K. Wagh, S.-H. Kim, D.-H. Kim, C. Lin, S.U. Lee, J.-H. Lee, Unveiling Dual-Linkage 3D Hexaiminobenzene Metal-Organic Frameworks towards Long-Lasting Advanced Reversible Zn-Air Batteries. Energy Environ. Sci. 12 (2019) 727.
(f) D. Feng, T. Lei, M.R. Lukatskaya, J. Park, Z. Huang, M. Lee, L. Shaw, S. Chen, A.A. Yakovenko, A. Kulkarni, J. Xiao, K. Fredrickson, J.B. Tok, X. Zou, Y. Cui, Z. Bao, Robust and conductive two-dimensional metal-organic frameworks with exceptionally high volumetric and areal capacitance, Nat. Energy 3 (2018) 30.
(g) D. Sheberla, J.C. Bachman, J.S. Elias, C.-J. Sun, Y. Shao-Horn, M. Dinca, Conductive MOF electrodes for stable supercapacitors with high areal capacitance, Nat. Mater. 16 (2017) 220.
(h) X. Huang, S. Zhang, L. Liu, L. Yu, G. Chen, W. Xu, D. Zhu, Superconductivity in a copper(ii) based coordination polymer with perfect kagome structure, Angew. Chem. Int. Ed. 57 (2018) 146.

[4] (a) S. Takaishi, M. Hosoda, T. Kajiwara, H. Miyasaka, M. Yamashita, Y. Nakanishi, Y. Kitagawa, K. Yamaguchi, A. Kobayashi, H. Kitagawa, Electroconductive porous coordination polymer Cu[Cu(Pdt)$_2$] composed of donor and acceptor building units, Inorg. Chem. 48 (2009) 9048.
(b) Y. Kobayashi, B. Jacobs, M.D. Allendorf, J.R. Long, Conductivity, doping, and redox chemistry of a microporous dithiolene-based metal-organic framework, Chem. Mater. 22 (2010) 4120.

[5] (a) M.E. Ziebel, L.E. Darago, J.R. Long, Control of electronic structure and conductivity in two-dimensional metal-semiquinoid frameworks of titanium, vanadium, and chromium, J. Am. Chem. Soc. 140 (2018) 3040.
(b) S. Benmansour, A. Abhervé, P. Gómez-Claramunt, C. Vallés- García, C.J. Gómez-García, Nanosheets of two-dimensional magnetic and conducting Fe(II)/Fe(III) mixed-valence metal-organic frameworks, ACS Appl. Mater. Interfaces 9 (2017) 26210.
(c) J.A. DeGayner, I.-R. Jeon, L. Sun, M. Dincă, T.D. Harris, 2D conductive iron-quinoid magnets ordering up to T_c = 105 K via heterogenous redox chemistry, J. Am. Chem. Soc. 139 (2017) 4175.

[6] (a) M.-H. Zeng, Q.-X. Wang, Y.-X. Tan, S. Hu, H.-X. Zhao, L.-S. Long, M. Kurmoo, Rigid pillars and double walls in a porous metal-organic framework: Single-crystal to single-crystal, controlled uptake and release of iodine and electrical conductivity, J. Am. Chem. Soc. 132 (2010) 2561.
(b) X. Zhang, I. da Silva, R. Fazzi, A.M. Sheveleva, X. Han, B.F. Spencer, S.A. Sapchenko, F. Tuna, E.J.L. McInnes, M. Li, S. Yang, M. Schröder, Iodine adsorption in a redox-active metal-organic framework: electrical conductivity induced by host-guest charge-transfer, Inorg. Chem. 58 (2019) 14145.

[7] (a) A.A. Talin, A. Centrone, A.C. Ford, M.E. Foster, V. Stavila, P. Haney, R.A. Kinney, V. Szalai, F.E. Gabaly, H.P. Yoon, F. Léonard, M.D. Allendorf, Tunable electrical conductivity in metal-organic framework thin-film devices, Science 343 (2014) 66.
(b) C. Schneider, D. Ukaj, R. Koerver, A.A. Talin, G. Kieslich, S.P. Pujari, H. Zuilhof, J. Janek, M.D. Allendorf, R.A. Fischer, High electrical conductivity and high porosity in a Guest@MOF Material: Evidence of TCNQ Ordering within Cu_3BTC_2, Micropores. Chem. Sci. 9 (2018) 7405.

[8] J.G. Park, M.L. Aubrey, J. Oktawiec, K. Chakarawet, L.E. Darago, F. Grandjean, G.J. Long, J.R. Long, Charge delocalization and bulk electronic conductivity in the mixed- valence metal-organic framework Fe(1, 2, 3-Triazolate)$_2$(BF_4)$_x$, J. Am. Chem. Soc. 140 (2018) 8526.

[9] (a) L.S. Xie, G. Skorupskii, M. Dinca, Electrically conductive metal-organic frameworks, Chem. Rev. 120 (2020) 8536–8580.
(b) X. Kuang, S. Chen, L. Meng, J. Chen, X. Wu, G. Zhang, G. Zhong, T. Hu, Y. Li, C.-Z. Lu, Chem. Commun. 55 (2019) 1643–1646.

[10] (a) L. Sun, T. Miyakai, S. Seki, M. Dincă, Mn_2(2, 5-disulfhydrylbenzene-1, 4-dicarboxylate): A microporous metal-organic framework with infinite (-Mn-S-)∞ chains and high intrinsic charge mobility, J. Am. Chem. Soc. 135 (2013) 8185.
(b) F. Gándara, F.J. Uribe-Romo, D.K. Britt, H. Furukawa, L. Lei, R. Cheng, X. Duan, M. O'Keeffe, O.M. Yaghi, Porous, conductive metal-triazolates and their structural elucidation by the charge-flipping method, Chem. Eur. J. 18 (2012) 10595.

[11] L. Liu, J.A. DeGayner, L. Sun, D.Z. Zee, T.D. Harris, Reversible redox switching of magnetic order and electrical conductivity in a 2D manganese benzoquinoid framework, Chem. Sci. 10 (2019) 4652.

[12] (a) J.Y. Koo, Y. Yakiyama, G.R. Lee, J. Lee, H.C. Choi, Y. Morita, M. Kawano, Selective formation of conductive network by radical-induced oxidation, J. Am. Chem. Soc. 138 (2016) 1776.
(b) X. Kuang, S. Chen, L. Meng, J. Chen, X. Wu, G. Zhang, G. Zhong, T. Hu, Y. Li, C.-Z. Lu, Supramolecular aggregation of a redox-active copper-naphthalenediimide network with intrinsic electron conduction, Chem. Commun. 55 (2019) 1643.
(c) G. Haider, M. Usman, T.-P. Chen, P. Perumal, K.-L. Lu, Y.-F. Chen, Electrically driven white light emission from intrinsic metal-organic framework, ACS Nano 10 (2016) 8366.
(d) D. Chen, H. Xing, Z. Su, C. Wang, Electrical conductivity and electroluminescence of a new anthracene-based metal-organic framework with π-conjugated zigzag chains, Chem. Commun. 52 (2016) 2019.
(e) L. Qu, H. Iguchi, S. Takaishi, F. Habib, C.F. Leong, D.M. D'Alessandro, T. Yoshida, H. Abe, E. Nishibori, M. Yamashita, Porous molecular conductor: electrochemical fabrication of through-space conduction pathways among linear coordination polymers, J. Am. Chem. Soc. 141 (2019) 6802.

[13] S.S. Park, E.R. Hontz, L. Sun, C.H. Hendon, A. Walsh, T. Van Voorhis, M. Dincă, Cation-dependent intrinsic electrical conductivity in isostructural tetrathiafulvalene-based microporous metal-organic frameworks, J. Am. Chem. Soc. 137 (2015) 1774.

[14] P.I. Scheurle, A. Mähringer, A.C. Jakowetz, P. Hosseini, A.F. Richter, G. Wittstock, D.D. Medina, T. Bein, A highly crystalline anthracene-based MOF-74 series featuring electrical conductivity and luminescence, Nanoscale 11 (2019) 20949.

[15] J.K. Sun, Q. Xu, Functional materials derived from open framework templates/precusros: Synthesis and applications, Energy Environ. Sci. 7 (2014) 2071.

[16] (a) R. Das, P. Pachfule, R. Banerjee, P. Poddar, Metal and metal oxide nanoparticles synthesis from metal organic frameworks (MOFs): finding the border of metal and metal oxides, Nanoscale 4 (2012) 591.
(b) S. Singha, A. Saha, S. Goswami, S.K. Dey, S. Payra, S. Banerjee, S. Kumar, R. Saha, A metal organic framework to CuO nanospheres of uniform morphologyfor synthesis of α-aminonitriles under solvent-free conditions along with crystal structure of the MOF, Cry. Growth Des. 18 (2018) 189.
(c) S. Ekambaram, K.C. Patil, M. Maaza, Synthesis of lamp phosphors: facile combustion approach, J. Alloys Compd. 393 (2005) 81-92.
(d) B.T. Sone, E. Manikandan, A. Gurib-Fakim, M. Maaza, Sm_2o_3 nanoparticles green synthesis via callistemon viminalis' extract, J. Alloys Compd. 650 (2015) 357-362.
(e) S. Khamlich, E. Manikandan, B.D. Ngom, J. Sithole, O. Nemraoui, I. Zorkani, Synthesis, characterization, and growth mechanism of α-cr_2o_3 monodispersed particles, J. Phys. Chem. Solids. 72 (2011) 714-718.
(f) S. Karthik, P. Siva, K.S. Balu, R. Suriyaprabha, V. Rajendran, M. Maaza, Acalypha indica-mediated green synthesis of ZnO nanostructures under differential thermal treatment: effect on textile coating, hydrophobicity, uv resistance, and antibacterial, Adv. Powder Technol. 28 (2017) 3184-3194.

(g) N. Mayedwa, N. Mongwaketsi, S. Khamlich, K. Kaviyarasu, N. Matinise, Green synthesis of nickel oxide, palladium and palladium oxide synthesized via aspalathus linearis natural extracts: physical properties & mechanism of formation, Appl Surf Sci. 446 (2018) 266-272.
(h) H. Guo, T.T. Li, W.W. Chen, L.X. Liu, J.L. Qiao, J. Zhang, Self-assembly formation of hollow Ni-Fe-O nanocage architectures by metal–organic frameworks with high-performance lithium storage, Sci. Rep. 5 (2015) 13310, 5.
(i) H.B. Wu, B.Y. Xia, L. Yu, X.-Y. Yu, X.W. Lou, Porous molybdenum carbide nano-octahedrons synthesized via confined carburization in metal–organic frameworks for efficient hydrogen production, Nature Comm. 6 (2015) 6512, 1.
(j) P. Panchfule, X. Yang, Q. Zhu, N. Tsumori, T. Uchida, Q. Xu, From Ru nanoparticle-encapsulated metal–organic frameworks to highly catalytically active Cu/Ru nanoparticles-embedded porous carbon, J. Mater. Chem. A 5 (2017) 4835.
(k) Z. Liang, C. Qu, D. Xia, R. Zou, Q. Xu, Atomically dispersed metal sites in MOF-based materials for electrocatalytic and photocatalytic energy conversion, Angew. Chem. Int. Ed. 57 (2018) 9604.

[17] (a) R. Dai, W. Sun, Y. Wang, Ultrasmall tin nanodots embedded in nitrogen-doped mesoporous carbon: Metal-organic-framework derivation and electrochemical application as highly stable anode for lithium ion batteries, Electrochim. Acta 217 (2016) 123.
(b) A.C. Nwanya, D. Obi, K.I. Ozoemena, R.U. Osuji, C. Awada, A. Ruediger, M. Maaza, F. Rosei, F.I. Ezema, Facile synthesis of nanosheet-like CuO film and its potential application as a high-performance pseudocapacitor electrode, Electrochimica Acta 198 (2016) 220-230.
(c) B.T. Sone, A. Diallo, X.G. Fuku, A. Gurib-Fakim, M. Maaza, Biosynthesized CuO nano-platelets: physical properties & enhanced thermal conductivity nanofluidics, Arab. J. Chem. 13 (2020) 160-170.
(d) A.C. Nwanya, M.M. Ndipingwi, N. Mayedwa, L.C. Razanamahandry, C.O. Ikpo, Maize (zea mays l.) fresh husk mediated biosynthesis of copper oxides: potentials for pseudo capacitive energy storage, Electrochimica Acta 301 (2019) 436-448.

[18] H. Pang, B. Guan, W. Sun, Y. Wang, Metal-organic-frameworks derivation of mesoporous nio nanorod for high-performance lithium ion batteries, Electrochim. Acta. 213 (2016) 351.

[19] (a) J. Wu, Y. Song, R. Zhou, S. Chen, L. Zuo, H. Hou, L. Wang, Zn–Fe–ZIF-derived porous $ZnFe_2o_4$/C@NCNT nanocomposites as anodes for lithium-ion batteries, J. Mater. Chem. A. 3 (2015) 7793.
(b) W.J. Meng, W. Chen, L. Zhao, Y. Huang, M.S. Zhu, Y. Huang, Y.Q. Fu, F.X. Geng, J. Yu, X.F. Chen, Porous Fe_3O_4/carbon composite electrode material prepared from metal–organic framework template and effect of temperature on its capacitance, Nano Energy 8 (2014) 133.

[20] C.F. Lee, Y.C. Liu, S.S. Badsara, Transition-metal-catalyzed C-S bond coupling reaction, Chem. Asian J. 9 (2014) 706.

[21] (a) S.F. Nielsen, E.O. Nielsen, G.M. Olsen, T. Liljefors, D. Peters, Novel potent ligands for the central nicotinic acetylcholine receptor: Synthesis, receptor binding, and 3D-QSAR analysis, J. Med. Chem. 43 (2000) 2217.
(b) G. De Martino, M.C. Edler, G. La Regina, A. Cosuccia, M.C. Barbera, D. Barrow, R.I. Nicholson, G. Chiosis, A. Brancale, E. Hamel, M. Artico, R. Silvestri, New arylthioindoles: potent inhibitors of tubulin polymerization. 2. structure-activity relationships and molecular modeling studies, J. Med. Chem. 49 (2006) 947.

[22] (a) S.V. Ley, A.W. Thomas, Modern synthetic methods for copper-mediated C(aryl)-O, C(aryl)-N, and C(aryl)-S Bond Formation, Angew. Chem. Int. Ed. 43 (2003) 5400.
(b) C. Sambiagio, S.P. Marsden, A.J. Blacker, P.C. McGowan, Chem. Soc. Rev. 43 (2014) 3525-3550.

[23] T. Punniyamurthy, L. Rout, Recent advances in copper-catalyzed oxidation of organic compounds, Coord. Chem. Rev. 252 (2008) 134.

[24] (a) K.E. Torraca, X. Huang, C.A. Parrish, S.L. Buchwald, An efficient intermolecular palladium-catalyzed synthesis of aryl ethers, J. Am. Chem. Soc. 123 (2001) 10770.
(b) J. Mondal, A. Modak, A. Dutta, A. Bhaumik, Facile C–S coupling reaction of aryl iodide and thiophenol catalyzed by cu-grafted furfural functionalized mesoporous organosilica, Dalton Trans. 40 (2011) 5228.
(c) G.B.B. Varadwaj, S. Rana, K.M. Parida, Stable amine functionalized montmorillonite supported Cu, Ni catalyst showing synergistic and cooperative effectiveness towards C-S coupling reactions, RSC Adv. 3 (2013) 7570.
(d) E. Sperotto, G.P.M. van Klink, J.G. de Vries, G. van Koten, Ligand-free copper-catalyzed C-S coupling of aryl iodides and thiols, J. Org. Chem. 73 (2008) 5625.

[25] (a) G.T. Venkanna, H.D. Arman, Z.J. Tonzetich, Catalytic C-S cross-coupling reactions employing Ni complexes of pyrrole-based pincer ligands, ACS Catal. 4 (2014) 2941.
(b) X. Xu, J. Liu, J.J. Zhang, Y.W. Wang, Y. Peng, Nickel-mediated inter- and intramolecular C-S coupling of thiols and thioacetates with aryl iodides at room temperature, Org. Lett. 15 (2013) 3, 550.
(c) O. Bistri, A. Correa, C. Bolm, Iron-catalyzed C-O cross-couplings of phenols with aryl iodides, Angew. Chem. Int. Ed. 47 (2008) 586.

[26] S. Mandal, M. Mukherjee, S. Hazra, Evolution of electronic structures of polar phthalocyanine substrate interfaces, ACS Appl. Mater. Interfaces 12 (2020) 45564–45573.

[27] Bruker, APEX2, SAINT and SADABS, BRUKER AXS, Inc., Madison, Wisconsin, USA, 2008.

[28] G.M. Sheldrick, Crytal structure refinement with SHELX, Acta Cryst. C71 (2015) 3–8.

[29] L.J. Farrugia, Wingx and ORTEP for windows, an update, J. Appl. Crystallogr. 45 (2012) 849–854.

[30] A.L. Spek, Structure validation in chemical crystallography, Acta Cryst. D65 (2009) 148–155.

[31] L.J. Farrugia, ORTEP-3 for windows - a version of ORTEP-III with a graphical user interface (GUI), J. Appl. Crystallogr. 30 (1997) 565.

[32] X. He, C. Lu, D. Yuan, L. Chen, Q. Zhang, C. Wu, Hydrothermal synthesis, crystal structures, and properties of a class of 2D coordination polymers, Eur. J. Inorg. Chem. (2005) 4598.

[33] (a) R. Kitaura, K. Seki, G. Akiyama, S. Kitagawa, Porous coordination-polymer crystals with gated channels specific for supercritical gases, Angew. Chem. Int. Ed. 42 (2003) 428.
(b) J. Zhang, S. Kitagawa, Supramolecular isomerism, framework flexibility, unsaturated metal center, and porous property of Ag(I)/Cu(I) 3, 3', 5, 5'-tetrametyl-4, 4'-bipyrazolate, J. Am. Chem. Soc. 130 (2008) 907.

[34] T.K. Maji, M. Ohba, S. Kitagawa, Transformation from a 2D stacked layer to 3D interpenetrated framework by changing the spacer functionality: Synthesis, structure, adsorption, and magnetic properties, Inorg. Chem. 44 (2005) 9225.

[35] M.C. Biesinger, Advanced analysis of copper X-ray photoelectron spectra, Surf. Interface Anal. 49 (2017) 1325–1334.

[36] (a) X. Lv, W. Bao, J. Org. Chem. 72 (2007) 3863.
(b) D. Ma, Q. Cai, N, N-dimethyl glycine-promoted ullmann coupling reaction of phenols and aryl halides, Org. Lett. 5 (2003) 3799.
(c) H.-J. Cristau, P.P. Cellier, S. Hamada, J.-F. Spindler, M. Taillefer, A general and mild ullmann-type synthesis of diaryl ethers, Org. Lett. 6 (2004) 913.
(d) S. Jammi, S. Sakthivel, L. Rout, T. Mukherjee, S. Mandal, R. Mitra, P. Saha, T. Punniyamurthi, Cuo nanoparticles catalyzed c-n, c-o and c-s cross coupling reaction: scope and mechanism, J. Org. Chem. 74 (2009) 1971-1976.

[37] A.R. Hajipour, F. Dordahan, F. Rafiee, M. Mahdavi, C–n cross-coupling reaction catalysed by efficient and reusable cuo/sio2 nanoparticles under ligand-free conditions, Appl. Organ. Chem. 28 (2014) 809–813.

[38] S. Sagadevan, P. Murugasen, Electrical properties of copper oxide nanoparticles, J. Nano Res. 30 (2015) 1.

CrystEngComm

ROYAL SOCIETY OF CHEMISTRY

PAPER

View Article Online
View Journal | View Issue

Cite this: *CrystEngComm*, 2021, **23**, 3510

Photo-responsive Schottky diode behavior of a donor–acceptor co-crystal with violet blue light emission†

Soumen Singha,[a] Rajkumar Jana,[ab] Rituparna Mondal,[ac] Partha Pratim Ray,[a] Partha Pratim Bag,[d] Kajal Gupta,[e] Nandan Pakhira,[e] Corrado Rizzoli,[f] Arabinda Mallick,[e] Sanjay Kumar *[a] and Rajat Saha *[ae]

Herein, we report the crystal structure, supramolecular structure, electronic transport properties and optoelectronic behaviour of a co-crystal made of tetrabromoterephthalic acid (TBTA) and quinoxaline (QUIN) (1 : 1). The sample has been characterized using thermogravimetric analysis and spectral techniques. Moreover, theoretical analyses of noncovalent interactions, optical properties and the band structure of the co-crystal have been performed. The co-crystal has been crystallized in an orthorhombic system with the *Pnma* space group and the constituent molecules assemble in the solid state by using O–H···N hydrogen bonding, π···π, Br···π and Br···O interactions. The ground state geometry optimization over the hydrogen bonded dimer by DFT method indicates that TBTA acts as the donor and QUIN as the acceptor within the self-assembled co-crystal. According to UV-vis spectroscopic study the bandgap of the co-crystal is ~3.18 eV. In the solid state it exhibits a broad emission band with a maximum at 405 nm while in aqueous medium its photoluminescence emission peaks are obtained at 350 and 403 nm. The values of the average fluorescence lifetime of the sample in aqueous medium are 3.38 ns at 352 nm and 4.94 ns at 403 nm. Under UV-irradiation, the co-crystal emits violet-blue light. The emission spectrum in solution phase shows a relative quantum yield of 0.018. Band structure calculation indicates that the co-crystal is a p-type semiconductor with a bandgap of 2.835 eV. Due to its semiconducting character, the ITO/co-crystal/Al sandwiched structured device acts as a Schottky barrier diode with rectification ratio, ideality factor, barrier height and series resistance of 41, 1.36, 0.70 eV, and 26.97 kΩ, respectively. The current through the device increases substantially under visible light exposure. Upon visible light illumination the values of electrical conductivity, mobility and carrier concentration increase by 35 (±0.5), 54 (±0.5) and 6 (±0.5)%, respectively, with respect to dark conditions. It has been shown that π···π and hydrogen bonding interactions can play a crucial role in producing the donor–acceptor (D–A) type co-crystal, semiconducting behaviour can be incorporated in the organic co-crystal utilizing π···π and hydrogen bonding interactions and weak intermolecular π···π, Br···π and Br···O interactions can act as the pathway for electrical conduction.

Received 5th January 2021,
Accepted 2nd March 2021

DOI: 10.1039/d1ce00020a

rsc.li/crystengcomm

Introduction

In recent times, photo-responsive organic semiconductors[1] have attracted enormous attention because of their significant application potential in photodetectors,[2] optical switches,[3] LED[4] and photovoltaic cells.[5] In this context, donor–acceptor molecular co-crystals connected by charge transfer and weak intermolecular interactions like hydrogen bonding[6] and π-interactions[7] which also have success in crystal engineering have emerged as the most promising material of this category.[8–11] The physicochemical properties of co-crystals are poles apart from the sum of their components. These properties can be tuned rationally by altering intermolecular interactions through judicious selection of the constituents. Recently, study of the semiconducting and optoelectronic

[a] *Department of Physics, Jadavpur University, Jadavpur, Kolkata-700032, WB, India. E-mail: kumars@phys.jdvu.ac.in, rajatinorg1@gmail.com*
[b] *Department of Physics, Techno India University, EM-4, Sector-V, Salt lake, Kolkata-700091, India*
[c] *Department of Electronics, Barrackpore Rastraguru Surendranath College, Barrackpore, West Bengal 700120, India*
[d] *Dumka Engineering College, Dumka, Jharkhand-814101, India*
[e] *Department of Chemistry, Kazi Nazrul University, Asansol-713340, WB, India*
[f] *Dipartimento SCVSA, Università di Parma, Parco Area delle Scienze 17/A, Parma, Italy*

† Electronic supplementary information (ESI) available: Experimental procedures, tables, relevant figures and other related documents. CCDC 1841621. For ESI and crystallographic data in CIF or other electronic format see DOI: 10.1039/d1ce00020a

behaviour of organic co-crystals/salts has attracted paramount attention due to their enormous application possibilities in next generation environment friendly electronic and optoelectronic devices in place of the Si-based devices used nowadays.[12–36] However, very few co-crystals exhibit photo-responsive properties.[15–36] Thorough investigation of the electronic and optoelectronic properties of a number of organic co-crystal based devices fabricated in laboratory conditions yielded very promising results in respect to their application possibilities in the area of light emitting diodes,[17] light emitting transistors,[18,19] lasers,[20] photoconductors,[21,22] and photovoltaic cells.[23]

Tsutsumi *et al.*, have reported the photovoltaic behaviour of a device fabricated by using DBTTF–TCNQ (dibenzotetrathiofulvalene–tetracyanoquinodimethane) co-crystal with narrow bandgap (0.7 eV).[24] The thin film solar cell made of tetracene-doped anthracene co-crystal exhibits an optical efficiency of 23.72%.[25] The highest power conversion efficiency achieved in fullerene and squarine co-crystal based heterojunction solar cells is 10%.[26] The organic p–n junction photovoltaic cell made from contorted hexabenzocoronene (donor) and spherical fullerene (acceptor) exhibits a good response but large scale production of the device has not yet been taken up due to lack of proper structural characterization of the co-crystal used.[27] W. Hu and co-workers have assessed the optoelectronic performance of several D–A type charge transfer co-crystals.[28–32] They have examined morphology dependant photo-responsive behaviour of two different co-crystals of perylene (P) and TCNQ (T) and shown that the on–off photocurrent ratios of the devices made of 1 : 1 and 3 : 1 P–T co-crystals under visible light illumination are 5.4 and 4.4, respectively.[30] In another article, they have shown that the bipyridylethylene (BPE)–1,2,4,5-tetracyanobenzene (TCNB) co-crystal can be used as an optical waveguide.[31] They have also designed photonic logic gate properties of an organic co-crystal composed of 4-(1-naphthylvinyl)pyridine and 1,2,4,5-tetracyanobenzene.[32] The field effect transistor (FET) fabricated by using the co-crystal of C_{60} and 5,10,15,20-tetrakis(3,5-dimethoxyphenyl)porphyrin (3,5-TPP) responds to NIR radiation.[33] The heterojunction device made from the acridine–trimesic acid co-crystal exhibits an ultrahigh on–off photocurrent ratio of the order of 10^4.[34] The electrical conductivity of co-crystal of 1,3,6,8-pyrenetetrasulfonic acid tetrasodium salt as donor and 1,1′-bibutyl-4,4′-bipyridinium dibromide as acceptor increases upon illumination with laser beam of wavelength 405 nm.[35] However, this co-crystal has low conductivity.[35]

Earlier we have reported the role of weak intermolecular interactions (like hydrogen bonding, π–π, Br···π and Br···O interactions) in the electrical response of tetrabromoterephthalic acid (TBTA) based multi-component semiconducting co-crystals through formation of Schottky barriers.[36] Recently, we have reported the photo-responsive behaviour of some organic co-crystal/salts based Schottky barrier diodes.[15] It is noteworthy that the weak intermolecular interactions between the donor and acceptor molecules of co-crystals can be utilized for generation of photocarriers.[1,5,15–23] Thus, from a fundamental view point of crystal engineering it appears that the possibility of forming a co-crystal utilizing charge transfer/π···π stacking between TBTA and quinoxaline (QUIN) molecules and having the supramolecular network formed by weak hydrogen bonding, π–π, Br···π and Br···O interactions can be explored in order to examine the role of such weak noncovalent interactions in the electronic transport properties and optoelectronic behaviour through a comprehensive study of the photo-responsive properties of a TBTA–QUIN based Schottky barrier diode.

Herein, we have designed a semiconducting-luminescent co-crystal of the poly-bromo organic molecule TBTA as donor and QUIN as acceptor (Fig. S1†) using the solvent evaporation method, characterized it using single crystal X-ray diffraction (SCXRD), UV-vis, luminescence lifetime measurements and fluorescence microscopic imaging techniques. Its photo-responsive properties have also been examined. Structural study reveals that this TBTA–QUIN co-crystal has been formed by the self-assembly of its constituents TBTA and QUIN through hydrogen bonding and π–π interactions and it has assembled in the solid state through supramolecular O–H···N hydrogen bonding, Br···O, Br···π and π–π interactions. Theoretical inspection of the energy levels of frontier molecular orbitals of the hydrogen bonded dimer shows that TBTA acts as donor while QUIN acts as acceptor. Band structure calculations show that the bandgap of the co-crystal is 2.835 eV and this value agrees well with the optical bandgap (3.18 eV) obtained from solid state UV-vis spectra. Under UV-irradiation the co-crystal emits violet-blue light. To examine the electrical response, thin film of the co-crystal is fabricated on an ITO surface and the ITO/co-crystal/Al sandwich structure exhibits "Schottky diode" behaviour with a rectification ratio of 45 in dark conditions. The conductivity of the co-crystal made device increases by 35 (±0.5)% upon visible light exposure and it exhibits "Schottky diode" behaviour with a rectification ratio of ~56.

Experimental section

This study includes the solvent evaporation synthesis of TBTA–QUIN co-crystal, X-ray single crystal structural characterization, density functional theory (DFT) based calculation of the binding energy and non-covalent interactions within the components, Hirshfeld surface analysis, spectroscopic study and its theoretical verification by DFT and periodic DFT calculations (details are provided in the ESI†). The *I–V* measurements in dark and under visible light illumination have been performed on an Al/co-crystal/ITO sandwich structure fabricated by using an SCU 2700 spin coating system. Aluminium (Al) electrode is deposited on the active thin film by a vacuum coating unit (12A4D of HINDHIVAC) using a shadow mask. The *I–V* characteristics, in dark and under visible light irradiation, of the co-crystal have been recorded using the two probe method using a

Keithley 2400 sourcemeter interfaced with a PC at applied bias voltage in the range of −2 to +2 V. The *I–V* measurements have been carried out in a dark box. The photo-responsive behaviour of the device has been investigated under AM 1.5 G photo-irradiation. Details of the *I–V* measurements are provided in the ESI.†

Results and discussion

Molecular and supramolecular structure of the co-crystal

Upon mixing equimolar ethanolic solutions of TBTA and QUIN (Fig. 1) the co-crystal was grown *via* the solvent evaporation method. Rhombohedral shaped (Fig. S1†) colourless single crystals were collected and characterized using the single crystal X-ray crystallographic technique (ESI†). Structural analysis reveals that the co-crystal crystallizes in the orthorhombic system with *Pnma* space group (Tables 1 and S1†). The asymmetric unit of the co-crystal contains half of each of the TBTA and QUIN molecules (Fig. S2†). In the molecule of TBTA, the carboxylic groups are almost perpendicular (angle between the plane of the phenyl ring and the plane of carboxylic acid group is 87.23°, Fig. S3†) to the plane of the phenyl ring. The C–O bond lengths (O1–C5 = 1.302(3) Å, O2–C5 = 1.192(3) Å) confirm the presence of the carboxylic acid group. The QUIN moiety is completely planar and is co-planar to the phenyl ring of the TBTA moiety.

Interestingly, the TBTA and QUIN molecules are connected by O–H···N hydrogen bonds to form the 1D supramolecular chains along the *b*-axis (Fig. 2, S4 and Table S2†). Two parallel 1D chains are connected by π···π interactions (Fig. S5 and Table S3†) between the TBTA and QUIN molecules to form a double layer which is further connected by Br···O interactions (Fig. S6 and Table S4†) to form a 2D supramolecular structure within the *ab*-plane (Fig. 2). These 2D sheets are further bridged by Br···π interactions (Table S5†) to form a 3D supramolecular network (Fig. S7†).

PXRD, thermal and IR analyses

The phase purity of the bulk material was characterized by PXRD analysis (Fig. S8†). Thermal analysis reveals two-step degradation of the co-crystal. The sample is stable up to 140 °C, and then for the 1st step of decomposition within the temperature range 140–220 °C the weight loss of the sample is nearly 24.5% indicating the removal of the QUIN moiety from the structure. In the next step the remaining part of the sample gets completely degraded in the temperature interval of 270–360 °C (Fig. S9†). The vibrational spectra recorded in ATR mode (Fig. S10†) show shifts in the frequency band positions corresponding to C═O and O–H vibrations in the co-crystal with respect to TBTA towards lower frequencies. This may be attributed to the weakening of C═O and O–H vibrations due to intermolecular hydrogen bonding interactions between TBTA and QUIN in the co-crystal.

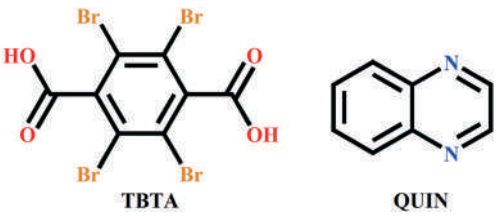

Fig. 1 Molecular structures of co-crystallizing components.

Table 1 Crystallographic data of the TBTA–QUIN co-crystal

Structure	Crystal form
System	Orthorhombic
Space group	*Pnma*
a (Å)	9.4972(18)
b (Å)	14.745(3)
c (Å)	13.181(2)
α (°)	90
V (Å^3)	1845.8(6)
Z, density	4, 2.202
CCDC no.	1841621

Inspection of noncovalent interactions within the co-crystal

Hirshfeld surface analysis

The Hirshfeld surface analysis provides more detailed information regarding the intermolecular interactions and the 2D fingerprint plot quantifies these interactions within the crystal structure (details are provided in the ESI†). The Hirshfeld surfaces were calculated over TBTA molecules (Fig. 3) and the 2D fingerprint plots (Fig. S11†) were analysed accordingly. The d_{norm} surface of TBTA was mapped over the fixed colour scale of −0.751 to 1.417 Å. It displays some bright circular red spots, which correspond to the short intermolecular O···H and N···H interactions. The light red spots correspond to the long intermolecular Br···O, Br···π, C···H and H···H interactions. The 2D fingerprint plots reveal that the O···H interactions comprise 17.0% of the total Hirshfeld surface and appear as a blunt spike with the lowest contact distance $d_i \approx 1.5$ Å and $d_e \approx 1.3$ Å. The N···H

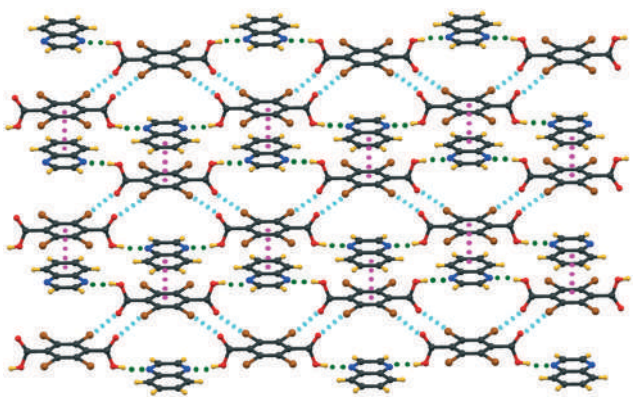

Fig. 2 2D supramolecular structure formed by hydrogen bonds (green), halogen bonds (cyan) and π···π interactions (magenta).

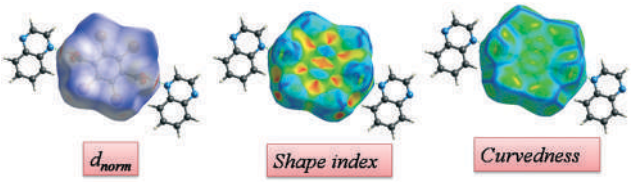

Fig. 3 Hirshfeld d_{norm}, shape index and curvedness surfaces of TBTA–QUIN around TBTA.

interactions cover 4.3% of the total surface and emerge as a sharp spike with contact distance $d_i \approx 0.6$ Å and $d_e \approx 1.0$ Å. The Br···C interaction corresponding to Br···π comprises 13.5% of the surface and appears as two spikes with average contact distance $d_e + d_i \approx 3.4$ Å. The C···H, Br···O, H···H and Br···H interactions are found in the 2D fingerprint plot with relative surface areas 2.3%, 18.4%, 7.1% and 27.4%, respectively as shown in Fig. S10.†

Intermolecular interaction energies

The quantitative view of the topology of the distribution of overall interaction energies sustaining the molecular components within the crystal structure have been calculated by two ways. Firstly on the basis of pair-wise interaction energies by summing up four energy components *viz.*, electrostatic (E_{el}), polarization (E_{pol}), dispersion (E_{dis}) and exchange repulsion (E_{rep}) on a structure-cluster mapped within 6 Å in the neighbourhood of each component (TBTA and QUIN) of the co-crystal to include long-range interactions. Secondly the binding energies of the four kinds of self-assembled dimeric model geometries focussing different kinds of intermolecular interactions (Fig. 4) were calculated from the difference of the energy of the system and the sum of individual components in the framework of DFT with counterpoise correction.

For a cluster of molecules within the 2 × 2 × 2 unit cell, graphical representation of the individual energy components has been simulated in the energy framework and is depicted in Fig. S12.† The interactions for different kinds of orientations of the component molecules within the crystals have been explored in the energy framework and are presented in Fig. S13–S15.† The electrostatic and dispersion energies coexisting together provide the total interaction energy for the self-assembly of the co-crystal. Signatures of electrostatic force due to the strong O–H···N hydrogen bonded arrays and dispersion force due to π-stacking interactions, Br···O halogen bonding with Br···π and C–H···π interactions within the constituents of the heterodimers have been detected in the interaction energy plots (Fig. S13 and S14†). The Br···O halogen bonding interactions between the TBTA homodimer have been detected to form a 2D-planar geometry made of a $R_2^2(10)$ network between the TBTA molecules (Fig. S15†).

On the other hand Fig. 4(a) describes the binding energy of the first model dimer considering only the O–H···N hydrogen bonding interactions, the second model (Fig. 4(b)) gives the binding energy of the weakly interacting π stacked dimer, the third and fourth models diagnose the intermolecular interactions between the homo-dimers, Br···O and Br···π interactions between two TBTA moieties (Fig. 4(c)) and C–H···π interactions between two QUIN moieties (Fig. 4(d)). The calculated values of these interactions as listed in Table 2 show comparable results.

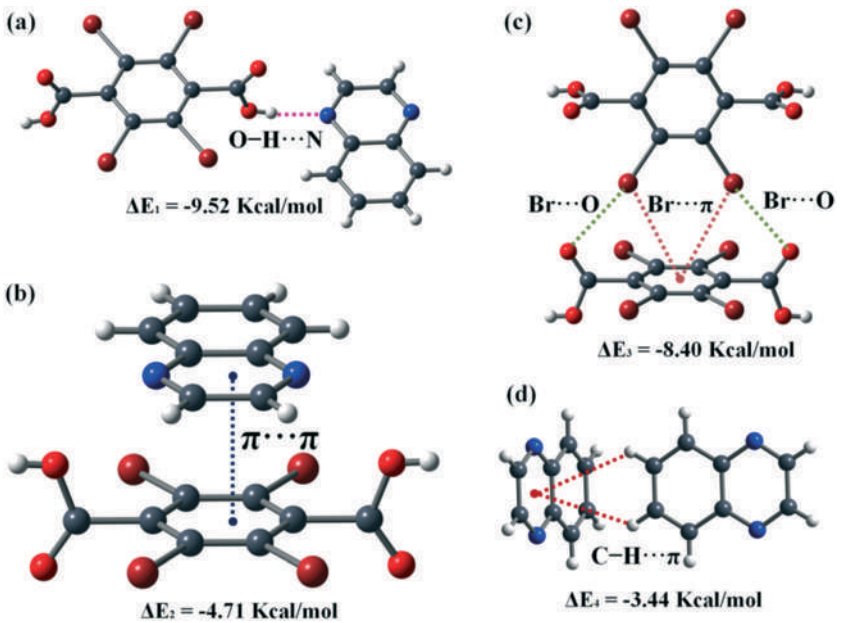

Fig. 4 Theoretical model geometries with the synthon energies describing (a) O–H···N hydrogen bonding interaction, (b) π···π interaction for the TBTA-QUIN hetero-dimer model structures, (c) Br···O and Br···π interactions within the TBTA homo-dimer and (d) C–H···π interactions between the QUIN homo-dimer model structure.

Table 2 Comparison between interaction energies calculated from the energy framework and binding energies from DFT computation

Pair	Interaction	Interaction energy	Binding energy
TBTA–QUIN heterodimer	O–H···N hydrogen bonding interactions	−50.5 kJ mol^{-1}	−9.52 kcal mol^{-1}
	π··· stacking interactions	−36.5 kJ mol^{-1}	−4.71 kcal mol^{-1}
TBTA homodimer	Br···O halogen bonding with Br···π	−31.4 kJ mol^{-1}	−8.40 kcal mol^{-1}
QUIN homodimer	C–H···π interactions	−11.6 kJ mol^{-1}	−3.44 kcal mol^{-1}
TBTA homodimers with $R_2^2(10)$ network forming a 2D-planar geometry	Br···O halogen bonding interaction between the TBTA homodimers	−19.0 kJ mol^{-1}	

QTAIM and NCI plot analysis

A qualitative analysis of the topological properties of the noncovalent interactions prevailing within the dimer geometries based on the electron density has been performed using the quantum theory of atoms in molecules (QTAIM). In the QTAIM distribution of critical points (CPs) and bond paths each noncovalent interaction is characterized by a bond CP (yellow sphere) and bond path interconnecting the atoms of two different molecular units and to visualize the nature of the non-covalent interactions (NCI), the reduced density gradient (RDG) has been represented by iso-density surfaces over the interacting dimers (Fig. 5). The nature of the interaction between the molecules within the dimer can be traced through a red–blue–green colour scheme on the calculated iso-surface where blue colour usually highlights strong attractive interaction whereas red points towards strong repulsive interaction. Weak interactions (attractive) are indicated by green colour.

Fig. 5(a) shows the QTAIM representation of the heterodimer, where the O–H···N hydrogen bond is portrayed by the bond critical point (BCP) represented by a yellow sphere and the bond path shown by a pink line interconnecting the H and N atoms. The small blue iso-surface located between the H and N atoms shows the NCI plot representation which confirms the presence of strong O–H···N hydrogen bonding interactions. Fig. 5(b) displays several BCPs connecting the π-systems of both the QUIN rings and the TBTA molecule, characterizing the π-stacking interaction. The extended green iso-surface between the π-stacked hetero-dimers indicates the weakly attractive nature of the interactions between the participating residues.

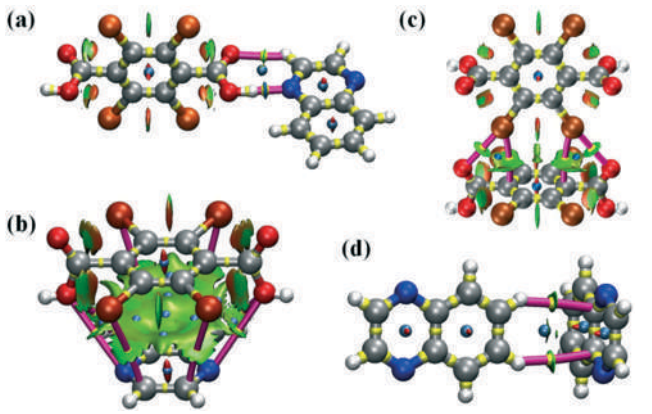

Fig. 5 AIM distribution of bond and ring critical points (yellow and tan spheres respectively), bond paths (magenta lines) and the nature of non-covalent interactions for the model dimeric geometries revealing (a) O–H···N strong H-bonding interaction, (b) π-stacking interaction, (c) Br···O and Br···π interactions and (d) C–H···π short contacts.

It can be observed that for the self-assembled homo-dimer (Fig. 5(c)) the distribution of bond critical points (CPs) and bond paths reveals two different types of interaction, one corresponds to the XB, where the Br and O atoms are interconnected by a bond CP and bond path and the other contact can be defined as a Br···π interaction that is characterized by a bond CP and bond path connecting the Br atom to one C-atom of the π-aromatic ring. The natures of weakly interacting Br···O and Br···π interactions are characterized by three separate green iso-surfaces between them. On the other hand Fig. 5(d) presents the similar distribution of bond critical points (CPs) and bond paths, revealing the C–H···π short contacts by a bond CP and bond path interconnecting the H atom to one C-atom of the π ring of QUIN. The strength of the interaction can be observed by four discrete green iso-surfaces between the QUIN homo-dimer and was found to be weak in nature.

Optical, electronic and electrical transport properties

Spectroscopic and light emitting behaviour

The optical properties of the co-crystal have been examined in both solid state and aqueous medium (Fig. 6). The solid state absorption spectrum of the co-crystal shows a broad band in the UV region while in the aqueous medium multiple peaks appear (Fig. 6(a)). The peaks obtained at lower wavelength can be attributed to π–π* transition while higher wavelength peaks are due to inter-ligand charge transfer (ILCT) between different moieties of the co-crystal. Usually, in the UV-vis reflectance spectra the band for the co-crystal formed by the charge transfer (CT) interaction appears at lower energy with respect to its individual components.[12] However, in the present case no such shifting of the band for the co-crystal has been observed, which discards the possibility of the presence of CT interaction between TBTA and QUIN moieties in the co-crystal (Fig. S16(a)†). The absorption spectra of the co-crystal in both solid state and solution phase show two major bands. The solution phase spectrum is blue shifted with respect to the solid state spectrum. The peaks in solution phase absorption spectrum are clearly resolved whereas for the solid state spectrum the

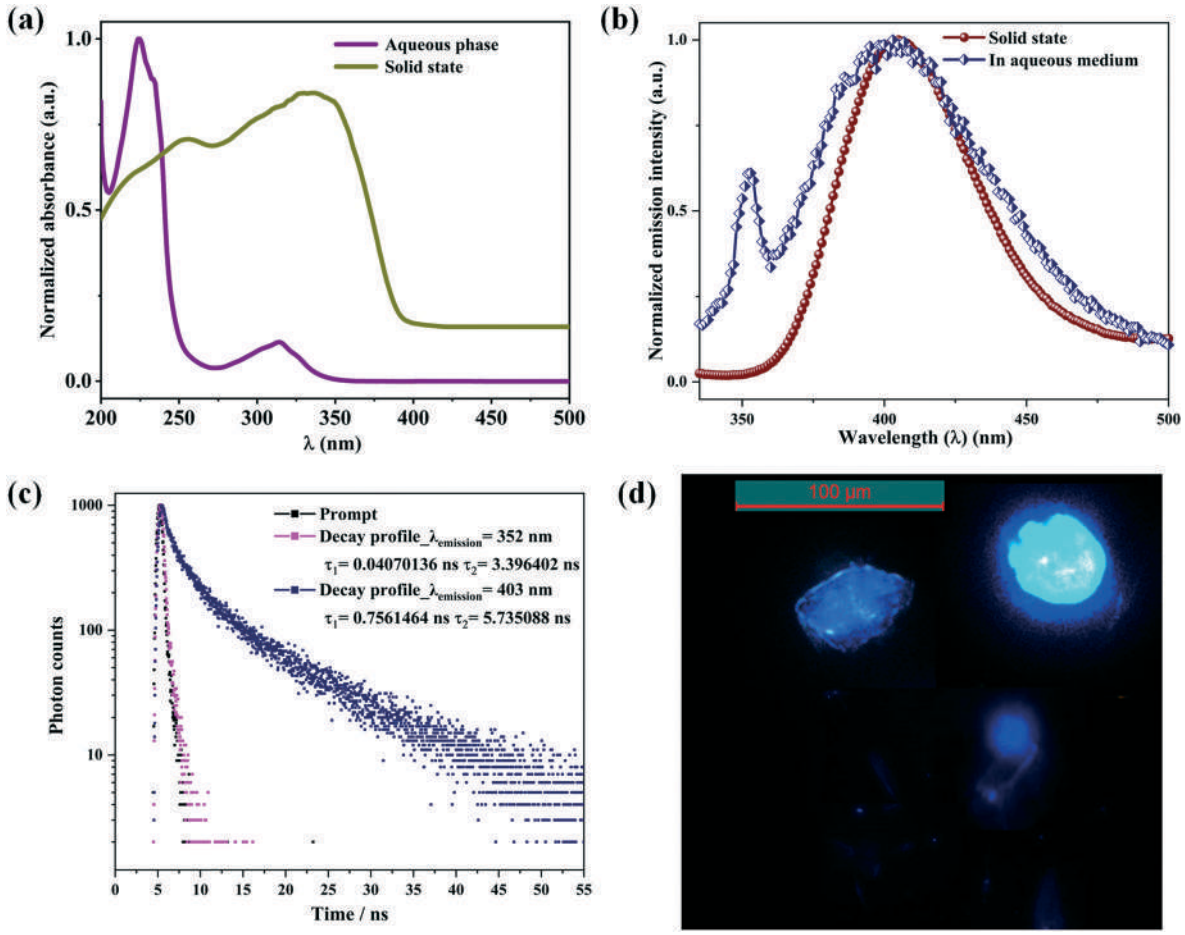

Fig. 6 (a) UV-vis absorption spectra of the sample in both solid state and aqueous medium, (b) steady state emission spectra of the sample in both solid state and aqueous medium (λ_{ex} = 313 nm, conc. = 10^{-4} mol l^{-1}), (c) lifetime profile of the sample in solution phase and (d) fluorescence image of the co-crystal. The spectra of the sample in solid state and in solution phase as shown in Fig. 6(a) and (b) are normalized to illustrate their differences.

band nature can be observed, which mainly arises due to the aggregation effect. Fig. S16(b)† depicts the absorption behaviour of the sample and its components in solution phase. By correlating the experimental and simulated absorption spectra of the sample in solution phase it has been shown that the co-crystal retains its supramolecular assembly in the aqueous medium (see ESI†).

The solid state emission spectrum of the co-crystal shows a broad band with a maximum at 405 nm while in aqueous medium it has two peaks with maxima at 350 nm and 403 nm (Fig. 6(b)). Such behaviour is due to the solid state aggregation effect within the multi-component material. Concentration dependent absorption and emission spectra of the sample have also been studied in solution phase (Fig. S17(a) and (b)†). With increasing concentration, the intensity of the peaks in the absorption spectra increases continuously; while in the emission spectra, the intensity of the peak at 350 nm decreases and it increases for the peak at 403 nm. Most probably self-assembled aggregation is responsible for the decrement and the incessant increase in the propensity of the inter-ligand charge transfer interaction with increasing concentration causes the significant enhancement in the intensity of the second peak.

Fluorescence lifetime is a very effective tool for probing the local environment around a fluorescent molecule and excited state interactions. The decay profiles of the sample recorded in aqueous environment have been fitted with a double-exponent (Fig. 6(c)) and the respective lifetime values τ_1 and τ_2 are provided in Table 3. The average lifetime values of the material in aqueous medium for those emission maxima were determined from the results of the time-resolved fluorescence spectroscopy using the equation: $\langle\tau_{av}\rangle = (a_1\tau_1^2 + a_2\tau_2^2)/(a_1\tau_1 + a_2\tau_2)$, where a_1, a_2 are the percentage contributions for these two lifetime values and are presented in Table 3.

The relative quantum yield (Φ_F) calculation from the luminescence measurement carried out in solution phase (considering only the area under the emission spectrum with maximum at 403 nm) using quinine sulfate (QS) in 0.1 M H_2SO_4 as the standard reference shows that the sample is minimally radiative with Φ_F = 0.018. The consequential radiative and non-radiative transition rate constants for this

Table 3 Lifetime values of the sample in aqueous environment

Monitoring wavelength (λ_{em})	a_1	τ_1 (ns)	a_2	τ_2 (ns)	$\langle\tau_{av}\rangle$ (ns)
352	0.17	0.04	0.83	3.39	3.38
403	0.59	0.75	0.41	5.73	4.94

a_1, a_2: percentage contributions for lifetime values; τ_1, τ_2: lifetime; and $\langle\tau_{av}\rangle$: average lifetime.

emission peak were extracted from the relations $k_r = \varphi_F/\tau_{av}$ and $k_{ir} = (1 - \varphi_F)/\tau_{av}$, respectively, and these values are found to be $k_r = 3.64 \times 10^6$ s^{-1} and $k_{ir} = 9.96 \times 10^8$ s^{-1}. The fluorescence microscopic image of the co-crystal under UV irradiation has been recorded (Fig. 6(d)). The co-crystal shows violet-blue emission from its edges as expected from the coordinate (0.151, 0.056) of the CIE chromaticity diagram ((Fig. S18(c)†) drawn from the solid state PL spectra.

Ground state structural and electronic properties

The molecular structure of the co-crystal has been optimized in the electronic ground state (S_0) in both the gaseous phase and in water medium employing the DFT method with the 6-311++G(d,p) basis set. The gas phase and solution phase optimized geometries of the co-crystal are presented in Fig. S18† and the coordinates are reported in Tables S6 and S7.† As the present sample is not a CT type co-crystal and the hydrogen bonding interaction is the strongest interaction between the components of the co-crystal, the hydrogen bonded heterodimer was chosen as the molecular unit of the co-crystal for all molecular level calculations. In the starting solid state geometry derived from the crystal structure a molecular unit of the co-crystal contains a TBTA and a QUIN moiety where the carboxylic groups of TBTA are perpendicular to the aromatic ring of TBTA and the aromatic ring of TBTA is coplanar with the QUIN ring. The relative orientations of the different fragments of the optimized geometry in the aqueous phase is almost the same as the solid state molecular structure. The slight difference between these conformations is because of the presence of solvent interactions in the aqueous phase. On the other hand, for the optimized geometry in the gaseous phase the aromatic ring of the TBTA molecule becomes perpendicular with respect to the QUIN moiety and the carboxylic groups turn coplanar with the QUIN moiety. Due to the absence of crystalline packing force the optimized geometry of the molecule in the gaseous phase exhibits such a substantially different conformation from the solid state molecular geometry. Except for the bonds with H atoms all the optimized bond lengths are within the appreciable limit of ~0.02 Å. In the solution phase optimized geometry the increment of the O–H bond dimension is more than the gaseous phase optimized geometry. Some of the selected bond lengths of the co-crystal are listed in Table S8.†

The isodensity surface plots (isodensity = 0.02 e Bohr^{-3}) of some of the selected frontier molecular orbitals (FMO) of both the optimized structures of the co-crystal along with their orbital energies are depicted in Fig. 7. For the FMOs the contributions coming from different parts of the co-crystal in terms of atomic contribution are obtained by the fragment analysis method, and energies of the FMOs along with the HOMO–LUMO energy differences are provided in Table S9.† It can be clearly seen that the FMOs for the geometries optimized in the gaseous phase and in water medium have different energies and the electron density distributions of the FMOs (Fig. 7) show different distribution of the isodensities over different parts of the molecules.

In the hydrogen bonded dimer the HOMO e-density is found over TBTA and the LUMO e-density is on QUIN for both the phases. Therefore for the ground state of the TBTA–QUIN self-assembly, TBTA will act as donor, whereas QUIN will act as acceptor. This observation is further supported by the calculation of the Mulliken charges over the atoms of the hydrogen bonded dimer geometry (Tables S10 and S11†). It may be noted that for both the phases all virtual orbitals subsequent to the LUMO are composed of contributions from a single entity. For both the phases, LUMO+1 to LUMO+3 are composed of the contribution from the TBTA moiety and LUMO+4 is composed of the sole contribution from the QUIN moiety. The HOMO−2 and HOMO−4 orbitals in the gaseous phase optimized structure and the HOMO−1 orbital in the aqueous medium optimized geometry are composed of sole contributions from the QUIN moiety. For all other occupied orbitals both the TBTA and QUIN moieties contribute in different ratios. All the % contributions are listed in Table S9.†

Singlet excited states and calculated absorption spectra

We have computed the theoretical UV-vis spectra of the co-crystal in both the gaseous state and aqueous medium using the ground state optimized geometries in the respective phases, with the help of the non-equilibrium approach of the time dependent density functional (TD-DFT) method. The energy of each excited state (S_n) represents the vertical excitation energy in electron volts (eV) from the ground state (S_0).

The theoretically (both in the gaseous and solution phases) and experimentally obtained UV-vis spectra of the co-crystal in aqueous medium are presented in Fig. 8. The absorption spectra of the co-crystal show multiple transitions and these excitations are primarily attributed to charge transfer transition between different moieties within the molecular unit of the co-crystals. The peaks in the experimental spectrum have been assigned by visual inspection. The values of theoretically calculated excitation wavelengths matching with experimental result, excitation energies, oscillator strengths and CI coefficients along with the corresponding most relevant transitions involved are presented in Tables S12 and S13.† Both the experimental and calculated spectral features of the co-crystal are more or less similar and lie in the UV region of the spectrum, except the fact that in the theoretical spectra there is a slight bathochromic shift relative to the experimental spectrum in the lower wavelength region.

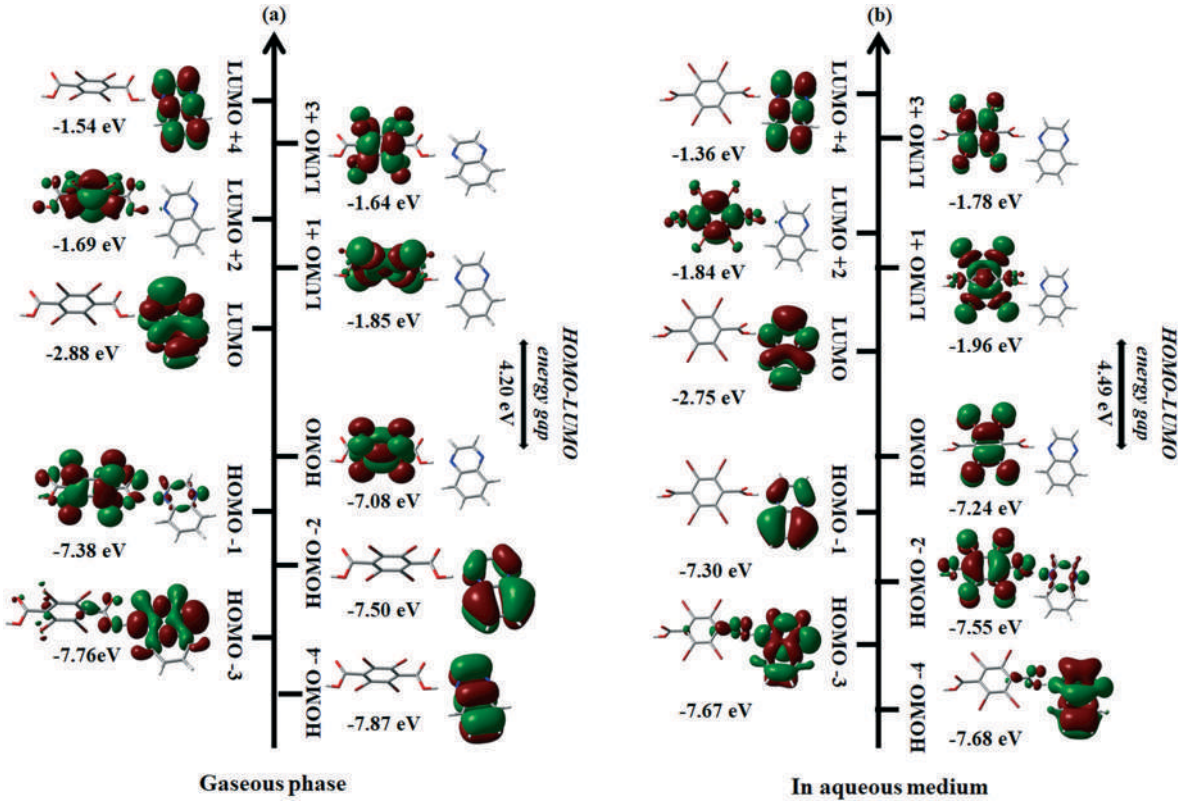

Fig. 7 Schematic representations of the selective FMOs of the co-crystal (a) in gaseous phase and (b) water medium.

The natural transition orbital (NTO) analysis based on the calculated transition density matrices allows us to identify and visualize the electronic transitions in terms of excitation from hole to electron of the singlet excitons. Further, the transition orbitals provide a graphical real-space representation of the transition densities associated with the molecular electronic excitations computed within the framework of TD-DFT. The NTOs of the co-crystal for the gaseous phase and water medium excitations are depicted in Fig. S19 and S20.† The experimental transition wavelength, most appropriate theoretical transitions and corresponding hole and electron NTOs involved along with the weights of the respective configuration λ ($\lambda \leq 1$, where the parameter λ actually refers to the fraction of the NTO pair contribution to a given electronic excitation) have been pictorially provided in Fig. S19 and S20.† These calculated NTOs corresponding to the main absorption band clearly indicate the π–π^* character of these transitions. Both the hole and electron orbitals are spread over the different parts of the co-crystal, establishing a generalised characteristic π (for holes) and π^* (for electrons) nature of orbitals.

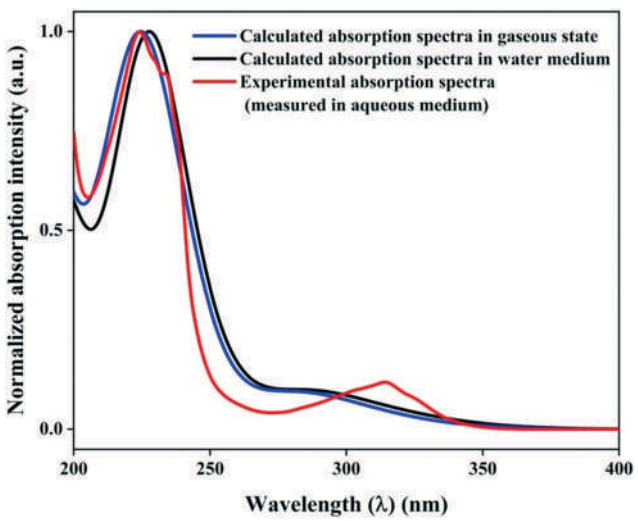

Fig. 8 Experimental absorption spectrum in aqueous medium along with the calculated absorption spectra in gaseous phase and water medium for the co-crystal at room temperature.

In Fig. S19† the lowest energy transition observed around 315 nm is found at *ca.* 308.49 nm (4.02 eV, $f = 0.0349$), which can be described by one set of NTOs (each with $\lambda = 0.98$) and is exclusively attributed to the π (QUIN) → π^* (QUIN) ILCT transition. The next UV transition observed near 294 nm is computed at 282.18 nm (4.39 eV, $f = 0.0861$) and can be ascribed to π (QUIN) → π^* (QUIN) ILCT transition. The most intense transition obtained ~237 nm is calculated at 232.75 nm (5.33 eV, $f = 0.2717$). This transition is due to n(N-QUIN) + π (TBTA) → π^* (TBTA) ILCT transition in association with a slight LLCT nature. The most appropriate calculated transition near the experimentally observed transition at 225 nm is found at 218.82 nm (5.67 eV, $f = 0.2295$). This transition has both LLCT and ILCT characters and can be

represented by π (TBTA + QUIN) → π* (TBTA) LLCT/ILCT transition. The experimentally observed UV-vis transitions of the co-crystal in water medium are theoretically interpreted in a similar manner and the results are summarized in Fig. S20.† So, the TD-DFT with NTO analysis establishes the excitations occurring due to inter/intra-molecular charge transfer interactions between TBTA and QUIN.

Electronic band structure and comparison with optical bandgap

The calculated band structure of the co-crystal along the high symmetry points of the 1st Brillouin zone is represented in Fig. 9(a) (and S21†). It shows that the bandgap of the co-crystal is 2.835 eV, which is close to the value of the optical bandgap (~3.179 eV) calculated from the absorption band edge of the solid state UV-vis spectra (Fig. 9(b)). The dispersions in the valence and conduction bands are clearly described in Fig. 9(a). The parameters corresponding to the band structure are given in Table S14.† The lowest energy (2.835 eV) of the CBs is located at the *G* point (CBM), whereas, the highest energy (0.000 eV) of the VBs is localized at the *Z* point (VBM). This indicates that this co-crystal is an indirect bandgap semiconductor. The calculated band gap shows a slightly smaller value compared to the experimental optical bandgap which is again a general flaw of DFT calculations with the GGA functional. So it can be said without ambiguity that the co-crystal is an indirect band p-type semiconductor with a wide bandgap.

Now, the bands can be assigned according to total and partial densities of states (DOS) as depicted in Fig. S22.† The resonance of C-2s, O-2s, N-2s and Br-4s states in conjunction with a partial amount of H-1s, C-2p, N-2p and O-2p states construct the VB located in the range −24.2 eV to −10.5 eV. The bottom portion of the VB is mainly dominated by the contribution from O-2p (21.4 electrons per eV) and N-2p (7.8 electrons per eV) orbitals. The next region above it is formed by C-2s (18.27 electrons per eV) and Br-4s (12.5 electrons per eV) orbitals. The top of the VB just below the Fermi level between the energy range −10.2 eV to the Fermi level (0.0 eV) are formed by the superposition of C-2p (35.8 electrons per eV) and Br-4p (30.70 electrons per eV) states in association with a considerable amount of contribution from N-2p (8.90 electrons per eV), O-2p (24.90 electrons per eV) and H-1s states. The topmost level of the VB (VBM ~ −1.02 eV ~ 0 eV) is formed due to the resonance of C-2p, N-2p and Br-4p orbitals. The conduction band (CB) just above the Fermi level ranging from 2.83 eV to 5.7 eV is formed due to the superposition of C-2p, N-2p and Br-4p orbitals mixing with a slight amount of O-2p orbitals where the states C-2p (8.35 electrons per eV) and N-2p (6.87 electrons per eV) dominate the bottom of the CB. The states C-2p and Br-4s mixing with a small amount of C-2s and H-1s have created the region ranging from 5.8 eV to 18.9 eV in the CB.

The partial density of state (PDOS) contribution of the two molecular units TBTA and QUIN in the total density of states for the co-crystal is depicted in Fig. S23.† In the PDOS, some peaks appearing at the same energy level (hybridization) for different atomic orbitals (Fig. S22†) and for different molecular fragments (Fig. S23†) clearly show the evidence of strong intermolecular interactions between the moieties of the co-crystal and intramolecular interactions within the moieties. The N-2p orbits hybridize with H-1s due to the resonance in peak positions from −13.5 eV to 0 eV implying partial charge transfer from H atoms to N atoms. So, the presence of strong H bonds between H atoms and N atoms is ensured. Again, a strong resonance is observed between the O-2p and Br-4p peaks within the range −7.9 eV to 0.0 eV. This can be argued to be the evidence of the presence of strong Br···O halogen interaction between the non-bonded atoms.

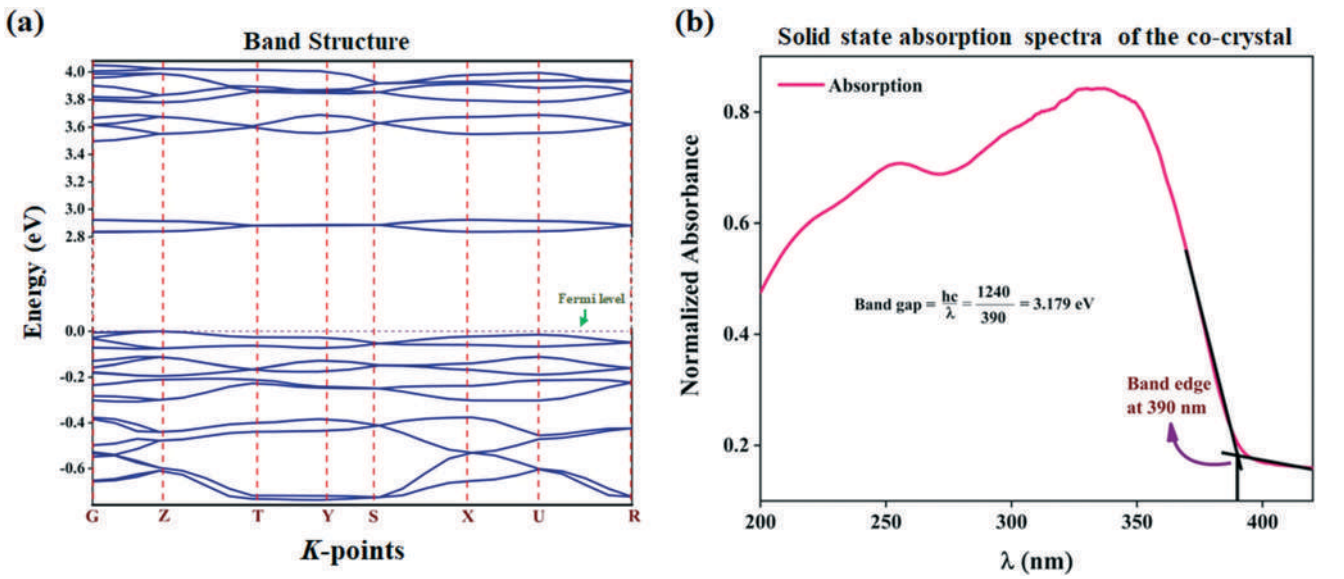

Fig. 9 (a) Calculated band structure zoomed in over the top of the VBs and bottom of CBs and (b) solid state UV-DRS spectrum of the co-crystal in the wavelength range 200 to 420 nm.

Optical properties from the electronic band structure

The electronic band structure calculation can provide insight regarding the optical response. The salient features of the parameters: real ($\varepsilon'(\omega)$) and imaginary ($\varepsilon''(\omega)$) parts of dielectric permittivity, reflectivity ($R(\omega)$), refractive index ($n(\omega)$), extinction coefficient ($k(\omega)$), optical conductivity ($\sigma(\omega)$), absorption coefficient ($\alpha(\omega)$) and energy-loss function ($L(\omega)$) as a function of frequency of the incident photon are displayed in Fig. 10 in the energy range 0–45 eV.

The plots of $\varepsilon''(\omega)$ and $\varepsilon'(\omega)$ against photon energy are shown in Fig. 10(a). The characteristic spectra for the $\varepsilon''(\omega)$ of the co-crystal comprise mainly four sharp peaks at 2.97, 7.12, 11.61 and 14.26 eV together with some shoulder peaks near 17.40 eV and beyond. At low frequency, the imaginary part $\varepsilon''(\omega)$ is zero and the threshold energy for the $\varepsilon''(\omega)$ is consistent with the bandgap of the material at equilibrium. At higher frequency (>35 eV), the $\varepsilon''(\omega)$ approaches to zero. The value of the static dielectric constant ($\varepsilon_s = \varepsilon'(0)$) is 2.98. The $\varepsilon'(\omega)$ fluctuates with increasing frequency and shows four peaks at 2.37, 6.11, 10.76 and 13.16 eV and afterward it starts decreasing, becoming negative in the energy range 19.20–24.32 eV which may be due to the metallic character of the sample in this energy range. At higher energy, the value of $\varepsilon'(\omega)$ again turns positive and is almost independent of energy ($\varepsilon'(\infty) \sim 0.80$).

The reflectivity spectrum of the sample as displayed in Fig. 10(b) shows two distinct peaks: one sharp and strong peak at 6.92 eV and another weak peak at 2.46 eV. A broad band appears in the energy range 9 to 29 eV due to the superposition of several peaks located at 11.66, 14.78, 19.74 and 23.42 eV (accompanied by a shoulder). The reflectivity of the material approaches to zero when the frequency reaches near 45 eV. The zero energy value of reflectivity (*i.e.*, $R(0)$) is 7% and up to 4.83 eV the value of the reflectivity remains within 8.8%. Due to such a low value of reflectivity, the compound is nearly transparent in the infrared and visible energy range. Now, materials with a low refractive index are suitable for application in optoelectronic devices such as LEDs and solar cells. In the entire frequency range, the calculated value of the reflectivity of the co-crystal is lower than that in inorganic compounds like the metal oxides and thus it can be used for fabricating optoelectronic devices. The highest value of reflectivity (21.08%) is observed at 23.42 eV. It has been observed that the reflectivity value attains maximum when the value of $\varepsilon'(\omega)$ becomes negative (Fig. 10(a) and (b)).

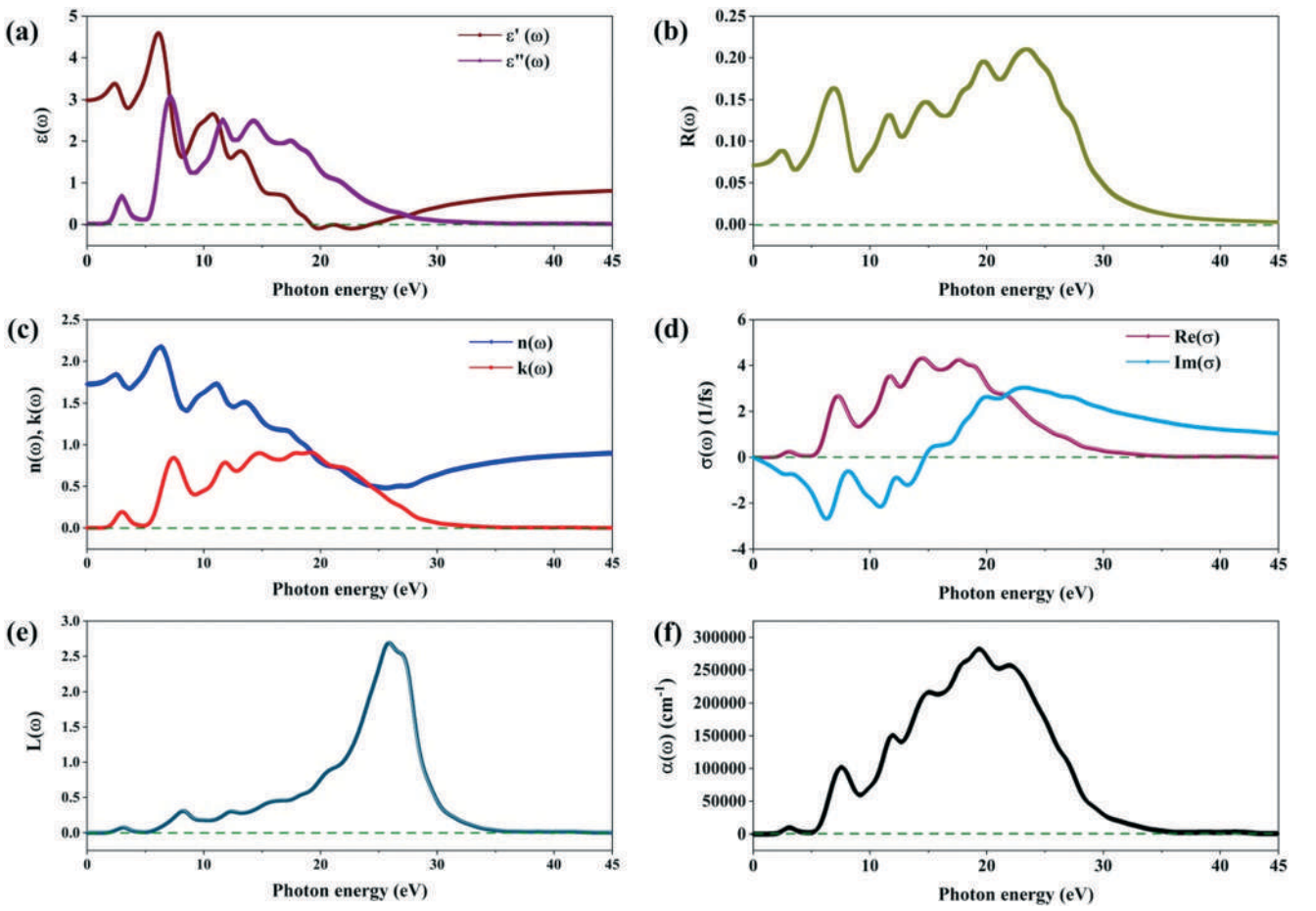

Fig. 10 The plot for (a) dielectric permittivity $\varepsilon(\omega)$; (b) reflectivity $R(\omega)$; (c) refractive index $n(\omega)$ and extinction coefficient $k(\omega)$; (d) optical conductivity $\sigma(\omega)$; (e) energy loss function $L(\omega)$ and (f) absorption coefficient $\alpha(\omega)$ of the co-crystal as a function of photon energy.

The co-crystal shows a non-zero value of refractive index $n(\omega)$ up to 45 eV (Fig. 10(c)). The value of $\varepsilon'(\omega)$ at zero energy ($\varepsilon'(0) = 2.98$) could be used to estimate the refractive index $n(\omega)$ at zero energy using the relationship $n(0) = [\varepsilon'(0)]^{1/2}$ and the estimated value of the static refractive index $n(0)$ for the co-crystal is found to be 1.73. From its zero energy value, the refractive index increases with frequency, reaching the maximum value of 2.17 at 6.23 eV. A value for the refractive index of more than one signifies that when the photons traverse through the material they get slowed down due to their interactions with the electrons. The extinction coefficient $k(\omega)$ (the imaginary part of the complex refractive index) shows two sharp peaks at 3.02 and 7.42 eV and satellite peaks at 11.84, 14.76, 17.94 and 19.13 eV to form a broad band. The $\varepsilon''(\omega)$ and $k(\omega)$ spectra display similar trends (Fig. 10(a) and (c)). The optical conductivity $\sigma(\omega)$ spectrum of the co-crystal is shown in Fig. 10(d). The real part of the complex conductivity exhibits peaks at 3.06, 7.24, 11.70 and 14.46 eV along with shallow shoulders located in the high energy region (~17.60 eV). The maximum value of the conductivity of the co-crystal was achieved at 14.46 eV with a magnitude of 4.32 1/fs.

The energy-loss function $L(\omega)$ (Fig. 10(e)) is an important optical parameter describing the energy loss of a fast moving photon traversing through a material. The peaks in the $L(\omega)$ spectrum represent the characteristics associated with the plasma resonance and the corresponding frequency is called the plasma frequency above which the material is a dielectric insulator [$\varepsilon'(\omega) > 0$] and below which the material behaves as a metal [$\varepsilon'(\omega) < 0$]. For this material the resonant energy loss is manifested by a strong band situated in the energy region 22 to 28 eV composed of peaks located at 20.84 (low intensity), 25.86 (intense peak) and 26.83 eV (shoulder). This region of plasma resonance corresponds to the region in which $\varepsilon'(\omega)$ is negative. Again, the peak for the plasma resonance associated with the $L(\omega)$ spectrum coincides with the trailing edges in the reflectivity spectra. The $\alpha(\omega)$ and $R(\omega)$ spectra are similar in the energy range 2.84 to 45 eV (Fig. 10(f)). In the low energy region distinct sharp peaks are observed at 3.10 and 7.55 eV followed by a strong broad band in the high energy region consisting of peaks located at 11.93 and 15.07 eV with the largest peak at 19.38 eV accompanied by two shoulder peaks at about 18.16 and 21.94 eV.

Electrical transport properties

According to UV-vis spectroscopic study and band structure calculation the co-crystal is a p-type semiconductor. So, to assess the electrical transport properties of the sample we have measured the current–voltage (*I–V*) characteristics of a device made of an ITO/co-crystal/Al sandwich structure (Fig. 11(a)) at room temperature. The *I–V* measurements have been performed in the applied bias voltage range from −2 to +2 V using the two-probe technique with the help of a Keithley 2400 source meter. The SEM micrograph of the active thin film of the co-crystal cast on the ITO surface is shown in Fig. 11(b). The *I–V* characteristic curves of the device in the dark and under visible light illumination are presented in Fig. 11(c). The forward current of the device rises rapidly in a nonlinear fashion while it is very low and remains almost constant in the reversed bias region. The device is displaying rectifying behaviour with on/off ratios of 41 and 56 at ±2 V in the dark and under visible light exposure, respectively. Thus, it is acting like a Schottky barrier diode due to the presence of the semiconducting co-crystal between the electrodes. Further, in the voltage range 0 to 0.8 V (region I) the *I–V* curves of the device under dark conditions and visible light illumination obey the equation $I = C_1 \exp(-C_2)[\exp(C_3V) - 1]$, where C_1, C_2 and C_3 are constants that depend on different parameters of the device, portraying the thermionic emission behaviour of a Schottky barrier diode whereas in the voltage range 0.8 to 2 V (region II) they follow the power law behaviour ($I \propto V^n$, with $n = 2$), manifesting that the space charge limited current (SCLC) controls the electrical transport mechanism of the device in this region (Fig. S25†). This clearly indicates that the device is a Schottky barrier diode.[36] Accordingly, we have analyzed region I using thermionic emission theory to determine the different parameters of the device while in region II, SCLC theory has been employed to estimate the electrical transport parameters of the device.

The values of the ideality factor (η), series resistance (R_s) and barrier height (ϕ_b) of the device have been calculated by analyzing the *I–V* curve of the device in region I in the framework of the model proposed by S. K. Cheung and N. W. Cheung[37] following the methodology reported earlier (details are provided in the ESI†). The effective charge carrier mobility (μ_{eff}), transit time (τ) and carrier concentration (n) of the device have been estimated using the Mott–Gurney law in the SCLC region (region II) following the standard approach described in the literature (details are provided in the ESI†) and utilizing the capacitance *versus* frequency plot of the device (Fig. S26†).[38–40] The values of all the parameters of the device are listed in Table 4. The value of η deviates from its ideal value of unity due to the presence of the series resistance, existence of the interface states and the barrier inhomogeneities.[41,42] Under light exposure, the values of μ_{eff} and n are increased by 54 (±0.5)% and 6 (±0.5)%, respectively, compared to those under dark conditions.

In dark conditions the value of electrical conductivity of the device is found to be 0.56×10^{-5} S m^{-1} and it increases to 0.76×10^{-5} S m^{-1} under light illumination (Table 4). The photo-responsive behaviour of the device has been verified by measuring the transient photocurrent of the device at 2 V under an illumination of 100 mW cm^{-2}. Fig. 11(d) represents the photocurrent (dark currents subtracted) *versus* time graph of the device. The device shows fast and reproducible photo-switching behaviour with light on and off (Fig. 11(d)). Photosensitivity (S) is an important parameter of photosensitive electronic devices and it is calculated with the help of the relationship, $S = (I_L - I_D)/I_D$ (ref. 43) where I_D and I_L are the dark current and photocurrent at +2 V, respectively. The value of S is calculated as 0.45.

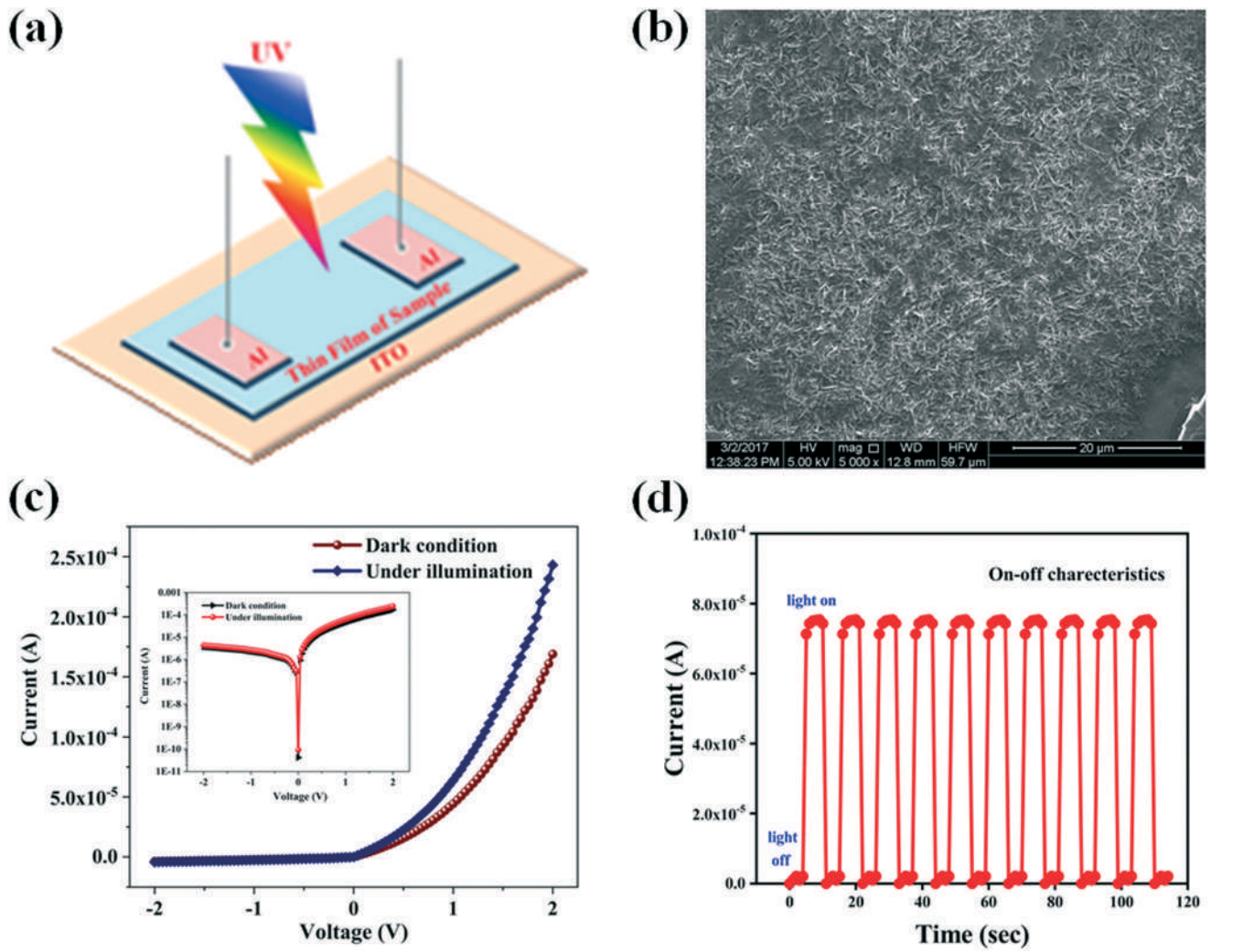

Fig. 11 (a) Schematic representation of the device, (b) SEM micrograph of the semiconducting layer, (c) photoconductive behaviour of the co-crystal, (d) on–off characteristics of the device.

Table 4 Important electrical and charge transport parameters of the Al/co-crystal/ITO device

Condition	On/off	S	η	R_s (kΩ)		Φ_b (eV)	$\sigma \times 10^{-5}$ (s m^{-1})	$\mu_{eff} \times 10^{-7}$ (m^2 V^{-1} S^{-1})	$\tau \times 10^{-7}$ (S)	$n \times 10^{20}$ (eV m^{-3})
				$dV/d\ln I$ *vs.* I	$H(I)$ *vs.* I					
Dark	41	0.45	1.36	26.97	26.50	0.70	0.56	4.44	3.9	3.57
Light	56		1.19	19.72	18.77	0.65	0.76	6.86	2.7	3.79

S: photosensitivity, η: ideality factor, R_s: series resistance, Φ_b: barrier height, σ: conductivity, μ_{eff}: mobility, τ: transit time, n: carrier concentration.

To the best of our knowledge, this is a unique report of a donor–acceptor co-crystal based photo-responsive Schottky barrier diode. The co-crystal acts as a semiconductor because of the presence of weak intermolecular interactions, more specifically π–π interactions, between the donor and acceptor molecules of the co-crystal, which helps in generation of carriers. It may be noted that the conductivity, mobility and carrier concentration of the device increase substantially under visible light illumination compared to the dark condition. This indicates that the co-crystal responds toward the visible light by generating photo carriers.

Theoretical investigation of the ground state energy levels of the frontier molecular orbitals of the hydrogen bonded dimer geometry of the co-crystal reveals that in the self-assembled co-crystal TBTA acts as donor whereas QUIN acts as acceptor when they interact through hydrogen bonding interactions. The Mulliken charge distribution analysis of the hydrogen bonded dimer (Table S11†) clearly indicates that an appreciable amount of charge has been transferred from donor TBTA to acceptor QUIN. Moreover, the MEP analysis has revealed that in the co-crystal the aromatic ring of the QUIN molecule is electron rich (π-e) while the aromatic ring

of TBTA is positively charged and acts as an electron deficient π-hole (π-h) (Fig. S24†). Thus, in the solid state, holes are created in the VB and the co-crystal acts as a p-type semiconductor as the concentration of holes in the VB is greater than the concentration of electrons in the CB. It may therefore be concluded that the π···π and hydrogen bonding interactions together play the key role in assembling the co-crystal and introducing the semiconducting behaviour in it. The weak intermolecular π–π, Br···π and Br···O interactions provide the pathway for electrical conduction.

Optoelectronic behaviour of a material can be understood by correlating the results of optical property analysis and the study of the electrical transport properties under light illumination. The absorption coefficient *versus* photon energy plot indicates the wavelengths prone to photon absorption whereas the optical conductivity *versus* photon energy plot provides the information regarding the change in conductivity due to photon absorption. From the theoretical calculations it has been found that when the co-crystal is exposed to a photon beam, the real part of the complex conductivity exhibits a peak at 3.06 eV and an absorption peak has been observed at 3.10 eV. Further the optical bandgap of the co-crystal is 3.17 eV and the calculated electronic bandgap is 2.835 eV. All these results together indicate that when the co-crystal is exposed to visible light it absorbs photons with energy ∼3 eV (the blue-violet region of visible light) and its conductivity increases in consequence of the photon absorption. It may be inferred that the bandgap energy is appropriate for transferring the electrons from the valence band to conduction band by absorbing the photons in the blue-violet region of the visible beam of light. Thus, holes are generated in the valence band and electron concentration in the conduction band increases. Therefore while performing the *I–V* measurements under visible light illumination, carriers have been generated due to the photo-responsive behaviour of the co-crystal. This leads to an increase in carrier concentration and subsequently the conductivity of the sample. Further NTO analysis reveals the presence of excitons in the sample. Thus there is another possibility that under visible light illumination the excitons in the co-crystal absorb energy from the incident photon beam and it breaks into electrons and holes and as a result the carrier concentration increases.

Conclusion

We have thoroughly examined the crystal structure, supramolecular structure, noncovalent interactions, band structure, optical properties, electronic transport mechanism and photo-responsive behaviour of a donor–acceptor co-crystal assembled by mainly π···π stacking and hydrogen bonding interactions along with minute contribution from halogen interactions. In conclusion, it has been shown that (i) apart from CT interaction, π···π and hydrogen bonding interactions can play a crucial role in formation of D–A type co-crystals, (ii) the co-crystal emits blue light under UV irradiation, (iii) a device fabricated with the co-crystal exhibits Schottky barrier diode behaviour and photo-responsive properties, (iv) the conductivity, mobility and carrier concentration of the co-crystal increase significantly upon visible light illumination, (v) π···π and hydrogen bonding interactions together can incorporate semiconducting behaviour, (vi) weak intermolecular π···π, Br···π and Br···O interactions provide the pathway for electrical conduction and (vii) in this sample carriers have been generated by transfer of electrons from the valence band to the conduction band or formation of electron/hole pairs by disintegration of excitons upon photon absorption.

Conflicts of interest

The authors declare no competing financial interest.

Acknowledgements

SS gratefully acknowledges DST, Govt. of India for providing a fellowship under the DST INSPIRE program. The PURSE and FIST programs of DST, Govt. of India are also acknowledged. Financial support from the UGC, New Delhi, DST, Govt. of India, through DRS (SAP-I) and FIST programs to Department of Physics, Jadavpur University are also acknowledged. RS also acknowledges SERB, Government of India for SERB-TARE project (File No: TAR/2018/000744).

References

1 C. Wang, H. Dong, L. Jiang and W. Hu, *Chem. Soc. Rev.*, 2018, **47**, 422–500.
2 D. Yang and D. Ma, *Adv. Opt. Mater.*, 2019, **7**, 1800522.
3 E. Orgiu, N. Crivillers, M. Herder, L. Grubert, M. Patzel, J. Frisch, E. Pavlica, D. C. Duong, G. Bratina, A. Salleo, N. Koch, S. Hecht and P. Samori, *Nat. Chem.*, 2012, **4**, 675–679.
4 M. Chaudhry, K. Muhieddine, R. Wawrzinek, J. Li, S. Lo and E. Namdas, *ACS Photonics*, 2018, **5**, 2137–2144.
5 Y. Yamamoto, G. Zhang, W. Jin, T. Fukushima, N. Ishii, A. Saeki, S. Seki, S. Tagawa, T. Minari, K. Tsukagoshi and T. Aida, *Proc. Natl. Acad. Sci. U. S. A.*, 2009, **106**, 21051–21056.
6 G. R. Desiraju, *Crystallogr. Rev.*, 2020, **26**, 64–65.
7 R. Thakuria, N. K. Nath and B. K. Saha, *Cryst. Growth Des.*, 2019, **19**, 523–528.
8 Y. Liu, Q. Zeng, B. Zou, Y. Liu, B. Xu and W. Tian, *Angew. Chem., Int. Ed.*, 2018, **57**, 15670–15674.
9 X. D. Wang, Z. Z. Li, M. P. Zhuo, Y. Wu, S. Chen, J. N. Yao and H. B. Fu, *Adv. Funct. Mater.*, 2017, **27**, 1703470.
10 M. Zhuo, Y. Tao, X. Wang, Y. Wu, S. Chen, L. Liao and L. Jiang, *Angew. Chem.*, 2018, **130**, 11470–11474.
11 S. J. Kang, S. Ahn, J. B. Kim, C. Schenck, A. M. Hiszpanski, S. Oh, T. Schiros, Y. Loo and C. Nuckolls, *J. Am. Chem. Soc.*, 2013, **135**, 2207–2212.
12 A. Mandal, A. Choudhury, P. K. Iyer and P. Mal, *J. Phys. Chem. C*, 2019, **123**, 18198–18206.
13 N. Yee, A. Dadvand and D. F. Perepichka, *Mater. Chem. Front.*, 2020, **4**, 3669–3677.

14 K. K. Ray, G. Campillo-Alvarado, H. Morales-Rojas, H. Höpfl, L. R. MacGillivray and A. V. Tivanski, *Cryst. Growth Des.*, 2020, **20**, 3–8.
15 S. Singha, S. Goswami, S. K. Dey, R. Jana, P. P. Ray, I. Saha, C. Rizzoli, P. Bag, S. Kumar and R. Saha, *CrystEngComm*, 2020, **22**, 8197–8207.
16 Z. Wang, F. Yu, J. Xie, J. Zhao, Y. Zou, Z. Wang and Q. Zhang, *Chem. – Eur. J.*, 2020, **26**, 3578–3585.
17 S. K. Park, J. H. Kim, T. Ohto, R. Yamada, A. O. F. Jones, D. R. Whang, I. Cho, S. Oh, S. H. Hong, J. E. Kwon, J. H. Kim, Y. Olivier, R. Fischer, R. Resel, J. Gierschner, H. Tada and S. Y. Park, *Adv. Mater.*, 2017, **29**, 1701346.
18 F. Cicoira and C. Santato, *Adv. Funct. Mater.*, 2007, **17**, 3421.
19 D. Liu, J. De, H. Gao, S. Ma, Q. Ou, S. Li, Z. Qin, H. Dong, Q. Liao, B. Xu, Q. Peng, Z. Shuai, W. Tian, H. Fu, X. Zhang, Y. Zhen and W. Hu, *J. Am. Chem. Soc.*, 2020, **142**, 6332–6339.
20 X. D. Wang, Z. Z. Li, M. P. Zhuo, Y. Wu, S. Chen, J. N. Yao and H. B. Fu, *Adv. Funct. Mater.*, 2017, **27**, 1703470.
21 W. Yu, X. Wang, J. Li, Z. Li, Y. Yan, W. Wang and J. Pei, *Chem. Commun.*, 2013, **49**, 54–56.
22 C.-H. Liu, M. R. Niazi and D. F. Perepichka, *Am. Ethnol.*, 2019, **131**, 2–11.
23 H. Zhang, L. Jiang, Y. Zhen, J. Zhang, G. Han, X. Zhang, X. Fu, Y. Yi, W. Xu, H. Dong, W. Chen, W. Hu and D. Zhu, *Adv. Electron. Mater.*, 2016, **2**, 1500423.
24 J. Tsutsumi, T. Yamada, H. Matsui, S. Haas and T. Hasegawa, *Phys. Rev. Lett.*, 2010, **105**, 226601.
25 G. Griffini, L. Brambilla, M. Levi, C. Castiglioni, M. Del Zoppo and S. Turri, *RSC Adv.*, 2014, **4**, 9893–9897.
26 T. Goh, J.-S. Huang, K. G. Yager, M. Y. Sfeir, C.-Y. Nam, X. Tong, L. M. Guard, P. R. Melvin, F. Antonio, B. G. Bartolome, M. L. Lee, N. Hazari and A. D. Taylor, *Adv. Energy Mater.*, 2016, **6**, 1600660.
27 S. J. Kang, S. Ahn, J. B. Kim, C. Schenck, A. M. Hiszpanski, S. Oh, T. Schiros, Y. Loo and C. Nuckolls, *J. Am. Chem. Soc.*, 2013, **135**, 2207.
28 L. Sun, W. Zhu, F. Yang, B. Li, X. Ren, X. Zhang and W. Hu, *Phys. Chem. Chem. Phys.*, 2018, **20**, 6009–6023.
29 W. Zhu, X. Zhang and W. Hu, *Sci. Bull.*, 2021, **66**, 512–520.
30 W. Zhu, Y. Yi, Y. Zhen and W. Hu, *Small*, 2015, **11**, 2150–2156.
31 W. Zhu, R. Zheng, X. Fu, H. Fu, Q. Shi, Y. Zhen, H. Dong and W. Hu, *Angew. Chem., Int. Ed.*, 2015, **54**, 6785–6789.
32 W. Zhu, L. Zhu, Y. Zou, Y. Wu, Y. Zhen, H. Dong, H. Fu, Z. Wei, Q. Shi and W. Hu, *Adv. Mater.*, 2016, **28**, 5954–5962.
33 T. Wakahara, K. Nagaoka, A. Nakagawa, C. Hirata, Y. Matsushita, K. Miyazawa, O. Ito, Y. Wada, M. Takagi, T. Ishimoto, M. Tachikawac and K. Tsukagoshi, *ACS Appl. Mater. Interfaces*, 2020, **12**(2), 2878–2883.
34 X.-G. Yang, Z.-M. Zhai, X.-M. Lu, L.-F. Ma and D. Yan, *ACS Cent. Sci.*, 2020, **6**, 1169–1178.
35 W. Yu, X. Wang, J. Li, Z. Li, Y. Yan, W. Wang and J. Pei, *Chem. Commun.*, 2013, **49**, 54.
36 S. K. Dey, R. Saha, S. Biswas, A. Layek, S. Middya, I. M. Steele, M. Fleck, P. P. Ray and S. Kumar, *Cryst. Growth Des.*, 2014, **14**, 207–221.
37 S. K. Cheung and N. W. Cheung, *Appl. Phys. Lett.*, 1986, **49**, 85–87.
38 N. F. Mott and R. W. Gurney, *Electronic Processes in Ionic Crystals*, Clarendon Press, Oxford, 1940.
39 J. A. Röhr, D. Moia, S. A. Haque, T. Kirchartz and J. Nelson, *J. Phys.: Condens. Matter*, 2018, **30**, 105901.
40 A. Dey, A. Layek, A. Roychowdhury, M. Das, J. Datta, S. Middya, D. Das and P. P. Ray, *RSC Adv.*, 2015, **5**, 36560–36567.
41 R. K. Gupta and F. Yakuphanoglu, *Sol. Energy*, 2012, **86**, 1539–1545.
42 M. Das, J. Datta, A. Dey, R. Jana, A. Layek, S. Middya and P. P. Ray, *RSC Adv.*, 2015, **5**, 101582–101592.
43 R. Jana, A. Dey, M. Das, J. Datta, P. Das and P. P. Ray, *Appl. Surf. Sci.*, 2018, **452**, 155–164.

A COMPARATIVE STUDY OF SOCIAL ANXIETY BETWEEN CESAREAN AND NON-CESAREAN SCHOOL CHILDREN

P. S. Patil[1] and P. Mahato[2]
[1-2]College of Physical Education, B.V.D.U., Pune, Dhankwadi
pradeep.patil090@gmail.com, mahatasudarshan@gmail.com

ABSTRACT

The purpose of the study was to compare the social anxiety between cesarean and non-cesarean school children. For this purpose researcher has selected One hundred (100) students of 5 schools of Purulia District, West Bengal. Comparative research design was adopted for the present study where comparison was drawn from cesarean and non - cesarean school children. Simple Random Sampling Method was used for selecting the sample from total population. Total Population was considering as a total number of male school going students i.e. 100 (20 from each school, 10 cesarean and 10 non-cesarean). Social Anxiety level was measured with the help of Spence Children's Anxiety Scale. The comparison between cesarean and non-cesarean children in reference to social anxiety the 't' test was applied at 0.05 level of significance. Result shows that there is difference between means of Cesarean and Non-Cesarean school children's, because the mean of Cesarean school children's is 71.62 which is greater than Non-Cesarean school children's is 55.72, and their Mean Difference is 15.9 and Standard Error is found 1.623, to see this difference is significant or not researcher applied 't' test. After applying 't' test it was found to be significant as the calculated 't' value (9.793) which is greater than tabulated 't' value (1.984) at 0.05 level of significance, which indicates or shows that there is significant difference in Social Anxiety between Cesarean and Non-Cesarean school children's. Concluding the above study it revealed that there is difference between means of Cesarean and Non-Cesarean school children's, and the Cesarean school children's shows high level of social anxiety as compared to Non-Cesarean school children's this may be attributed that during operation the mother is very stress and tense due to the worry about her children that what will happen by this arising situation cesarean children may face the social anxiety as compared to non-cesarean children.

Keyword: *Social Anxiety, Cesarean & Non-Cesarean School Children*

Introduction

Humans have evolved to give birth in a social and cultural context and there is evidence those women who are supported emotionally during labor today experience lower rates of medical intervention in the birth process. On the other hand, of course, there are circumstances under which emotional support alone is not sufficient for delivery of a healthy infant and other forms of intervention are essential.

Now days, it has been most probably observed that women request cesarean section even when there is not a clear medical indication that it is necessary for a variety of reasons. In many of the delivery cases, a woman may acquiesce to cesarean section when a doctor suggests it, despite the fact that continuing to labor may have resulted in a healthy, vaginally delivered infant. The word 'acquiesce' addresses issues of power, self-sufficiency and consent, which may all be absent in a high-tech hospital setting. Besides, many women do not have the confidence to challenge or question their attendants. In fact, low confidence has been shown to be one of the most grounded psychological predictors for elective cesarean section. Consider some of the expressions that are utilized to describe challenges or difficulties to the birth process: 'failure to progress', 'incompetent cervix', 'inefficient contractions', and 'uterine dysfunction'. If a woman who has been in labor for a long time and hears some of these expressions decides to acquiesce when surgery is suggested?

As we know the evolution of upright walking in our ancestors from an ape-like quadruped form involved a major restructuring of the muscles involved in locomotion and the bones associated with each muscle. These anatomical changes for locomotion also led to significant restructuring which lies within the pelvic girdle. The birth canal in different other apes is different it may be elongated (like the overall pelvis) in the anterior posterior plane and maintains this shape and orientation from the inlet to the outlet. It is also shallow throughout. Today virtually all women in societies need help during delivery from families and relatives. The most probable purpose behind

this reason is for emotional support at a time when the normally gregarious female feels vulnerable. In evolutionary terms, the main reason for seeking assistance or help is for emotional support.

The research scholar being a student of physical education has a great interest in games and sports. He has participated in different games and sports throughout all the physical education courses. During his participation throughout all the physical education courses he always thought that the child born through cesarean may be differ with non – cesarean with reference to the various health parameters.

The research scholar himself born through cesarean so based on his personal observation, interest and with further consults of teachers, experts and supervisor decided to undertake the study "A comparative study of Social Anxiety between cesarean and non-cesarean school children"

Methodology

The purpose of the study was to compare the social anxiety between cesarean and non-cesarean school children. For this purpose researcher has selected One hundred (100) students of 5 schools of Purulia District, West Bengal. Comparative research design was adopted for the present study where comparison was drawn from cesarean and non - cesarean school children. Simple Random Sampling Method was used for selecting the sample from total population. Total Population was considering as a total number of male school going students i.e. 100 (20 from each school, 10 cesarean and 10 non-cesarean).

Social Anxiety Test: Social Anxiety level was measured with the help of Spence Children's Anxiety Scale. The Spence Children's Anxiety Scale contains 44 statements or questions, in which 38 questions indicate specific anxiety syndrome whereas 6 questions are positive items and planned to prevent orientation toward anxiety problem. Among 38 questions, 6 are related to obsessive-compulsive disorder; six to separation anxiety; six to social phobia; 6 to generalized anxiety; 5 deals with fear of physical injuries; and the remaining questions reflect panic with agora-phobia. With the prior permission from the principal, class teacher, and sports teacher it was distributed to the students and the same were collected back after having filled by the students. Scoring was done as per method describe in the manual.

Statistical Analysis

The comparison between cesarean and non-cesarean children in reference to social anxiety the 't' test was applied at 0.05 level of significance.

TABLE

Comparison of Social Anxiety between Cesarean and Non-Cesarean School Children

SOCIAL ANXIETY		
Children	**Cesarean**	**Non-Cesarean**
Mean	71.62	55.72
SD	5.681	9.975
MD	15.9	
SE	1.623	
DF	98	
OT	**9.793***	
TT	1.984	

*Significant at 0.05

tabulated 't' at $df_{(98)} = 1.984$

Table reveals that there is difference between means of Cesarean and Non-Cesarean school children's, because the mean of Cesarean school children's is 71.62 which is greater than Non-Cesarean school children's is 55.72, and their Mean Difference is 15.9 and Standard Error is found 1.623, to see this difference is significant or not researcher applied 't' test. After applying 't' test it was found to be significant as the calculated 't' value (9.793) which is greater than tabulated 't' value (1.984) at 0.05 level of significance, which indicates or shows that there is significant difference in Social Anxiety between Cesarean and Non-Cesarean school children's.

GRAPH

Graphical representation of Mean of Social Anxiety of Cesarean and Non-Cesarean School Children

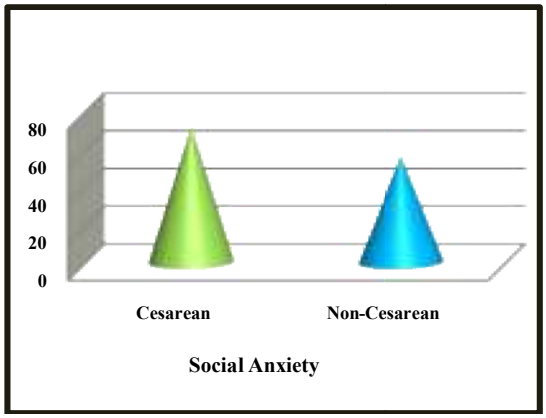

Conclusion

Concluding the above study it revealed that there is difference between means of Cesarean and Non-Cesarean school children's, because the mean of Cesarean school children's is 71.62 which is greater than Non-Cesarean school children's is 55.72. After applying 't' test it was found to be significant as the calculated 't' value is greater than tabulated 't' value , which indicates or shows that there is significant difference in Social Anxiety between Cesarean and Non-Cesarean school children's. The difference may be attributed that during operation the mother is very stress and tense due to the worry about her children that what will happen by this arising situation cesarean children may face the social anxiety as compared to non-cesarean children.

Reference

1. Kanwar R. C., "Educational and Sports Psychology", Amit Brothers Publication: Nagpur, 2007.
2. Handelzalts J. E., et. al., "Personality, fear of childbirth and cesarean delivery on demand", ACTA Obstetricia et. Gynecologica, Vol. 91, 2012.
3. Karabulut E. O., et. al., "The examination of the state-trait anxiety levels of the male football players at the age of 13-15 in terms of different variables", Journal of Kirsehir Education Faculty, Vol. 14, Issue (1), 2013.
4. https://socialanxietyinstitute.org/what-is-social-anxiety, 8:20 p.m., 06-05-2020
5. Wadey, et. al., "Basic Psychological Skills Usage and Competitive Anxiety Responses: Perceived Underlying Mechanisms", Research Quarterly for Exercise Sport, Vol. 79, Issue (3), 2008.

ISSN 0973-3671 Volume 13 No. 1 2020

JOURNAL OF THE DEPARTMENT OF ENGLISH

UGC-CARE Enlisted National Level Peer Reviewed Annual Journal

VIDYASAGAR UNIVERSITY
Midnapore, West Bengal, India

Contents

Memories of Subjective and Objective Violence of Amritsar Massacre in Bali Rai's *City of Ghosts*[1]

Indrajit Mukherjee

Abstract

Amritsar is a site of contestation and representation that always cries for a trajectory of resistance and protest against all forms of dehumanization and genocide perpetrated by the regime of terror and enforcement. The ferocious onslaught and assimilationist mentality of the colonizer silenced the colonized into dumb anguish of horror. Applying Žižek's theory of violence and Nora's notion of sites of memory, this paper seeks to explore how Bali Rai's heart-rendering tale *City of Ghosts* (2009) brings back the memory of black horror and unhealed trauma of soul-sapping scheme of random bloodshed engineered by Dyer and his Co. from the points of view of three young men, Gurdial, Jeevan, and Bissen Singh, through constructing the national memory of Amritsar as a patchwork of fact and fiction. I will also represent how this present fiction uses the ghostly figure of Heera who appears in each man's narrative to provide an alternative worldview from the perspectives of the marginalised.

Keywords: Resistance, Violence, Sites of Memory, Trauma, Dyer.

Introduction

The Jallianwala Bagh massacre alias Amritsar massacre is considered to be one of the most phantasmagorical experiences in the history of Indian politics because the warnings of Acting Brigadier Edward Harry Dyer to his fellow troops to hurl bullets from their Enfield Mark IV rifles into a large gathering of unarmed demonstrators butchered and battered the lives of at least four hundred people on the threshold of their undone years in an enclosed park on the auspicious occasion of Baisakhi of 1919. The historian Kim Wagner gives an example of this violence in his recently published book on Amritsar massacre thus: "the troops keep shooting and loading, shooting and loading, the piles of cartridges growing at their feet. The ground is littered with dead bodies, and a small girl is crying next to the bloodied corpse of her mother" (Wagner xv). The nation raised its voice in fierce protest and gave rise to secret centres of violence when open discussions and lawful movements bore no fruit. Even after one hundred years of this mass murder, we did not receive any formal apology from the British Govt., although Churchill, David Cameron and Theresa May expressed regret for this massacre or recently Archbishop of Canterbury felt ashamed

ROCK PEBBLES

A Peer-Reviewed Journal of Multidisciplinary Studies
UGC - CARE listed vide Sl. No. 168, Gr. D
September 2020 Vol. XXIV No. III

Cover Art
Title : Immersion in Enlightenment
Artist : Kala Ratn Sonjaye Maurya
Sir J.J. Institute of Applied Art, Mumbai, Maharastra

Correspondence Address
H.O : NARANPUR, Post: KODANDAPUR, Via: DEVIDWAR
Dist.: JAJPUR, ODISHA, INDIA, PIN Code-755007
Bhubaneswar Office : Qrs. No. D-17, Unit-6, Bhubaneswar - 751001.
Delhi Office : H-97, Gyan Mandir Road, Jaitpur Extn., Ph.-I, Badarpur, New Delhi - 110044
e-mail : rockpebbles 2007@rediffmail.com / rockpebbles2010@gmail.com
website : www.rockpebblesindia.com
Cell - 9437009135 / 9437449490, WhatsApp-9861012630 / 7978238911

CONTENTS

"The Storm is over": Negotiating Darwinism and Post-Apocalyptic Milieu in Jack London's *The Scarlet Plague*

Indrajit Mukherjee

Abstract ■ Presently, the COVID 19 crisis gives birth to a number of questions in our minds about the post-apocalyptic scenario: Will the crisis be a catalystfor a major social change? Will there be anarchy and the politics of extremism, or will there be a rise of dictatorship? Will we, as part of the Post-Corona world, be driven by scientific-rational thinking and ethics, or will we move on to another catastrophe by relying on the destiny of blind faith and religious hypocrisy? Will we emphasize more on our moral grounds, or will we become more courageous in sympathetic mobilization in the face of future disasters? Will we encourage the free flow of information so that our democratic institutions can be more efficient and humane? Will we increase the distance between the state and the people? Should we continue to live a self-centred life as we did before in our personal lives, or should we be careful in our social responsibilities and sympathetic to the needs and problems of 'others'? The representation of pandemic in literature reflects our fears and despairs about illness and societal crumbling while simultaneously representing us that survival is possible and that rebuilding ourselves into something new is not only necessary but also inevitable. Charged with social Darwinism and racism, Jack London's*The Scarlet Plague*(1912) is an important illustration of post-apocalyptic fiction because it brings out the novelist's delineation in his notions of human and social atavism in the text's inspection on the brink of destruction of the human civilization by "a fast-acting and untreatable plague" (Berkove 135). After discussing how people's attitudes towards these kinds of pandemic alter from time to time, this paper seeks to address these questions engaging Darwinism and Post-Apocalyptic world in this almost-forgotten short fiction.

Keywords: COVID-19, plague, pandemic, Darwinism, post-apocalyptic world

Introduction

"And once the storm is over, you won't remember how you made it through, how you managed to survive….. When you come out of the storm, you won't be the same person who walked in"

— Murakami (4).

The famous Japanese writer Haruki Murakami's observation in his *magnum opus*, entitled *Kafka on the Shore* (2002), takes us to the ongoing problem of negotiating

Middle Flight

SSM JOURNAL OF ENGLISH LITERATURE AND CULTURE
UGC CARE – LISTED NATIONAL LEVEL PEER REVIEWED JOURNAL

VOL. 9 November 2020 No. 1

(ISSN 2319-7684)

SPECIAL VOLUME ON

Health, Environment and Humanity in Literature

DEPARTMENT OF ENGLISH

S. S. MAHAVIDYALAYA
KESHPUR, PASCHIM MEDINIPUR
PIN: 721150, WEST BENGAL, INDIA

CONTENTS

Volume 4

2020

JAST

A Peer Reviewed Multidisciplinary Research Journal

Published by:
M.U.C. Women's College, West Bengal, INDIA

Journal of Arts, Science and Teaching

(A Peer Reviewed Multidisciplinary Research Journal)

ISSN: 2395-4553
Volume 4
August 2020

Published by
MAHARAJADHIRAJ UDAY CHAND WOMEN'S COLLEGE

Estd: 1955
Government Sponsored Degree College
(A Constituent College of the University of Burdwan)
Reaccredited by NAAC (3rd Cycle): Grade-B+ (CGPA-2.64)
B.C. Road, Rajbati, Burdwan-713104
West Bengal, India
Phone: 0342- 2533168 / 2531900
E-mail: mucwcburdwan@gmail.com

Date of Publication: 5th August 2020

Food and Power in the Food-stories of Mahasweta Devi

Kalyan Chatterjee,
Assistant Professor of English (WBES),
Government General Degree College, Purulia, West Bengal, India

&

Krishnapada Mandal,
Assistant Professor of English,
Nistarini College, Purulia, West Bengal, India

Abstract: Negotiation of the food-ways and eating by the powerful and the powerless emerges as the distinguishing factor between two classes. An examination of the exercise of power over the act of eating reveals how power operates through food and the act of eating in the short stories of Mahasweta Devi.

Keywords: *class, food, oppression, power, rice, starvation*

Citing literary occurrences as instances, ranging from the *Bible* (the *Genesis*) to Dickens's *Great Expectations* and Lewis Caroll's *Alice's Adventures in Wonderland*, Mervyn Nicholson, in his article "Food and Power: Homer, Caroll, Atwood and Others" (1987), describes how food is a "power crystal" round which revolves the relationship between the divinity and the mere mortals (or the ruler and the ruled, or the powerful and the powerless) with the former allotting the latter food befitting the position of the mortal in the hierarchy of beings. Obedience to these acts of apportioning marks an acceptance of one's own place in this order, whereas disobedience to these–as in the case of Adam and Eve–becomes an archetypal crime punishable without mercy. Strict adherence to the rule of obedience in terms of food is of paramount importance, because food "is the material means of growth, where growth may be defined as gaining power" (39): a threatening phenomenon for the ruler/ the powerful/ the divinity. In Mahasweta's stories like "Rice" ("Bhaat", First pub. in 1975), "Rice" ("Bhaat", First pub. in 1982), "Salt" ("Noon", First pub. in 1978), "Fish" ("Maachh", First pub. in 1978), "Flood" ("Baan", First pub. in 1968), "Birthday Party" ("Janmatithi", First pub. in 1975) and "The Fairy Tales of Mohanpur" ("Mohanpurer Rupkatha", First pub. in

IJCRT.ORG ISSN : 2320-2882

INTERNATIONAL JOURNAL OF CREATIVE RESEARCH THOUGHTS (IJCRT)

An International Open Access, Peer-reviewed, Refereed Journal

"The post-humanist logos": The Political Dogs in Nabarun Bhattacharya's Lubdhak.

Krishnapada Mandal

Assistant Professor of English Nistarini College, Purulia, W.B.

Abstract:

Posthumanism takes a critical stance towards humanism and it urges humans to respect and respond to non-human worlds and to reject the essentialist and hierarchical divisions between culture and nature. The aim of my article is to explore how the dogs in Nabarun Bhattacharya's *Lubdhak* (2006) take part in the *post*-humanist *logos* and interrogate the exploitation of animals. The novel opens a new discourse regarding animal life and rights and situates the animals at the centre of the text. The essay aims at recognizing the power of animals to interrupt, surprise, and reconstitute human commonality. Its focus is on how the street dogs' organization and their discourse on Human (its development, rationalism, invention, use and misuse of scientific knowledge) challenge and interrupt anthropocentrism. It will be argued how far the gaze of the animal breaks the hold of reason's plan by admitting an "alterity" to reason within the temporal continuum.

Keywords: Nabarun Bhattacharya; post-anthropocentric subject; animal gaze; empathy; alterity.

In the "Foreword: The Political Animal" (2008), Chris Danta and Dimitris Vardoulakis write: "The political animal is neither the subject who writes each article, nor the subject matter of each contribution. Rather, it is that which enables both the subject of writing and writing itself to belong to the *polis*. As we imagine it, the act of writing begins with the gaze of the political animal." (5) Nabarun Bhattacharya's *Lubdhak* is a text that engages 'the gaze of the political animal'. This paper intends to explore how the novel *Lubdhak* addresses and presents the dogs, principally, through the analysis of the animal gaze. Keeping Jacques Derrida, Cary Wolfe, who demonstrates that to adopt a posthumanist approach to animals is to address the unexamined framework of *speciesism,* Chris Danta and Dimitris Vardoulakis's study of animals as a backdrop, I would proceed to evaluate how the dogs in Nabarun Bhattacharya's *Lubdhak* (2006) take part in the *post*-humanist *logos* and interrogate the exploitation of animals. It would be an assessment of how the said novel opens a new discourse

regarding animal life and rights and situates the animals at the centre of the text. The human characters in the novel of Bhattacharya will be viewed from Posthumanist stance that urges humans "to respect and respond to non-human worlds" (Ryan 69). Adopting Chris Danta and Dimitris Vardoulakis' "The Political Animal" (2008) that opines that, "the animal also becomes political, in the sense that it conditions the possibility of singularity and of identity" (Danta and Vardoulakis 5), I would aim at recognizing the power of animals to interrupt, surprise, and reconstitute human commonality. This essay's focus is on how the street dogs' organization and their discourse on Human (its development, rationalism, invention, use and misuse of scientific knowledge) challenge and "interrupt" anthropocentrism. It will be argued how far the gaze of the animal breaks the hold of reason's plan by admitting an "alterity" to reason within the temporal continuum.

The oppression of the non-human animals is ensured in the current conceptualization of human. What Derrida does in philosophy, Bhattacharya does in literature. Derrida's speaks of the capacity of the animals to perceive 'our' existence, to acknowledge 'our' presence, without which, 'I' (the human) would not exist. In his *foreword* about the novel *Lubdhak* (2006), Nabarun Bhattacharya writes: "the right to the sphere of life is not only of man, but of all (living being)" (translation mine) (10). Both Derrida and Bhattacharya want to "move from 'the ends of man', that is the confines of man, to 'the crossing of borders' between man and animal." (Derrida 372) In short, while Derrida's interest is in what the animal gaze says about human consciousness, Bhattacharya, in some different context, continues deconstructing the established meaning of life in a language which is completely human (language): "by the loss of life, what do we mean? Of course, we mean human life" (Translation mine) (Bhattacharya 10). This is how the novel opens a new discourse regarding animal life and rights and situates the animals at the centre of the text.

While describing the gradual growth of *Kaan-Gojano*'s (name of dog) ear, Bhattacharya comments that, "…the dormant power of the multidimensional life is a magical realism." (Translation mine) (17) This opinion of Bhattacharya addresses Posthumanism that takes a critical stance towards humanism and urges humans to respect and respond to non-human worlds and to reject the essentialist and hierarchical divisions between culture and nature. Bhattacharya's text is written in the Posthuman condition that, as in her *The Posthuman* (2013) Rosi Braidotti comments, "introduces a qualitative shift in our thinking about what exactly is the basic unit of common reference for our species, our polity and our relationship to the other inhabitants of this planet." (1-2)

Lubdhak was first published in the festive season edition of Bengali Magazine *Disha*, later being published as a stand-alone book from Abhijan Publishers on January, 2006. Set in a city, Kolkata, the novel thematizes on the organization and revolution of the street dogs. At the turn of the century, the city undergoes beautification for which the street dogs must be driven out. After a long debate on the economic feasibilities and other associated issues, the authority has decided to imprison the dogs within Pinjrapoles (a place for encaging the abandoned animals). These Pinjrapoles resemble the concentration camps. A single Pinjrapole can accommodate more than hundred and seventeen dead dogs the body of which would become food for the

'এবং মহুয়া' -বিশ্ববিদ্যালয় মঞ্জুরী আয়োগ (U.G.C.- CARE List) অনুমোদিত
তালিকার অন্তর্ভুক্ত। ২০২০ সালে প্রকাশিত ৮৬ পৃ.
তালিকার ৬০ পৃ. এবং ৮৪ পৃ. উল্লেখিত।

এবং মহুয়া

(বাংলা ভাষা, সাহিত্য ও গবেষণাধর্মী মাসিক পত্রিকা)

২৩ তম বর্ষ, ১৩১ সংখ্যা, মার্চ, ২০২১

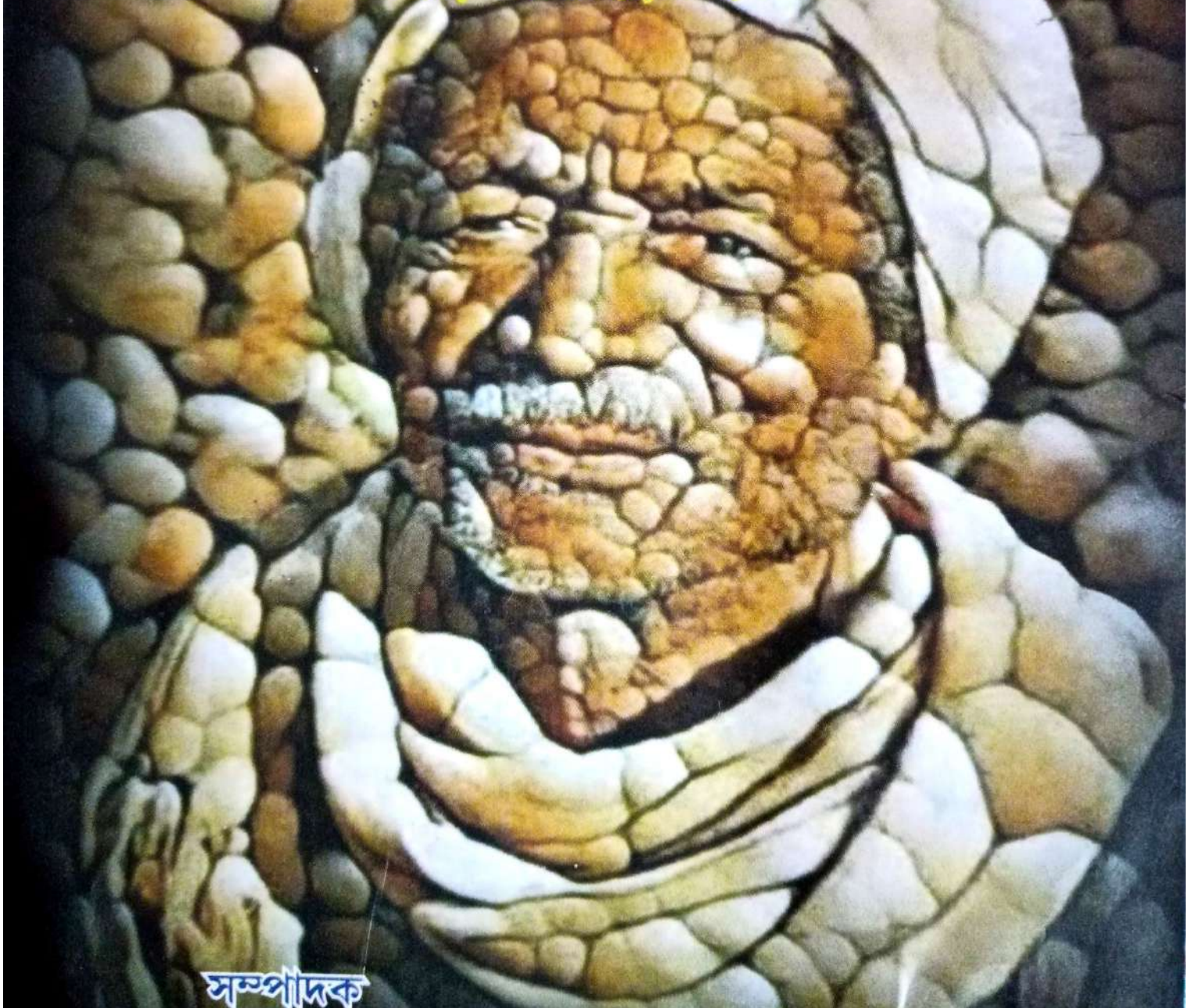

সম্পাদক
ডা. মদনমোহন বেরা

কে.কে. প্রকাশন
গোলকুঁয়াচক, মেদিনীপুর, প.বঙ্গ।

'এবং মহুয়া' -বিশ্ববিদ্যালয় মঞ্জুরী আয়োগ (UGC-CARE)
অনুমোদিত তালিকার অন্তর্ভুক্ত।
২০২০সালে প্রকাশিত ৮৬পৃ.তালিকার ৬০ পৃ.এবং ৮৪পৃ.উল্লেখিত।

এবং মহুয়া

(বাংলা ভাষা, সাহিত্য ও গবেষণাধর্মী মাসিক পত্রিকা)

২৩তম বর্ষ, ১৩১ সংখ্যা
মার্চ,২০২১

সম্পাদক
ড. মদনমোহন বেরা

সহসম্পাদক
পায়েল দাস বেরা
মৌমিতা দত্ত বেরা

যোগাযোগ :
ড. মদনমোহন বেরা, সম্পাদক।
গোলকুঁয়াচক, পোষ্ট-মেদিনীপুর,৭২১১০১,জেলা-প.মেদিনীপুর, প.বঙ্গ।
মো.-৯১৫৩১৭৭৬৫৩

কে.কে. প্রকাশন
গোলকুঁয়াচক, মেদিনীপুর, পশ্চিমবঙ্গ।

U.G.C.- CARE List approved journal, Indian Language-Arts and Humanities Group, out of 86 pages placed in Page 60 & 84.

EBONG MAHUA

Bengali Language, Literature, Research and Referred with Peer-Review Journal

23th Year, 131 Volume

March, 2021

Published By

K. K. Prakashan

Golekuachawk, P.O.-Midnapur,721101.W.B.

DTP and Printed By

K.K.Prakashan

Cover Designed By

Kohinoorkanti Bera

Special Editorial Co-ordinator

Amit Kumar Maity

Communication :

Dr. Madanmohan Bera, Editor.

Golekuachawk, P.O.-Midnapur, 721101. W.B.

Mob.-9153177653

Email- madanmohanbera51@gmail.com /

kohinoor bera @ gmail.com

Rs 500

Biomedical
Communication

BBRC
Bioscience Biotechnology
Research Communications

Biosc.Biotech.Res.Comm. Vol 13 No (4) Oct-Nov-Dec 2020 Pp 1942-1946

Corona Virus -19 Lockdown and its Impact on the Educational Status of Undergraduate Students of South Bengal, India

Animesh Mandal[1] and Rajendra Prasad Mondal[2*]

[1]*Department of Zoology, Nistarini College Purulia, West Bengal, India*

[2*]*Department of Zoology, Bankura Sammilani College, Bankura, West Bengal, India*

ABSTRACT

The pandemic of coronavirus (COVID-19) has directly or indirectly affected human civilization and has recently given a tremendous challenge to humanity for leading a normal life. Academic and research activities of students have been very much hampered during this period. Education is an important vehicle through which students can analyze while making life decisions. Through proper education, they will get important knowledge, including basic facts, job skills, and cultural norms values. Education prepares our students to think properly about communication, social interaction, ethics, environment and sustainability. Although online classes are being organized by many educational institutions, rural students face a lot of problems in attending such classes. So, to access the impact of COVID-19 on the educational status of the undergraduate students, an online survey was done in the form of an online Google form and it was circulated to students of Bankura and Purulia district through several Facebook groups as well as WhatsApp and Telegram contacts with the help of college teachers. The Google form was designed in such a way, that students can respond only one time by using one email and it can be generated using one device at a time. A total of 170 students actively participated in this online survey platform. 37% of respondents said that their average study time decreases during these days. More than 40% of online classes missed by 21% of students and 20-40% of online classes missed by 38% of students due to poor network connectivity in their locality. The number of missed online classes increased during the afternoon and evening because of internet connectivity problems. Sometimes students faced headaches and eye irritations due to the excessive use of smartphones, so few classes were also missed for these reasons. In view of these issues some initiatives are urgently needed to reduce the psychological stress of students during the COVID-19 lockdown situation.

KEY WORDS: PANDEMIC; ON-LINE; GOOGLE; NETWORK; STUDENT; PSYCHOLOGICAL STRESS.

ARTICLE INFORMATION

*Corresponding Author: rpmondal09@gmail.com
Received 18th Oct 2020 Accepted after revision 14th Dec 2020
Print ISSN: 0974-6455 Online ISSN: 2321-4007 CODEN: BBRCBA

Thomson Reuters ISI Web of Science Clarivate Analytics USA and Crossref Indexed Journal

NAAS Journal Score 2020 (4.31) SJIF: 2020 (7.728)

Online Contents Available at: http//www.bbrc.in/
DOI: http://dx.doi.org/10.21786/bbrc/13.4/46

INTRODUCTION

Human civilization has now faced a tremendous challenge from the novel severe acute respiratory syndrome coronavirus (SARS-Cov-2) in different countries. On January 30, 2020, the World Health Organization (WHO) declared Corona Virus Disease (COVID- 19) outbreak as an international public health emergency. Corona virus circulates in some wild animals like bats and transmitted to humans. It can cause severe respiratory symptoms along with symptoms of common cold and fever(Zhu

et al.,2020). The disease was first reported in China in December 2019 and now rapidly spread in many countries from Asia, Europe, and Africa(Jones,2020).The disease has now spread to 217countries and territories around the world and the total number of confirmed infected people is 42,055,863 people throughout the globe. In India, the disease was first reported on 30 January 2020 in Kerala from a student who returned from Wuhan, China. Now the total number of confirmed infected people is 7814682 till now across India (24th October, 2020) (WHO, COVID-19 Database). In West Bengal, many districts are also affected by this virus. The main problem of this outbreak is there are no specific treatments for these viruses to date. However, only one can reduce the chances of infection by only maintaining basic personal hygiene and social distancing from infected persons (Rubin and Wessely, 2020; Pulla, 2020).

Most of the people are now primarily restricted to their homes, owing to nationwide lockdowns and home-confinement strategies implemented in the majority of the COVID-19-hit countries to prevent the spread of the disease among communities (Rubin and Wessely,2020; Pulla,2020).This outbreak directly has hampered the normal lifestyle of people; many persons have lost their jobs and are facing tremendous mental stress. Due to the global outbreak of corona virus disease (COVID-19), the psychological issues have rapidly increased the public health burden of various persons (Totaleset al., 2020). Similarly, in this situation, the daily schedules of school, college, and university students are very much hampered and delays in academic activities mostly affected due to the closure of academic institutions (Cao et al., 2020). For college students, heightened levels of psychological distress and downstream negative academic consequences are prevalent under normal circumstances. During this adverse situation, education institutions shifted their classroom teaching to an online mode of teaching which would be expected to create academic stress for students. This creates a lot of problems in India because as per the 2017-18 national sample survey report only 24% of Indian household share internet facilities for education (Cao et al., 2020).

66% of the Indian population lives in rural areas where network connectivity is poor and only a little over 15% of rural households have access to internet services. In urban areas, only 42% of the population have access to internet services. More than 40% household has access to the internet in the states like Punjab, Kerala, Delhi, Uttarakhand and Himachal Pradesh whereas the proportion is less than 20% in the states of West Bengal, Bihar, Odisha, Assam, Andhra Pradesh, Jharkhand (Mukherjee and Roy,2020). During this online mode of teaching, students may experience reduced motivation toward studies, increased pressures for self-learning, changes in daily routines, and higher rates of dropout occur during this pandemic situation(Grubicet al.,2020).

In south Bengal regions, good percentages of student belonging to SC/ST/OBC and minority categories and many of them are even first-generation learners. This region is economically backward and no big industries are established in these regions. Students of this region are very talented, hard-working and procure top positions in board examinations in different University examinations in comparison to other districts of West Bengal (Mukherjee and Roy, 2020).In this background, the present study was planned online to evaluate the consequences and impact of Covid-19 lockdown among undergraduate students of South Bengal, India. During the online survey mainly students from two districts namely Bankura and Purulia were targeted. Through this study, we tried to understand their sociological status, mental health condition, pros and cons of the online mode of teaching during the lockdown situation.

MATERIAL AND METHODS

For understanding the impact of Covid-19 lockdown among undergraduate students of South Bengal, India, an online survey was conducted from 11th August to 24th August 2020. The survey was done in the form of an online Google form and it was circulated to students of Bankura and Purulia district through several Facebook groups as well as WhatsApp and Telegram contacts with the help of college teachers. The Google form was designed in such a way, that students can respond only one time by using one email and it can be generated using one device at a time. Due to the online mode of the survey, we specified our eligibility criteria (only students of South Bengal, India) to restrict its spread to a specific geography. The self-administered a questionnaire consisting of basic information about the students' names, age, gender, and the semester of study. Similarly, other questions were set to evaluate the effect of lockdown on their study, health as well as to understand the socio-demographic standards and psychological effects. The questionnaire was also included related to COVID-19 disease, its health hygiene, and information gathering related to this disease during the lockdown.

Figure 1: Number of family members in each student

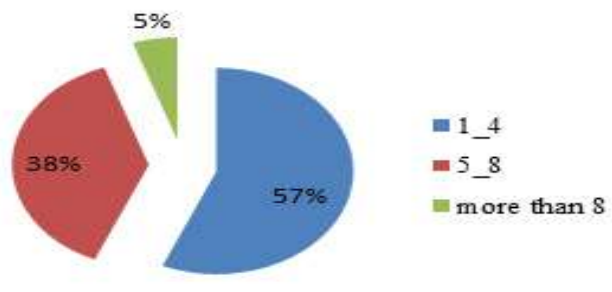

RESULTS AND DISCUSSION

A total of 170 responses were obtained from undergraduate students in the study period through the Google form survey platform. The data collected from respondents were analyzed and presented in Figures. Among 170 respondents, 26% of responses received from final six-

semester students, and only 9% of responses received from new second-semester students. Other semester students moderately participated in this online survey. The data are shown in Figure I revealed that 57% of students belonged to nuclear families and only 5% of student have belonged from joint family. The data shown in Figure II revealed that the majority of the respondents (44%) had only one toilet in their house and only 3% of students had no toilet, and family members still used open space for the toilet (Mukherjee and Roy, 2020).

Figure 2: Number of the toilet in each student family

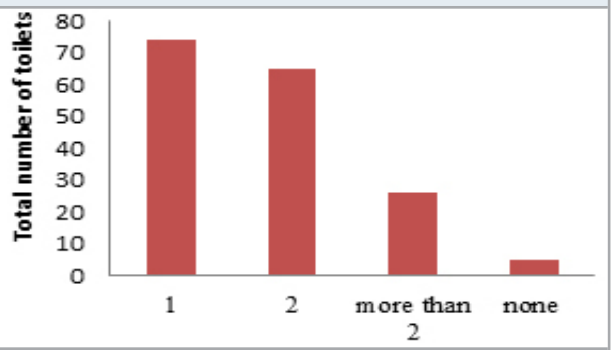

The data shown in Figure III revealed that the average time of use of smart phones increased in the majority of the respondent's during the COVID-19 lockdown period. Out of 170 respondents, 70 students regularly used smart phone more than 4 hours in social media and 74 students used 2-4 hours in social media and it will directly affect the academic performance of students. Most respondents admitted that their study time decreased during the lockdown period. According to the internet and mobile association of India report 2019, 67% of men had access to the internet whereas in women it is only about 33%. This type of gender-wise disparity is very much prominent in villages areas where 72% of access done by men and 28% by women. But due to pandemic situation students are forced to attend their online classes so the disparity reduced from percentage proportion of men: women of72:28(all India level) to 58:42 (approx.) in south Bengal regions (Mukherjee and Roy, 2020).

The data shown in Figure IV revealed that during lockdown majority of the respondents (47%) received information related to COVID 19 and its precautions through social media like WhatsApp and Facebook. 13% from television, 13% from the governmental announcement, and 8 % from the newspaper. According to Dubey et al.,(2020)social media must be used for good purposes to educate people about symptoms and transmission COVID -19 diseases during this pandemic situation. At the same time implementation of strict governmental laws and legislation is needed to stop the spreading of fake news, rumours, disinformation, and misinformation (Dubeyet al.,2020).Similarly, Guptaet al., (2020) documented that the sleep pattern of respondents was very much influenced by the lockdown. Shift to a later bedtime, delayed sleep onset, daytime napping increased are very common among many people's (Gupta et al., 2020). Similarly, more than 40% of people faced anxiety and depression during this lockdown and pandemic situation (Grover et al., 2020).

Figure 3: Average time of Smartphone used during lockdown

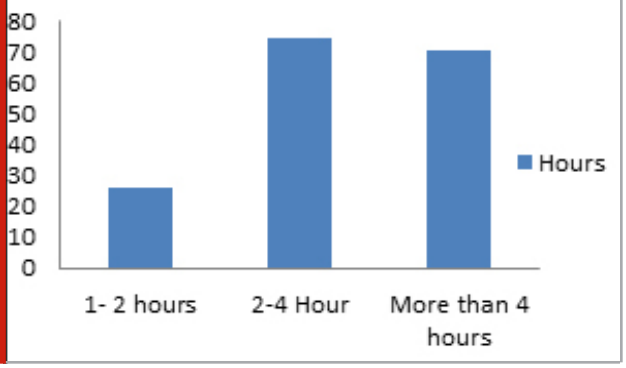

Figure 4: Awareness creates against COVID-19

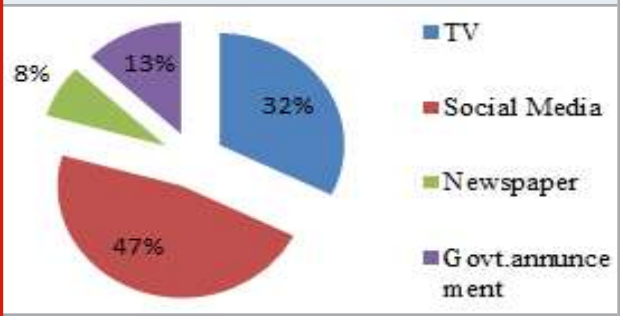

Figure 5: Types of ration card among student family

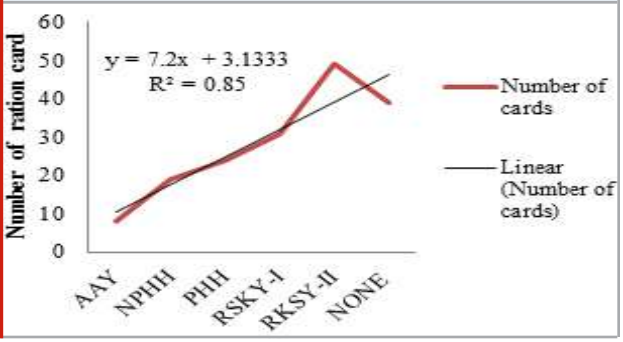

Figure 6: Bodyweight change during the lockdown

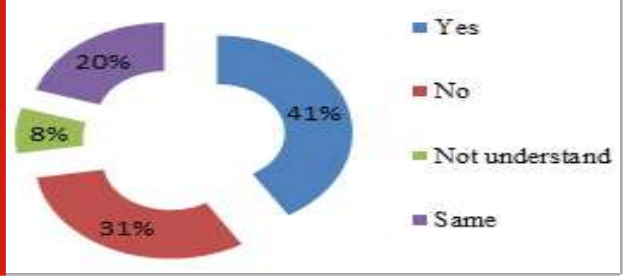

The data shown in Figure V revealed that most of the respondents have RKSY types of ration card and few students came from economically backward family. Till today few families do not have any ration cards. So, students from economically backward suffer a lot to attend the online classes. Similarly, the data shown in Figure VI reveals that 41% respondent gains their body weight during lockdown period because of leading sedentary life. The data were shown in Figure VII revealed that among all, 21% of students missed more than 40% of online classes, 38% missed 20-40% of online classes due to poor network connectivity in their locality. The number of online classes missed increases during the afternoon and evening because of connectivity problems as well as the exhaust of net data pack due to spending more time with smart phones during the daytime by students. Another survey also supported that due to closure of the educational institution, loss of classes and restricted social connections worsened pre-existing mental health conditions of 83% of young respondents(Youngminds,2020).

Dangi and George (2020) also showed that 76.44% of students suffered severe anxiety and 23.66% of students were having moderate anxiety in this lockdown period in their study area (Dangi and Mathew,2020). Sometimes students face headaches and eye irritation due to the use of excess time on smart phones so few classes also missed due to this reason. During the lockdown period, students were compelled to stay at home so during leisure time students learn many things. Girl students learned to prepare many food items from the internet, some prepare beautiful drawings as well as stitch work. Boys also spend time with physical exercise and nature study of their surroundings by using smart phones. Few students actively took part in many international and national online webinars which allow them the opportunity to listen to many things from reputed resource persons from home during this lockdown period (Dangi and Mathew, 2020).

Figure 7: Missed online classes due to poor internet connectivity

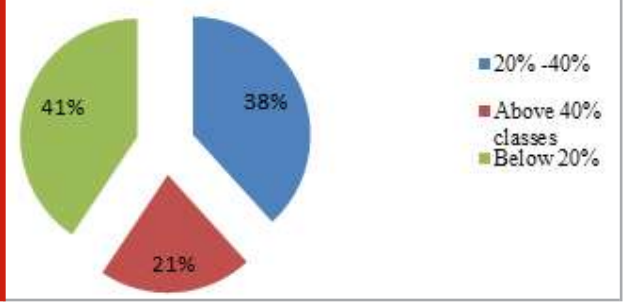

CONCLUSION

In the last two decades, mankind faced five pandemics like SARS (2002), Swine flu (2009), MERS (2012), Ebola (2014), and COVID-19 (2019). COVID-19 produces long-lasting effects on the various strata of people in society including students. The current pandemic situation does not obey the geographical boundary, race, religion, caste, and language. It creates psychological, social, economic, religious problems as well as depression and anxiety among people all over the world. It also produces immense agony among student fraternity who are already burdened with their semester and competitive exams, research and academic activities. This study showed that students are trying to adapt the new mode of online teaching but 21% of students missed more than 40% of online classes due to poor network connectivity in their locality. This creates a lot of mental anxiety among students along with loss of study time and restricted social connections. So, to reduce mental weakness and anxiety, educational institutions should have to conduct motivational sessions and set up one mental health helpline number. Arrangement of awareness programmes at both personal and community levels is urgently needed to reduce the psychological stress of students during the COVID-19 lockdown situation.

ACKNOWLEDGEMENTS

We want to acknowledge Principal, Bankura Sammilani College, Bankura and Principal, Nistarini College, Purulia for the help and support for conducting the survey work. Thanks are also due to the student respondents who have actively participated in this online survey.

Conflict of interest: The authors declare that they have no conflict of interest.

REFERENCES

Cao, W., Fang, Z., Hou, G., Han, M., Xu, X., Dong, J and Zheng, J. (2020). The psychological impact of the COVID-19 epidemic on college students in China. Psychiatr. Res,287: 112934.doi: 10.1016/j.psychres.2020.112934.

Dangi, R.R and Mathew, G. (2020). Psychological Perception of Students during COVID-19 Outbreak in India. High Technology Letters, 26(6): 142-144.

Dubey, S., Biswas, P., Ghosh, R., Chatterjee, S., Dubey, M.J., Chatterjee, S., Lahiri, D and Lavie, C.J. (2020). Psychosocial impact of COVID-19 Diabetes and Metabolic Syndrome: Clinical Research and Reviews, 14 (2020): 779e788 https://doi.org/10.1016/j.dsx.2020.05.035

Grover, S., Sahoo, S., Mehra, A., Avasthi, A., Tripathi, A., and Subramanyan, A. (2020). Psychological impact of COVID-19 lockdown: An online survey from India. Indian J Psychiatry, 62:354-62.

Grubic, N., Badovinac, S., and Johri, A.M. (2020). Student mental health in the midst of the COVID-19 pandemic: A call for further research and immediate solutions. International Journal of Social Psychiatry, 66(5): 517– 18.

Gupta, R., Grover, S., Basu, A., Krishnan, V., Tripathi, A and Subramanyam, A, (2020). Changes in sleep pattern

and sleep quality during COVID 19 lockdown. Indian J Psychiatry, 62:370-78.

Jones, D.S. (2020). History in a crisis - lessons for covid-19. N. Engl. J. Med,382, 1681-1683.

Mukherjee, S.K and Roy, A.K. (2020). A Statistical Survey of On-line Class - Performances in different Colleges under Bankura University. Innovation the research concept, 5(6): E16-22.

Pulla, P. (2020). Covid-19: India imposes lockdown for 21 days and cases rise. BMJ 2020; 368: m1251.PMID: 32217534.

Rubin, G.J and Wessely, S. (2020). The psychological effects of quarantining a city. BMJ, 368:m313. doi: 10.1136/bmj.m313. PMID: 31992552.

Torales, J., Higgins, M. O., Castaldelli-Maia, J. M and Ventricle, A. (2020). The outbreak of COVID-19 coronavirus and its impact on global mental health. International Journal of Social Psychiatry, 66(4):317-20.

Youngminds, Y. (2020). Coronavirus: Impact on young people with mental health needs. https://youngminds.org.uk/ media/3708/coronavirus-report_march2020.pdf

Zhu, W., Xie, K., Lu, H., Xu, L., Zhou, S and Fang, S. (2020). Initial clinical features of suspected Coronavirus Disease 2019 in two emergency departments outside of Hubei, China. J. Med. Virol, 1525-32. doi:10.1002/jmv.25763

ijlpr 2020; doi 10.22376/ijpbs/lpr.2021.11.1.L44-48

International Journal of Life science and Pharma Research

Research Article

Zoology for Novel drug discovery

Socio-Economic Conditions and Occupational Health Hazards of Fish Hook Makers in Rural Bengal

Animesh Mandal[1] and Rajendra Prasad Mondal[2*]

[1]*Department of Zoology, Nistarini College Purulia, West Bengal, India*

[2*] *Department of Zoology, Bankura Sammilani College, Bankura, West Bengal, India*

Abstract: Fish hook making is subject to health risks In the rural areas of West Bengal, a notable part of population is engaged in fish related activities in diverse ways either instantaneously or incidentally. The sector of activity of fish hook making is essentially rural and it being most haphazard, no focus has been given to the occupational health problems of these workers by politicians, planners, administrators and scientists. The objectives of our study is to access the occupational health hazards of fish hook makers and to give essential suggestions for the mitigation measures of those hazards resulting in a more desirable quality of life for the countryside inhabitants. A standardized structured questionnaire, with modification to suit the local context was used to collect the data. Data was analyzed in the form of percentage (%),mean and standard deviation. Out of the total 51 respondents 15 weremale and 36 were female. It revealed that in supreme number of cases hook workers experience hazards due tomachinery induced injury, musculo-skeletal disease, eye disease, skin disease due to working in unhealthy workplaces, manual handling of machines and not using personal protective equipments. So, fish hook makers need a notable degree of consciousness through regular safety training for minimizing their occupational health hazards.,

Keywords: Fish hook, health, countryside, inhabitants, musculo-skeletal, eye disease, safety training

***Corresponding Author**

Rajendra Prasad Mondal , Department of Zoology, Bankura Sammilani College, Bankura, West Bengal, India

Recieved On 23 April 2020
Revised On 19 May 2020
Accepted On 10 June 2020
Published On 01 January 2021

Funding This research did not receive any specific grant from any funding agencies in the public, commercial or not for profit sectors.

Citation Animesh Mandal and Rajendra Prasad Mondal , Socio-Economic Conditions and Occupational Health Hazards of Fish Hook Makers in Rural Bengal.(2020).Int. J. Life Sci. Pharma Res.11(1), L44-48 http://dx.doi.org/10.22376/ijpbs/lpr.2021.11.1.L44-48

1. INTRODUCTION

Fish is used as the favourite food item of people of West Bengal. So a large population of the villagers is engaged with the fishing and fishing gear related work in rural areas. From ancient times, man tried out various ways for catching fish and using hook is one of such methods. Hook is a simple, easy to operate and selective fishing device.[1] Excavation of a unique late bronze age copper fish-hook from Bet Dwarka Island, Gujarat, west coast of India proved that advanced hook fishing technology existed in ancient India.[2] In hook fishing, partly fixed baits are offered to the fish and fish swallows the bait and hook attached fish can be hauled from the water.[3] Hooks may be in different shapes, sizes, thickness of wires, and types of end of the shank (Figure- 1).Nowadays hooks that are made well-tempered and durable, are specially protected by galvanizing, bronzing, tinning, or enamelling to prevent corrosion. The corrosion resistance of different types of fishing hooks has been studied by many authors.[4]

Fig1. Different types fish hook

Fig 2. Data collection from hook makers

In Bankura district of West Bengal, a few villagers are engaged in making fish hooks. The financially backward sections of people, who have not much traditional education, are engaged in this work. They make fish hooks along with other household activities to support their family financially. They made different types of fish hooks like Ton, Ring, Boya according to the demand of the market. The fish hooksare made by rural people in their own homes and are collected from the workers by the businessmen. So the female members in the families and few men who do not have job security around the year or few months, are engaged in this type of work. They earn something for the betterment of their families. Thus this sector is vital and an important sector of rural economy in Bankura district. The workers use unsafe and unguarded machinery and their occupational environment is not hygienic. So this occupation is not devoid of health hazards. Various types of health related problems are observed among them. On the other hand, as this occupation is rural and being most unrecognized, no focus has been given to the health problems of these workers by plan makers, politicians, and scientists. Only very few studies have been carried out to document different properties of fishing hooks but many studies were done on the fishing efficiency of the hooks.[5-6]Socioeconomic status of individuals is the strongest indicator of people's life that provides social, economic, cultural and political characteristics of people, households, community groups, and institutions.[7-8]In rural areas, the socio-economic status of individuals is divided into three categories namely high, middle and low. Low socioeconomic status and its correlates, such as lower education, poverty and poor health, ultimately affect our society as a whole.[9]We have chosen this topic to assess the socioeconomic status and occupational health hazards of fish hook makers and to give essential suggestions for the mitigation measures of those hazards resulting in a more desirable quality of life for the countryside inhabitants.

2. MATERIALS AND METHODS

Field investigations were conducted in five villages namely Salbedia, Kendbana, Bankanti, Ghutgoria and Pratappur belonging to Bankura district of West Bengal, India during the time span of October,2019 to February, 2020, where a notable mass of fish hook makers are found . In these villages, more than 150 hook makers are engaged in hook making profession. A premeditated ordered questionnaire, with moderation to match the local perspective was used to gather the data from fish hook makers.The data was evaluated in the shape of percentile(%),mean and standard deviation. Selection of sample and preparation of standard questionnaires are the fundamental part of this research. Before answering all the questions were thoroughly discussed with the respondents. .Questions were asked in their leisure hour so that they can get enough time for answering all the questions. The selected respondents were interviewed to collect information about socioeconomic background of the fish hook makers relating to age, sex, number of family members, education, income of the family followed by the procedure applied by Ganguly et al, 2016.[10] During Interview their socioeconomic status, educational level, daily average income, available governmental facility, and health hazards were also asked (Figure-2).

3. STATISTICAL ANALYSIS

Statistical analysis of the experimental data was performed using the computer software's "STAT PLUS 2007 (Trial version)"for calculation of mean and standard error to analyse different types of health hazards among respondents. "MS EXCEL 2007" is used to find out the percentage of various parameters like comparison of age groups among male and female, educational status among male and female respondents, family size and monthly income of hook makers from hook making.

4. RESULT AND DISCUSSION

From our study it was found that among all respondents, 70.58% were female and 29.41% were male. Majority of the respondents (41.17%) were belonging to the age group of 20-40 years, surprisingly they were all females.

This was due to males engaging in other work like agriculture, business. As fish hook making is a household profession so females prefer this profession with their daily household activities. This may give some kind of women empowerment. The number of female workers decreases with their old age as evident from the observation of age group data belonging to 60-80 years where males were predominant. This may reveal that when males are unable to do outside work they tend to do hook making rather than just sitting lazily at home. Figure 3 shows that 23.52% female respondentsbelong to the age group 40-60 and 5.85% from 60-80 age groups (Figure 3). This may be due to the reason that they are more physiologically active during the 20-40 years of age group when they are capable of doing hook making with other household activities. As we know education transforms human from the shape of social backwardness to light of social amelioration, from ignorance to enlightenment, and a nation from under-development to foster social and economic development.[11]If we consider educational status of the respondents of these villages, it was revealed that female workers are more educated than male workers. Among male workers majority (11.76%) were belonging to standard IV-VII class whereas among female workers majority (29.41%) were belonging to class VIII-IX. Not only that but a significant portion of female respondents (17.64%) were belonging to class X and above (Figure-4). This may be due to higher educated males had chosen another better occupation or due to financial crisis they were compelled to discontinue theirstudy and search alternative.

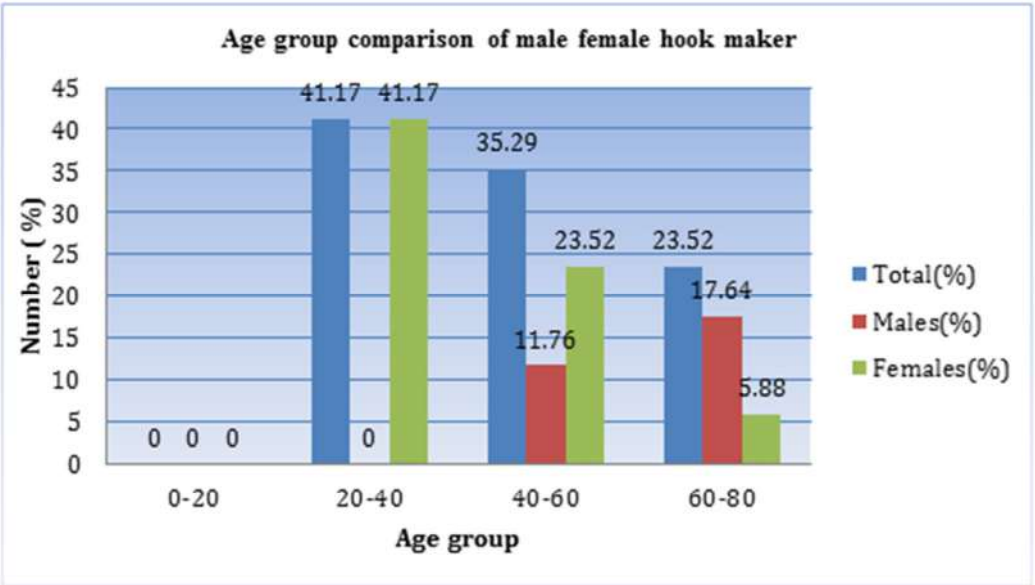

Fig3. Age group comparison between male and female hook maker

Maximum number of respondents earnRs. 2000 to 2500 per month. A small portion (5.88%) earn up to Rs. 1000 per month, 29.41% earn rupees 1500-2000, 17.64% earn rupees 1000-1500 and 11.76% earn rupees above 2500 per month(Figure 6). So it may be told that if the income increases according to the increasing price rate of the commodities more people will get interested and would engage themselves in this work by using their leisure time (Figure. 4).If we take a look at the family structure, it is clearthat the majority of the respondents (50.01%) are belonging to such a family that consists of up to 3 members only. Only a small fraction (7.14%) of workers belongs to a large family consisting of 8 members. This may reveal that when the number of family members increases then people tend to choose another occupation (Figure. 5).

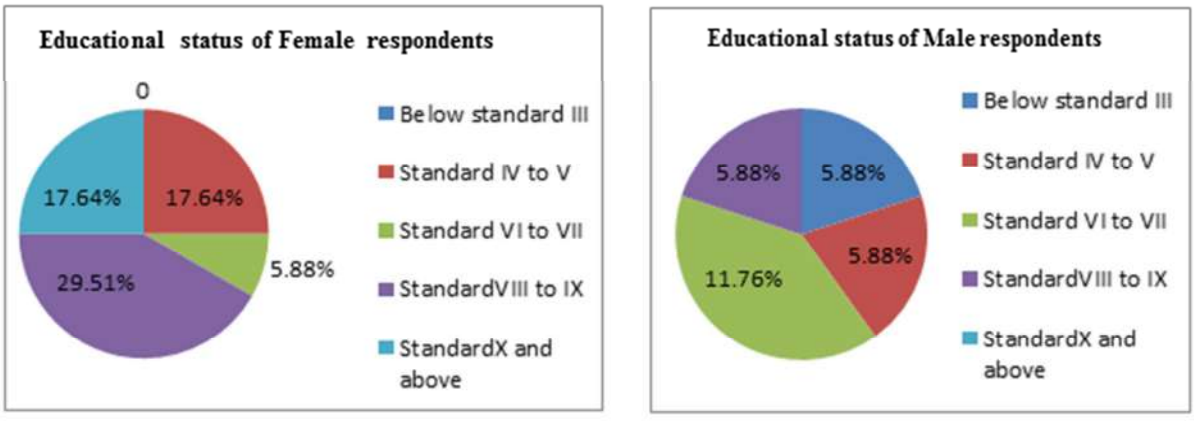

Fig4. Comparison of educational status between male and female hook maker

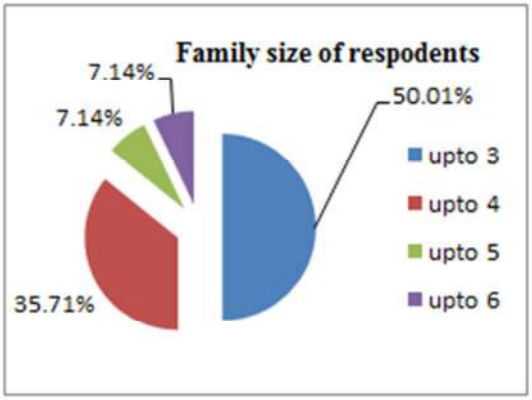

Fig 5. Family size of hook makers

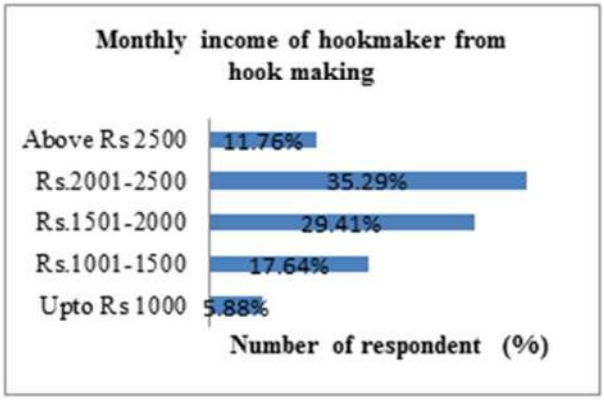

Fig 6. Monthly income of hook makers

Majority (71.42%) of the respondentshave a PHH type of ration card, 28.57% of the respondents possess the RKSY1 type of ration card. So it is evident that fish hook makers were generally a poorer section of society. Thus this section is indispensable and a significant section of economy in rural areas in Bankura district of West Bengal. Fish hook makers experienced various types of occupational health problems. Occupational disease occurred due to an exposure to risk factors arising from work activity. It was estimated that an average of 137 persons die from occupational disease in each day and an additional 17 die from injuries throughout the world.[12] Occupational health hazards are becoming a serious concern of this sector also. Low back disorders are common, musculoskeletal injuries, particularly due to working in stooped postures in many people working in different factories.[13] .Repeated exposures to vibrations and jarring motions while operating mechanical equipment.[14-15]also create various health hazards. In aquaculture, musculoskeletal injuries occur due to repetitive lifting or hand feeding, lifting of heavy cages or bags of feed, prolonged non-neutral postures at workstations, and tractor use.[16-17] In this study site majority of the male respondentsuffers from musculo-skeletal disease like pain in the body muscles, joints, neck regions, tendons, ligaments where as majority of females suffer from machinery induced injury due to mal handling and not using personal protection equipments.Among five villages average machinery induced injury in males are 1.40±1.14 , whereas average musculo-skeletal disease among males are 1.60±1.14. A large portion of male workers suffer from machinery induced injury (40%), eye disease (0.60±0.89), and skin disease (0.60±0.56). Females also suffer from machinery induced injury (3.40±1.51), skin disease (2.80±1.30) and eye disease (1.80±0.83) at older age. In each village musculo-skeletal diseases are also common among female workwe(3.00±1.22) (Figure 7). Skin disease may be due to worker's negligence about personal health and hygiene or they get very little time to maintain their proper health care. Eye disease may be due to working for a long time under dim light and metal particlesemerging during preparation of fish hook. Similar type of observation found among crafting communities, who work in poorly ventilated and inadequately lighted rooms. Workers have to work under unhygienic conditions leading to various health problems.[18]

Table 1. Various types of health hazards among hook makers

Types of health hazards	Affected males (%)	Affected females (%)
Machinery induced injury	1.40±1.14	3.40±1.51
Musculoskeletal disease	1.60±1.14	3.00±1.22
Skin disease	0.60±0.56	2.80±1.30
Eye disease	0.60±0.89	1.80±0.83

4. CONCLUSION

From our study,we can deduce that different types of occupational health hazards are regularly found among fish hook makers. So there is a need of notable degree of consciousness and sensitization through frequent safety training to reduce the health hazards. Under these circumstances, if various government sectors and NGO's came forward to overcome the hazards of these fish hook makers then in near future many other poor people engage themselves in this work to raise their socio economic standard.

5. RECOMMENDATION

Elicited from the perception of the current study we propose following recommendation:

1. Unsafe and unguarded manual handling of machines should be renewed.
2. Conscientious handling of machines, wires, marketable fish hooks and proper maintaining of machinery are necessary to avoid dreadful injuries.
3. Wearing PPE like protective goggles, hand gloves, jacket at the time of working can prevent the prevalence of accidents.
4. Occupational environment should be properly maintained.
5. Workers should pay attention to maintain their proper health and hygiene to avoid skin disease.
6. Workers should get systematic and consistent safety training to make aware of various types of protective measures to avoid hazards.
7. There is urgency of more illuminative investigation in attention of prior detection, safeguard and management

of job related diseases damages amongst fish hook makers.

6. ACKNOWLEDGEMENTS

We want to acknowledge Principal, Bankura Sammilani College, Bankura and Principal, Nistarini College, Purulia for their kind help and support for conducting the survey work. We acknowledge the help received from the hook makers of Salbedia, Kendbana, Bankanti, Ghutgoria and Pratappur village belonging to Bankura district of West Bengal, India for documenting their l knowledge.

7. AUTHORS CONTRIBUTION STATEMENT

Mr AnimeshMandal conceptualized and gathered data with regard to this work.MrRajendra Prasad Mondal analyzed these data.The necessary inputs towards the designing of the manuscript were given by Mr AnimeshMandal.Both the authors discussed the methodology and results and contributed to the final manuscript**.**

8. CONFLICT OF INTEREST

Conflict of interest declared none.

9. REFERENCES

1. Anon, A. Circle hooks outfish traditional halibut hooks. Mar Fish Rev. 1983;45:10-2.Available link: https://spo.nmfs.noaa.gov/sites/default/files/pdf-content/mfr4510-127.pdf
2. Gaur AS, Tripathi S, Tripathi S. Dwarka: An Ancient Harbour. Current Science.2004; 86(9):1256- 60. www.jstor.org/stable/24109935
3. Brandt VA. Fish catching methods of the world. Fishing Surrey.United Kingdom: news Books Limited. p. 393; 1984. Available from: https://www.wiley.com/en-us/Von+Brandt%27s+Fish+Catching+Methods+of+the+World%2C+4th+Edition-p-9780852382806.
4. Kitano Y, Satoh K, Yamane K, Sakai H. The corrosion resistance of tuna long-line fishing hook using fish monofilament, Nippon Suisan Gakkaishi (Japan)(Formerly Bull. Japan. Soc. Sci.Fish. 199; 56(11): 1765-72.
5. Varghese MD, George VC, GopalakrishnaPillai AG, Radhalakshmi K. Properties and performance of fishing hooks. FishTechnol. 1997;34:39-44.http://www.fao.org/3/a-i4017e.pdf.
6. Thomas SN, Odappazham G, Meenakumari B, Ashraf PM. Fishing hooks: a review. Fish Technol. 2007;44:1-16. https://www.academia.edu/9107725/Fishing_Hooks_A_Review.
7. Hanif MS, Iqbal KJ, Javid A, Khan N, Irfan I, Majeed H, Altaf M. Socio economic status of fishermen community, south Punjab, Pakistan. Punjab UnivJZool. 2019;34(2):115-18. doi:10.17582/journal.pujz/2019.34.1.115.118.
8. Marmot MG, Kogevinas M, Elston MA. Social/economic status and disease. Annu RevPublHealth. 1987;8:111-35. doi: 10.1146/annurev.pu.08.050187.000551, PMID 3555518.
9. Banerjee S. A study of relationship between socio-economic status and academic achievement of SC and ST students of secondary level in the district of Bankura in West Bengal.IntJ ApplRes. 2015;1(10):521-2. http://www.allresearchjournal.com/archives/2015/vol1issue10/PartH/1-9-193-741.pdf.
10. Ganguly M, Patsa MK,Ghosh A, Ganguly A.An Insight to the bell metal Industry of Bankura, West Bengal, India. IntJ Life Sci. 2016a;105-11. https://www.semanticscholar.org/paper/An-Insight-to-the-Bell-metal-Industry-of-Bankura-%2C-Ganguly-Patsa/4ff7179e278189c7ee20931fa8c12fef9d5dab99
11. Pattanaik BK,Singh MM.Sarva Siksha Abhiyan and Inclussive Education. Kurukshtra. 2011;59(7):16-19. http://yojana.gov.in/cms/(S(dzcartnbtrykky45ia4qrv55))/pdf/Kurukshetra/English/2011/May.pdf
12. Centers for Disease Control and Prevention (CDC). 1996. National Occupation Research Agenda, morbidity and mortality weekly report, 45: 445- 446 CDC. 1996. http://www.cdc.gov/nchs/data/nhanes/nhanCDC. 1996.
13. National Center for Health Statistics. CDC. 1996..
14. Fathallah FA, Miller BJ, Miles JA. Low back disorders in agriculture and the role of stooped work: scope, potential interventions, and research needs. J AgricSaf Health. 2008;14(2):221-45. doi: 10.13031/2013.24352, PMID 18524286.
15. Hostens I, Ramon H. Descriptive analysis of combine cabin vibrations and their effect on the human body. J Sound Vib. 2003;266(3):453-64. doi: 10.1016/S0022-460X(03)00578-9.
16. Mayton AG, Kittusamy NK, Ambrose DH, Jobes CC, Legault ML. Jarring/jolting exposure and musculoskeletal symptoms among farm equipment operators. Int J IndErgon. 2008;38(9-10):758-66. doi:10.1016/j.ergon.2007.10.011.
17. Moreau DTR, Neis B. Occupational Health and safety hazards in Atlantic Canadian aquaculture: laying the groundwork for prevention. Mar Pol. 2009;33(2):401-11. doi: 10.1016/j.marpol.2008.09.001.
18. Nonnenmann MW, Hussain A, Shirley M, Shepherd S, Gilmore K,Levin JL. Risk factors for musculoskeletal symptoms among crawfish farmers in Louisiana—a pilot study. J Agromed. 2010;15(4):386-93. doi: 10.1080/1059924X.2010.510440, PMID 20954034.
19. Ganguly M, Daripa A, Patsa MK, GangulyA. Assessment of Nutritional status, Socio-economic conditions and Occupational Health hazards of Conch shell workers of Bankura,West Bengal.IntJ Curr Res. 2016;8(3):28530-36.http://www.crdeepjournal.org/wp-content/uploads/2016/12/Vol-5-2-11-IJLS.pdf.
20. Satpathi MK. Terracotta Craft of Panchmura: Problems and Possibilities. Chitrolekha. International Magazine on Art and Design.2011;1(2). Available link:http://www.chitrolekha.com/V1/n2/07_Terracotta_crafts_of_Panchmura_Problems_and_Possibilities.pdf

Research & Reviews: Journal of Agriculture and Allied Sciences

e-ISSN:2347-226X
p-ISSN:2319-9857

IMPACTS OF AMBIENT AIR POLLUTION ON Mangifera indica GROWING AT PURULIA, PURULIA DISTRICT, W. B., INDIA

MOUMITA SINHA[1], SABYASACHI MUKHOPADHYAY*[2]

[1,2] Department of Environmental Science, Nistarini College, Purulia, W.B. (India)

Research Article

Received date: 18/04/2021
Accepted date: 25/04/2021
Published date: 29/04/2021

***For Correspondence**

SABYASACHI MUKHOPADHYAY

Keywords: Air pollution, Mangifera indica, biochemical characteristics, APTI.

ABSTRACT

In present days, growing industrialization and vehicular traffic are immense threat to ambient air quality in most of the urban areas. Few plants are sensitive and few are tolerant to air pollution in urban as well as in industrial habitats. Purulia have high emission of air pollutants mainly due to contribution of automobile exhaust, small industries, and domestic heating. In the month of February-March of 2019, impact of air pollution on Mango (Mangifera indica) leaves was investigated considering their biochemical characteristics and APTI values. Three samples were sampled considering control (Bongabari) and commercial areas (Renny Road, and Chawk Bazar) investigated by standard methods and APTI was calculated. Highest APTI was observed at control area (i.e., 18.52) followed by 12.79 at Renny Road and 11.54 at Chawk Bazar. It reveals that, between two commercial sampling points in Purulia town, Chawk Bazar shows more remarkable threatened condition.

e-ISSN:2347-226X
p-ISSN:2319-9857

INTRODUCTION

Plants are essential to balance both the nature and people's lives. Green plants, i.e., those possessing chlorophyll, are able to manufacture their own food and give off oxygen in the process of photosynthesis, in which water and carbon dioxide are combined by the energy of light. Plants are the ultimate source of food and metabolic energy for nearly all animals. Besides foods (e.g., grains, fruits, and vegetables), plant products are vital to humans include wood and wood products, fibres, drugs, oils, latex, pigments, and resins. Coal and petroleum are fossil substances of plant origin. Thus plants provide people not only sustenance but shelter, clothing, medicines, fuels, and the raw materials from which numerous other products are made. Pollution is now a common place term that our ears are attuned to. We hear about the various forms of pollution and read about it through the mass media. Irrespective of indoors or outside, air pollution is one such form that refers to the contamination of the air. A physical, biological or chemical alteration to the air in the atmosphere can be termed as pollution which occurs as and when any harmful gases, dust, smoke enters into the atmosphere and makes it difficult to survive for plants, animals and humans as the air becomes dirty. Growing industrialization and vehicular traffic especially in the urban areas of India is a great threat to air quality. The identification and categorization of plants into sensitive and tolerant groups is important because the former can serve as indicators and the latter as sinks for the air pollutants in urban and industrial habitats. Plant selection for their sensitivity or tolerance level to air pollutants is important because the sensitive plants can serve as bio-indicator and the tolerant plants as sink for controlling air pollution in urban and industrial areas. Purulia have high emission of air pollutants, which is degrading the ambient air quality day by day. There is now great concern that air pollutants especially sulfur dioxide, ozone, and oxides of nitrogen can change the physiological processes of plants, thereby affecting patterns of growth. Air pollutants cause damage to leaf cuticles and affect stomata conductance. They can also have direct impacts on photosynthetic systems, leaf longevity, and patterns of carbon allocation within plants. Pollutants interact with other environmental factors, and may change plant-environment relationships on a regional scale (Winner, 1981). Various strategies exist for controlling atmospheric pollution, but vegetation provides one of the natural ways of cleansing the atmosphere by absorption of gaseous and some particulate matter through leaves (Varshney, 1985). Lots of work has been performed to study the response of traffic load on plants (Angold, 1997) and also the impact of industries on plants (Chaphekar, 1972; Dwivedi and Tripathi, 2007). The degradation of air quality is a major environmental issue that affects many urban and industrial areas and the surrounding regions worldwide. On the basis of air pollution indices like adsorption or absorption, different plant groups were classified into sensitive, intermediate, moderately tolerant plant groups (Singh et al., 1991). To screen plants for their sensitivity or tolerance level to air pollutants, large number of plants parameter has been used including leaf or stomatal conductance, ascorbic acid, relative water content, membrane permeability, peroxidase activity, chlorophyll content and leaf extract pH (Choudhary and Rao, 1977; Keller and Schwager, 1977; Sivakumaran and Hall, 1978; Farooq and Beg, 1980; Winner, 1981; Eckert an Houston, 1982; William and Christopher, 1986; Singh et al., 1991; Tripathi et al., 1991; Namita et al., 2009). To indicate the susceptibility level of plant, pollutioninduced changes in individual parameters are usually quantified and correlated with the level of plant response. The combination of the biochemical and physiological parameters gave a more reliable result than those of individual parameter. Therefore, combination of parameters.

MATERIALS AND METHODS

The major sources of pollutants in Purulia town are automobile exhaust, small industries, and domestic heating. Sample, i.e., Mangifera indica leaves, collected from Bongabari (S1as control zone, 3.0 km far from Purulia town); Renny Road (S2), and Chawk Bazar (S3) which are the heart and prime commercial area of the Purulia town, were investigated with respect to their biochemical characteristics and APTI values. For this purpose, the mature leaf samples (fifth from top) of the most common plant in the

e-ISSN:2347-226X
p-ISSN:2319-9857

region such as Mangifera indica (Mango) were collected in the month of February-March, 2019. For each species, five individuals were identified and each sample was taken in triplicate. Care was taken to see that all plants had, as far as possible, the same ecological condition with respect to light, water, soil and pollutant exposure. The collected samples were analyzed for ascorbic acid, chlorophyll; relative water content and leaf extract pH. The mean values of different parameters were used for computing the index. Total chlorophyll content was estimated using the method of Singh et al. (1991). Briefly, for chlorophyll estimation, 200 mg of leaf material directly harvested from the plants was ground in mortar and pestle with a small quantity of acid washed sand in 80% acetone. The absorbance of the filtered extract was measured through spectrophotometer (Genesis 6, Thermo Electron) at 645 nm and 663 nm. Equation 1 was used to calculate total chlorophyll.

$$\text{Total chlorophyll (mg/g)} = \frac{V\,(20.2\times A645 + 8.02\times A663)\times V}{1000\times W}$$

Where, A645 = Absorbance at 645nm; A663 = Absorbance at 663nm; V = Total volume of extract; W = Weight of leaf material in gram

For Ascorbic acid, 0.5 g of fresh leaf sample was homogenized with 20 ml of extracting solution (5 g oxalic acid + 0.75 g EDTA in 1000 ml of distilled water). It was centrifuged for 15 min at 6000xg and the supernatant collected. The supernatant (1 ml) was added to 2,6dichlorophenol indophenol (DCPIP) (5ml of 20 µg/ml), the solution was turning pink. The optical density of the mixture was taken at 520 nm (Es). After taking the optical density (OD) of the mixture one drop of ascorbic acid was added to bleach the pink colour and again the OD was taken at the same wavelength (Et). The OD of DCPIP solution was also taken at 520 nm (Eo). The standard curve was prepared by using different concentration of ascorbic acid by following the same method. Individual leaves of different plant species were excised and weighed immediately. They were dipped into water in a beaker. After 8 hr the leaves were blotted and reweighed before being dried at 80ºC for 24 hr and reweighed. For determination of leaf pH, 5 g of leaf samples was well homogenized with 50 ml deionized water and pH of the suspension was measured with a digital pH meter (Hanna Instrument, Germany).

$$\text{APTI} = \frac{[A\,(T + P)] + R}{10}$$

Where, A is ascorbic acid content of leaf in mg/g dry weight, T is total chlorophyll content of leaf in mg/g dry weight, P is leaf extract pH and R is % relative water content of leaf. The total sum is divided by 10 to obtained APT

RESULTS AND DISCUSSION

Parameter	Control (S1)	S2	S3
Total chlorophyll (mg/g dry weight)	11.98	8.12	4.07
Leaf extract pH	9.4	7.2	7.0
Ascorbic acid (mg/g dry weight)	4.12	3. 28	3.12
Relative water content (%)	89.78	71.35	74.06
APTI	17.26	12.16	10.86

Table-1: Results obtained after analysis

e-ISSN:2347-226X
p-ISSN:2319-9857

From the Table-1, it clear that in Purulia town, there was very serious impacts on plants from the air pollution. In Bongabari, every parameter is in good state, which depict that there was less stress on *Mangifera indica* than in case of Purulia. Between two sampling point in Purulia town, Chawk Bazar shows more threatened figure, which is very remarkable. APTI determinations are of importance because with increased industrialization, there is increasing danger of deforestation due to air pollution. The results of such studies are therefore handy for future planning and may be helpful to bring out possible control measures. It is worth noting that combining a variety of parameters gave a more reliable result than when based on a single biochemical parameter.

REFERENCES

1. Angold P G (1997), *The impact of a road upon adjacent health land vegetation effects on plant species composition*, **J. Appl. Ecol**., 34: 409-417.
2. Chaphekar SB (1972), *Effect of atmospheric pollutants on plants in Bombay*, **J. Biol. Sci.**, 15: 1-6.
3. Choudhary CS, Rao DN (1977), *Study on some factors in plants controlling their susceptibility to SO2 pollution,* **Proc. Indian National Sci. Acad.**, 43: 236-241.
4. Choudhury P, Banerjee D (2009), *Biomonitoring of air quality in the industrial town of asansol using the air pollution tolerance index approach,* **Res. J. Chem. Environ**. 13(1): 46-51.
5. Dwivedi AK, Tripathi BD (2007), *Pollution tolerance and distribution pattern of plants in surrounding area of coal-fired industries*, **J. Environ. Biol.** 28(2): 257-263
6. Eckert RT, Houston DB (1982), *Foliar peroxidase and acid phosphatise activity response to low level SO2 exposer in eastern white pine clones*. **Forestry Sci.** 28: 661-664.
7. Farooq M, Beg MU (1980), *Effect of aqueous SO2 on the membrane permeability of common Indian tree leaves,* **New Botanisz**: 7: 213-217.
8. Keller T, Schwager H (1977), *Air pollution and ascorbic acid,* **Eur. J. Forestry Pathol**. 7: 338-350.
9. Lakshmi PS, Sravanti KL, Srinivas N (2008), *Air pollution tolerance index of various plant species growing in industrial areas*, **The Ecoscan** 2(2): 203-206.
10. Namita J, Chauhan A, Joshi PC (2009), *Impact of industrial air pollutants on some biochemical parameters and yield in wheat and mustard plants,* **Environmentalist**, 29(4): 398-404.
11. Singh SK, Rao DN (1983), *Evaluation of plants for their tolerance to air pollution.* **In: Proceeding of Symposium on Air Pollution Control, Vol.1. Indian Association of Air Pollution Control, New Delhi**, 218-224.
12. Singh SK, Rao DN, Agrawal M, Pande J, Narayan D (1991), *Air pollution tolerance index of plants*. **J. Env. Manag**. 32: 45-55.
13. Singh SK, Rao DN, Agrawal M, Pande J, Narayan D (1991), *Air pollution tolerance index of plants,* **J. Env. Manag**. 32: 45-55.
14. Sivakumaran S, Hall MA (1978), *Effect of age and water stress in endogenous levels of plants growth regulators in Euphorbia lathyrus*. **J. Exp. Bot**. 29: 195-205.

e-ISSN:2347-226X
p-ISSN:2319-9857

15. Tripathi BD, Tripathi A, Mishra K (1991), *Atmospheric dust fall deposits in Varanasi city,* **Atmos. Environ**. 258: 109-112.
16. Varshney CK (1985), *Role of plant in indicating, monitoring and mitigating air pollution,* In: Air pollution and pants: **A state-of-The-Art Report** (Eds. GV Subrahmanium, DN Rao, CK Varshney and DK Viswas). Ministry of Environment and Forests. New Delhi, pp. 146- 170.
17. William EW, Christopher JA (1986), *Absorption of air pollution by plants, and consequences for growth,* **Trends Ecol. Evol**. 1(1): 15-18.
18. Winner WE (1981), *The effects of SO2 on photosynthesis and stomatal behavior of mediterranean-climate shrubs and herbs*. **In: Componenet of productivity of Mediterranean climate region- basic and applied aspects** (Eds. NS Margaris and HA Mooney). Dr. W Junk Publishers: 91-103.

UGC CARE LIST – SCIENCE (Updated July 2020)

Sr.No.	Journal Title	Publisher	ISSN	E-ISSN	Action
1	Acta Fytotechnica et Zootechnica	Slovak University of Agriculture in Nitra	1335-258X	1336-9245	Indexed in Scopus
2	Acta Geographica Debrecina, Landscape and Environment Series	Department of Landscape Protection and Environmental Geography, University of Debrecen	1789-4921	1789-7556	View
3	Acta Graphica	Faculty of Graphic Arts, University of Zagreb	0353-4707	1848-3828	View
4	Acta Universitatis Apulensis	Department of Mathematics and Informatics, University of Alba Iulia	1582-5329	NA	View
5	Acta Universitatis Matthiae Belii Series Mathematics	Department of Mathematics Faculty of Natural Sciences, Matej Bel University	1338-712X	1338-7111	View
6	ADBU Journal of Engineering Technology	Assam Don Bosco University	NA	2348-7305	View
7	Advanced Engineering Forum	Trans Tech Publications Inc.	2234-9898	2234-991X	View
8	Advanced Materials Research	Scientific.Net	1022-6680	1662-8985	View
9	Advanced Science Letters	American Scientific Publishers	1936-6612	1936-7317	Discontinued from July 2020
10	Advances and Applications in Mathematical Sciences	Mili Publications	0974-6803	NA	View
11	Advances in Agriculture	Hindawi Limited	2356-654X	2314-7539	View
12	Advances in Environment Research	Techno Press	2234-1722	2234-1730	View
13	Advances in Zoology and Botany	Horizon Research Publishing	2331-5083	2331-5091	View
14	African Diaspora Journal of Mathematics	Mathematical Research Publisher	1539-854X	NA	View
15	Afrika Statistika	Saint-Louis Senega University	2316-090X	NA	View
16	Agricultural Research Journal	Punjab Agricultural University	2395-1435	2395-146X	View

UGC CARE LIST – SCIENCE (Updated July 2020)

17	AIMS Molecular Science	AIMS Press	NA	2372-0301	View
18	AIS Transactions on Human- Computer Interaction	Association for Information Systems	NA	1944-3900	View
19	Al Ameen Journal of Medical Sciences	Al Ameen Medical College	0974-1143	NA	View
20	Albanian Journal of Mathematics	Department of Mathematics and Statistics, Oakland University	1930-1235	NA	View
21	Algological Studies	Schweizerbart Science Publishers	1864-1318	2363-7080	View
22	Aligarh Journal of Statistics	Department of Statistics and Operations Research, Aligarh Muslim University	0971-0388	NA	View
23	Analytical Chemistry Letters	Taylor and Francis	2229-7928	2230-7532	View
24	Ancient Science of Life	AVP Research Foundation	0257-7941	2249-9547	View
25	Animal Systematics, Evolution and Diversity	Korean Society of Systematic Zoology	NA	2234-8190	View
26	Annales Mathematiques Blaise Pascal	Mathematical laboratory, Blaise Pascal University of Clermont-Ferrand	1259-1734	2118-7436	View
27	Annals of Ayurvedic Medicine	Society of Ayurvedic Physicians of India	2277-4092	2347-6923	View
28	Annals of Faculty Engineering Hunedoara-International Journal of Engineering	Faculty of Engineering Hunedoara, University Politehnica Timisoara	1584-2665	1584-2673	Discontinued from July 2020
29	Annals of National Academy of Medical Sciences	National Academy of Medical Sciences	2454-5635	2454-5635	View
30	Annals of Plant and Soil Research	G. K. V. Society	0972-1959	2347-6036	View
31	Annals of West University of Timisoara-Mathematics and Computer Science	Sciendo, De Gruyter	NA	1841-3307	View
32	Annals. Food Science and Technology	Valahia University Press	2065-2828	2344-4916	View
33	Antennae: The Journal of Nature in Visual Culture	University of Strathclyde	1756-9575	NA	View

UGC CARE LIST – SCIENCE (Updated July 2020)

34	Applied Ecology and Environmental Sciences	Science and Education Publishing	2328-3912	2328-3920	View
35	Applied Water Science	Springer	2190-5487	2190-5495	View
36	Arab Journal of Forensic Sciences and Forensic Medicine	Arab Society for Forensic Sciences and Forensic Medicine	1658-6786	1658-6794	View
37	Arab Journal of Mathematical Sciences	Elsevier	1319-5166	NA	Indexed in Scopus
38	Arabian Journal of Mathematics	Springer	2193-5343	2193-5351	View
39	Archives of Medicine and Health Sciences	Yenepoya University	2321-4848	2321-6085	View
40	Arctoa: A Journal of Bryology	KMK Scientific Press Ltd.	0131-1379	NA	View
41	Asian Journal of Agriculture and Development	Southeast Asian Regional Center for Graduate Study and Research in Agriculture	1656-4383	2599-3879	View
42	Asian Journal of Organic and Medicinal Chemistry	Asian Publication Corporation	NA	2456-8937	View
43	Atmospheric and Oceanic Science Letters	Taylor and Francis	1674-2834	2376-6123	Indexed in Scopus
44	Autism and Developmental Language Impairments	Sage Publications	2396-9415	NA	View
45	Ayu	Institute For Post Graduate Teaching & Research in Ayurveda	0974-8520	0976-9382	View
46	Bharatiya Vaigyanik evam Audyogik Anusandhan Patrika	National Institute of Science Communication and Information Resources	0771-7706	0975-2412	View
47	Big Data and Society	Sage Publications	2053-9517	NA	View
48	Biochemistry Insights	Sage Publications	1178-6264	1178-6264	Discontinued from July 2020
49	Bioengineering	MDPI	2306-5354	NA	Indexed in Scopus

UGC CARE LIST – SCIENCE (Updated July 2020)

50	Biological Theory	Springer	1555-5542	1555-5550	View
51	Biotechnology Research and Innovation	Elsevier	2452-0721	NA	View
52	Biotecnologia Vegetal	Instituto De Biotecnologia De Las Plantas	1609-1841	2074-8647	View
53	Blde University Journal of Health Sciences	BLDE University	2468-838X	2456-1975	View
54	Botanicheskii Zhurnal	Sankt-Peterburgskaya Izdatel'Skaya Firma Nauka	0006-8136	2658-6339	View
55	Bryophyte Diversity and Evolution	Magnolia Press	2381-9677	2381-9685	View
56	Bulgarian Journal of Physics	Heron Press Ltd.	1310-0157	1314-2666	View
57	Bulletin of Calcutta Mathematical Society	Calcutta Mathematical Society	0008-0659	NA	View
58	Bulletin of Faculty of Pharmacy, Cairo University	Faculty of Pharmacy, Cairo University	1110-0931	NA	Discontinued from Jan. 2020
59	Bulletin of the Ecological Society of America	Ecological Society of America	NA	2327-6096	View
60	Canadian Journal of Disability Studies	Canadian Studies Disability Association	1929-9192	NA	View
61	Case Report in Rheumatology	Hindawi Limited	2090-6889	2090-6897	View
62	Caucasian Entomological Bulletin	Institute of Arid Zones SSC RAS	NA	1814-3326	View
63	Chemistry and Biology Interface	Indian Society of Chemists and Biologists	NA	2249-4820	Discontinued from Jan. 2020
64	Chinese Herbal Medicines	Elsevier	1674-6384	2589-3610	Discontinued from Jan. 2020
65	Cogent Environmental Science	Taylor and Francis	NA	2331-1843	View

UGC CARE LIST – SCIENCE (Updated July 2020)

66	Communications Faculty of Sciences University of Ankara Series A1: Mathematics and Statistics	Faculty of Science, Ankara University	1303-5991	2618-6470	View
67	Complex Analysis and its Synergies	Springer	NA	2197-120X	View
68	Computational Methods for Differential Equations	University of Tabriz	2345-3982	2383-2533	View
69	Concrete Operators	Walter de Gruyter	NA	2299-3282	View
70	Contraception and Reproductive Medicine	BioMed Central Ltd.	NA	2055-7426	View
71	Convergent Science Physical Oncology	Institute of Physics Publishing	NA	2057-1739	Discontinued from Feb. 2020
72	Creative Mathematics and Informatics	Depatament of Mathematics and Computer Science, Tehnical University of Cluj- Napoca	1584-286X	1843-441X	View
73	Crux Mathematicorum	Canadian Mathematical Society	1706-8142	1496-4309	View
74	Cubo, A Mathematical Journal	Department of Mathematics and Statistics, University of La Frontera	0716-7776	0719-0646	View
75	Current Biochemical Engineering	Bentham Science Publishers	2212-7119	2212-7127	View
76	Current Botany	TathQeef Scientific Publishing	NA	2220-4822	View
77	Current Catalysis	Bentham Science Publishers	2211-5447	2211-5455	View
78	Current Dermatology Reports	Springer	NA	2162-4933	Indexed in Scopus
79	Current Green Chemistry	Bentham Science Publishers	2213-3461	2213-347X	View
80	Current Medicine Research and Practice	Elsevier	2352-0817	NA	View
81	Current Microwave Chemistry	Bentham Science Publishers	2213-3356	2213-3364	View
82	Current Opinion in Biomedical Engineering	Elsevier	2468-4511	NA	View
83	Current Physical Chemistry	Bentham Science Publishers	1877-9468	1877-9476	View

UGC CARE LIST – SCIENCE (Updated July 2020)

84	Current Sustainable/Renewable Energy Reports	Springer	NA	2196-3010	View
85	Current Traditional Medicine	Bentham Science Publishers	2215-0838	2215-0846	View
86	Current World Environment	Enviro Research Publishers	0973-4929	2320-8031	View
87	Curtis's Botanical Magazine	John Wiley and Sons, Inc.	NA	1467-8748	View
88	Data Science and Engineering	Springer	2364-1185	2364-1541	Indexed in Scopus
89	Defence Life Science Journal	Defence Scientific Information and Documentation Centre	2456-379X	2456-0537	View
90	Differential Geometry- Dynamical Systems	Balkan Society of Geometers, Geometry Balkan Press	NA	1454-511X	View
91	Discussiones Mathematicae- General Algebra and Applications	Faculty of Mathematics Computer Science and Econometrics, University of Zielona Gora	1509-9415	2084-0373	View
92	Ecology, Economy and Society- the INSEE Journal	Indian Society of Ecological Economics	2581-6152	2581-6101	View
93	Ecosystem Health and Sustainability	Taylor and Francis	2096-4129	2332-8878	Indexed in Scopus
94	Ela Journal of Forestry and Wildlife	Ela Foundation	2319-4361	NA	View
95	Electronic Journal of Mathematical Analysis and Applications	Department of Mathematics and Computer Sciences, Alexandria University	NA	2090-729X	View
96	Environmental and Experimental Biology	University of Latvia	1691-8088	2255-9582	View
97	Eurasian Journal of Forest Science	Eurasscience Journals	NA	2147-7493	Discontinued from Sept. 2019
98	European Journal of Medicinal Plants	Sciencedomain International	2231-0894	NA	Discontinued from Feb. 2020

UGC CARE LIST – SCIENCE (Updated July 2020)

99	Fasciculi Mathematici	Poznan University of Technology, Institute of Mathematics	0044-4413	NA	View
100	Food Science and Human Wellness	Beijing Academy of Food Sciences	2213-4530	NA	Indexed in Scopus
101	Fractional Differential Calculus	Element d.o.o.	1847-9677	NA	View
102	Fungal Biology and Biotechnology	BioMed Central Ltd.	2054-3085	NA	View
103	Future Journal of Pharmaceutical Sciences	Springer	2314-7245	2314-7253	View
104	Fuzzy Systems and Soft Computing	Tver State University	1819-4362	NA	View
105	Ganita	Bharata Ganita Parishada	0046-5402	NA	View
106	Gardens Bulletin Singapore	National Parks Board, Singapore Botanic Gardens	0374-7859	2382-5812	View
107	Genomics and Computational Biology	Johannes Gutenberg University	NA	2365-7154	View
108	Geographical Review of India	The Geographical Society of India	0375-6386	NA	View
109	Gravitational and Space Research	American Society for Gravitational and Space Research	NA	2332-7774	Discontinued from Feb. 2020
110	Gujarat Agricultural University Research Journal	Sardarkrushinagar Dantiwada Agricultural University	0250-5193	NA	View
111	Gulf Journal of Mathematics	Canadian University of Dubai	NA	2309-4966	View
112	Hepatoma Research	OAE Publishing Inc.	2394-5079	2454-2520	Discontinued from Sept. 2019
113	High Voltage	Institution of Engineering and Technology	NA	2397-7264	Indexed in Web of Science
114	Hill Geographer	Geographical Society of the North-Eastern Hill Region	0970-5023	NA	View
115	Hippocratic Journal of Unani Medicine	Central Council for Research in Unani Medicine	0974-1291	NA	View

UGC CARE LIST – SCIENCE (Updated July 2020)

116	Horticultural Plant Journal	KeAi Publishing Communications Ltd	2095-9885	2468-0141	Indexed in Scopus
117	ICTACT Journal on Communication Technology	ICT Academy	0976-0091	2229-6948	View
118	ICTACT Journal on Image and Video Processing	ICT Academy	0976-9099	0976-9102	View
119	ICTACT Journal on Microelectronics	ICT Academy	2395-1672	2395-1680	View
120	ICTACT Journal on Soft Computing	ICT Academy	0976-6561	2229-6956	View
121	IET Cyber- Physical Systems: Theory and Applications	Institution of Engineering and Technology	NA	2398-3396	Indexed in Scopus
122	Indian Dermatology Online Journal	Indian Association of Dermatologists, Venereologists and Leprologists	2229-5178	2249-5673	View
123	Indian Hydrobiology	Krishnamurthy Institute of Algology, Madras Christian College	0971-6548	NA	View
124	Indian Journal of Aerobiology	Indian Aerobiological Society	0971-1546	NA	View
125	Indian Journal of Allergy Asthma and Immunology	Indian College of Allergy Asthma and Immunology	0972-6691	2320-4745	View
126	Indian Journal of Animal Nutrition	Animal Nutrition Society of India	0970-3209	2231-6744	Discontinued from Sept. 2019
127	Indian Journal of Continuing Nursing Education	College of Nursing, Christian Medical College	2230-7354	NA	View
128	Indian Journal of Dairy Science	Indian Dairy Association	0019-5146	2454-2172	View
129	Indian Journal of Dental Sciences	Himachal Pradesh University	0976-4003	2231-2293	View
130	Indian Journal of Geography and Environment	Department of Geography and Environment Management, Vidyasagar University	0972-7388	NA	View
131	Indian Journal of Geosciences	Geological Society of India	2229-3574	2582-3485	View
132	Indian Journal of Gerontology	Indian Gerontological Association	0971-4189	NA	View
133	Indian Journal of Gynecologic Oncology	Springer	2363-8397	2363-8400	Indexed in Scopus

UGC CARE LIST – SCIENCE (Updated July 2020)

134	Indian Journal of Hill Farming	Indian Association of Hill Farming	0970-6429	NA	View
135	Indian Journal of Psychiatric Nursing	Indian Society of Psychiatric Nurses	2231-1505	2666-528X	View
136	Indian Journal of Sexually Transmitted Diseases and AIDS	Indian Association for the Study of Sexually Transmitted Diseases	2589-0557	2589-0565	View
137	Indian Journal of Small Ruminants	Indian Society for Sheep and Goat Production and Utilization	0971-9857	0973-9718	View
138	Indian Journal of Sugarcane Technology	Association of Sugarcane Technologists of India	0970-3233	NA	View
139	Indo Global Journal of Pharmaceutical Sciences	Indo Global Journal of Pharmaceutical Sciences	NA	2249-1023	View
140	Indonesian Journal of Forestry Research	Ministry of Environment and Forestry, Republic of Indonesia	2355-7079	2406-8195	View
141	Industrial Engineering Journal	Indian Institution of Industrial Engineering	2581-4915	NA	View
142	INFOCOMP Journal of Computer Science	Department of Computer Science, Federal University of Lavras	NA	1982-3363	View
143	Information and Inference: A Journal of the IMA	Oxford University Press	2049-8764	2049-8772	View
144	Integers	Colgate University and Charles University	NA	1553-1732	View
145	International Journal of Advanced Medical and Health Research	Jawaharlal Institute of Postgraduate Medical Education and Research	2349-4220	2350-0298	View
146	International Journal of Advanced Pervasive and Ubiquitous Computing	IGI Global	1937-965X	1937-9668	View
147	International Journal of Advances in Engineering Sciences and Applied Mathematics	Springer	0975-0770	0975-5616	View
148	International Journal of Agricultural System	Graduate School, Hasanuddin University	2337-9782	2580-6815	View
149	International Journal of Agricultural Technology	Association of Agricultural Technology in Southeast Asia	2630-0613	2630-0192	Indexed in Scopus

UGC CARE LIST – SCIENCE (Updated July 2020)

150	International Journal of Applied and Basic Medical Research	Basic Medical Scientists Association	2229-516X	2250-2858	View
151	International Journal of Applied Exercise Physiology	Asian Exercise and Sports Science Association	2322-3537	NA	Discontinued from Jan. 2020
152	International Journal of Applied Industrial Engineering	IGI Global	2155-4153	2155-4161	View
153	International Journal of Applied Logistics	IGI Global	1947-9573	1947-9581	View
154	International Journal of Applied Nonlinear Science	Inderscience Publishers	1752-2862	1752-2870	View
155	International Journal of Architecture, Engineering and Construction	International Association for Sustainable Development and Management	1911-110X	1911-1118	View
156	International Journal of Artificial Intelligence and Soft Computing	Inderscience Publishers	1755-4950	1755-4969	View
157	International Journal of Biomedical and Clinical Engineering	IGI Global	2161-1610	2161-1629	View
158	International Journal of Computational Intelligence Studies	Inderscience Publishers	1755-4977	1755-4985	View
159	International Journal of Computer Theory and Engineering	International Journal of Computer Theory and Engineering	1793-8201	NA	View
160	International Journal of Computer Vision and Image Processing	IGI Global	2155-6997	2155-6989	View
161	International Journal of Creative Interfaces and Computer Graphics	IGI Global	1947-3117	1947-3125	View
162	International Journal of Data Science and Analytics	Springer	2364-415X	2364-4168	View
163	International Journal of Design Engineering	Inderscience Publishers	1751-5882	1751-5874	View

UGC CARE LIST – SCIENCE (Updated July 2020)

164	International Journal of Digital Curation	Digital Curation Centre, University of Edinburgh	NA	1746-8256	View
165	International Journal of Digital Literacy and Digital Competence	IGI Global	1947-3494	1947-3508	View
166	International Journal of Ecology and Environmental Sciences	National Institute of Ecology	0377-015X	2320-5199	View
167	International Journal of Economic and Environmental Geology	Society of Economic Geologists and Mineral Technologists, Department of Geology, University of Karachi	NA	2223-957X	Discontinued from July 2020
168	International Journal of Electrochemistry	Hindawi Limited	2090-3529	2090-3537	View
169	International Journal of Energy Optimization and Engineering	IGI Global	2160-9500	2160-9543	View
170	International Journal of Geosynthetics and Ground Engineering	Springer	2199-9260	2199-9279	Indexed in Scopus
171	International Journal of Green Computing	IGI Global	1948-5018	1948-5026	View
172	International Journal of Information Communication Technologies and Human Development	IGI Global	1935-5661	1935-567X	View
173	International Journal of Information Security Science	Department of Computer Engineering, Gazi University	NA	2147-0030	View
174	International Journal of Information Technology	Springer	2511-2104	2511-2112	View
175	International Journal of Information Technology and Electrical Engineering	International Journal of Information Technology and Electrical Engineering	NA	2306-708X	View
176	International Journal of Insect Science	Sage Publications	1179-5433	1179-5433	Discontinued from July 2020

UGC CARE LIST – SCIENCE (Updated July 2020)

177	International Journal of Interdisciplinary Telecommunications and Networking	IGI Global	1941-8663	1941-8671	View
178	International Journal of Masonry Research and Innovation	Inderscience Publishers	2056-9467	2056-9459	Indexed in Scopus
179	International Journal of Materials, Mechanics and Manufacturing	International Association of Computer Science and Information Technology	1793-8198	NA	View
180	International Journal of Mathematics and Statistics	Centre for Environment and Socio- Economic Research Publications	0974-7117	0973-8347	View
181	International Journal of Monitoring and Surveillance Technologies Research	IGI Global	2166-7241	2166-725X	View
182	International Journal of Nano Dimension	Islamic Azad University, Tonekabon Branch	2008-8868	2228-5059	Discontinued from Jan. 2020
183	International Journal of Next- Generation Computing	Perpetual Innovation	2229-4678	0976-5034	View
184	International Journal of Operations Research	Department of Management Sciences, TamKang University	1813-713X	1813-7148	View
185	International Journal of Pharmaceutical Investigation	Phcog.Net	2230-973X	2230-9713	View
186	International Journal of Pharmaceutical Sciences and Drug Research	MRI Publication Pvt. Ltd.	NA	0975-248X	View
187	International Journal of Pharmaceutical Sciences and Nanotechnology	Pharma Book Syndicate	NA	0974-3278	View
188	International Journal of Quantitative Structure-Property Relationships	IGI Global	2379-7487	2379-7479	View

UGC CARE LIST – SCIENCE (Updated July 2020)

189	International Journal of Renewable Energy Technology	Inderscience Publishers	1757-3971	1757-398X	View
190	International Journal of Statistics and Reliability Engineering	Indian Association for Reliability and Statistics	2350-0174	2456-2378	View
191	International Journal of Yoga	Swami Vivekananda Yoga Anusandhana Samsthana	0973-6131	2231-2714	View
192	International Research Journal of Plant Science	International Research Journals Publishing House	2141-5447	NA	View
193	Involve: A Journal of Mathematics	Mathematical Sciences Publishers	1944-4176	1944-4184	View
194	Iranian Journal of Mathematical Chemistry	University of Kashan	2226-6489	2008-9015	Discontinued from Sept. 2019
195	IRCF Journal Reptiles and Amphibians: Conservation and Natural History	The International Reptile Conservation Foundation	2330-3956	2332-4961	View
196	Isecure- The ISC International Journal of Information Security	Iranian Society of Cryptography	2008-2045	2008-3076	View
197	Jahan- e- Tib	Central Council for Research in Unani Medicine	0974-1372	NA	View
198	Jnanabha	Vijnana Parishad of India	0304-9892	2455-7463	View
199	Journal of Advanced Mathematical Studies	Fair Partners Society for the Promotion of Science	2065-3506	2065-5851	View
200	Journal of Advanced Scientific Research	Sciensage	NA	0976-9595	View
201	Journal of Aerospace Sciences and Technologies	Aeronautical Society of India	0972-950X	NA	View
202	Journal of Algebra and Related Topics	Faculty of Mathematical Sciences, University of Guilan	2345-3931	2382-9877	Discontinued from Jan. 2020
203	Journal of Animal Ethics	University of Illinois Press	2156-5414	2160-1267	View

UGC CARE LIST – SCIENCE (Updated July 2020)

204	Journal of Applied Biology and Biotechnology	Open Science Publishers	2455-7005	2347-212X	Discontinued from Sept. 2019
205	Journal of Applied Mathematics and Computational Mechanics	Institute of Mathematics, Czestochowa University of Technology	2299-9965	2353-0588	View
206	Journal of Aquatic Biology and Fisheries	Department of Aquatic Biology and Fisheries, University of Kerala	2321-340X	NA	View
207	Journal of Ayurveda	National Institute of Ayurveda	2321-0435	NA	View
208	Journal of Biologically Active Products from Nature	Taylor and Francis	2231-1866	2231-1874	Indexed in Scopus
209	Journal of Bioresources	Rajiv Gandhi University, Center with Potential for Excellence in Biodiversity	2394-4315	2582-2276	View
210	Journal of Calcutta Mathematical Society	Calcutta Mathematical Society	0080-0659	NA	View
211	Journal of Cancer Metastasis and Treatment	OAE Publishing Inc.	2394-4722	2454-2857	View
212	Journal of Cellular Immunotherapy	Shanghai Hengrun Biomedical Technology Research Institute	2352-1775	NA	Discontinued from July 2020
213	Journal of Classical Analysis	Element d.o.o.	1848-5979	1848-5987	View
214	Journal of Climate Change	IOS Press	2395-7611	2395-7697	View
215	Journal of Construction Management	National Institute of Construction Management and Research	0970-3675	NA	View
216	Journal of Dental Research and Review	Dr. D. Y. Patil VIdyapeeth	2348-2915	2348-3172	View
217	Journal of Dental Research Dental Clinics Dental Prospects	Tabriz University of Medical Sciences	2008-210X	2008-2118	View
218	Journal of Dermatology and Dermatologic Surgery	Saudi Society of Dermatology and Dermatologic Surgery	2352-2410	2352-2429	View
219	Journal of Diabetology	Diabetes In Asia Study Group	2543-3288	2078-7685	View

UGC CARE LIST – SCIENCE (Updated July 2020)

220	Journal of Digital Forensics, Security and Law	Association of Digital Forensics, Security and Law	1558-7215	1558-7223	View
221	Journal of Dynamical Systems and Geometric Theories	Taylor and Francis	1726-037X	2169-0057	View
222	Journal of Epilepsy Research	Korean Epilepsy Society	2233-6249	2233-6257	View
223	Journal of Experimental Biology and Agricultural Sciences	Horizon Publisher India	NA	2320-8694	Discontinued from Jan. 2020
224	Journal of Family and Community Medicine	Saudi Society of Family and Community Medicine	2230-8229	2229-340X	View
225	Journal of Family Medicine and Primary Care	Family Medicine and Primary Care Trust	2249-4863	2278-7135	View
226	Journal of Food, Agriculture and Environment	WFL Publisher Ltd.	1459-0255	1459-0263	View
227	Journal of Forensic Dental Sciences	Indian Association of Forensic Odontology	0975-1475	0975-2137	View
228	Journal of Fractional Calculus and Applications	Department of Mathematics and Computer Sciences, Alexandria University	2090-584X	2090-5858	View
229	Journal of Fungi	MDPI	NA	2309-608X	Indexed in Scopus
230	Journal of Geophysics	Association of Exploration Geophysicists	0257-1412	NA	View
231	Journal of Geriatric Mental Health	Indian Association for Geriatric Mental Health	2348-9995	2395-3322	View
232	Journal of Global Resources	Institute of Sustainable Development, Environmental and Scientific Research	2395-3160	2455-2445	Discontinued from Jan. 2020
233	Journal of Himalayan Ecology and Sustainable Development	Department of Environmental Science, University of Kashmir	0973-7502	NA	Discontinued from Jan. 2020

UGC CARE LIST – SCIENCE (Updated July 2020)

234	Journal of Hyperstructures	University of Mohaghegh Ardabili	2251-8436	2322-1666	View
235	Journal of Indian Association of Public Health Dentistry	Indian Assiciation of Public Health Dentistry	2319-5932	2350-0484	View
236	Journal of Indian College of Cardiology	Indian College of Cardiology	1561-8811	2213-3615	View
237	Journal of Indian Orthodontic Society	Sage Publications	0301-5742	0974-9098	View
238	Journal of Indian Water Works Association	Indian Water Works Association	0970-275X	NA	View
239	Journal of Insect Biodiversity	Ataturk University	2147-7612	NA	View
240	Journal of International Clinical Dental Research Organisation	International Clinical Dental Research Organisation	2231-0754	2231-5357	View
241	Journal of Laboratory Physicians	The Indian Association of Laboratory Physicians	0974-2727	0974-7826	View
242	Journal of Linear and Topological Algebra	Central Tehran Branch, Islamic Azad University	2252-0201	2345-5934	View
243	Journal of Mahatma Gandhi Institute of Medical Sciences	Mahatma Gandhi Institute of Medical sciences	0971-9903	2347-1948	View
244	Journal of Marine Medical Society	Marine Medical Society of India	0975-3605	2589-1235	View
245	Journal of Mathematical Computational Science	SCIK Publishing Corporation	1927-5307	NA	View
246	Journal of Mathematical Extension	Islamic Azad University, Shiraz Branch	1735-8299	2476-7719	View
247	Journal of Mathematical Research and Applications	Dalian University of Technology and China Society for Industrial and Applied Mathematics	2095-2651	NA	View
248	Journal of Microbiology and Infectious Diseases	Department of Microbiology, Fatih University	2146-3158	2146-9369	View
249	Journal of Microscopy and Ultrastructure	Saudi Society of Microscopes	NA	2213-8803	View
250	Journal of Mycology and Plant Pathology	Indian Society of Mycology and Plant Pathology	0971-9393	0975-4180	View
251	Journal of Nanostructure in Chemistry	Springer	2008-9244	2193-8865	View

UGC CARE LIST – SCIENCE (Updated July 2020)

252	Journal of Nonlinear Analysis and Optimization: Theory and Applications	Department of Mathematics, Naresuan University	1906-9685	NA	View
253	Journal of Oilseed Brassica	Society for Rapeseed- Mustard Research	0976-1454	2230-7753	View
254	Journal of Optimization	Hindawi Limited	2356-752X	0231-4648	View
255	Journal of Oral and Maxillofacial Radiology	School of Dentistry	2321-3841	2321-385X	View
256	Journal of Partial Differential Equations	Global Science Press	1000-940X	2079-732X	View
257	Journal of Physics Communications	Institute of Physics Publishing	NA	2399-6528	View
258	Journal of Post- Harvest Technology	Department of Food Science and Postharvest Technology, Bihar Agricultural University	NA	2348-4330	View
259	Journal of Radiation Research and Applied Sciences	Taylor and Francis	NA	1687-8507	Indexed in Scopus and Web of Science
260	Journal of Rajasthan Academy of Physical Sciences	Rajasthan Academy of Physical Sciences	0972-6306	NA	View
261	Journal of Scientific Research	Faculty of Sciences, Rajshahi University	2070-0237	2070-0245	View
262	Journal of Scientific Research	Institute of Science, Banaras Hindu University	0447-9483	NA	View
263	Journal of Scientific Temper	National Institute of Science Communication and Information Resources	2278-2788	2278-2796	View
264	Journal of Self- Assembly and Molecular Electronics	River Publishers	2245-4551	2245-8824	View
265	Journal of Spices and Aromatic Crops	Indian Society for Spices	0971-3328	NA	View

UGC CARE LIST – SCIENCE (Updated July 2020)

266	Journal of Statistical Distributions and Applications	Springer	NA	2195-5832	Indexed in Scopus
267	Journal of Statistical Theory and Applications	Atlantis Press	1538-7887	2214-1766	View
268	Journal of Statistics Applications and Probability	Natural Sciences Publishing	2090-8423	2090-8431	Indexed in Scopus
269	Journal of Stress Physiology and Biochemistry	Siberian Institute of Plant Physiology and Biochemistry	NA	1997-0838	View
270	Journal of Sustainable Metallurgy	Springer	2199-3823	2199-3831	Indexed in Scopus
271	Journal of Sustainable Mining	Elsevier	2300-3960	NA	Indexed in Scopus
272	Journal of Sustainable Water in the Built Environment	American Society of Civil Engineers	NA	2379-6111	Indexed in Scopus
273	Journal of Taibah University for Science	Elsevier	NA	1658-3655	Indexed in Web of Science
274	Journal of the Botanical Society of Bengal (print only)	Botanical Society of Bengal	0971-2976	NA	View
275	Journal of the Chungcheong Mathematical Society	The Chungcheong Mathematical Society	1226-3524	2383-6245	View
276	Journal of the French Statistical Society	Societe Francaise De Statistique	NA	2102-6238	View
277	Journal of the Geographical Institute "Jovan Cvijic" SASA	Geographical Institute “Jovan Cvijić” SASA	0350-7599	1821-2808	Indexed in Scopus
278	Journal of the Indian Association of Sedimentologists	Indian Association of Sedimentologists	0970-3268	2582-2020	View
279	Journal of the Indian Society of Soil Science	Indian Council of Agricultural Research	0974-0228	NA	Indexed in Scopus
280	Journal of the Indian Statistical Association	Indian Statistical Association	0537-2585	NA	View

UGC CARE LIST – SCIENCE (Updated July 2020)

281	Journal of the Indonesian Mathematical Society	Indonesian Mathematical Society	2086-8952	2460-0245	View
282	Journal of the Korean Society of Mathematical Education Series B: The Pure and Applied Mathematics	The Korean Society of Mathematical Education	1226-0657	2287-6081	View
283	Journal of the Maharaja Sayajirao University of Baroda (print only)	Maharaja Sayajirao University of Baroda	0025-0422	NA	View
284	Journal of the Marine Biological Association of India	The Marine Biological Association of India	0025-3146	2321-7898	View
285	Journal of the Numismatic Society of India (print only)	Numismatic Society of India	0029-6066	NA	View
286	Journal of Traditional and Folk Practices	Jawaharlal Nehru Tropical Botanic Garden and Research Institute	2278-5906	NA	View
287	Journal of Tropical Forestry and Environment	Department of Forestry and Environmental Science, University of Sri Jayewardenepura	2235-9370	2235-9362	View
288	Journal of Tropical Life Science	Universitas Brawijava	2087-5517	2527-4376	View
289	Journal of Veterinary and Animal Sciences	Kerala Veterinary and Animal Sciences University	0971-0701	2582-0605	View
290	Journal of Water and Environmental Nanotechnology	Iran Nanotechnology Initiative Council and Iranian Environmental Mutagen Society	2476-7204	2476-6615	View
291	Journal on Systemics, Cybernetics and Informatics	International Institute of Informatics and Cybernetics	1690-4532	1690-4524	Discontinued from July 2020
292	Karbala International Journal of Modern Science	University of Karbala	2405-609X	2405-6103	Indexed in Scopus
293	Kavaka	Mycological Society of India	0379-5179	NA	View

UGC CARE LIST – SCIENCE (Updated July 2020)

294	Khayyam Journal of Mathematics	Tusi Mathematical Research Group and Department of Pure Mathematics, Ferdowsi University of Mashhad	NA	2423-4788	Indexed in Scopus
295	Kobe Journal of Mathematics	Kobe University	0289-9051	NA	View
296	Korean Journal of Mathematics	Kangwon-Kyungki Mathematical Society	1976-8605	2288-1433	View
297	Lignocellulose	Department of Cellulose and Paper Technology, Shahid Beheshti University	2322-1577	2252-0287	Discontinued from Feb. 2020
298	Malaya Journal of Matematik	University Press	2319-3786	2321-5666	View
299	Malaysian Journal of Chemistry	Institute Kimia Malaysia	NA	2550-1658	View
300	Maritime Affairs: Journal of the National Maritime Foundation of India	Taylor and Francis	0973-3159	1946-6609	View
301	Mathematical and Computational Applications	MDPI	1300-686X	2297-8747	Discontinued from Feb. 2020
302	Mathematical Forum	The Registrar, Dibrugarh University	0972-9852	NA	View
303	Mathematical Sciences	Springer	2008-1359	2251-7456	View
304	Mathematical Sciences and Applications E-Notes	Mathematical Sciences and Applications E- Notes	NA	2147-6268	Discontinued from Feb. 2020
305	Mathematics in Engineering, Science and Aerospace	Cambridge Scientific Publishers	2041-3165	0204-1316	Indexed in Scopus
306	Mechanics of Advanced Materials and Modern Processes	Springer	NA	2198-7874	View
307	Medical Journal of Dr. D. Y. Patil Vidyapeeth	Dr D. Y. Patil Vidyapeeth	2589-8302	2589-8310	View

UGC CARE LIST – SCIENCE (Updated July 2020)

308	Medical Sciences	MDPI	NA	2076-3271	Discontinued from Sept. 2019
309	Microbiology Insights	Sage Publications	1178-6361	1178-6361	View
310	Microorganisms	MDPI	NA	2076-2607	Indexed in Web of Science
311	Nano Convergence	Springer	NA	2196-5404	Indexed in Scopus and Web of Science
312	Nanocomposites	Taylor and Francis	2055-0324	2055-0332	Indexed in Scopus
313	Nanomaterials and Energy	ICE Publishing	2045-9831	2045-984X	View
314	Nanosystems: Physics, Chemistry, Mathematics	St. Petersburg National Research University of Information Technologies, Mechanics and Optics	2220-8054	2305-7971	View
315	National Journal of Maxillofacial Surgery	Maxillofacial Society of India	0975-5950	2229-3418	View
316	Natural Products and Bioprospecting	Springer	2192-2195	2192-2209	View
317	Nelumbo (Bulletin of Botanical Survey of India)	Botanical Survey of India	0976-5069	2455-376X	View
318	Neotropical Biodiversity	Taylor and Francis	NA	2376-6808	Indexed in Scopus
319	New Disease Reports	British Society for Plant Pathology	2044-0588	NA	Indexed in Scopus
320	New Zealand Journal of Mathematics	Department of Mathematics, The University of Auckland	NA	1179-4984	View
321	New Zealand Journal of Physiotherapy	Physiotherapy New Zealand	0303-7193	2230-4886	Indexed in Scopus

UGC CARE LIST – SCIENCE (Updated July 2020)

322	Nigerian Journal of Natural Products and Medicine	Nigerian Society of Pharmacognosy	NA	1118-6267	View
323	Notulae Scientia Biologicae	University of Agricultural Sciences and Veterinary Medicine	2067-3205	2067-3264	View
324	Opec Energy Review	John Wiley and Sons, Inc.	NA	1753-0237	View
325	Open Journal of Psychiatry and Allied Sciences	Academy Publisher	2394-2053	2394-2061	View
326	ORYZA- An International Journal on Rice	Association of Rice Research Workers	0474-7615	2249-5266	View
327	Palaeovertebrata	Department of Paleontology, Institut des Sciences de l' Evolution	0031-0247	2274-0333	View
328	Paleobios	University of California	0031-0298	NA	View
329	Personalized Medicine Universe	International Society of Personalized Medicine	2186-4950	NA	View
330	Philosophy, Theory and Practice in Biology	Michigan Publishing	1949-0739	2475-3025	View
331	Physics Education	Indian Association of Physics Teachers	NA	0970-5953	View
332	Proceeding in Applied Mathematics and Machanics	John Wiley and Sons, Inc.	NA	1617-7061	View
333	Proceedings of the Zoological Society	Springer	0373-5893	0974-6919	View
334	Protection and Control of Modern Power Systems	Springer	2367-2617	2367-0983	Indexed in Scopus
335	Punjab University Journal of Mathematics	Department of Mathematics, University of Punjab	1016-2526	NA	View
336	Radiation Protection and Environment	Indian Association for Radiation Protection	0972-0464	2250-0995	View
337	Ratio Mathematica	Academy of Piceno Aprutina Dei Velati	1592-7415	2282-8214	View
338	Record of the Zoological Survey of India	Zoological Survey of India Kolkata	0375-1511	2581-8686	View
339	Reinwardtia	Research Center for Biology- LIPI	0034-365X	2337-8824	View

UGC CARE LIST – SCIENCE (Updated July 2020)

340	Reliability: Theory and Applications	Gnedenko Forum	NA	1932-2321	View
341	Research and Reviews: A journal of Pharmaceutical Science	STM Journals	NA	2229-7006	Discontinued from Sept. 2019
342	Research and Reviews: A Journal of Toxicology	STM Journals	2349-1264	2231-3834	Discontinued from Sept. 2019
343	Research and Reviews: Journal of Agriculture and Allied Sciences	Research and Reviews	2319-9857	2347-226X	View
344	Research Journal of Agricultural Science an International Journal	Centre for Advanced Research in Agricultural Science	0976-1675	2249-4538	View
345	Research Journal of Textile and Apparel	Emerald Publishing Limited	1560-6074	2515-8090	Indexed in Scopus
346	Review of Agrarian Studies	Foundation for Agrarian Studies	2248-9002	NA	View
347	Review of Science, Mathematics and ICT Education	Department of Educational Science and Early Childhood Education, University of Patras	1791-261X	1792-3999	View
348	Rheumatology and Therapy	Springer	2198-6576	2198-6584	View
349	Rivista Italiana di Ornitologia- Research in Ornithology	Page Press	0035-6875	2385-0833	View
350	Romanian Journal of Biology- Zoology	Publishing House of the Romanian Academy	2248-3799	1843-7761	View
351	Romanian Journal of Biophysics	Publishing House of the Romanian Academy	1220-515X	1843-424X	View
352	Rubber Science	Rubber Research Institute of India	2454-4841	2454-485X	View
353	SA Heart Journal	South African Heart Association	1996-6741	2071-4602	View
354	SAARC Journal of Agriculture	SAARC Agriculture Centre	1682-8348	2312-8038	View
355	Samriddhi: A Journal of Physical Sciences, Engineering and Technology	Institute of Technology, School of Management Sciences	2229-7111	2454-5767	View
356	Sao Paulo Journal of Mathematical Sciences	Springer	1982-6907	2316-9028	Indexed in Scopus

UGC CARE LIST – SCIENCE (Updated July 2020)

357	Sarajevo Journal of Mathematics	Department of Natural Sciences and Mathematics, Academy of Sciences and Arts of Bosnia and Herzegovina	1840-0655	2233-1964	View
358	Scandinavian Journal of Forensic Science	Sciendo, De Gruyter	NA	2353-0707	View
359	Science and Technology Journal	Mizoram University	2321-3388	NA	View
360	Scientific Studies and Research, Series Mathematics and Informatics	Vasile Alecsandri University of Bacau	2457-497X	2067-3566	View
361	Sema Journal	Springer	2254-3902	2281-7875	View
362	Serdica Mathematical Journal	Bulgarian Academy of Sciences, Institute of Mathematics and Informatics	1310-6600	NA	View
363	Shape Memory and Superelasticity	Springer	2199-384X	2199-3858	View
364	South East Asian Journal of Mathematics and Mathematical Sciences	Ramanujan Society of Mathematics and Mathematical Sciences	0972-7752	NA	View
365	Southeast Asian Bulletin of Mathematics	Department of Mathematics, Yunnan University	0129-2021	0219-175X	View
366	Sri Lanka Journal of Psychiatry	Sri Lanka College of Psychiatry	2012-6883	2579-2008	View
367	Statistica	Department of Statistical Sciences Paolo Fortunato, University of Bologna	0390-590X	1973-2201	View
368	Statistics and Applications	Society of Statistics, Computer and Applications	NA	2454-7395	View
369	Stochastic Modeling and Applications	MUK Publications and Distributions	0972-3641	NA	View
370	Sustainability, Agri, Food and Environmental Research	Universidad Catolica de Temuco	0719-3726	NA	View
371	TANG [Humanitas Medicine]	Association of Humanitas Medicine	NA	2233-8985	View
372	The Electronic International Journal Advanced Modeling and Optimization	Research Institute for Informatics	NA	1841-4311	View
373	The Holistic Approach to Environment	Association for Promotion of Holistic Approach to Environment	NA	1848-0071	View

UGC CARE LIST – SCIENCE (Updated July 2020)

374	The Horological Journal	British Horological Institute	0018-5108	NA	View
375	The Indian Fern Journal	Indian Fern Society	0970-2741	NA	Discontinued from Sept. 2019
376	The Indian Forester	Indian Forester	0019-4816	NA	View
377	The Journal of Analysis	Springer	NA	2367-2501	View
378	The Journal of Community Informatics	The Journal of Community Informatics	1712-4441	NA	View
379	The Journal of Cytology and Genetics	Society of Cytologists and Geneticists	0253-7605	NA	View
380	The Journal of Indian Geophysical Union	Indian Geophysical Union	0971-9707	0257-7968	Discontinued from Sept. 2019
381	The Journal of Plant Science Research	Prints Publication Pvt. Ltd.	0970-2539	0976-3880	View
382	The Journal of Research Angrau	Acharya N. G. Ranga Agricultural University	0970-0226	NA	View
383	The Mathematical Gazette	Cambridge University Press	0025-5572	2056-6328	View
384	The Mathematics Educator	Association of Mathematics Educators	0218-9100	NA	View
385	The Mathematics Student	Indian Mathematical Society	0025-5742	NA	View
386	The Nucleus	Pakistan Institute of Nuclear Science and Technology	0029-5698	2306-6539	View
387	The Ring	Sciendo, De Gruyter	NA	2083-3520	View
388	Thematics Journal of Geography	Thematic Publication	2277-2995	NA	Discontinued from Jan. 2020
389	Topological Algebra and its Applications	Walter de Gruyter	NA	2299-3231	View
390	Transactions on Combinatorics	University of Isfahan	2251-8657	2251-8665	Indexed in Scopus
391	Tropical Plant Research	Society for Tropical Plant Research	2349-9265	2349-1183	Discontinued from Jan. 2020
392	Tuberculosis Research and Treatment	Hindawi Limited	2090-150X	2090-1518	View

UGC CARE LIST – SCIENCE (Updated July 2020)

393	TWMS Journal of Pure and Applied Mathematics	Turkic World Mathematical Society	2076-2585	2219-1259	View
394	Uttar Pradesh Journal of Zoology	Uttar Pradesh Zoological Society	0256-971X	NA	View
395	Vietnam Journal of Computer Science	World Scientific Publishing	2196-8888	2196-8896	View
396	Water History	Springer	1877-7236	1877-7244	View
397	Water Science	Taylor and Francis	NA	1110-4929	View
398	Women's Reproductive Health	Taylor and Francis	2329-3691	2329-3713	View
399	World Journal of Meta Analysis	Baishideng Publishing Group Inc.	NA	2308-3840	View
400	World Journal of Science, Technology and Sustainable Development	Emerald Publishing Limited	2042-5953	2042-5945	View

Accepted Manuscript

Journal of Algebra and its Applications

Article Title:	On the prime spectrum of an le-module
Author(s):	M. Kumbhakar, A. K. Bhuniya
DOI:	10.1142/S0219498821502200
Received:	14 April 2019
Accepted:	05 July 2020
To be cited as:	M. Kumbhakar, A. K. Bhuniya, On the prime spectrum of an le-module, *Journal of Algebra and its Applications*, doi: 10.1142/S0219498821502200
Link to final version:	https://doi.org/10.1142/S0219498821502200

On the prime spectrum of an le-module

M. Kumbhakar and A. K. Bhuniya

Department of Mathematics, Nistarini College, Purulia-723101, India.
Department of Mathematics, Visva-Bharati, Santiniketan-731235, India.
manaskumbhakar@gmail.com, anjankbhuniya@gmail.com

Abstract

Here we continue to characterize a recently introduced notion, le-modules ${}_RM$ over a commutative ring R with unity [7]. This article introduces and characterizes Zariski topology on the set $Spec(M)$ of all prime submodule elements of M. Thus we extend many results on Zariski topology for modules over a ring to le-modules. The topological space $Spec(M)$ is connected if and only if $R/Ann(M)$ contains no idempotents other than $\overline{0}$ and $\overline{1}$. Open sets in the Zariski topology for the quotient ring $R/Ann(M)$ induces a base of quasi-compact open sets for the Zariski-topology on $Spec(M)$. Every irreducible closed subset of $Spec(M)$ has a generic point. Besides, we prove a number of different equivalent characterizations for $Spec(M)$ to be spectral.

Keywords: Rings; complete lattice; le-modules; prime spectrum; Zariski topology.
AMS Subject Classifications: 54B35, 13C05, 13C99, 06F25.

1 Introduction

W. Krull [20] recognized that many properties on ideals in a commutative ring are independent on the fact that they are composed of elements. Hence those properties can be restated considering ideals to be an undivided entity or element of a suitable algebraic system. In the abstract ideal theory, the ideals are considered to be elements of a multiplicative lattice, a lattice with a commutative multiplication and satisfies some axioms. Ward and Dilworth [10], [11], [31], [32], [33], [34], [35], contributed many significant results in abstract ideal theory via the residuation operation on a multiplicative lattice. In [11] Dilworth redefined principal elements and obtained the Noether primary

decomposition theorems. The multiplicative theory of ideals were continued towards dimension theory, representations problem and many other overlaping areas by D. D. Anderson, E. W. Johnson, J. A. Johnson, J. P. Ladiaev, K. P. Bogart, C. Jayaram and many others. For the proper references of these articles we refer to [3]. Also we refer to [22] for more discussions on abstract ideal theory.

Success achieved in abstract ideal theory naturally motivated researchers to consider abstract submodule theory, which today is known as the theory of lattice modules. E. W. Johnson and J. A. Johnson [15], [18], introduced and studied Noetherian lattice modules. They also considered lattice modules over semilocal Noetherian lattice. Whitman [36] introduced principal elements in a lattice module and extended Nagata's principle of idealization to lattice modules. Nakkar and Anderson [29] studied localization in lattice modules. There are many articles devoted to lattice modules, to mention a few [16], [17], [19], [28], [36].

This article is a continuation of our present project on le-modules, an algebraic structure motivated by lattice modules over a multiplicative lattice. Our goal is to develop an "abstract submodule theory" which will be capable to give insight about rings more directly. The system we choose is a complete lattice M with a commutative and associative addition which is completely join distributive and admits a module like left action of a commutative ring R with 1. Since we are taking left action of a ring R not of the complete modular lattice of all ideals of R, we hope that influence of arithmetic of R on M will be easier to understand. For further details and motivation for introducing le-modules we refer to [7, 21].

In this article we introduce and study Zariski topology on the set $Spec(M)$ of all prime submodule elements of an le-module ${}_RM$. It is well established that the Zariski topology on prime spectrum is a very efficient tool to give geometric interpretation of the arithmetic in rings [2], [14], [26], [30], [37] and modules [1], [5], [6], [12], [13], [23], [24], [25], [27]. Here we have extended several results on Zariski topology in modules to le-modules.

In addition to this introduction, this article comprises six sections. In Section 2, we recall definition of le-modules and various associated concepts from [7]. Also we discuss briefly on the Zariski topology in rings and modules. Section 3, introduces Zariski topology $\tau^*(M)$ on the set $Spec(M)$ of all prime submodule elements of an le-module ${}_RM$, and proves the equivalence of a different characterization of $\tau^*(M)$ by the ideals of the ring R. Annihilator $Ann(M)$ of an le-module ${}_RM$ is defined so that it is an ideal of R. This induces a natural connection between $Spec(M)$ and $Spec(R/Ann(M))$. Section 4 establishes some basic properties of this natural connection. As a consequence, we deduce that $Spec(M)$ is connected if and only if $\overline{0}$ and $\overline{1}$ are the only idempotents

of the ring $R/Ann(M)$. Section 5 finds a base for the Zariski topology on $Spec(M)$ consisting of quasi-compact open sets. Section 6 characterizes irreducible closed subsets and generic points in $Spec(M)$ showing that these two notions are closely related. Section 7 proves the equivalence of a number of different characterizations for $Spec(M)$ to be spectral.

2 Preliminaries

Throughout the article, R stands for a commutative ring with 1. The cardinality of a set X will be denoted by $|X|$.

First we recall the definition of an le-module and various associated concepts from [7]. Here by an *le-semigroup* we mean $(M, +, \leqslant, e)$ such that $(M, \leq)$ is a complete lattice, $(M, +)$ is a commutative monoid with the zero element 0_M and for all $m, m_i \in M, i \in I$ it satisfies $m \leq e$ and

(S) $m + (\vee_{i\in I} m_i) = \vee_{i\in I}(m + m_i)$.

Let R be a ring and $(M, +, \leqslant, e)$ be an le-semigroup. If there is a mapping $R \times M \longrightarrow M$ which satisfies

(M1) $r(m_1 + m_2) = rm_1 + rm_2$;

(M2) $(r_1 + r_2)m \leqslant r_1m + r_2m$;

(M3) $(r_1r_2)m = r_1(r_2m)$;

(M4) $1_Rm = m; \quad 0_Rm = r0_M = 0_M$;

(M5) $r(\vee_{i\in I} m_i) = \vee_{i\in I} rm_i$,

for all $r, r_1, r_2 \in R$ and $m, m_1, m_2, m_i \in M, i \in I$ then M is called an *le-module* over R. It is denoted by ${}_RM$ or by M if it is not necessary to mention the ring R.

From (M5), we have,

(M5)′ $m_1 \leqslant m_2 \Rightarrow rm_1 \leqslant rm_2$, for all $r \in R$ and $m_1, m_2 \in M$.

An element n of an le-module ${}_RM$ is said to be a *submodule element* if $n+n, rn \leqslant n$, for all $r \in R$. We denote the set of all submodule elements of M by $S(M)$. We call $n \in S(M)$ proper if $n \neq e$. Note that $0_M = 0_Rn \leqslant n$, for every $n \in S(M)$. Also for each $n \in S(M)$, $n+n \leqslant n = n+0_M \leqslant n+n$ shows that $n + n = n$, i.e., every submodule element of M is an idempotent. We define the sum of the family $\{n_i\}_{i\in I}$ of submodule elements in ${}_RM$ by:

$$\sum_{i\in I} n_i = \vee\{(n_{i_1} + n_{i_2} + \cdots + n_{i_k}) : k \in \mathbb{N}, and\ \ i_1, i_2, \cdots, i_k \in I\}.$$

Since ${}_RM$ is assumed to be complete, $\sum_{i\in I} n_i$ is well defined. It is easy to check that $\sum_{i\in I} n_i$ is a submodule element of M.

If n is a submodule element in ${}_RM$, then we denote

$$(n : e) = \{r \in R : re \leqslant n\}.$$

Then $0_R \in (n : e)$ implies that $(n : e) \neq \emptyset$. One can check that $(n : e)$ is an ideal of R. For submodule elements $n \leqslant l$ of an le-module ${}_RM$, we have $(n : e) \subseteq (l : e)$. Also if $\{n_i\}_{i\in I}$ be an arbitrary family of submodule elements in ${}_RM$, then $(\wedge_{i\in I} n_i : e) = \cap_{i\in I}(n_i : e)$.

We call $(0_M : e)$ the annihilator of ${}_RM$. It is denoted by $Ann(M)$. Thus

$$\begin{aligned} Ann(M) &= \{r \in R : re \leqslant 0_M\} \\ &= \{r \in R : re = 0_M\}. \end{aligned}$$

For an ideal I of R, we define

$$Ie = \vee\{\textstyle\sum_{i=1}^{k} a_i e : k \in \mathbb{N}; a_1, a_2, \cdots, a_k \in I\}$$

Then Ie is a submodule element of M. Also for any two ideals I and J of R, $I \subseteq J$ implies that $Ie \leqslant Je$. The following result, proved in [7], is useful here.

Lemma 2.1. *Let ${}_RM$ be an le-module and $n \in S(M)$. Then for any ideal I of R, $Ie \leqslant n$ if and only if $I \subseteq (n : e)$.*

Now we recall some notions from rings and modules. An ideal P in a ring R is called *prime* if for every $a, b \in R$, $ab \in P$ implies that $a \in P$ or $b \in P$. We denote the set of all prime ideals of a ring R by X^R or $Spec(R)$. For every ideal I of R, we define

$$\begin{aligned} &V^R(I) = \{P \in Spec(R) : I \subseteq P\},\ \ and \\ &\tau(R) = \{X^R \setminus V^R(I) : I\ is\ an\ ideal\ of\ R\}. \end{aligned}$$

Then $\tau(R)$ is a topology on $Spec(R)$, which is known as the *Zariski topology* on $Spec(R)$. There are many enlightening characterizations associating arithmetical properties of R and topological properties of $Spec(R)$ [30].

Let M be a left R-module. Then a proper submodule P of M is called a *prime submodule* if for every for $r \in R$ and $n \in M$, $rn \in P$ implies that either $n \in P$ or $rM \subseteq P$. We denote the set of all prime submodules of M by $Spec(M)$.

For a submodule N of M, $(N : M) = \{r \in R : rM \subseteq N\}$ is an ideal of R. There is a topology $\tau(M)$ on $Spec(M)$ such that the closed subsets are of the form

$$V(N) = \{P \in Spec(M) : (N : M) \subseteq (P : M)\}.$$

The topology $\tau(M)$ is called the Zariski topology on M. Associating arithmetic of a module over a ring R with the geometry of the Zariski topology on M is an active area of research on modules [1], [6], [12], [13], [23], [24], [25], [27].

The notion of prime submodule elements was introduced in [7], which extends prime submodules of a module over a ring. A proper submodule element p of an le-module ${}_RM$ is said to be a *prime submodule element* if for every $r \in R$ and $n \in M$, $rn \leqslant p$ implies that $r \in (p : e)$ or $n \leqslant p$. The *prime spectrum* of M is the set of all prime submodule elements of M and it is denoted by $Spec(M)$ or X^M. For $P \in Spec(R)$, we denote

$$Spec_P(M) = \{p \in Spec(M) : (p : e) = P\}.$$

We also have the following relation between prime submodule elements of an le-module ${}_RM$ and prime ideals of R.

Lemma 2.2. *[7] If p is a prime submodule element of ${}_RM$, then $(p : e)$ is a prime ideal of R.*

Also we refer to [4], [8] for background on commutative ring theory, to [9] for fundamentals on topology and to [22] for details on multiplicative theory of ideals.

3 The Zariski topology on an le-module

In this section we give the definition and an alternative characterization of Zariski topology on the prime spectrum $Spec(M)$ of an le-module M. For any submodule element n of M, we consider two different types of varieties $V(n)$ and $V^*(n)$ defined by

$$V(n) = \{p \in Spec(M) : n \leqslant p\}; \ \ and$$
$$V^*(n) = \{p \in Spec(M) : (n : e) \subseteq (p : e)\}.$$

Then $V(n) \subseteq V^*(n)$ for every submodule element n of M.

Proposition 3.1. *Let ${}_RM$ be an le-module. Then*

(i) $V^*(0_M) = X^M = V(0_M)$;

(ii) $V^*(e) = \emptyset = V(e)$;

(iii) *For an arbitrary family of submodule elements* $\{n_i\}_{i\in I}$ *of* M,
(a) $\cap_{i\in I} V^*(n_i) = V^*(\sum_{i\in I}(n_i : e)e)$;
(b) $\cap_{i\in I} V(n_i) = V(\sum_{i\in I} n_i)$;

(iv) *For any two submodule elements* n *and* l *of* M,
(a) $V^*(n) \cup V^*(l) = V^*(n \wedge l)$;
(b) $V(n) \cup V(l) \subseteq V(n \wedge l)$.

Proof. (i) and (ii) are obvious. Also the proofs of $(iii)(b)$ and $(iv)(b)$ are similar to $(iii)(a)$ and $(iv)(a)$ respectively. Hence we prove here only $(iii)(a)$ and $(iv)(a)$.
$(iii)(a)$ Let $p \in \cap_{i\in I} V^*(n_i)$. Then $(n_i : e) \subseteq (p : e)$ implies that $(n_i : e)e \leqslant (p : e)e \leqslant p$, for all $i \in I$. Consequently $\sum_{i\in I}(n_i : e)e \leqslant p$ and so $(\sum_{i\in I}(n_i : e)e : e) \subseteq (p : e)$. Hence $p \in V^*(\sum_{i\in I}(n_i : e)e)$ and it follows that $\cap_{i\in I} V^*(n_i) \subseteq V^*(\sum_{i\in I}(n_i : e)e)$. Next let $p \in V^*(\sum_{i\in I}(n_i : e)e)$. Then for any $j \in I$, $(n_j : e) \subseteq ((n_j : e)e : e) \subseteq (\sum_{i\in I}(n_i : e)e : e) \subseteq (p : e)$ implies that $p \in V^*(n_j)$ and so $V^*(\sum_{i\in I}(n_i : e)e) \subseteq \cap_{i\in I} V^*(n_i)$. Thus $\cap_{i\in I} V^*(n_i) = V^*(\sum_{i\in I}(n_i : e)e)$.
$(iv)(a)$ Now $n \wedge l \leqslant n$ and $n \wedge l \leqslant l$ implies that $V^*(n) \cup V^*(l) \subseteq V^*(n \wedge l)$. Let $p \in V^*(n \wedge l)$. Then $(n \wedge l : e) \subseteq (p : e)$ implies that $(n : e) \cap (l : e) \subseteq (p : e)$. Since $(p : e)$ is a prime ideal, either $(n : e) \subseteq (p : e)$ or $(l : e) \subseteq (p : e)$. Hence $p \in V^*(n) \cup V^*(l)$ and it follows that $V^*(n \wedge l) \subseteq V^*(n) \cup V^*(l)$. Therefore $V^*(n) \cup V^*(l) = V^*(n \wedge l)$. □

Thus we see that the collection $\{V(n) \mid n$ is a submodule element of $M\}$ is not closed under finite unions and hence fails to be the set of all closed subsets of any topology on X^M. For any ideal I, Ie is a submodule element of M. Now we see that the subcollection $\{V(Ie) \mid I$ is an ideal of $R\}$ is closed under finite unions.

Lemma 3.2. *Let* ${}_RM$ *be an le-module. Then for any ideals* I *and* J *in* R,
(i) $V(Ie) \cup V(Je) = V((I \cap J)e) = V((IJ)e)$;
(ii) $V^*(Ie) \cup V^*(Je) = V^*((I \cap J)e) = V^*((IJ)e)$. *In particular,* $V^*(re) \cup V^*(se) = V^*((rs)e)$ *for any* $r, s \in R$.

Proof. (i) First $I \cap J \subseteq I$ implies that $(I \cap J)e \leqslant Ie$ and so $V(Ie) \subseteq V((I \cap J)e)$. Similarly $V(Je) \subseteq V((I \cap J)e)$, and we have $V(Ie) \cup V(Je) \subseteq V((I \cap J)e)$. Also $IJ \subseteq I \cap J$ implies that $V((I \cap J)e) \subseteq V((IJ)e)$. Now let $p \in V((IJ)e)$. Then $(IJ)e \leqslant p$ implies that $IJ \subseteq (p : e)$. Since

$(p : e)$ is a prime ideal, either $I \subseteq (p : e)$ or $J \subseteq (p : e)$. Then either $Ie \leqslant (p : e)e \leqslant p$ or $Je \leqslant (p : e)e \leqslant p$. Hence $p \in V(Ie) \cup V(Je)$ and it follows that $V((IJ)e) \subseteq V(Ie) \cup V(Je)$. Thus $V(Ie) \cup V(Je) \subseteq V((I \cap J)e) \subseteq V((IJ)e) \subseteq V(Ie) \cup V(Je)$. This completes the proof.
(ii) Similar. □

We denote,

$$\mathcal{V}(M) = \{V(n) : n \in S(M)\},$$
$$\mathcal{V}^*(M) = \{V^*(n) : n \in S(M)\},$$
$$\mathcal{V}'(M) = \{V(Ie) : I \text{ is an ideal of } R\}.$$

From Proposition 3.1, it follows that there exists a topology, $\tau(M)$ say, on $Spec(M)$ having $\mathcal{V}(M)$ as the collection of all closed sets if and only if $\mathcal{V}(M)$ is closed under finite unions. In this case, we call the topology $\tau(M)$ the *quasi-Zariski topology* on $Spec(M)$. Also from Proposition 3.1, it is evident that for any le-module ${}_RM$ there always exists a topology, $\tau^*(M)$ say, on $Spec(M)$ having $\mathcal{V}^*(M)$ as the family of all closed sets. This topology $\tau^*(M)$ is called the *Zariski topology* on $Spec(M)$. In this article we focus on the basic properties of the Zariski topology $\tau^*(M)$. By Lemma 3.2, it follows that $\mathcal{V}'(M)$ induces a topology, $\tau'(M)$ say, on $Spec(M)$ for every le-module ${}_RM$.

Now we study the interrelations among these three topologies $\tau(M)$, $\tau^*(M)$ and $\tau'(M)$.

Proposition 3.3. *Let ${}_RM$ be an le-module and $n, l \in S(M)$. If $(n : e) = (l : e)$ then $V^*(n) = V^*(l)$. The converse is also true if both n and l are prime.*

Proof. It follows from the definition of $V^*(n)$ that if $(n : e) = (l : e)$ then $V^*(n) = V^*(l)$.

Conversely suppose that $V^*(n) = V^*(l)$ and both n and l are prime. Since n is prime, $n \in V^*(n) = V^*(l)$ and so $(l : e) \subseteq (n : e)$. Similarly $(n : e) \subseteq (l : e)$ and hence $(n : e) = (l : e)$. □

Proposition 3.4. *Let ${}_RM$ be an le-module, n be a submodule element of M and I be an ideal of R. Then*
(i) $V^*(n) = \cup_{P \in V^R((n:e))} Spec_P(M)$;
(ii) $V^*(n) = V^*((n : e)e) = V((n : e)e)$;
(iii) $V(Ie) = V^*(Ie)$. *In particular* $V(re) = V^*(re)$ *for every* $r \in R$.

Proof. (i) Let $p \in V^*(n)$. Then $(n : e) \subseteq (p : e)$ and so $p \in \cup_{P \in V^R((n:e))} Spec_P(M)$, since $(p : e)$ itself a prime ideal. Thus $V^*(n) \subseteq \cup_{P \in V^R((n:e))} Spec_P(M)$. Also let $p \in \cup_{P \in V^R((n:e))} Spec_P(M)$. Then there

exists a prime ideal $P_0 \in V^R((n:e))$ such that $p \in Spec_{P_0}(M)$. This implies that $(n:e) \subseteq P_0 = (p:e)$, i.e., $p \in V^*(n)$. Hence $\cup_{P \in V^R((n:e))} Spec_P(M) \subseteq V^*(n)$. Therefore $V^*(n) = \cup_{P \in V^R((n:e))} Spec_P(M)$.
(ii) Since $(n:e)e \leqslant n$, $V^*(n) \subseteq V^*((n:e)e)$. Let $p \in V^*((n:e)e)$. Then $((n:e)e:e) \subseteq (p:e)$. Now $(n:e) \subseteq ((n:e)e:e)$ implies that $(n:e) \subseteq (p:e)$ and so $p \in V^*(n)$. Thus $V^*((n:e)e) \subseteq V^*(n)$ and hence $V^*(n) = V^*((n:e)e)$. Let $p \in V^*(n)$. Then $(n:e) \subseteq (p:e)$ which implies that $(n:e)e \leqslant (p:e)e \leqslant p$, i.e., $p \in V((n:e)e)$. Thus $V^*(n) \subseteq V((n:e)e)$. Also let $p \in V((n:e)e)$. Then $(n:e)e \leqslant p$ implies $((n:e)e:e) \subseteq (p:e)$. Thus $p \in V^*((n:e)e) = V^*(n)$ and hence $V((n:e)e) \subseteq V^*(n)$. Therefore $V^*(n) = V((n:e)e) = V^*((n:e)e)$.
(iii) The proof is omitted since it is easy to prove. □

Theorem 3.5. *For any le-module ${}_RM$, the Zariski topology $\tau^*(M)$ on $Spec(M)$ is identical with $\tau'(M)$.*

Proof. It is suffices to prove that $\mathcal{V}^*(M) = \mathcal{V}'(M)$. Let $V^*(n)$ be a closed set in $\mathcal{V}^*(M)$ for some $n \in S(M)$. Then by Proposition 3.4(ii), $V^*(n) = V((n:e)e) = V(Ie)$, where $(n:e) = I$, an ideal of R. Thus every closed set in $\mathcal{V}^*(M)$ is a closed set in $\mathcal{V}'(M)$ and hence $\mathcal{V}^*(M) \subseteq \mathcal{V}'(M)$. Now let $V(Ie)$ be a closed set in $\mathcal{V}'(M)$ for some ideal I of R. Again by Proposition 3.4(iii), $V(Ie) = V^*(Ie)$. Since Ie is a submodule element of M, $V(Ie)$ is a closed set in $\mathcal{V}^*(M)$. Thus $\mathcal{V}'(M) \subseteq \mathcal{V}^*(M)$. Therefore $\mathcal{V}^*(M) = \mathcal{V}'(M)$. □

An le-module M is called a *top le-module* if $\mathcal{V}(M)$ is closed under finite unions. Hence if M is a top le-module, then $\tau(M) = \{X^M \setminus V(n) \mid n \in S(M)\}$ becomes a topology on X^M.

Clearly $\mathcal{V}'(M) \subseteq \mathcal{V}(M)$. Then by Theorem 3.5, $\mathcal{V}^*(M) = \mathcal{V}'(M) \subseteq \mathcal{V}(M)$ and hence the quasi-Zariski topology $\tau(M)$ on $Spec(M)$ is finer than the Zariski topology $\tau^*(M)$.

4 Relation between Spec(M) and Spec(R/Ann(M))

Let ${}_RM$ be an le-module. Then $Ann(M)$ is an ideal of R, which allows us to consider the quotient ring $\overline{R} = R/Ann(M)$. The image of every element $r \in R$ and every ideal I of R such that $Ann(M) \subseteq I$ under the canonical epimorphism $\phi : R \to R/Ann(M)$ will be denoted by $\overline{r}$ and $\overline{I}$, respectively. Then for every prime ideal P of R and $Ann(M) \subseteq P$, the ideal $\overline{P}$ is prime in $\overline{R}$. Hence the mapping $\psi : X^M \to X^{\overline{R}}$ defined by

$$\psi(p) = \overline{(p:e)} \text{ for every } p \in X^M$$

is well defined. We call ψ the *natural map* on X^M.

In this section we study relationship of X^M and $X^{\overline{R}}$ under the natural map. Here we are interested in conditions under which ψ is injective, surjective, open, closed, and homeomorphic.

Proposition 4.1. *For any le-module ${}_RM$, the natural map ψ of X^M is continuous for the Zariski topologies; more precisely , $\psi^{-1}(V^{\overline{R}}(\overline{I})) = V(Ie)$ for every ideal I of R containing $Ann(M)$.*

Proof. Let I be an ideal of R containing $\mathrm{Ann}(M)$ and let $p \in \psi^{-1}(V^{\overline{R}}(\overline{I})$. Then there exists some $\overline{J} \in V^{\overline{R}}(\overline{I})$ such that $\psi(p) = \overline{J}$, i.e., $(p : e)/Ann(M) = J/Ann(M)$. This implies that $(p : e) = J \supseteq I$ and so $Ie \leqslant (p : e)e \leqslant p$. Hence $p \in V(Ie)$. Therefore $\psi^{-1}(V^{\overline{R}}(\overline{I})) \subseteq V(Ie)$. Now let $q \in V(Ie)$. Then $I \subseteq (Ie : e) \subseteq (q : e)$ implies that $\overline{I} = I/Ann(M) \subseteq (q : e)/Ann(M) = \overline{(q : e)}$. Hence $q \in \psi^{-1}(V^{\overline{R}}(\overline{I}))$. Thus $V(Ie) \subseteq \psi^{-1}(V^{\overline{R}}(\overline{I}))$. Therefore $\psi^{-1}(V^{\overline{R}}(\overline{I})) = V(Ie)$. □

Proposition 4.2. *The following conditions are equivalent for any le-module ${}_RM$:*
(i) The natural map $\psi : X^M \to X^{\overline{R}}$ is injective;
(ii) For every $p, q \in X^M$, $V^*(p) = V^*(q)$ implies that $p = q$;
(iii) $|Spec_P(M)| \leqslant 1$ for every $P \in Spec(R)$.

Proof. $(i) \Rightarrow (ii)$: Let $V^*(p) = V^*(q)$. Then $(p : e) = (q : e)$ which implies that $(p : e)/Ann(M) = (q : e)/Ann(M)$. Thus $\psi(p) = \psi(q)$ and hence $p = q$, since ψ is injective.
$(ii) \Rightarrow (iii)$: Let $p, q \in Spec_P(M)$, where $P \in Spec(R)$. Then $(p : e) = P = (q : e)$ which implies that $V^*(p) = V^*(q)$. Hence $p = q$, by (ii).
$(iii) \Rightarrow (i)$: Let $p, q \in X^M$ be such that $\psi(p) = \psi(q)$. Then $(p : e)/Ann(M) = (q : e)/Ann(M)$. This implies that $(p : e) = (q : e) = P$, say. Thus $p, q \in Spec_P(M)$ and so $p = q$, by (iii). Therefore ψ is injective. □

Theorem 4.3. *Let ${}_RM$ be an le-module and $\psi : X^M \to X^{\overline{R}}$ be the natural map of X^M. If ψ is surjective, then ψ is both closed and open. More precisely, for every $n \in S(M)$, $\psi(V^*(n)) = V^{\overline{R}}(\overline{n : e})$ and $\psi(X^M - V^*(n)) = X^{\overline{R}} - V^{\overline{R}}(\overline{n : e})$.*

Proof. By the Proposition 4.1, we have ψ is a continuous map and $\psi^{-1}(V^{\overline{R}}(\overline{I})) = V(Ie)$, for every ideal I of R containing $Ann(M)$. Thus for every $n \in S(M)$, $\psi^{-1}(V^{\overline{R}}(\overline{n : e})) = V((n : e)e) = V^*(n)$. This implies that $\psi(V^*(n)) = \psi o \psi^{-1}(V^{\overline{R}}(\overline{n : e})) = V^{\overline{R}}(\overline{n : e})$, since ψ is surjective. Similarly $\psi(X^M - V^*(n)) = \psi(\psi^{-1}(X^{\overline{R}}) - \psi^{-1}(V^{\overline{R}}(\overline{n : e}))) = \psi(\psi^{-1}(X^{\overline{R}} - V^{\overline{R}}(\overline{n : e}))) = \psi o \psi^{-1}(X^{\overline{R}} - V^{\overline{R}}(\overline{n : e})) = X^{\overline{R}} - V^{\overline{R}}(\overline{n : e})$. Thus ψ is both closed and open. □

Corollary 4.4. *Let ${}_RM$ be an le-module and $\psi : X^M \to X^{\overline{R}}$ be the natural map of X^M. Then ψ is bijective if and only if ψ is homeomorphic.*

A commutative ring R with 1 is said to be a *quasi-local ring* if it has a unique maximal ideal.

Theorem 4.5. *Let ${}_RM$ be an le-module and $\psi : X^M \to X^{\overline{R}}$ be the surjective natural map of X^M. Then the following statements are equivalent:*
(i) $X^M = Spec(M)$ is connected;
(ii) $X^{\overline{R}} = Spec(\overline{R})$ is connected;
(iii) The ring $\overline{R}$ contains no idempotent other than $\overline{0}$ and $\overline{1}$.
Consequently, if either R is a quasi-local ring or $Ann(M)$ is a prime ideal of R, then both X^M and $X^{\overline{R}}$ are connected.

Proof. $(i) \Rightarrow (ii)$: From Proposition 4.1, we have that ψ is a continuous map. Then (ii) follows from the fact that ψ is surjective and continuous image of a connected space is connected.
$(ii) \Rightarrow (i)$: Let $X^{\overline{R}}$ be connected. If possible assume that X^M is disconnected. Then X^M must contain a non-empty proper subset Y which is both open and closed. By Theorem 4.3, $\psi(Y)$ is a non-empty subset of $X^{\overline{R}}$ that is both open and closed. We assert that $\psi(Y)$ is a proper subset of $X^{\overline{R}}$. Since Y is open, $Y = X^M - V^*(n)$ for some submodule element n of M. Then by Theorem 4.3, $\psi(Y) = \psi(X^M - V^*(n)) = X^{\overline{R}} - V^{\overline{R}}(\overline{n : e})$. Therefore, if $\psi(Y) = X^{\overline{R}}$, then $V^{\overline{R}}(\overline{n : e}) = \emptyset$. Now suppose that $\overline{(n : e)} \neq \overline{R}$. Then $\overline{(n : e)}$ is a proper ideal of $\overline{R}$ and so contained in a maximal ideal, say $\overline{P}$ of $\overline{R}$, which is also a prime ideal of $\overline{R}$. Thus $\overline{(n : e)} \subseteq \overline{P}$ and hence $\overline{P} \in V^{\overline{R}}(\overline{n : e})$, i.e., $V^{\overline{R}}(\overline{n : e}) \neq \emptyset$, a contradiction. Thus $\overline{(n : e)} = \overline{R}$, i.e., $n = e$. This implies that $Y = X^M - V^*(n) = X^M - V^*(e) = X^M$, which is an absurd since Y is a proper subset of X^M. Thus $\psi(Y)$ is a proper subset of $X^{\overline{R}}$ and hence $X^{\overline{R}}$ is disconnected, a contradiction. Therefore $X^M = Spec(M)$ is connected.

The equivalence of (ii) and (iii) is well-known [8]. □

5 A base for the Zariski topology on Spec(M)

For any element r of a ring R, the set $D_r = X^R - V^R(rR)$ is open in X^R and the family $\{D_r : r \in R\}$ forms a base for the Zariski topology on X^R. Each D_r, in particular $D_1 = X^R$ is known to be quasi-compact. In [23], Chin-Pi Lu introduced a base for the Zariski topology on $Spec(M)$ for any R-module M, which is similar to that on X^R. In this section, we introduce a base for the Zariski topology on X^M for any le-module ${}_RM$.

For each $r \in R$ we define,

$$X_r = X^M - V^*(re).$$

Then every X_r is an open set in X^M. Note that $X_0 = \emptyset$ and $X_1 = X^M$.

Proposition 5.1. *Let ${}_RM$ be an le-module with the natural map $\psi : X^M \to X^{\overline{R}}$ and $r \in R$. Then*
(i) $\psi^{-1}(D_{\overline{r}}) = X_r$; and
(ii) $\psi(X_r) \subseteq D_{\overline{r}}$; the equality holds if ψ is surjective.

Proof. (i) $\psi^{-1}(D_{\overline{r}}) = \psi^{-1}(X^{\overline{R}} - V^{\overline{R}}(\overline{r}\overline{R})) = \psi^{-1}(X^{\overline{R}}) - \psi^{-1}(V^{\overline{R}}(\overline{r}\overline{R})) = \psi^{-1}(V^{\overline{R}}(\overline{0})) - \psi^{-1}(V^{\overline{R}}(\overline{rR})) = V(0_M) - V(rRe) = X^M - V(re) = X^M - V^*(re) = X_r$, by Proposition 4.1 and Proposition 3.4(iii).
(ii) It follows from (i). □

Now we have a useful lemma which will be used in the next theorem:

Lemma 5.2. *Let ${}_RM$ be an le-module.*
(i) For every $r, s \in R$, $X_{rs} = X_r \cap X_s$.
(ii) For any ideal I in R, $V^*(Ie) = \cap_{a\in I} V^*(ae)$.

Proof. (i) $X_{rs} = X^M - V^*((rs)e) = X^M - (V^*(re) \cup V^*(se)) = (X^M - V^*(re)) \cap (X^M - V^*(se)) = X_r \cap X_s$, by Lemma 3.2$(ii)$.
(ii) Let $p \in V^*(Ie)$. Then $(Ie : e) \subseteq (p : e)$. Now for all $a \in I$, $ae \leqslant Ie$ implies that $(ae : e) \subseteq (Ie : e) \subseteq (p : e)$. Thus $p \in V^*(ae)$ for all $a \in I$ and so $p \in \cap_{a\in I} V^*(ae)$. Hence $V^*(Ie) \subseteq \cap_{a\in I} V^*(ae)$. Also let $p \in \cap_{a\in I} V^*(ae)$. Then for all $a \in I$, $p \in V^*(ae) = V(ae)$, by Proposition 3.4, which implies that $ae \leqslant p$. Thus for any $k \in \mathbb{N}$ and $a_1, a_2, \cdots, a_k \in I$, $a_1e + a_2e + \cdots + a_ke \leqslant p$ and hence $Ie \leqslant p$. Then $(Ie : e) \subseteq (p : e)$ and so $p \in V^*(Ie)$. Hence $\cap_{a\in I} V^*(ae) \subseteq V^*(Ie)$. Therefore $V^*(Ie) = \cap_{a\in I} V^*(ae)$. □

Theorem 5.3. *Let ${}_RM$ be an le-module. Then the set $B = \{X_r : r \in R\}$ forms a base for the Zariski topology on X^M which may be empty.*

Proof. If $X^M = \emptyset$, then $B = \emptyset$ and theorem is trivially true in this case. Let $X^M \neq \emptyset$ and U be an any open set in X^M. Then $U = X^M - V^*(Ie)$ for some ideal I of R, since $\mathcal{V}^*(M) = \mathcal{V}'(M) = \{V^*(Ie) = V(Ie) : I \text{ is an ideal of } R\}$, by Proposition 3.4. By above lemma $V^*(Ie) = \cap_{a\in I} V^*(ae)$. Hence $U = X^M - V^*(Ie) = X^M - \cap_{a\in I} V^*(ae) = \cup_{a\in I}(X^M - V^*(ae)) = \cup_{a\in I} X_a$. Thus B is a base for the Zariski topology on X^M. □

A topological space T is called *quasi-compact* if every open cover of T has a finite subcover. Every finite space is quasi-compact, and more generally every space in which there is only a finite number of open sets is quasi-compact. A subset Y of a topological space T is said to be quasi-compact if the subspace Y is quasi-compact. By a *quasi-compact open subset* of T we mean an open subset of T which is quasi-compact. To avoid ambiguity, we would like to mention that a compact topological space is a quasi-compact Hausdorff space. Quasi-compact spaces are of use mainly in applications of topology to algebraic geometry and are seldom featured in other mathematical theories, where on the contrary compact spaces play an important role in different branches of mathematics. To keep uniformity in terminology we continue with the term quasi-compact.

Theorem 5.4. *Let ${}_RM$ be an le-module and the natural map $\psi : X^M \to X^{\overline{R}}$ is surjective. Then the following statements hold:*

(i) The open set X_r in X^M for each $r \in R$ is quasi-compact. In particular, the space X^M is quasi-compact.

(ii) The quasi-compact open sets of X^M are closed under finite intersection and form an open base.

Proof. (i) Since $B = \{X_r : r \in R\}$ forms a base for the zariski topology on X^M by Theorem 5.3, for any open cover of X_r, there is a family $\{r_\lambda : \lambda \in \Lambda\}$ of elements of R such that $X_r \subseteq \cup_{\lambda\in\Lambda} X_{r_\lambda}$. By Proposition 5.1$(ii)$, $D_{\overline{r}} = \psi(X_r) \subseteq \cup_{\lambda\in\Lambda}\psi(X_{r_\lambda}) = \cup_{\lambda\in\Lambda} D_{\overline{r_\lambda}}$. Since $D_{\overline{r}}$ is quasi-compact, there exists a finite subset Λ' of Λ such that $D_{\overline{r}} \subseteq \cup_{\lambda\in\Lambda'} D_{\overline{r_\lambda}}$. Hence $X_r = \psi^{-1}(D_{\overline{r}}) \subseteq \cup_{\lambda\in\Lambda'} X_{r_\lambda}$, by Proposition 5.1$(i)$. Thus for each $r \in R$, X_r is quasi-compact.

(ii) To prove the theorem it suffices to prove that the intersection of two quasi-compact open sets of X^M is a quasi-compact set. Let $C = C_1 \cap C_2$, where C_1, C_2 are quasi-compact open sets of X^M. Since $B = \{X_r : r \in R\}$ is an open base for the Zariski topology on X^M, each C_i, $i = 1, 2$, is a finite union of members of B. Then by Lemma 5.2, it follows that C is also a finite union of members of B. Let $C = \cup_{i=1}^n X_{r_i}$ and let Ω be any open cover of C. Then Ω also covers each X_{r_i} which is quasi-compact by (i). Hence each X_{r_i} has a finite subcover of Ω and so does C. Thus C is quasi-compact. The other part of the theorem follows from the existence of the open base B. □

6 Irreducible closed subsets and generic points

For each subset Y of X^M, we denote the closure of Y in Zariski topology on X^M by $\overline{Y}$, and meet of all elements of Y by $\Im(Y)$, i.e. $\Im(Y) = \wedge_{p\in Y} p$. One can check that $\Im(Y)$ is a submodule element of

M. For each subset Y of $Spec(R)$, we denote the intersection $\cap_{P\in Y}P$ of all elements of Y by $\Im^R(Y)$

Proposition 6.1. *Let ${}_RM$ be an le-module and $Y \subseteq X^M$. Then $V^*(\Im(Y)) = \overline{Y}$. Hence Y is closed if and only if $V^*(\Im(Y)) = Y$.*

Proof. To prove the result it is sufficient to prove that $V^*(\Im(Y))$ is the smallest closed subset of X^M containing Y. Now for all $p \in Y$, $\Im(Y) = \wedge_{p\in Y}p \leqslant p$ implies that $(\Im(Y) : e) \subseteq (p : e)$, i.e., $p \in V^*(\Im(Y))$. Hence $Y \subseteq V^*(\Im(Y))$. Now let $V^*(n)$ be any closed subset of X^M such that $Y \subseteq V^*(n)$. Then for every $p \in Y$, $(n : e) \subseteq (p : e)$ and so $(n : e) \subseteq \cap_{p\in Y}(p : e) = (\wedge_{p\in Y}p : e) = (\Im(Y) : e)$. Also let $q \in V^*(\Im(Y))$. Then $(n : e) \subseteq (\Im(Y) : e) \subseteq (q : e)$ implies that $q \in V^*(n)$. Thus $V^*(\Im(Y)) \subseteq V^*(n)$. Therefore $V^*(\Im(Y)) = \overline{Y}$. □

For an le-module ${}_RM$, we denote $\Phi = \{(p : e)|p \in X^M\}$. Then $\Phi \subseteq X^R$, by Lemma 2.2. We say P is a maximal element of Φ if for any $Q \in \Phi$, $P \subseteq Q$ implies that $P = Q$. Recall that a topological space is a T_1-space if and only if every singleton subset is closed.

Proposition 6.2. *Let ${}_RM$ be an le-module and $p \in X^M$. Then*

(i) $\overline{\{p\}} = V^*(p)$;

(ii) For any $q \in X^M$, $q \in \overline{\{p\}}$ if and only if $(p : e) \subseteq (q : e)$ if and only if $V^*(q) \subseteq V^*(p)$;

(iii) The set $\{p\}$ is closed in X^M if and only if
- *(a) $P = (p : e)$ is a maximal element of Φ, and*
- *(b) $Spec_P(M) = \{p\}$, i.e., $|Spec_P(M)| = 1$;*

(iv) $Spec(M)$ is a T_1-space if and only if
- *(a) $P = (p : e)$ is a maximal element of Φ for every $p \in X^M$, and*
- *(b) $|Spec_P(M)| \leqslant 1$ for every $P \in Spec(R)$.*

Proof. (i) It follows from Proposition 6.1 by taking $Y = \{p\}$.
(ii) It is an obvious result of (i).
(iii) Let $\{p\}$ be closed in X^M. Then by (i), $\{p\} = V^*(p)$. To show $P = (p : e)$ is a maximal element of Φ, let $Q \in \Phi$ be such that $P \subseteq Q$. Since $Q \in \Phi$ there is a prime submodule element q of X^M such that $(q : e) = Q$. Then $(p : e) \subseteq (q : e)$ which implies that $q \in V^*(p) = \{p\}$. Thus $p = q$ and so $P = Q$. For (ii) suppose that q be any element of $Spec_P(M)$. Then $(q : e) = P = (p : e)$ implies that $q \in V^*(p) = \{p\}$ and hence $q = p$.

Conversely, we assume that the conditions (a) and (b) hold. Let $q \in V^*(p)$. Then $(p : e) \subseteq (q : e)$ and so $P = (p : e) = (q : e)$, by (a). Now (b) implies that $p = q$, i.e., $V^*(p) \subseteq \{p\}$. Also $\{p\} \subseteq V^*(p)$. Thus $\{p\} = V^*(p)$, i.e., $\{p\}$ is closed in X^M by (i).
(iv) Note that (b) is equivalent to that $|Spec_P(M)| = 1$ for every $P \in \Phi$. Thus, by (iii), it follows that $\{p\}$ is closed in X^M for every $p \in X^M$. Hence X^M is a T_1-space. □

A topological space T is called *irreducible* if for every pair of closed subsets T_1, T_2 of T, $T = T_1 \cup T_2$ implies $T = T_1$ or $T = T_2$. A subset Y of T is *irreducible* if it is irreducible as a subspace of T. By an *irreducible component* of a topological space T we mean a maximal irreducible subset of T. Also if a subset Y of a topological space T is irreducible, then its closure $\overline{Y}$ is so. Since every singleton subset of X^M is irreducible, its closure is also irreducible. Now by Proposition 6.2(i), we have the following result:

Corollary 6.3. *$V^*(p)$ is an irreducible closed subset of X^M for every prime submodule element p of an le-module ${}_RM$.*

From Proposition 6.2(i) and from the fact that X^M is T_0 if and only if the closures of distinct points in X^M are distinct, the following result is immediate.

Corollary 6.4. *The following conditions are equivalent for any le-module ${}_RM$:*
(i) X^M is a T_0-space;
(ii) For every $p, q \in X^M$, $V^*(p) = V^*(q)$ implies that $p = q$.

It is well known that a subset Y of $Spec(R)$ for any ring R is irreducible if and only if $\Im^R(Y)$ is a prime ideal of R [8]. Let M be a left R-module. Then a subset Y of $Spec(M)$ is irreducible if $\Im^M(Y) = \cap_{P \in Y} P$ is a prime submodule of M, but the converse is not true in general [23]. In the following result we show that the situation in an le-module ${}_RM$ is similar to the modules over a ring. Interestingly, the converse of this result in an le-module ${}_RM$ is directly associated with the ring R.

Proposition 6.5. *Let ${}_RM$ be an le-module and $Y \subseteq X^M$. If $\Im(Y)$ is a prime submodule element of M then Y is irreducible. Conversely, if Y is irreducible then $\Psi = \{(p : e) | p \in Y\}$ is an irreducible subset of $Spec(R)$, i.e., $\Im^R(\Psi) = (\Im(Y) : e)$ is a prime ideal of R.*

Proof. Let $\Im(Y)$ be a prime submodule element of M. Then by Corollary 6.3, $V^*(\Im(Y)) = \overline{Y}$ is irreducible and hence Y is irreducible. Conversely, suppose that Y is irreducible. Since ψ is continuous by Proposition 4.1, the image $\psi(Y)$ of Y under the natural map ψ of X^M is an irreducible

subset of $X^{\overline{R}}$. Hence $\Im^{\overline{R}}(\psi(Y)) = \overline{(\Im(Y) : e)}$ is a prime ideal of $X^{\overline{R}}$. Thus $\Im^R(\Psi) = (\Im(Y) : e)$ is a prime ideal of R so that Ψ is an irreducible subset of $Spec(R)$. □

Also we have some other characterization of the irreducible subsets of X^M.

Proposition 6.6. *Let ${}_RM$ be an le-module. Then the following statements hold:*

(i) If $Y = \{p_i | i \in I\}$ is a family of prime submodule elements of M which is totally ordered by "$\leqslant$", then Y is irreducible in X^M.

(ii) If $Spec_P(M) \neq \emptyset$ for some $P \in Spec(R)$, then
   (a) $Spec_P(M)$ is irreducible, and
   (b) $Spec_P(M)$ is an irreducible closed subset of X^M if P is a maximal ideal of R.

(iii) Let $Y \subseteq X^M$ be such that $(\Im(Y) : e) = P$ is a prime ideal of R. Then Y is irreducible if $Spec_P(M) \neq \emptyset$.

Proof. (i) It is suffices to show that $\Im(Y) = \wedge_{i\in I} p_i$ is a prime submodule element. Let $r \in R$ and $n \in M$ be such that $n \nleqslant \Im(Y)$ and $r \notin (\Im(Y) : e) = (\wedge_{i\in I} p_i : e) = \cap_{i\in I}(p_i : e)$. Then there exists l and k such that $n \nleqslant p_l$ and $r \notin (p_k : e)$. Since Y is totally ordered, either $p_l \leqslant p_k$ or $p_k \leqslant p_l$. Let $p_l \leqslant p_k$. Then $r \notin (p_l : e)$ and $n \nleqslant p_l$ implies that $rn \nleqslant p_l$, since p_l is a prime submodule element. Thus $rn \nleqslant \wedge_{i\in I} p_i = \Im(Y)$. Hence $\Im(Y)$ is a prime submodule element.
(ii) Let $Spec_P(M) \neq \emptyset$ for some $P \in Spec(R)$. Then $\Im(Spec_P(M))$ is a proper submodule element of M.
(a) Assume that $r \in R$ and $n \in M$ be such that $rn \leqslant \Im(Spec_P(M))$ and $n \nleqslant \Im(Spec_P(M))$. Since $n \nleqslant \Im(Spec_P(M))$, there exists $p \in X^M$ with $(p : e) = P$ such that $n \nleqslant p$. Now $rn \leqslant \Im(Spec_P(M)) \leqslant p$ and $n \nleqslant p$ implies that $re \leqslant p$, since p is a prime submodule element. Thus $r \in (p : e) = P = (\Im(Spec_P(M)) : e)$. Therefore $\Im(Spec_P(M))$ is a prime submodule element and hence $Spec_P(M)$ is irreducible.
(b) We prove that $Spec_P(M) = V^*(Pe)$ so that $Spec_P(M)$ is closed. Let $q \in Spec_P(M)$. Then $(q : e) = P \subseteq (Pe : e)$. Since P is a maximal ideal of R, $(Pe : e) = P = (q : e)$, and so $q \in V^*(Pe)$. Thus $Spec_P(M) \subseteq V^*(Pe)$. Also let $q \in V^*(Pe)$. Then $P \subseteq (Pe : e) \subseteq (q : e)$ which implies that $(q : e) = P$, since P is a maximal ideal. Thus $q \in Spec_P(M)$ and hence $V^*(Pe) \subseteq Spec_P(M)$. Therefore $Spec_P(M) = V^*(Pe)$.
(iii) Let p be any element of $Spec_P(M)$. Then $(p : e) = P = (\Im(Y) : e)$ which implies that $V^*(p) = V^*(\Im(Y)) = \overline{Y}$, by Proposition 6.1. Thus $\overline{Y}$ is irreducible and hence Y is irreducible. □

Let Y be a closed subset of a topological space T. An element $y \in Y$ is called a *generic point* of Y if $Y = \overline{\{y\}}$. Proposition 6.2(i) shows that every prime submodule element p of M is a generic point of the irreducible closed subset $V^*(p)$ in X^M. Now we prove that every irreducible closed subset of X^M has a generic point.

Theorem 6.7. *Let ${}_RM$ be an le-module and the natural map $\psi : X^M \to X^{\overline{R}}$ be surjective. Then the following statements hold.*

(i) Then $Y \subseteq X^M$ is an irreducible closed subset of X^M if and only if $Y = V^*(p)$ for some $p \in X^M$. Every irreducible closed subset of X^M has a generic point.

(ii) The correspondence $p \mapsto V^*(p)$ is a surjection of X^M onto the set of irreducible closed subsets of X^M.

(iii) The correspondence $V^*(p) \mapsto \overline{(p : e)}$ is a bijection of the set of irreducible components of X^M onto the set of minimal prime ideals of $\overline{R}$.

Proof. (i) Let Y be an irreducible closed subset of X^M. Then $Y = V^*(n)$ for some submodule element n of M. By Proposition 6.5, we have $(\Im(V^*(n)) : e) = (\Im(Y) : e) = P$ is a prime ideal of R. Then $P/Ann(M) \in X^{\overline{R}}$. Since ψ is surjective, there exists a prime submodule element p of X^M such that $\psi(p) = P/Ann(M)$, i.e., $(p : e)/Ann(M) = P/Ann(M)$ and hence $(p : e) = P = (\Im(V^*(n)) : e)$. Therefore $V^*(\Im(V^*(n))) = V^*(p)$. Since $V^*(n)$ is closed, $V^*(\Im(V^*(n))) = V^*(p)$ implies $V^*(n) = V^*(p)$, by Proposition 6.1. Thus $Y = V^*(n) = V^*(p)$.

Converse part follows from Corollary 6.3.

Now it follows from $V^*(p) = \overline{\{p\}}$ that every irreducible closed subset of X^M has a generic point.
(ii) Follows from (i).
(iii) First assume that $V^*(p)$ is an irreducible component of X^M. Then $V^*(p)$ is maximal in the set $\{V^*(q) : q \in X^M\}$. Clearly $\overline{(p : e)}$ is a prime ideal of $\overline{R}$. To show $\overline{(p : e)}$ is minimal let $\overline{P}$ be a prime ideal of $\overline{R}$ such that $\overline{P} \subseteq \overline{(p : e)}$. Then $P \subseteq (p : e)$. Since ψ is surjective there exists $q \in X^M$ such that $\psi(q) = \overline{P}$, i.e., $\overline{(q : e)} = \overline{P}$. Therefore $(q : e) = P \subseteq (p : e)$ and hence $V^*(p) \subseteq V^*(q)$. Since $V^*(p)$ is maximal in the set $\{V^*(q) : q \in X^M\}$, $V^*(p) = V^*(q)$. Thus $(p : e) = (q : e) = P$ and so $\overline{P} = \overline{(p : e)}$.

Next let $\overline{P}$ be a minimal prime ideal of $\overline{R}$. Since ψ is surjective there exists $p \in X^M$ such that $(p : e) = P$. From Corollary 6.3, $V^*(p)$ is an irreducible subset of X^M. Now let $q \in X^M$ be such that $V^*(p) \subseteq V^*(q)$. Then $(q : e) \subseteq (p : e) = P$ which implies that $\overline{(q : e)} \subseteq \overline{P}$. Since $\overline{P}$ is minimal,

$\overline{(q:e)} = \overline{P}$. Thus $(q:e) = P = (p:e)$ and so $V^*(p) = V^*(q)$. Therefore $V^*(p)$ is an irreducible component of X^M. This completes the proof. □

7 X^M as a spectral space

A topological space T is called *spectral* if it is T_0, quasi-compact, the quasi-compact open subsets of T are closed under finite intersection and form an open basis, and each irreducible closed subset of T has a generic point. Importance of spectral topological space is that a topological space T is homeomorphic to $Spec(R)$ for some commutative ring R if and only if T is spectral. Any closed subset of a spectral topological space with the induced topology is spectral.

From Theorem 5.4 and Theorem 6.7(i), it follows that X^M satisfies all the conditions to be a spectral space except being T_0.

Now we have the following equivalent characterizations for X^M to be spectral.

Theorem 7.1. *Let ${}_RM$ be an le-module and the natural map $\psi : X^M \to X^{\overline{R}}$ be surjective. Then the following conditions are equivalent:*

(i) X^M *is a spectral space;*

(ii) X^M *is a* T_0*-space;*

(iii) For every $p, q \in X^M$, $V^*(p) = V^*(q)$ *implies that* $p = q$*;*

(iv) $|Spec_P(M)| \leqslant 1$ *for every* $P \in Spec(R)$*;*

(v) ψ *is injective;*

(vi) X^M *is homeomorphic to* $X^{\overline{R}}$*.*

Proof. Equivalence of (ii) and (iii) follows from Corollary 6.4, equivalence of (iii), (iv) and (v) follows from Proposition 4.2 and equivalence of (v) and (vi) follows from Corollary 4.4.
$(i) \Rightarrow (ii)$: It follows from the definition of spectral space.
$(ii) \Rightarrow (i)$: This follows from Theorem 5.4 and Theorem 6.7(i). □

An le-module ${}_RM$ is called a *multiplication le-module* if every submodule element n of M can be expressed as $n = Ie$, for some ideal I of R. Let n be a submodule element of a multiplication le-module ${}_RM$. Then there exists an ideal I of R such that $n = Ie$. For each $k \in \mathbb{N}$ and $a_i \in (n:e)$, we have

$$a_1e + a_2e + \cdots + a_ke \leqslant n + n + \cdots + n(k\ times) = n$$

Hence $(n : e)e \leqslant n$. Also $n = Ie$ implies $I \subseteq (n : e)$ which implies that $n = Ie \leqslant (n : e)e$. Thus $(n : e)e = n$.

Theorem 7.2. *Let ${}_RM$ be a multiplication le-module and the natural map $\psi : X^M \to X^{\overline{R}}$ be surjective. Then X^M is a spectral space.*

Proof. First we show that X^M is T_0. Let l and n be two distinct elements of X^M. If possible let $V^*(l) = V^*(n)$. Then $(l : e) = (n : e)$ which implies that $l = (l : e)e = (n : e)e = n$, a contradiction. Thus $\overline{\{l\}} = V^*(l) \neq V^*(n) = \overline{\{n\}}$, by Proposition 6.2($i$). Hence X^M is T_0. Thus the theorem follows from Theorem 5.4 and Theorem 6.7(i). □

Thus assuming surjectivity of the natural map $\psi : X^M \longrightarrow X^{\overline{R}}$ gives us several equivalent characterizations for X^M to be spectral. In other words, surjectivity of ψ is a very strong condition to imply that X^M is spectral. Now we prove some conditions for X^M to be spectral, which do not assume surjectivity of the natural map $\psi : X^M \longrightarrow X^{\overline{R}}$.

Theorem 7.3. *Let ${}_RM$ be an le-module and $\psi : X^M \longrightarrow X^{\overline{R}}$ be the natural map of X^M such that the image $Im\,\psi$ of ψ is a closed subset of $X^{\overline{R}}$. Then X^M is a spectral space if and only if ψ is injective.*

Proof. Set $Y = Im\ \psi$, Since $X^{\overline{R}}$ is a spectral space and Y is a closed subset of $X^{\overline{R}}$, Y is spectral for the induced topology. Suppose that ψ is injective. Then $\psi : X^M \to Y$ is a bijection and by Proposition 4.1, $\psi : X^M \to Y$ is continuous. Now we show that ψ is closed. Let $V^*(n)$ be a closed subset of X^M for some submodule element n of M. Then $Y' = Y \cap V^{\overline{R}}(\overline{(n : e)})$ is a closed subset of Y. Also $\psi^{-1}(Y') = \psi^{-1}(Y \cap V^{\overline{R}}(\overline{(n : e)})) = \psi^{-1}(Y) \cap \psi^{-1}(V^{\overline{R}}(\overline{(n : e)})) = X^M \cap \psi^{-1}(V^{\overline{R}}(\overline{(n : e)})) = \psi^{-1}(V^{\overline{R}}(\overline{(n : e)})) = V((n : e)e) = V^*(n)$ by Proposition 4.1. Since $\psi : X^M \to Y$ is surjective, $\psi(V^*(n)) = \psi(\psi^{-1}(Y')) = Y'$, a closed subset of Y. Thus $\psi : X^M \to Y$ is a homeomorphism and hence X^M is a spectral space. Conversely, let X^M be a spectral space. Then X^M is a T_0-space and so ψ is injective by Corollary 6.4 and Proposition 4.2. □

Theorem 7.4. *Let ${}_RM$ be an le-module such that $Spec(M) = X^M$ is a non-empty finite set. Then X^M is a spectral space if and only if $|Spec_P(M)| \leqslant 1$ for every $P \in Spec(R)$.*

Proof. The finiteness of $|X^M|$ implies that X^M is quasi-compact and the quasi-compact open subsets of X^M are closed under finite intersection and forms an open base. We show that every irreducible

closed subset of X^M has a generic point. Let $Y = \{p_1, p_2, \cdots, p_n\}$ be an irreducible closed subset of X^M. Then $Y = \overline{Y} = V^*(\Im(Y)) = V^*(p_1 \wedge p_2 \wedge \cdots \wedge p_n) = V^*(p_1) \cup V^*(p_2) \cup \cdots \cup V^*(p_n) = \overline{\{p_1\}} \cup \overline{\{p_2\}} \cup \cdots \cup \overline{\{p_n\}}$. Since Y is irreducible, $Y = \overline{\{p_i\}}$ for some i. Therefore by Hochster's characterization of spectral spaces, X^M is a spectral space if and only if X^M is a T_0-space. Hence by Corollary 6.4 and Proposition 4.2, it follows that X^M is a spectral space if and only if $|Spec_P(M)| \leqslant 1$ for every $P \in Spec(R)$. □

References

[1] J. Abuhlail, A dual Zariski topology for modules, *Topology Appl.* **158** (2011) 457-467.

[2] D. D. Anderson, Abstract commutative ideal theory without chain condition, *Algebra Universalis* **6** (1976) 131-145.

[3] D. D. Anderson and E. W. Johnson, Abstract ideal theory from Krull to the present, in: Ideal theoretic methods in commutative algebra(Columbia, MO, 1999), *Lecture notes in Pure and Appl. Math.*, Marcel Dekkar, New York, **220** (2001) 27-47.

[4] M. F. Atiyah and I. G. Macdonald, *Introduction to Commutative Algebra*, Addison-Wesley Publishing Co., 1969.

[5] M. Behboodi, A generalization of the classical krull dimension for modules, *J. Algebra* **305** (2006) 1128-1148.

[6] M. Behboodi and M. R. Haddadi, Classical Zariski topology of modules and spectral spaces I, *International Electronic Journal of Algebra* **4** (2008) 104-130.

[7] A. K. Bhuniya and M. Kumbhakar, Uniqueness of primary decompositions in Laskerian le-modules, *Acta Math. Hunga.* **158(1)** (2019) 202-215.

[8] N. Bourbaki, *Commutative Algebra*, Springer-Verlag, 1998.

[9] N. Bourbaki, *General Topology*, Part I, Addison-Wesley, 1966.

[10] R. P. Dilworth, Non-commutative residuated lattices, *Trans. Amer. Math. Soc.* **46** (1939) 426-444.

[11] R. P. Dilworth, Abstract commutative ideal theory, *Pacific J. Math.* **12** (1962) 481-498.

[12] T. Duraivel, Topology on spectrum of modules, *J. Ramanujan Math. Soc.* **9(1)** (1994) 25-34.

[13] D. Hassanzadeh-Lelekaami and H. Roshan-Shekalgourabi, Prime submodules and a sheaf on the prime spectra of modules, *Comm. Algebra* **42(7)** (2014) 3063-3077.

[14] M. Hochster, Prime ideal structure in commutative rings, *Trans. Amer. Math. Soc.* **137** (1969) 43-60.

[15] J. A. Johnson, a-adic completions of Noetherian lattice modules, *Fund. Math.* **66** (1970) 347-373.

[16] J. A. Johnson, Quotients in Noetherian lattice modules, *Proceedings of the American Mathematical Society* **28(1)** (1971) 71-74.

[17] J. A. Johnson, Noetherian lattice modules and semi-local comletions, *Fund. Math.* **73** (1971) 93-103.

[18] E. W. Johnson and J. A. Johnson, Lattice modules over semi-local Noether lattices, *Fund. Math.* **68** (1970) 187-201.

[19] E. W. Johnson and J. A. Johnson, Lattice Modules over principal element domains, *Comm. in Algebra* **31(7)** (2003) 3505-3518.

[20] W. Krull, Axiomatische begründung der allgemeinen idealtheorie, *Sitz-ber. phys.-med. Soz. Erlangen* **56** (1924) 47-63.

[21] M. Kumbhakar and A.K. Bhuniya, On irreducible pseudo-prime spectrum of topological le-modules, *Quasigroups and Related Systems* **26(2)** (2018) 251-262.

[22] M. D. Larsen and P. J. McCarthy, *Multiplicative theory of ideals*, Academic Press, Volume-43, 1971.

[23] C. P. Lu, The Zariski topology on the prime spectrum of a module, *Houston J. Math.* **25(3)** (1999) 417-432.

[24] C. P. Lu, A module whose prime spectrum has the surjective natural map, *Houston J. Math.* **33(1)** (2007) 125-143.

[25] C. P. Lu, Modules with Noetherian spectrum, *Comm. Algebra* **38(3)** (2010) 807-828.

[26] D. Lu and W. Yu, On prime spectrum of commutative rings, *Comm. Algebra* **34** (2006) 2667-2672.

[27] R. McCasland, M. Moore, and P. Smith, On the spectrum of a module over a commutative ring, *Comm. Algebra* **25(1)** (1997) 79103.

[28] H. M. Nakkar and D. D. Anderson, Associated and weakly associated prime elements and primary decomposition in lattice modules, *Algebra Universalis* **25** (1988) 296-209.

[29] H. M. Nakkar and D. D. Anderson, Localization of associated and weakly associated prime elements and supports of lattice modules of finite length, *Studia Scientiarum Mathematicarum Hungarica* **25** (1990) 263-273.

[30] N. Schwartz and M. Tressl, Elementary properties of minimal and maximal points in Zariski spectra, *J. Algebra* **323** (2010) 2667-2672.

[31] M. Ward, Residuation in structures over which a multiplication is defined, *Duke Math. Jour.* **3** (1937) 627-636.

[32] M. Ward, Structure residuation, *Ann. of Math.* **39** (1938) 558-568.

[33] M. Ward and R.P. Dilworth, Residuated lattices, *Trans. Amer. Math. Soc.* **35** (1939) 335-354.

[34] M. Ward and R.P. Dilworth, The lattice theory of Ova, *Ann. of Math.* **40(3)** (1939) 600-608.

[35] M. Ward and R.P. Dilworth, Evaluations over residuated structures, *Ann. of Math.* **40** (1939) 328-338.

[36] D. G. Whitman, On ring theoretic lattice submodules, *Fund. Math.* **70** (1971) 221-229.

[37] G. Zhang, W. Tong, and F. Wang, Spectrum of a noncommutative ring, *Comm. Algebra* **34(8)** (2006) 2795-2810.

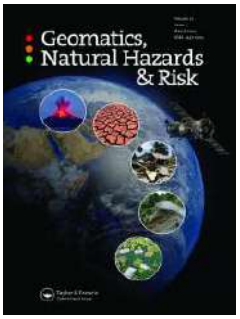

Geomatics, Natural Hazards and Risk

ISSN: (Print) (Online) Journal homepage: https://www.tandfonline.com/loi/tgnh20

Robustness analysis of machine learning classifiers in predicting spatial gully erosion susceptibility with altered training samples

Tusar Kanti Hembram, Sunil Saha, Biswajeet Pradhan, Khairul Nizam Abdul Maulud & Abdullah M. Alamri

To cite this article: Tusar Kanti Hembram, Sunil Saha, Biswajeet Pradhan, Khairul Nizam Abdul Maulud & Abdullah M. Alamri (2021) Robustness analysis of machine learning classifiers in predicting spatial gully erosion susceptibility with altered training samples, Geomatics, Natural Hazards and Risk, 12:1, 794-828, DOI: 10.1080/19475705.2021.1890644

To link to this article: https://doi.org/10.1080/19475705.2021.1890644

Published online: 10 Mar 2021.

JHSP DWFV. RDWZUDOKDcDUGV DRG ULVN
5254. aSC045. RS04. : @7 ; 5;
kwtvA1gslGuj 142042; 214@7: 8: 2805254O4; @2977

Robustness analysis of machine learning classifiers in predicting spatial gully erosion susceptibility with altered training samples

bïyfwNfszoJjr gvfr [a], aïsoqafnf [a], Coy fpjjzUvfinfs [b,c,d], Nnfoïvq Sofr Bgiï qRfïqji [d,e] fsi Bgiïqpfn R. Bofr vo [f]

[a]Ghtduwp hrwsi Jhsjudtk. Zrl huvlw si Jsyu Edrjd. P dogd. b hvwEhrjdo Lrgld B [b]Wkh Fhrwh isu Dg drfhg P sghodrj drg Jhsvtdvldo Lrisupdvlsr V vwhpv)FDP JLV,. Idfyov si Hrjlrhhulrj drg Lrisupdvlsr Whfkrsosj. Zrl huvlw si Whfkrsosj V grh. RVb. Dywudd B [c]Ghtduwp hrwsi Hrhuj drg P lrhudo Uhvsyufhv Hrjlrhhulrj. Vhrnsrj Zrl huvlw. Vhsyo Uhtyedf si NsuhdB [d]Hduwk Sevhu dvlsr Fhrwh. Lrvwyvh si Fdpdvh Fkdrjh. Zrl huvlw Nhedrjvddr P dod vld. Edrjl. Vhodrjsu P dod vld B [e]Ghtduwp hrwsi Fllo Hrjlrhhulrj. Idfyov si Hrjlrhhulrj drg Eylov Hr lusrphrw Zrl huvlw Nhedrjvddr P dod vld. ZNP Edrjl. Vhodrjsu P dod vld B [f]Ghtduwp hrwsi Jhsosj (Jhstk vlfv. Fsohjh si Vflhrfh. Nlrj Vdyg Zrl huvlw. Ul dgk. Vdyg l Dudeld

ABSTRACT

bnj uvjyjsz vjyjfvbm oszjsiji zt fyyjyy znj vtrgïyzsjyy tl znvjyj utuïdqwr fhnosj qjfvsosmr tijqy, qj. vfsitr ltvjyz (WH), gttyzji vjmvjyydts zvjyj (CWb) fsi sf j gf jy (SC) os yufzdfqmïoqq jwtrydts yïyhjuzoqoqpz r tijqqpsmos Nfoszo Wbjwgfyos, Ksidf. B mïoqq os js-ztw r fu tl 209 mïoqqpy fy uvjyufvjyi znvtrïmn lojqj yïwj fsi l ttmqj jfvzn or fmjvjy. Htoqt osmznj 80/30 vfzdt, znvjyj vfsitr q yfr uqji mvtrïuy tl fqzjvji zvfrososmfsi foqpfzdts mïoqq yjzy l 1, l 2 fsi l 3 jvjy uvjyufvjyi ltwr tijqqpsmmïoqq jwtrydts yïyhjuzoqoqpz. cyosmosltw fzdts mfos vfzdt fsi r ïqzohtqpsjfwz fsfqyoy, 14 mïoqq htsiozdtsosmlfhztvy (l EH) jvjy yjqjhzji. bnj ioyhwor osfzdts fgoqpz fsi vjyofgoqpz tl znj r tijqy jvjy r jfyïvjyi znvtrïmn Nfuuf htjlldhojsz, jlldhojsh, vjyhjojw tujvfzosm hnfvfhzjvoyzdh hïwj, vtrtz-r jfs-yvïfvjy-jwtrw (WRaG) fsi r jfs-fgytdqjzj-jwtrw (RBG). bnj yzfgoqpz tl znj r fhnosj qjfvsosmr tijqy fy jyzo r fzji g htr ufvosmznj fhhïvfh yzfzoyzdhy fsi znj ijufvzïvjy os fvjyfqtïzhtr jy fr tsmoszvfr-r tijq fsi oszjwr tijq WH r tijq fy ltïsi fy znj r tyz htsyoyzjsz. d ozn znj nomjyz r jfs BcE (0.A03), jlldhojsh (A1.18), Nfuuf htjlldhojsz (0.935) fsi qt jyz WRaG (0.1A2) fsi RBG (0.091), WH fy ltïsi zt gj r tvjy htsyoyz-jsz njs znj zvfrososmfsi foqpfzdts ifzf yjzy jvjy fqzjvji. bnj jlljhzojsjyy tl jfhn osuïz lEHy fy ijzjwr osji ïyosmr fu vjyr t fqyjsyozoqz fsfqyoy zjhnsovïj. bnoy yzïi htïqi gj yïu-utwzoj os fyhjwzfososmr tijqi jud r jszltwr fuuosmmïoqq jwtr-ydts fsi r fsfmosmznj qfsi vjyytïvhj.

ARTICLE HISTORY

Uhfhl hg 4: Myr h 5252
Dffhtvhg 42 l heuydu 5254

KEYWORDS

P dfklrh dhdurlrj Bjyoo
husvlsr BJLVBdovhuhg jyoo
vdp t dhvBLrgld

Elv drhhwTudgkdr elv drhhv@udgkdr Cywv0hgy0dy

scientific reports

Check for updates

OPEN

Measuring landslide vulnerability status of Chukha, Bhutan using deep learning algorithms

Sunil Saha[1], Raju Sarkar[2]✉, Jagabandhu Roy[1], Tusar Kanti Hembram[3], Saroj Acharya[4], Gautam Thapa[5] & Dowchu Drukpa[6]

Landslides are major natural hazards that have a wide impact on human life, property, and natural environment. This study is intended to provide an improved framework for the assessment of landslide vulnerability mapping (LVM) in Chukha Dzongkhags (district) of Bhutan. Both physical (22 nos.) and social (9 nos.) conditioning factors were considered to model vulnerability using deep learning neural network (DLNN), artificial neural network (ANN) and convolution neural network (CNN) approaches. Selection of the factors was conceded by the collinearity test and information gain ratio. Using Google Earth images, official data, and field inquiry a total of 350 (present and historical) landslides were recorded and training and validation sets were prepared following the 70:30 ratio. Nine LVMs were produced i.e. a landslide susceptibility (LS), one social vulnerability (SV) and a relative vulnerability (RLV) map for each model. The performance of the models was evaluated by area under curve (AUC) of receiver operating characteristics (ROC), relative landslide density index (R-index) and different statistical measures. The combined vulnerability map of social and physical factors using CNN (CNN-RLV) had the highest goodness-of-fit and excellent performance (AUC = 0.921, 0.928) followed by DLNN and ANN models. This approach of combined physical and social factors create an appropriate and more accurate LVM that may—support landslide prediction and management.

[1]Department of Geography, University of Gour Banga, Malda, West Bengal, India. [2]Department of Civil Engineering, Delhi Technological University, Delhi, India. [3]Department of Geography, Nistarini College, Purulia, West Bengal, India. [4]National Centre for Hydrology and Meteorology, Thimphu, Bhutan. [5]Royal Government of Bhutan Projects, Phuentsholing, Bhutan. [6]Department of Geology and Mines, Ministry of Economic Affairs, Thimphu, Bhutan. ✉email: rajusarkar@dce.ac.in

Available online at www.sciencedirect.com

ScienceDirect

Cp nzoq uz cffmoq b q qmot ( )

ADVANCES IN SPACE RESEARCH (a COSPAR publication)

.hauhylht.er p /orecvh/cut

K n up qz qy nxq y mot uzq xqmzuzs mffff fimot q rfi xmzp xupq oqff unuxu y mffffuzs uzs pu q qz my ffxuzs mufi m Hm cuwwuy Kuy mxm mz - Izpum

c zuxcmt m[a,*] - Mfs mnmzpt b fi [a] - Eu mqq Umpt mz [b,c,d] - d m Omz uKqy n my [e]

[a] Dht dvxp hrxsi Ghslvdtm, Wrnzhwvnx si Gsyv Bdrld, N dogd-732103, b hwx Bhrldq Irgnd
[b] Unh Chrxvh isv Agzdrfhg N sghonrl drg Ghswtdxulo Irisvp dxusr T wvhp w (CAN GIT), Fdfyox si Erlrrhlwnrl drg Irisvp dxusr Uhfmrsosl, Wrnzhwvnx si Uhfmrsosl T grh, OTb 2007, Aywxdond
[c] Chrxhv si E fhohrfh isv Cop dxh Cmdrlh Shwhdvfm Knrl Aegyal n Wrnzhwvnx, R. P. Bs 80234, Jhggdm21589, Tdygn Avdend
[d] Edvxm Pewhvzdxusr Chrxvh, Irwvnyxh si Cop dxh Cmdrlh, Wrnzhwvnx Khedrlwldr N dal vnd, Bdrln43600, N dal vnd
[e] Dht dvxp hrxsi Ghslvdtm, Onwdlvrrn Csohlh, Ryvyod-723101, b hwx Bhrldq Irgnd

b qoqu qp 2: Mfz m 3132= qoqu qp uz q uqp rfi y 23 R m 3132=nooqff qp 31 R m 3132

Pmzp xupq u mnus ff finxqy uz tqyfi z mzfi qsufiz mxfi q tq fi xp/cuwwuy Kuy mxm mz qsufiz u mxfi q uzs r fiy xmzp xupq ff finxqy / dtu p ' y mz finvqo u q m fi sqzq mq xmzp xupq oqff unuxu y mff (PcR) ofiz upq uzs tqt n up qz qy nxq fir y mot uzq xqmzuzs mffff fimot q uzs pu q qz my ffxq mufi / b mzpfiy I fi q (b I) m tq nmq oxm u q mz qz qy nxq ut nmssuzs - b fi mufiz I fi q (b d I) - mzp b mzpfiy c n ffmoq (b c) R q moxm u q q q qp rfi ffmumx xmzp xupq y fipqxuzs / I u - ofixqo qp 97 xmzp xupq xfiomufiz t fi st qpp uz q usmufiz mzp r fiy cuwwuy pu uo pum q fi oq q q y mffffqp m mxmzp xupq uz qz fi / F fixqo qp xmzp xupq xfiomufiz q q omqsfi u qp uz fi muzuzs mzp q uzs pmmq mzpfiy x uzs rfi my ffxq mufi (61;61 - 71;51 - 81;41 mzp 91;31) / Emqp fiz tq rfi my ffxuzs mufi mzp r qqz ofizpufizuzs rmo fi - m fi mxfir u qqz PcR q qff qffmqp uzs b I - Enssuzs. b I (E. b I) - b d I. b I mzp b c. b I uz J Ic ffxmrfi y / I fi m q uzs tqyfipqxuzs moo mo mzp ofiy ffmufiz my fizs tq q - tq mqm zpq tq qoqu q fiffq muzs ot mmo. q u uo (Ce b TF) mzp fi tq mu uomx y q t fip ot m fifi . y qmz. ffi mq. q fi (b R c H) - y qmz. mn fix q. q fi (R CH) mzp b . uzpq y q t fip q q qp / dtq fi q mxx ff fi ouqzo fir b c. b I (Ce F @ 1/982 - 1/958 fir 61%;61% - Ce F @ 1/: 36 - 1/: 42 fir 71%;51% - Ce F @ 1/: 44 - 1/: 4: fir 81%;41% = Ce F @ 1/: 38 - 1/: 44 fir 91%;31%) m rfi zp fi nq n mz umx s qmq tmz tq q x fir b I - E. b I - mzp b d I. b I / dtq b c. b I y fipqx mzp 81;41 my ffxq mufi tmp tq tustq sfifipzq . fir. mzp moo mo m ffq tq b R c H - R CH - mzp b . uzpq y q t fip / I tq y fi q - tq y fipqx nmqp fiz b c. b I u mff fiy uuzs mzp mooqff mnxq m fir y mffffuzs qsufiz mx xmzp xupq /

Kh svgw Pmzp xupq oqff unuxu = J Ic = R q moxm u q = Hz qy nxq y mot uzq xqmzuzs = Hm cuwwuy Kuy mxm m

ca

Kuy mxm mz qsufiz fir Izpum u tqyfi zm mx t m mp fizq - m qo qp n xmzp xupq mzp qm t ffi mwq / Cffff fi u y mqx 91% fir xmzp xupq uz Izpum fioo uz t u mqm (Tzmst q mx/ - 3123) / cuwwuy u tq ffm fir t q Kuy mxm m t q q xmzp xupq u m qfioo uzs ff finxqy / dtu mqmu r q. ffi qz x m qo qp n tq xmzp xupq q q qm p q fi t qm mzrmxx p uzs tq y fiz fifiz uy q (b fi q mx/ - 312:) / b qoqz x - xmzp xupq t m q uzo qm qp uz t u m qm - m qo uzs xurq mzp ff fiffq p q fi y ot mz t ffffis qz uo uz q rq qz oq (R wmzq - 3125 = c m wm q mx/ - 2: : 6) /

* Ffi q fffizpuzs m t fi /
E-p dnv dggvhwvhw zusqfi/99B sy mx/ofiy (c/ cmt m) - vns mnmzpt . fi 2: : 2B sy mx/ofiy (M b fi) - nu mqq/ff npt mzB /qp /m (E/ Umpt mz) - mff xm2: : 2B sy mx/ofiy (d/O/ Kqy n my) /

j vs ub/grl.r t i /10.1017/mcut.2021.06.01:
0283-1188/© 2021 ORaSCV. Swddujhg d Pouhylht E.b. Coot lij vu thuht yhg.

Uqmq ouq t u m uoxq m; c/ cmt m - M b fi - E/ Umpt mz q mx/ - K n up qz qy nxq y mot uzq xqmzuzs mffff fimot q rfi xmzp xupq oqff unuxu y mffffuzs uzs pu q qz my ffxuzs mufi m Hm cuwwuy Kuy mxm mz - Izpum - Cp nzoq uz cffmoq b q qmot - t ff :00pfiu/fi s021/21270/m /3132/16/129

ISSN : 2249-9318
Peer-Reviewed and Refereed Research Journal
UGC Approved Journal No: 41369

अनुसंधान

(छायावाद पर केन्द्रित अंक)

वर्ष : 16 अंक : 15-16 जनवरी-दिसम्बर, 2020

प्रकाशक
अनुसंधान समिति
हिंदी एवं आधुनिक भारतीय भाषा विभाग
इलाहाबाद विश्वविद्यालय, प्रयागराज

छायावाद में क्रांति का स्वरूप और निराला

डॉ. पोर्शिया सरकार*

क्रांति और संघर्ष से मानव सभ्यता का रिश्ता बहुत पुराना है। सभ्यता के प्रारंभ से लेकर अब तक उसने जितने भी पड़ाव पार किए उसके पीछे की कहानी कहीं न कहीं क्रांति और संघर्ष से जुड़ी हुई है। पूरे विश्व में जितने भी बदलाव और परिवर्तन हुए हैं उसके पीछे क्रांति और संघर्ष का हाथ है। विश्व के हरेक कला और साहित्य का सृजन इन्हीं की देन है। समय-समय में जितने भी संत, योगी, चिंतक, कवि, साहित्यकार और कलाकार हुए हैं उनका जीवन आदर्श भी इसकी स्याही से लिखी गई है।

हिन्दी साहित्य का सम्पूर्ण इतिहास भी इन्ही संघर्षों का लेखा-जोखा है। मनुष्य अपनी सभी जीवनानुभूतियों को साहित्य में प्रकाशित करता जाता है। वह अपने आसपास की परिस्थिति, परिवेश और विसंगतियों से ही नवीन प्रेरणा ग्रहण करता है। चाहे वह आदि कवि वाल्मीकी हो या अन्य कवि। साहित्य और कला में इसी क्रांति और संघर्ष की गूंज सुनाई पड़ती है। इसी क्रम में हिन्दी साहित्य को अगर लिया जाए तो हमें पता चलेगा कि प्राचीनकाल से लेकर आधुनिककाल तक अनगिनत क्रांतिकारी कवियों ने अपने हुंकारों से साहित्य के पन्नों को भर दिया। चाहे वह कवि चंद हो या भूषण, कबीर हो या निराला। हिन्दी साहित्य के प्रत्येक काल की शुरुआत इसी विद्रोह से हुई है। और अगर छायावाद की बात करें तो पाएंगे कि प्राचीन बंधनों को काटकर नवीनता की और बढ़ना और स्थूलता के स्थान पर सूक्ष्मता की स्थापना करना ही इस काल का लक्ष्य रहा। इस काल में क्रांति और संघर्ष की बात की जाए तो निराला के बिना अधूरा सा लगेगा। इसी प्रसंग में युगांतकारी कवि निराला को अगर देखें तो पाएंगे उनका संपूर्ण जीवन ही संघर्षों से जूझते हुए बीता। उन्हें जीवनभर विरोधों और विवादों का सामना करना पड़ा। वे हिन्दी के ऐसे बिरले कवियों में से एक है जिन्हें आजीवन आर्थिक तंगी, ठोकरे और अवहेलना मिली। इसलिए वे तत्कालीन समाज में व्याप्त शोषण, दमन असमानता, अज्ञानता एवं रूढ़िवादिता को देखकर भी अनदेखा नहीं कर सके। उनके साहित्य में भी यही मुखरित हुआ है। वे सन् 1916 से 1953 ई. तक निरंतर साहित्य में लीन रहे। उनकी कुछ छायावादी रचनाएँ अनामिका, परिमल, गीतिका और तुलसीदास है। हिन्दी साहित्य में निराला को एक ऐसे कवि के रूप में माना जाता है जिन्होंने साहित्य में कदम ही रखा विद्रोह और क्रांति के साथ। इसका अच्छा खासा उदाहरण सन् 1916 ई. में प्रकाशित 'जुही की कली' कविता है। उन्होंने काव्य के बंधनों को ही नहीं तोड़ा बल्कि समाज के रूढ़िगत बंधनों से भी समाज को मुक्त करने का प्रयास किया। उनके काव्य के विषय भी अनेक रूपता लिए हुए हैं। उनके काव्य में कही उमड़-घुमड़ कर गरजता हुआ बादल है तो कहीं विधवा और भिक्षुकों के बच्चों का क्रंदन है। एक ओर अनके काव्य में विद्रोह की आग है तो दूसरी ओर नारी के अद्वितीय सौंदर्य की झांकी। परन्तु अपनी कविताओं के माध्यम से वर्गीय शोषण, सामाजिक वैशम्य और राजनैतिक स्वार्थपरता के विरुद्ध पचंड विद्रोह करना ही उनका सबसे महत्वपूर्ण लक्ष्य रहा। इसी प्रसंग में डॉ.नरेन्द्र द्वारा संपादित 'हिन्दी साहित्य के इतिहास' पुस्तक में उनके कथन को देखा जा सकता है। वे लिखते है-"जैसे-जैसे युग बदलता है, कवि

* सहायक अध्यापिका, हिन्दी विभाग, निस्तारिणी कॉलेज, पुरुलिया, पश्चिम बंगाल

डाक-पंजीयन म.प्र./भोपाल/4-472/2021-23
पोस्टिंग दिनांक : प्रतिमाह दिनांक 2 से 3, पृष्ठ सं. 112
प्रकाशन दिनांक : 1 से 1 प्रतिमाह

आर.एन.आई क्र. : 38470/83
आई.एस.एस.एन. क्र. : 2456-7167

मूल्य 25/-

39 वाँ वर्ष

मई 2021

अक्षरा

194

साहित्य की मासिकी

हास्य-व्यंग्य और रेणु का कथेतर साहित्य

- पोर्शिया सरकार

जन्म - 18 जून 1978।
शिक्षा - एम.ए., पीएच.डी।
रचनाएँ - एक पुस्तक प्रकाशित।

रेणु एक ऐसे कथाकार हैं, जिनको अपनी रचनाओं में अपने समय की नब्ज को पकड़ने की अनोखी ताकत है। उनका कथेतर साहित्य तत्कालीन जीवन संघर्ष, दु:ख, द्वंद्व, संकटबोध और तनाव उत्पन्न करने वाली परिस्थितियों को प्रकट करते हुए भी आज अप्रासंगिक नहीं है। कथेतर विधाओं में रेणु अपनी गहन अनुभूतियों के जरिए इतिहासबोध तक जाते हैं। रेणु के कथेतर साहित्य में वर्णित समय-समाज एक सम्पूर्ण युगबोध है।

जब हम फणीश्वरनाथ रेणु का नाम लेते हैं, तो हमारे मन में 'मैला आँचल' या 'परती परिकथा' या फिर 'तीसरी कसम' की याद आने लगती है। वे एक ऐसे कथा-शिल्पी हैं, जिन्होंने सफेद कागज के टुकड़ों पर मानवीय संवेदनाओं को साकार किया है। उनका सम्पूर्ण साहित्य सत्यानुभूतियों की मार्मिक अभिव्यक्ति है। रेणु का कथा साहित्य अमर है और कथेतर साहित्य अद्वितीय। उन्होंने रिपोर्ताज, रपट, संस्मरण, रेखाचित्र, साक्षात्कार, पत्र, निबंध, हास्य-व्यंग्य, कविता, गद्यगीत आदि विभिन्न साहित्यिक विधाओं में लेखन-कार्य किया है। हिन्दी जगत में इतनी सारी साहित्यिक विधाओं में लिखनेवाले साहित्यकार विरल ही हैं।

रेणु के कथेतर साहित्य में हास्य-व्यंग्य की चर्चा करने से पहले हमें इतिहास जानना होगा। हास्य-व्यंग्य की शुरुआत कब से साहित्य में हुई, यह बताना कठिन है, पर सरल भाषा में कहा जा सकता है कि यह शब्द का वह गूढ़ अर्थ है, जो उसकी व्यंजना शक्ति के द्वारा प्रकट होता है। प्राचीन काल से लेकर अब तक विभिन्न विधाओं के जरिए कवियों ने हास्य-व्यंग्य को प्रस्तुत किया है। संस्कृत वाङ्मय में भी कई कविताओं में इसे देखा जा सकता है।

हास्य-व्यंग्य के मूल स्रोत को अगर हम देखने की कोशिश करेंगे, तो हमें पता चलेगा कि इसकी परम्परा काफी पुरानी है। यह हमारी संस्कृति, सभ्यता और जीवन दर्शन में रचा-बसा है। भारतीय संस्कृति में प्राचीन काल से ही जन्म, मृत्यु, प्रकृति और मानव मात्र की समस्त सूक्ष्म अनुभूतियों को महत्ता प्रदान की गई है। भारतीय संस्कृति प्रकृति के कण-कण में व्याप्त आनंद और रस की फुहार को ही नाना रूपों में साहित्य और कला के जरिए प्रस्तुत करती है।

भारत में हर उत्सव, पूजा-पाठ, अनुष्ठान आदि सुख, शांति और समृद्धि के लिए मनाए जाते हैं। उत्सव हमारे आनंद के प्रतीक हैं। अक्सर इसी की छाया साहित्य में पड़ने पर हास्य का जन्म होता है, परन्तु आधुनिक काल तक आते-आते हास्य के क्षेत्र में कई महत्त्वपूर्ण परिवर्तन हुए। भारतीय विद्वानों ने इसे एक स्वतंत्र विधा न मानकर सभी साहित्यिक विधाओं में व्याप्त रहनेवाला रस माना है और यह भी माना है कि हास्य और व्यंग्य दोनों एक-दूसरे से भिन्न हैं। इस मत का

Reg. No. 694/2009-10

Impact Factor : 5.029

ISSN : 2250-1193

Anukriti

An International Peer Reviewed Refereed Research Journal

Vol. 10, No. 3 Year-10 March, 2020

PEER REVIEWED JOURNAL

Published by

SRIJAN SAMITI PUBLICATION

VARANASI (U.P.), INDIA

Mob. 9415388337, **E-mail :** anukriti193@rediffmail.com, **Website :** anukritijournals.com

अनुक्रमणिका

Reg. No. 694/2009-10
Anukriti (An International Peer Reviewed Refereed Research Journal), Vol. 10, No. 3, March, 2020
Impact Factor : 5.029
ISSN : 2250-1193

रेणु के रिपोर्ताज में राजनैतिक चेतना

डॉ0 पोर्शिया सरकार
सहायक अध्यापिका, हिन्दी विभाग, निस्तारिणी कॉलेज, पुरुलिया

रेणु के सम्पूर्ण कथेतर साहित्य की बात करें तो उन्होंने गद्य की प्रत्येक विधा में अपनी लेखनी चलाई है। उनके द्वारा लिखे गए रिपोर्ताज अपने आप में बेजोड़ हैं। उदाहरण के तौर पर 'विदापत नाच', 'हड्डियों का पुल', 'नए सवेरे की आशा', 'एकलव्य के नोट्स', 'पुरानी कहानी : नया पाठ', 'भूमिदर्शन की भूमिका', 'पटना जल प्रलय', 'सरहद के उस पार' आदि। ये सारे रिपोर्ताज विभिन्न विषय वस्तुओं को समेटे हुए हैं, लेकिन इनके केन्द्र में आम इंसान है, जो शोषित और अवहेलित है।

रेणु द्वारा रचित सत्रह रिपोर्ताज आज उपलब्ध हैं। रिपोर्ताजों का संबंध समाज और जीवन के विविध पक्षों से है। इनमें रेणु के समय के जन की आशा, आकांक्षा, संघर्ष, आस्था–अनास्था का चित्रण किया गया है। उनका पहला रिपोर्ताज सन् 1945 में प्रकाशित हुआ और अन्तिम सन् 1975 में। 31 वर्षों में लिखे गए रेणु के रिपोर्ताज मानव के सामाजिक, आर्थिक और राजनीतिक समस्याओं से संबद्ध हैं। रेणु के कई रिपोर्ताज भारतीय राजनैतिक परिवेश का दस्तावेज हैं। मात्र भारतीय कहना गलत होगा क्योंकि उन्होंने बंग्लादेश और नेपाल की राजनीति का भी बारीकी से निरीक्षण किया है। रेणु ने अनेक राजनैतिक दलों का चित्रण किया है, जिसमें कांग्रेस, हिन्दू महासभा और समाजवादी दल भी हैं। इन सभी दलों के कार्यकलापों का बिना किसी पूर्वाग्रह के उन्होंने चित्रण किया है।

रेणु आजीवन राजनीति से जुड़े रहे। वे स्वीकारते हैं–"जीवन की शुरूआत राजनीति से की थी मैंने, अथवा किसी 'नीति' से, कह नहीं सकता, मगर राजनीति हमारे लिए 'दाल–भात' की तरह है।" वास्तव में उनके लिए राजनीति एक माध्यम था मजदूरों, कृशकों एवं गरीबों को उनका अधिकार दिलाने का। चाहे वह किसान आन्दोलन, काश्त संघर्श तथा मील–मजदूरों की हड़ताल ही क्यों न हो, उन्होंने लोगों का साथ दिया। उन्होंने सन् 1952 तक सक्रिय राजनीति की थी। इसमें उन्हें सफलता नहीं मिली, परन्तु राजनीति को उन्होंने अपने से अलग नहीं होने दिया। साथ ही साथ उन्होंने संघर्श के दौरान किए गए अनुभवों को अपने रिपोर्ताज में लिपिबद्ध किया। उनके अधिकांश रिपोर्ताज जो कि खासतौर पर सूखे और बाढ़ पर केन्द्रित हैं, उनमें भी तत्कालीन राजनेताओं के गतिविधियों को देखा जा सकता है। रेणु के अधिकांश रिपोर्ताज विभिन्न पार्टियों की 'राजनीति' या यूँ कह सकते हैं 'स्वार्थपरता' को दर्शाता है।

स्वतंत्रता–पूर्व भारतीयों ने जिस सुख एवं समृद्धि का सपना देखा था, उसे आजादी के पश्चात् शक्तिशाली और अवसरवादी राजनेताओं ने चकनाचूर कर दिया। जिसके कारण जनता का नेताओं से मोह भंग हो गया। रेणु ने अपने रिपोर्ताजों में नेताओं के झूठे वादे और वोट की माँग पर भी व्यंग्य किया है। नेता चुनाव–पूर्व इन्कलाब का झूठा स्वप्न दिखाकर गरीब जनता को ठगते हैं। जैसे ही इन्हें वोट मिल जाता है, ये अपनी ही तिजोरियों को भरने लगते हैं। यानी इनके 'नाम बड़े पर दर्शन छोटे' होते हैं। जनता भी नेताओं को पहचानने लगी। जनता को आजादी झूठी लगती है। वह रंगे सियारों को पहचानने लगी है। वह जानती है कि राजनीतिज्ञ ही उनकी जिन्दगी में समस्याओं को जन्म देने का कार्य कर रहे हैं।

रेणु ने अपने रिपोर्ताजों में भ्रष्टाचार में लिप्त कांग्रेसी सरकार के चट्टे–बट्टों को बेनकाब किया है। वे राजनीति और उससे जुड़े लोगों के हर तरह के पैंतरे से परिचित हैं। वे राजनीतिज्ञों और जमींदारों के गठबंधन को भी देखते हैं। यह गठबंधन किसानों के लिए घातक है।

रेणु का राजनीतिक कदम केवल अपने देश और अपने क्षेत्र विशेश तक सीमाबद्ध नहीं था। उन्होंने अपने देश ही नहीं संपूर्ण विश्व–मानव समाज के शोशक वर्ग के खिलाफ आवाज उठाया है। वे भारत के साथ नेपाल, बांग्लादेश यहाँ तक की चीन की जनता के दुःख–दर्द के साथ जुड़े हुए थे।

'हड्डियों का पुल' रिपोर्ताज में रेणु ने बिहार के सूखाग्रस्त इलाके का वर्णन किया है, जहाँ लोग सारूख और करमी पर ही जीवित रहते हैं, पर जमींदारों एवं साहूकारों का शोषण–चक्र अपनी पूरी शक्ति से घूमता है। सरकार भी इनसे मिली हुई। भारतीय समाज आज जिस शोशण और बदहाली का शिकार है उसके लिए जिम्मेदार भारतीय शासन व्यवस्था है। रेणु ने लगभग अधिकांश रिपोर्ताज में मानव–विद्रोह को किसी न किसी रूप में दर्शाया है। रेणु क्रांति की आवश्यकता को हर क्षेत्र में महसूस करते हैं। सही अर्थों में राजनीतिक सुधार ही जीवन के हरेक क्षेत्र में इन्कलाब की शुरूआत है।

JOURNAL FOR SOCIAL REALITY

Quarterly (English & Hindi)

ISSN 2349 - 9710

Vol. 7 Oct. - Dec., 2020 No. 4

Editor

Dr. Sachidanand Prasad

Associate Professor, Head, Dept. of Philosophy,
R.R.S. College, Mokama, Patna, Bihar

Institute for Social Development & Research

Gari Hotwar, Ranchi - 835217 (Jharkhand)

No. 4
ISSN 2349-9710, Peer Reviewed Journal, JSR, Vol. 7(4), 2020, ISDR, Ranchi.

रेणु के रिपोर्ताज 'बिदापत-नाच' में दलित समाज

डॉ. पोर्शिया सरकार
सहायक अध्यापिका, हिन्दी विभाग, निस्तारिणी कॉलेज, पुरूलिया, पश्चिम बंगाल

जब हम फणीश्वर नाथ 'रेणु' का नाम लेते हैं, तो हमारे मन में 'मैला आँचल' या 'परती परिकथा' या फिर 'तीसरी कसम' की याद आने लगती है। बहुत कम लोग जानते हैं कि उन्होंने बहुत समृद्ध कथेत्तर साहित्य का सृजन किया है। रेणु का कथा-साहित्य अमर है और कथेत्तर साहित्य अद्वितीय। परन्तु उनकी कथेत्तर साहित्य की अपेक्षा उनकी कथा साहित्य की चर्चा अधिक हुई है। उनका कथेत्तर साहित्य सत्यानुभूतियों की मार्मिक अभिव्यक्ति है। रेणु ने कथेत्तर साहित्य के विभिन्न विधाएँ जैसे- रपट, रिपोर्ताज, संस्मरण, रेखाचित्र, जीवनी, कविता, हास्य-व्यंग्य, गद्य-गीत, साक्षात्कार, निबंध एवं पत्र आदि को बड़े सुंदर ढंग से प्रस्तुत किया है। उन्होंने विषय के रूप में दलित समाज, गरीबी, महामारी, बेकारी और शोषण में जर्जित मनुष्य को इनमें शामिल किया। रेणु का सम्पूर्ण कथेत्तर साहित्य उनके जीवन संकल्प 'सबार ऊपरे मानुष सत्य' का ही साकार रूप है।

लेकिन हम यहाँ मात्र रिपोर्ताजों में दलित चेतना की बात करेंगे? वैसे रेणु ने बाढ़, अकाल एवं युद्ध से सम्बंधित अनेक रिपोर्ताजों को लिखा है। साथ ही साथ लोक-जीवन, समाज-व्यवस्था, खेल, कृषि, रीति-रिवाज, संस्कार, आस्था, मनोरंजन (फिल्म) आदि विभिन्न विषयों पर महत्त्वपूर्ण रिपोर्ताजों की रचना की है। उदाहरण के तौर पर 'विदापत-नाच', 'हड्डियों का पुल', 'नए सवेरे की आशा', 'सरहद के उस पार', 'एकलव्य के नोट्स', 'पुरानी कहानी : नया पाठ', 'भूमि दर्शन की भूमिका' और 'पटना जल प्रलय' आदि। उनके रिपोर्ताजों की कुल संख्या सत्रह है जो अपने-आप में बेजोड़ है। इनमें निम्न वर्ग का जीवन सत्य, कृषि समस्या, अन्नाभाव, हिन्दु-मुसलमान एकता, राजनैतिक दाव-पेंच एवं टूटते परिवार का दर्द है। उनकी ये रिपोर्ताज किसी-न-किसी रूप में सर्वहारा और

Environment and Ecology 37 (3) : 728—731, July—September 2019
Website: environmentandecology.com ISSN 0970-0420

Physico-Chemical Quality of Soil of Agro-Fields Along Side Heavy Transportation Burdened Barakar Road, Bongabari, Purulia, WB, India

Moumita Sinha, Priyanka Dutta

Received 1 February 2019; Accepted 2 March 2019; Published on 23 March 2019

Abstract Present study was undertaken to observe the physico-chemical characteristics of soil collected from agro-fields adjacent to the highly traffic burdened Barakar Road, Bongabari, Purulia. These fields ,most of the time, are exposed to the heavy automobile emission. Simultaneously, for control study, soil samples were collected from agro-field near Purana Kali Mandir, Ketika, Purulia where fields are far away from heavy automobile emissions. Soil samples were collected from both of the agro-field surface areas within the depth 0-10 cm. Parameters like bulk density, particle density, organic carbon, pH, EC, soil moisture, available nitrogen, phosphorus, potassium, Cu, Zn, Pb and Cd of soil samples were estimated. pH of Bongabari area is less acidic ($p<0.01$) than that of control area ; Cu and Pb concentration were significantly enhanced in the road side field ($p<0.01$) than in interior region, soil moisture, available nitrogen, available potassium, Zn and Cd concentration were reduced significantly ($p<0.01$) in the road side area. Study guesses that the changes in physico-chemical characteristics and comparatively elevated concentration of Pb and Cu in Bongabari area may be due to the impact of automobile emission. In the second part of the investigation, the changing pattern in soil physico-chemical characteristics was investigated between two zones of the same agro-field. A set of 5 soil samples were collected from 0-10 m horizontal range from Barakar Road whereas another set of similar number of soil samples were collected from the 25—35 m range horizontally from the said road. Analytical data revealed that soil density, organic carbon, pH, available nitrogen, available potassium and Zn concentration were significantly higher ($p<0.01$, $p<0.05$) in the range 0-10 m from the road and soil moisture, phosphorus, Cu, Pb and Cd concentration were found significantly higher ($p<0.01$, $p<0.05$) in the range 25—35m. It was observed that changes in soil characteristics were more prominent in the range 25—35 m than the other one; Pb, Cu and Zn concentration were also found significantly ($p<0.01$) higher in this range.

Keywords Soil density, NPK, Soil pH, Soil organic carbon, Soil Pb.

Moumita Sinha*
Assistant Professor, Department of Environmental Science, Nistarini College, D. B. Road, Purulia (Sidho Kanho Birsha University), WB, India

Priyanka Dutta
Department of Environmental Science, The University of Burdwan, Burdwan, WB, India
e-mail : moumitanistarini@rediffmail.com
sinhanayek@gmail.com
*Corresponding author

www.aensi.in /Index in Cosmos ISSN 0025-1348 (P), 2456-1356 (O) UGC APPROVED

Received: 4 February Revised: 9 February Accepted: 19 February

Present Scenario of Women in Higher Education in India-Opportunities and Challenges

Moumita Sinha
Assistant Professor, Department of Environmental Science,
Nistarini College (Under SKBU), Purulia-723101, WB

Abstract

Education has a vital role in dynamic nature of a society as well as a country towards affirmative direction. Liberalism of a society appreciably depends on the educational rank and educational quality of women, because women are the exclusive hauler of prospect generation. Children initiate their first learning from their mothers. Children find outknowledge to build up their characters, to expand good traits and morals within them from their mothers. So, if a woman becomesskilled, then entire society, entire nation will be educated. Currently in our country women education especially their enrollment in higher education are being emphasized. Without higher educational qualities or degrees, women will not be able to compete with others in job market; in upshot of that they will be economically dependent on other family members; unemployment, pitiable educational status, gender biasness will make them incapable in family as well as in society. But great past and present instances of world explain to about huge potentiality of women. Women higher educational status and empowerment are urgently required for the concurrent richness of our society. To extend the essence of higher study among women and lessening gender gap in higher education, India Government has thought the matter seriously and initiatedfew action plans successfully. Besides the Co-education colleges, institutes and universities, a number of colleges and universities are dedicated solely for women studies. Financial assistanceas scholarship, stipends are being provided to the optimal poor meritorious girl pupils to carry out their higher education in spite of a number of barriers like poverty, pressure from family as well as society due to conservativeness; early marriage, burden of domestic work as well as responsibilities towards family members, nourishment of offspring, gender biasness in family; child labour; enhanced frequency of violence, crime and injustice to them. An effort has been granted in current review article to share the present scenario of women education after 12th standard. The opportunities or amenities they are being provided as well as the challenges or the barriers they are facing in the way of higher studies are discussed in recent paper.

Keywords: education, women education, higher education, scholarships, women studies.

Introduction

Education is the main driving force of a society that compelled a society to move forward. Education helps in character building; it motivates the manifestation of human soul, broadens the mind, light of education makes shower of knowledge upon human. Education plays an important role for all but it is especially significant for women. Without proper education, society has to remain in grave danger.

Giele and Smock (1977) in her 'Women's Roles and Status in Eight Countries' observes:

"Education for women has both microscopic and macroscopicimplication that is education may transform that attitude and self image of the individual women while on a social level it often alters the balance in male-female roles and widens sphere of permissible feminine activities"

Gmail

Search mail

Remittance voucher - sinhanayek@gmail.com - Gmail

(4)

Compose

Inbox 45

Starred

Snoozed

Sent

Drafts 9

More

MOUMITA +

No recent chats
Start a new one

Environment and Ecology
to me

Dear Colleague

The payment information is received for your Paper No. MR 4216

Your paper is tentatively scheduled for journal volume.37(3B) 2019.

Note: Please do not write separate email every time regarding same MR no. and always reply to this same email conversa No.

Journal is enlisted in UGC and NAAS
NAAS Rating = 4.18

Editor
Environment and Ecology
Website: www.environmentandecology.com

1/1

Scientific and Environmental Research Institute

Date: 08th August 2018

To
Moumita Sinha, Sabyasachi Mukhopadhyay, Trisha Biswas

Dear Author,

I am pleased to inform you that your paper titled **"Evaluation Of Physico-Chemical Properties Of Agro-Field Soil Alongside Barakar Road Near Bongabari Krishak Bazar, Purulia District, W.B. (India)"** has been **selected** by the Editorial Board and will be published in the book titled "Recent Trends in Agriculture, Environment, Sustainability and Life Sciences" with ISBN 978-81-8914-059-5.

We shall inform you after the publication.

Wish you a best of luck.

Dr. Tanmoy Rudra
Mobile: 9831446832

Scientific and Environmental Research Institute
42, Station Road, Rahara, Kolkata- 700118, West Bengal, INDIA
Telephone: +91 33 2568 0277 **Mob:** +91 9830063122
E-mail: seri.inst@gmail.com **Web:** www.seri.org.in

Quasigroups and Related Systems **26** (2018), 251 – 262

On irreducible pseudo-prime spectrum of topological le-modules

Manas Kumbhakar and Anjan Kumar Bhuniya

Abstract. An le-module M over a ring R is a complete lattice ordered additive monoid having the greatest element e together with a module like action of R. A proper submodule element n of ${}_RM$ is called *pseudo-prime* if $(n : e) = \{r \in R : re \leqslant n\}$ is a prime ideal of R. In this article we introduce the *Zariski topology* on the set X_M of all pseudo-prime submodule elements of M and discuss interplay between topological properties of the Zariski topology on X_M and algebraic properties of M. If ${}_RM$ is pseudo-primeful, then irreducibility of X_M and $\mathrm{Spec}(R/Ann(M))$ are equivalent. Also there is a one-to-one correspondence between the irreducible components of X_M and the minimal pseudo-prime submodule elements in M. We show that if R is a Laskerian ring then X_M has only finitely many irreducible components.

1. Introduction

Inspired by the theory of multiplicative lattices [1], [17], [18], [19], [20], and lattice modules [7], [8], [9], [10], [11], [14], [21], we introduced the notion of le-modules in [2]. An le-module is a complete lattice ordered monoid endowed with a module like action of a commutative ring. Motivation behind introducing this new notion is to create a new avenue similar to what we do in module theory for studying commutative rings. In [2] and [12] we find several results on the interplay between properties of an le-module M and properties of the ring R acting on M. We considered uniqueness of primary decompositions of the primary submodule elements in a Laskerian le-module in [2].

In this article, we introduce the Zariski topology on the set X_M of all pseudo-prime submodule elements of an le-module M over a commutative ring R. Inspiration comes from the enlightening interplay between the Zariski topology on the prime spectrum $\mathrm{Spec}(R)$ of a commutative ring R and the ring theoretic properties of R [6], [13], [15], [16]; and interplay between the Zariski topology on the pseudo-prime spectrum of a module A over R and the algebraic properties of ${}_RA$ and R [4], [5]. Besides basic characterizations of the Zariski topology on X_M, we find several conditions on M under which X_M may be an irreducible topological space.

The organization of this article is as follows. This introduction is followed by

2010 Mathematics Subject Classification: 54B35, 54B99, 13C05, 13C99, 06F25.
Keywords: pseudo-prime element, Zariski topology, topological le-module, irreducible space.

a section to recap definition and basic properties of le-modules. Also we recall a few notions on rings. In Section 3, we introduce the *Zariski topology* on X_M and characterize its basic properties. We show that X_M is always T_0 and it is T_1 if and only if each pseudo-prime submodule element of ${}_RM$ is maximal in X_M. Annihilator of M is an ideal of R, which induces a natural mapping ψ from X_M into $\mathrm{Spec}(R/Ann(M))$. Interplay of the properties of X_M and $Spec(R/Ann(M))$ is reflected prominently in the nature of this natural map ψ. Here we show that if ψ is surjective, then connectedness of X_M implies the connectedness of $\mathrm{Spec}(R/Ann(M))$. Section 4 characterizes irreducibility of X_M. If ψ is surjective then irreducibility of X_M and $\mathrm{Spec}(R/Ann(M))$ are equivalent. As a consequence of the necessary and sufficient characterization of the irreducible closed subsets, presented here, we establish a bijective correspondence between the irreducible components of X_M and the minimal pseudo-prime submodule elements of ${}_RM$. Also we prove that if a ring R is Laskerian then for every le-module ${}_RM$, the pseudo-prime spectrum X_M has only finitely many irreducible components.

2. Preliminaries

In this article, every ring R is commutative and contains 1; and $\mathbb{N}$ denotes the set of all natural numbers. An *le-semigroup* $(M, +, \leqslant, e)$ is such that $(M, \leqslant)$ is a complete lattice with the greatest element e, $(M, +)$ is a commutative monoid with the zero element 0_M and for all $m, m_i \in M, i \in I$ it satisfies

(S) $m + (\vee_{i\in I} m_i) = \vee_{i\in I}(m + m_i)$.

Let R be a ring and $(M, +, \leqslant, e)$ be an le-semigroup. Then M is called an *le-module* over R if there is a mapping $R \times M \longrightarrow M$ which satisfies

(M1) $r(m_1 + m_2) = rm_1 + rm_2$,

(M2) $(r_1 + r_2)m \leqslant r_1m + r_2m$,

(M3) $(r_1r_2)m = r_1(r_2m)$,

(M4) $1_Rm = m$; $\quad 0_Rm = r0_M = 0_M$,

(M5) $r(\vee_{i\in I}(m_i)) = \vee_{i\in I}(rm_i)$,

for all $r, r_1, r_2 \in R$ and $m, m_1, m_2, m_i \in M$, and $i \in I$.

We denote an le-module M over R by ${}_RM$ or by M. From $(M5)$, we have,

(M5)$'$ $m_1 \leqslant m_2 \Rightarrow rm_1 \leqslant rm_2$, for all $r \in R$ and $m_1, m_2 \in M$.

An element n of M is said to be a *submodule element* if $n + n, rn \leqslant n$, for all $r \in R$. We call a submodule element n proper if $n \neq e$. Note that $0_M = 0_Rn \leqslant n$, for every submodule element n of M. Also $n + n = n$, i.e., every submodule element of M is an idempotent. Let $\{n_i\}_{i\in I}$ be a family of submodule elements of M. Then their sum is defined by:

$$\sum_{i\in I} n_i = \bigvee\{(n_{i_1} + n_{i_2} + \cdots + n_{i_k}) : k \in \mathbb{N}, and\ \ i_1, i_2, \cdots, i_k \in I\}.$$

It is easy to check that $\sum_{i\in I} n_i$ is a submodule element of M.

For an ideal I of R, we define

$$Ie = \bigvee\{\sum_{i=1}^{k} a_i e : k \in \mathbb{N}; a_1, a_2, \cdots, a_k \in I\}$$

Then Ie is a submodule element of M. Also for any two ideals I and J of R, $I \subseteq J$ implies that $Ie \leqslant Je$.

Let n be a submodule element of M. We denote

$$(n : e) = \{r \in R : re \leqslant n\}.$$

Then $(n : e)$ is an ideal of R. For any two submodule elements n, l of M, $n \leqslant l$ implies that $(n : e) \subseteq (l : e)$. Also if $\{n_i\}_{i\in I}$ is an arbitrary family of submodule elements in ${}_RM$, then $(\wedge_{i\in I} n_i : e) = \cap_{i\in I}(n_i : e)$. For every submodule element n of ${}_RM$ and ideal I of R, $Ie \leqslant n$ if and only if $I \subseteq (n : e)$. This result, proved in [2], is useful here.

A proper submodule element n of an le-module ${}_RM$ is called a *pseudo-prime submodule element* if $(n : e)$ is a prime ideal of R. The *pseudo-prime spectrum* of ${}_RM$ is the set of all pseudo-prime submodule elements of M and it is denoted by X_M. A pseudo-prime submodule element p of M is said to be *maximal* if for any pseudo-prime submodule element q of M, $p \leqslant q$ implies $p = q$. Minimal pseudo-prime submodule elements are defined dually. A submodule element n of M is said to be *pseudo-semiprime* if n is a meet of some pseudo-prime submodule elements of M. A pseudo-prime submodule element p of M is called *extraordinary* if for any two pseudo-semiprime submodule elements n and l of M, $n \wedge l \leqslant p$ implies that either $n \leqslant p$ or $l \leqslant p$. An le-module ${}_RM$ is said to be *topological* if $X_M = \emptyset$ or every pseudo-prime submodule element of M is extraordinary.

For every submodule element n of M, we denote

$$V(n) = \{l \in X_M : n \leqslant l\}.$$

The following result have some use in this article.

Lemma 2.1. (cf. [12]) *Let ${}_RM$ be an le-module. Then for any ideals I and J of R, $V((IJ)e) = V(Ie) \cup V(Je) = V((I \cap J)e)$.*

Now we recall some notions from rings. We denote the set of all prime ideals of R by $\mathrm{Spec}(R)$. A topology, known as the *Zariski topology* is defined on $\mathrm{Spec}(R)$. The closed sets in the Zariski topology on $\mathrm{Spec}(R)$ are of the form

$$V^R(I) = \{P \in Spec(R) : I \subseteq P\}$$

There are many useful characterizations associating arithmetical properties of R and topological properties of $\mathrm{Spec}(R)$ [13], [15], [16].

3. Pseudo-prime spectrum of topological le-modules

Here we introduce a topology on X_M analogous to the Zariski topology on the set of all pseudo-prime submodules of a module over a ring.

Lemma 3.1. *Let ${}_RM$ be an le-module. Then*

(*i*) $V(0_M) = X_M$.

(*ii*) $V(e) = \emptyset$.

(*iii*) $\cap_{i\in I}V(n_i)=V(\sum_{i\in I} n_i)$ *for any family of submodule elements* $\{n_i\}_{i\in I}$ *of* M.

Proof. (*i*) and (*ii*) are obvious.
(*iii*). We have $V(\sum_{i\in I} n_i) \subseteq V(n_i)$ for each $i \in I$, and hence $V(\sum_{i\in I}(n_i)) \subseteq \cap_{i\in I}V(n_i)$. Now let $p \in \cap_{i\in I}V(n_i)$. Then $n_i \leqslant p$ for all $i \in I$ implies that $\sum_{i\in I} n_i \leqslant p$, and so $p \in V(\sum_{i\in I}(n_i))$. Thus $\cap_{i\in I}V(n_i) \subseteq V(\sum_{i\in I} n_i)$. Consequently, $\cap_{i\in I}V(n_i) = V(\sum_{i\in I} n_i)$. □

Let us denote

$$\mathcal{V}_R(M) = \{V(n)\colon\ n \text{ is a submodule element of } M\}.$$

In general, $\mathcal{V}_R(M)$ is not closed under finite unions. If $\mathcal{V}_R(M)$ is closed under finite unions, then the le-module ${}_RM$ is called a *top le-module* [12]. Thus an le-module ${}_RM$ is a *top le-module* if and only if for every submodule elements n, l of M there is a submodule element k of M such that $V(n) \cup V(l) = V(k)$. Also we assume that every le-module ${}_RM$ such that $X_M = \emptyset$ is a top le-module. Following result shows that the classes of top and topological le-modules are same and establishes an useful characterization of the le-modules in this class.

Theorem 3.2. *The following statements are equivalent for an le-module* ${}_RM$.

(*i*) ${}_RM$ *is a top le-module.*

(*ii*) *Every pseudo-prime submodule element of* M *is extraordinary.*

(*iii*) $V(n) \cup V(l) = V(n \wedge l)$, *for any pseudo-semiprime submodule elements* n *and* l *of* M.

Proof. If $X_M = \emptyset$ then the results hold trivially. Suppose $X_M \neq \emptyset$.
$(i) \Rightarrow (ii)$. Let p be any pseudo-prime submodule element of M and let n and l be two pseudo-semiprime submodule elements of M such that $n \wedge l \leqslant p$. Since ${}_RM$ is a top le-module, there exists a submodule element k of M such that $V(n) \cup V(l) = V(k)$. Now $n = \wedge p_i$, for some collection of pseudo-prime submodule elements p_i of M. Then $n \leqslant p_i$ implies that $p_i \in V(n) \subseteq V(k)$ for each $i \in I$. It follows that $k \leqslant p_i$ for each $i \in I$ and hence $k \leqslant n$. Similarly $k \leqslant l$. Thus $k \leqslant n \wedge l$ which implies that $V(n \wedge l) \subseteq V(k)$. Now $V(n) \cup V(l) \subseteq V(n \wedge l) \subseteq V(k) = V(n) \cup V(l)$. So, $V(n) \cup V(l) = V(n \wedge l)$. Also $p \in V(n \wedge l) = V(n) \cup V(l)$ shows that either

$p \in V(n)$ or $p \in V(l)$, i.e., either $n \leqslant p$ or $l \leqslant p$. Hence p is extraordinary.

$(ii) \Rightarrow (iii)$. Let n and l be two pseudo-semiprime submodule elements of M. We have $V(n) \cup V(l) \subseteq V(n \wedge l)$. Let $p \in V(n \wedge l)$. Then p is a pseudo-prime submodule element and $n \wedge l \leqslant p$. Since p is extraordinary, either $n \leqslant p$ or $l \leqslant p$, equivalently, either $p \in V(n)$ or $p \in V(l)$. Hence $p \in V(n) \cup V(l)$. Consequently, $V(n) \cup V(l) = V(n \wedge l)$.

$(iii) \Rightarrow (i)$. Let n and l be any two submodule elements of M. If $V(n) = \emptyset$, then $V(n) \cup V(l) = V(l)$ and the result holds. Assume that both $V(n)$ and $V(l)$ are nonempty. Then $V(n) \cup V(l) = V(\wedge_{p \in V(n)} p) \cup V(\wedge_{p \in V(l)} p) = V((\wedge_{p \in V(n)} p) \wedge (\wedge_{p \in V(l)} p))$, by (iii). Thus ${}_RM$ is a top le-module. □

From the equivalence of (i) and (ii) in the above result, we have:

Corollary 3.3. *An le-module ${}_RM$ is a top le-module if and only if it is a topological le-module.*

Thus in view of Lemma 3.1, it follows that $\mathcal{V}_R(M)$ satisfies the axioms of a topological space for the closed subsets if and only if ${}_RM$ is topological. If ${}_RM$ is a topological le-module, then this topology is said to be the *Zariski topology* on X_M.

Henceforth, in this article, we assume that every le-module ${}_RM$ is a topological le-module.

Recall that a topological space X is T_1 if and only if every singleton subset of X is a closed subset. For each subset Y of X_M, we denote the closure of Y in X_M by $\overline{Y}$, and meet of the elements of Y by $\Im(Y)$, i.e., $\Im(Y) = \wedge_{p \in Y} p$. If $Y = \emptyset$, then we take $\Im(Y) = e$.

A subset Y of a topological space X is called *dense* in X if Y has non-empty intersection with every non-empty open subset of X. Equivalently, Y is dense in X if and only if $\overline{Y} = X$.

Proposition 3.4. *Let ${}_RM$ be an le-module and $Y \subseteq X_M$.*

- (i) *Then $\overline{Y} = V(\Im(Y))$. Hence Y is closed if and only if $Y = V(\Im(Y))$. In particular, $\overline{\{l\}} = V(l)$, for every $l \in X_M$.*
- (ii) *If $0_M \in Y$, then Y is dense in X_M.*
- (iii) *X_M is a T_0-space.*
- (iv) *X_M is a T_1-space if and only if each pseudo-prime submodule element of M is a maximal element in X_M.*

Proof. (i). Clearly $Y \subseteq V(\Im(Y))$. Let $V(n)$ be any closed subset of X_M containing Y. Since $\Im(V(n)) \leqslant \Im(Y)$, we have $V(\Im(Y)) \subseteq V(\Im(V(n))) = V(n)$. Thus $V(\Im(Y))$ is the smallest closed subset of X_M containing Y. Hence, $\overline{Y} = V(\Im(Y))$.

(ii). This is clear by (i).

(iii). Let n and l be two distinct elements of X_M. Then by (i),

$$\overline{\{n\}} = V(n) \neq V(l) = \overline{\{l\}}.$$

Now by the fact that a topological space is a T_0-space if and only if the closures of distinct elements are distinct, we conclude that X_M is a T_0-space.

(iv). Let X_M be a T_1-space and let p be a pseudo-prime submodule element of M. Then $\{p\}$ is closed, hence

$$\{p\} = \overline{\{p\}} = V(p), \text{ by } (i).$$

Thus p is a maximal element in X_M.

Conversely, suppose p is a maximal element in X_M, then by (i), we have

$$\overline{\{p\}} = V(p) = \{p\}.$$

Thus $\{p\}$ is closed and hence X_M is a T_1-space. □

Let ${}_RM$ be an le-module. Then the ideal $(0_M : e)$ of R is called the *annihilator* of M. It is denoted by $Ann(M)$. Thus

$$Ann(M) = \{r \in R : re \leqslant 0_M\} = \{r \in R : re = 0_M\}.$$

Consider the canonical epimorphism $\phi : R \to R/Ann(M)$. The image of every element r and every ideal I of R such that $Ann(M) \subseteq I$ under $\phi : R \to R/Ann(M)$ will be denoted by $\overline{r}$ and $\overline{I}$ respectively. It is well known in quotient rings that for every prime ideal P of R such that $Ann(M) \subseteq P$, the ideal $\overline{P} = P/Ann(M)$ is prime in $\overline{R} = R/Ann(M)$. Hence the mapping $\psi : X_M \to Spec(\overline{R})$ defined by

$$\psi(p) = \overline{(p : e)} \text{ for every } p \in X_M$$

is well defined. We call ψ the *natural map* on X_M. An le-module ${}_RM$ is called *pseudo-primeful* if either $M = 0_M$ or $M \neq 0_M$ and the natural map ψ is surjective. Also ${}_RM$ is called *pseudo-injective* if the natural map ψ is injective.

Recall that if I is an ideal of a ring R, then the *radical* of I is defined by

$$\text{Rad}(I) = \{a \in R : a^n \in I, \text{for some positive integer } n\}$$

Since R is commutative $\text{Rad}(I)$ is also an ideal of R and $I \subseteq Rad(I)$. Also $\text{Rad}(I)$ is the intersection of all prime ideals P such that $I \subseteq P$. An ideal I of R is called a *radical ideal* if $I = Rad(I)$.

Proposition 3.5. *Let ${}_RM$ be a nonzero pseudo-primeful le-module and I be a radical ideal of R. Then $(Ie : e) = I$ if and only if $Ann(M) \subseteq I$. In particular, Pe is pseudo-prime submodule element of M for every prime ideal P of R containing $Ann(M)$.*

Proof. Assume that $Ann(M) \subseteq I$. Since I is a radical ideal, $Ann(M) \subseteq I = \cap_{I \subseteq P_i} P_i$, where P_i are prime ideals of R. Since ${}_RM$ is a pseudo-primeful le-module and $Ann(M) \subseteq P_i$, there exists a pseudo-prime submodule element p_i of M such that $(p_i : e) = P_i$. Therefore $I \subseteq (Ie : e) = ((\cap_{I \subseteq P_i} P_i)e : e) \subseteq \cap_{I \subseteq P_i}(P_i e : e) = \cap_{I \subseteq P_i} P_i = I$. Hence $(Ie : e) = I$. □

It is well known that the prime spectrum $\mathrm{Spec}(R)$ of a ring R is connected if and only if R contains no idempotents other than 0 and 1 [3]. Now we have the following:

Theorem 3.6. *Let ${}_RM$ be a pseudo-primeful le-module and the pseudo-prime spectrum X_M be connected. Then Spec$(\overline{R})$ is connected and hence the ring $\overline{R}$ contains no idempotents other than $\overline{0}$ and $\overline{1}$.*

Proof. First we show that the natural map $\psi : X_M \to Spec(\overline{R})$ is continuous. Let I be an ideal of R such that $Ann(M) \subseteq I$ and $p \in \psi^{-1}(V^{\overline{R}}(\overline{I}))$. Then there exists $\overline{J} \in V^{\overline{R}}(\overline{I})$ such that $\psi(p) = \overline{J}$, i.e, $\overline{(p:e)} = \overline{J}$. This implies that $(p:e) = J \supseteq I$ and so $Ie \leqslant (p:e)e \leqslant p$. Hence $p \in V(Ie)$. Therefore $\psi^{-1}(V^{\overline{R}}(\overline{I})) \subseteq V(Ie)$. Now let $q \in V(Ie)$. Then $I \subseteq (Ie:e) \subseteq (q:e)$ implies that $\overline{I} \subseteq \overline{(q:e)}$. Hence $q \in \psi^{-1}(V^{\overline{R}}(\overline{I}))$. Thus $V(Ie) \subseteq \psi^{-1}(V^{\overline{R}}(\overline{I}))$. Therefore $\psi^{-1}(V^{\overline{R}}(\overline{I})) = V(Ie)$. Hence ψ is continuous. Thus the theorem follows from the fact that the map ψ is surjective and the continuous image of a connected set is connected. □

4. Irreducible pseudo-prime spectrum

A topological space X is *irreducible* if and only if for every pair of closed subsets Y_1, Y_2 of X, $X = Y_1 \cup Y_2$ implies $X = Y_1$ or $X = Y_2$. A nonempty subset Y of a topological space X is called an *irreducible subset* if the subspace Y of X is irreducible. An *irreducible component* of a topological space X is a maximal irreducible subset of X. A subset Y of X is irreducible if and only if its closure $\overline{Y}$ is irreducible. Thus irreducible components of X are closed. Since every singleton subset of X_M is irreducible, its closure is also irreducible.

The following result is a direct consequence of Proposition 3.4(i) and hence we omit the proof.

Lemma 4.1. *$V(l)$ is an irreducible closed subset of X_M for every pseudo-prime submodule element l of an le-module ${}_RM$.*

Theorem 4.2. *Let ${}_RM$ be a nonzero pseudo-primeful le-module. Then the following statements are equivalent:*

(i) *X_M is an irreducible space;*

(ii) *Spec$(\overline{R})$ is an irreducible space;*

(iii) *$V^R(Ann(M))$ is an irreducible space;*

(iv) *$Rad(Ann(M))$ is a prime ideal of R;*

(v) *$X_M = V(Ie)$ for some $I \in V^R(Ann(M))$.*

Proof. $(i) \Rightarrow (ii)$. In the proof of Theorem 3.6, we have seen that the mapping $\psi : X_M \to Spec(\overline{R})$ is continuous. Thus (ii) follows from the fact that ψ is surjective and continuous image of an irreducible space is irreducible.

$(ii) \Rightarrow (iii)$. Note that the mapping $\phi : Spec(\overline{R}) \to Spec(R)$ defined by $\overline{P} \mapsto P$ is a homeomorphism. Hence $V^R(Ann(M))$ is an irreducible space.

$(iii) \Rightarrow (iv)$. Obvious.

$(iv) \Rightarrow (v)$. Assume that $\mathrm{Rad}(Ann(M))$ is a prime ideal of R. Then by Proposition 3.5, $(Rad(Ann(M)))e$ is a pseudo-prime submodule element of M. Let $p \in X_M$. Then $Rad(Ann(M)) \subseteq (p : e)$ which implies that $(Rad(Ann(M)))e \leqslant (p : e)e \leqslant p$. Thus $p \in V((Rad(Ann(M)))e)$ and hence $X_M = V(Ie)$, where $I = Rad(Ann(M)) \in V^R(Ann(M))$.

$(v) \Rightarrow (i)$. This is a direct consequence of the Proposition 3.5 and Lemma 4.1. □

For a submodule element n of M, the *pseudo-prime radical* of n, denoted by $\mathbb{P}rad(n)$, is the meet of all pseudo-prime submodule elements of M containing n, that is,

$$\mathbb{P}rad(n) = \wedge_{p \in V(n)} p.$$

If $V(n) = \emptyset$, then we set $\mathbb{P}rad(n) = e$. Note that $n \leqslant \mathbb{P}rad(n)$ and that $\mathbb{P}rad(n) = e$ or $\mathbb{P}rad(n)$ is a pseudo-semiprime submodule element of M. Also $V(n) = V(\mathbb{P}rad(n))$. A submodule element n of M is said to be a *pseudo-prime radical submodule element* if $n = \mathbb{P}rad(n)$.

It is well-known that in a ring R, a subset Y of $\mathrm{Spec}(R)$ is irreducible if and only if $\Im(Y)$ is a prime ideal of R [3]. The next theorem is a analogue of this fact for topological le-modules.

Theorem 4.3. *Let ${}_RM$ be an le-module and $Y \subseteq X_M$. Then $\Im(Y)$ is a pseudo-prime submodule element of M if and only if Y is irreducible in X_M.*

Proof. Let Y be irreducible, I and J be two ideals of R such that $IJ \subseteq (\Im(Y) : e)$. Then $(IJ)e \leqslant \Im(Y)$. Now, we have

$$Y \subseteq V(\Im(Y)) \subseteq V((IJ)e) = V(Ie) \cup V(Je), \text{ by Lemma 2.1.}$$

Since Y is irreducible, so either $Y \subseteq V(Ie)$ or $Y \subseteq V(Je)$. Hence, either $Ie \leqslant (\mathbb{P}rad(Ie)) = \Im(V(Ie)) \leqslant \Im(Y)$ or $Je \leqslant (\mathbb{P}rad(Je)) = \Im(V(Je)) \leqslant \Im(Y)$. This implies that $I \subseteq (\Im(Y) : e)$ or $J \subseteq (\Im(Y) : e)$. Thus $\Im(Y)$ is a pseudo-prime submodule element of M.

Conversely let $\Im(Y)$ be a pseudo-prime submodule element of M and let $Y \subseteq Y_1 \cup Y_2$, where Y_1 and Y_2 are two closed subset of X_M. Then there exist submodule elements n and l of M such that $Y_1 = V(n)$ and $Y_2 = V(l)$. Hence

$$\mathbb{P}rad(n) \wedge \mathbb{P}rad(l) = \Im(V(n)) \wedge \Im(V(l)) = \Im(V(n) \cup V(l)) = \Im(Y_1 \cup Y_2) \leqslant \Im(Y).$$

Since ${}_RM$ is a topological le-module, $\Im(Y)$ is an extraordinary submodule element. Hence, We have $\imath rad(n) \leqslant \Im(Y)$ or $\mathbb{P}rad(l) \leqslant \Im(Y)$. Thus $Y \subseteq V(\Im(Y)) \subseteq V(\mathbb{P}rad(n)) = V(n) = Y_1$ or $Y \subseteq Y_2$. Therefore Y is irreducible. □

For every $I \in Spec(R)$, we denote

$$X_{M,I} = \{p \in X_M : (p : e) = I\}.$$

Corollary 4.4. *Let ${}_RM$ be an le-module, n be a submodule element of M and $I \in Spec(R)$. Then*

(*i*) *$V(n)$ is irreducible in X_M if and only if $\mathbb{P}rad(n)$ is a pseudo-prime submodule element of M.*

(*ii*) *X_M is an irreducible topological space if and only if $\mathbb{P}rad(0_M)$ is a pseudo-prime submodule element of M.*

(*iii*) *If $X_{M,I} \neq \emptyset$ then $X_{M,I}$ is an irreducible space.*

Proof. (*i*). Since $\mathbb{P}rad(n) = \Im(V(n))$, the result follows from Theorem 4.3.

(*ii*). This is obvious.

(*iii*). We have $(\Im(X_{M,I}) : e) = (\wedge_{p \in X_{M,I}} p : e) = \cap_{p \in X_{M,I}}(p : e) = I \in \mathrm{Spec}(R)$ and hence the result follows from Theorem 4.3. □

Corollary 4.5. *Let ${}_RM$ be an le- module such that $0_M \in X_M$. Then X_M is an irreducible space.*

Let Y be closed subset of a topological space X. An element $y \in Y$ is called a *generic point* of Y if $Y = \overline{\{y\}}$. In Proposition 3.4, we have seen that every element l of X_M is a generic point of the irreducible closed subset $V(l)$. The next theorem shows that the irreducible closed subset of X_M are determined completely by the pseudo-prime submodule elements of M. Also there is a one-to-one correspondence between the set of minimal pseudo-prime submodule elements of M and the set of irreducible components of X_M.

Theorem 4.6. *Let ${}_RM$ be an le-module and $Y \subseteq X_M$.*

(*i*) *Then Y is an irreducible closed subset of X_M if and only if $Y = V(p)$ for some $p \in X_M$. Thus every irreducible closed subset of X_M has a generic point.*

(*ii*) *The correspondence $V(p) \mapsto p$ is a bijection of the set of all irreducible components of X_M onto the set of all minimal pseudo-prime submodule elements of M.*

Proof. (*i*). Let Y be an irreducible closed subset of X_M. Then there exists a submodule element n of M such that $Y = V(n)$. By Theorem 4.3,

$$\Im(Y) = \Im(V(n)) = \mathbb{P}rad(n) \in X_M.$$

Hence $Y = V(n) = V(\mathbb{P}rad(n))$. Converse part follows from the Lemma 4.1.

(ii). Let Y be an irreducible component of X_M. Then Y is an irreducible closed subset of X_M and so by (i), we have $Y = V(p)$ for some $p \in X_M$. Since each irreducible component is a maximal irreducible closed subset, $V(p)$ is a maximal irreducible closed subset of X_M. Let q be a pseudo-prime submodule element of M such that $q \leqslant p$. Then $V(q)$ is an irreducible closed subset and $V(p) \subseteq V(q)$ implies that $V(p) = V(q)$. Thus $p = q$. Hence p is a minimal element of X_M.

Now let p be a minimal element of X_M. Then by Corollary 4.1, $V(p)$ is an irreducible closed subset of X_M. Let $V(p) \subseteq V(q)$ for some $q \in X_M$. Then

$$q = \mathbb{P}rad(q) = \Im(V(q)) \leqslant \Im(V(p)) = \mathbb{P}rad(p) = p,$$

and hence $p = q$. Therefore $V(p) = V(q)$. Thus $V(p)$ is an irreducible component of X_M. □

Theorem 4.7. *Let ${}_RM$ be a pseudo-primeful le-module. Then the mapping $\phi : V(p) \mapsto \overline{(p : e)}$ is a bijection from the set of all irreducible components of X_M onto the set of all minimal prime ideals of $\overline{R}$.*

Proof. Let $V(p)$ be an irreducible component of X_M. Then by Theorem 4.6(ii), p is a minimal pseudo-prime submodule element of M and so $(p : e)/Ann(M)$ is a prime ideal of $\overline{R}$. We show that $(p : e)/Ann(M)$ is a minimal prime ideal of $\overline{R}$. Let $J/Ann(M) \in Spec(R/Ann(M))$ be such that $J/Ann(M) \subseteq (p : e)/Ann(M)$. Then $Je \leqslant (p : e)e \leqslant p$. Since ${}_RM$ is pseudo-primeful and Je is a proper submodule element of M, Je is a pseudo-prime submodule element of M with $(Je : e) = J$, by Proposition 3.5. By the minimality of p, $Je = p$ and hence $(p : e)/Ann(M) = J/Ann(M)$. Thus $(p : e)/Ann(M)$ is a minimal prime ideal of $\overline{R}$. Thus ϕ is well-defined.

Now suppose that $P/Ann(M)$ is a minimal prime ideal of $R/Ann(M)$. Then by Proposition 3.5, $(Pe : e) = P$ and Pe is a pseudo-prime submodule element of M. To show Pe is a minimal pseudo-prime submodule element of M let $q \leqslant Pe$ for some pseudo-prime submodule element q of M. Then $(q : e)/Ann(M) \subseteq (Pe : e)/Ann(M) = P/Ann(M)$. By the minimality of $P/Ann(M)$ we have $(q : e)/Ann(M) = P/Ann(M)$ and so $(q : e) = P$. Thus $Pe = (q : e)e \leqslant q \leqslant Pe$ which implies that $q = Pe$. Hence Pe is a minimal pseudo-prime submodule element of M. Therefore $V(Pe)$ is a irreducible component of X_M by Theorem 4.6(ii). Thus ϕ is a surjection. Now let $V(p)$ and $V(q)$ be two irreducible components of X_M such that $\overline{(p : e)} = \overline{(q : e)}$. Then by Theorem 4.6$(ii)$, both p and q are minimal pseudo-prime submodule elements of M. It follows from $\overline{(p : e)} = \overline{(q : e)}$ that $(p : e) = (q : e)$ which implies that $(p : e)e \leqslant (q : e)e \leqslant q$. Now by Proposition 3.5, $(p : e)e$ is a pseudo-prime submodule element, and hence, by the minimality of q, $(p : e)e = q$. Then $q \leqslant p$ and so $q = p$. Therefore, $V(p) = V(q)$. Hence ϕ is an injection. □

A ring R is called *Laskerian* if every proper ideal of R has a primary decomposition. In the following result we show that if R is a Laskerian ring then the irreducible components of X_M are precisely determined by the primary decomposition of the ideal $\mathrm{Ann}(M)$ of R and they are finite in numbers.

Theorem 4.8. *Let ${}_RM$ be a nonzero pseudo-primeful le-module. Then the following statements hold:*

(*i*) *The set of all irreducible components of X_M is of the form*

$$T = \{V(Ie) : I \text{ is a minimal element of } V^R(Ann(M)).$$

(*ii*) *If R is a Laskerian ring then X_M has only finitely many irreducible components.*

Proof. (i). Let Y be an irreducible component of X_M. Then by Theorem 4.6(i), $Y = V(n)$ for some $n \in X_M$. Now $(n : e)$ is a prime ideal of R containing $\mathrm{Ann}(M)$ so by Proposition 3.5, $(n : e)e$ is a pseudo-prime submodule element of M. Also $(n : e)e \leqslant n$ implies that $Y = V(n) \subseteq V((n : e)e)$. Since Y is irreducible component of X_M, $V(n) = V((n : e)e)$. Thus $(n : e)e = n$. We show that $(n : e)$ is a minimal element of $V^R(Ann(M))$. Let $J \in V^R(Ann(M))$ be such that $J \subseteq (n : e)$. Then $J/Ann(M) \in Spec(R/Ann(M))$. Since ${}_RM$ is a pseudo-primeful le-module, there exists $l \in X_M$ such that $(l : e) = J$. Also $(l : e)e$ is a pseudo-prime submodule element of M, by Proposition 3.5. Then $Y = V(n) \subseteq V((l : e)e)$ and so $V(n) = V((l : e)e)$, since Y is irreducible component. Thus $n = (l : e)e \leqslant l$ which implies that $(n : e) \subseteq (l : e) = J \subseteq (n : e)$. Hence $(n : e) = J$.

Now let $Y \in T$. Then there exists a minimal element J of $V^R(Ann(M))$ such that $Y = V(Je)$. Since ${}_RM$ is a pseudo-primeful le-module, Je is a pseudo-prime submodule element of M and $(Je : e) = J$, by Proposition 3.5. Thus $V(Je)$ is an irreducible space, by Lemma 4.1. Let $Y = V(Je) \subseteq V(l)$ for some $l \in X_M$. Then $Je \in V(l)$ implies that $l \leqslant Je$ which implies that $(l : e) \subseteq (Je : e) = J$. By the minimality of J we have $(l : e) = J$. Thus $Je = (l : e)e \leqslant l$ and so $V(l) \subseteq V(Je)$. Hence $Y = V(Je) = V(l)$ and so Y is an irreducible component of X_M.

(ii). Let R be a Laskerian ring then every proper ideal of R has a primary decomposition. Let I be a minimal element of $V^R(Ann(M))$ and $Ann(M) = \cap_{i=1}^{n} Q_i$ is a minimal primary decomposition. Then there exists $1 \leqslant i \leqslant n$ such that $Q_i \subseteq I$ and hence by minimality of I we have $I = Rad(Q_i)$. Thus irreducible components of X_M are $V(Rad(Q_i)e)$, by (i). □

References

[1] **D.D. Anderson**, *Multiplicative lattices*, Dissertation, University of Chicago, (1974).

[2] **A.K. Bhuniya and M. Kumbhakar**, *Uniqueness of primary decompositions in Laskerian le-modules*, https://www.researchgate.net/publication/326342684.

[3] **N. Bourbaki**, *Commutative Algebra*, Springer-Verlag, (1998).

[4] **D. Hassanzadeh-Lelekaami and H. Roshan-Shekalgourabi**, *Pseudo-prime submodules of modules*, Math. Reports **18(68)** (2016), 591 – 608.

[5] **D. Hassanzadeh-Lelekaami and H. Roshan-Shekalgourabi**, *Topological dimension of pseudo-prime spectrum of modules*, Commun. Korean. Math. Soc. **32** (2017), 553 – 563.

[6] **M. Hochster**, *Prime ideal structure in commutative rings*, Trans. Amer. Math. Soc. **137** (1969), 43 – 60.

[7] **J.A. Johnson**, *a-adic completion of Noetherian lattice module*, Fund. Math. **66** (1970), 341 – 371.

[8] **J.A. Johnson**, *Quotients in Noetherian lattice modules*, Proc. Amer. Math. Soc. **28(1)** (1971), 71 – 74.

[9] **J. A. Johnson**, *Noetherian lattice modules and semi-local comletions*, Fund. Math. **73** (1971), 93 – 103.

[10] **E.W. Johnson and J.A. Johnson**, *Lattice modules over semi-local Noether lattices*, Fund. Math. **68** (1970), 187 – 201.

[11] **E.W. Johnson and J.A. Johnson**, *Lattice modules over principal element domains*, Commun. Algebra **31** (2003), 3505 – 3518.

[12] **M. Kumbhakar and A.K. Bhuniya**, *Pseudo-prime submodule elements of an le-module*, https://www.researchgate.net/publication/329339509.

[13] **D. Lu and W. Yu**, *On prime spectrum of commutative rings*, Comm. Algebra **34** (2006), 2667 – 2672.

[14] **H.M. Nakkar and D.D. Anderson**, *Associated and weakly associated prime elements and primary decomposition in lattice modules*, Algebra Universalis **25** (1988), 196 – 209.

[15] **J. Ohm and R.L. Pendleton**, *Rings with Noetherian spectrum*, Duke Math. J. **35** (1968), 631 – 639.

[16] **N. Schwartz and M. Tressl**, *Elementary properties of minimal and maximal points in Zariski spectra*, J. Algebra **323** (2010), 2667 – 2672.

[17] **M. Ward**, *Residuation in structures over which a multiplication is defined*, Duke Math. J. **3** (1937), 627 – 636.

[18] **M. Ward**, *Structure residuation*, Ann. Math. **39** (1938), 558 – 568.

[19] **M. Ward and R.P. Dilworth**, *Residuated lattices*, Trans. Amer. Math. Soc. **35** (1939), 335 – 354.

[20] **M. Ward and R.P. Dilworth**, *The lattice theory of Ova*, Ann. Math. Soc. **40(3)** (1939), 600 – 608.

[21] **D.G. Whitman**, *On ring theoretic lattice modules*, Fund. Math. **70** (1971), 221 – 229.

Received August 19, 2018

M. Kumbhakar
Department of Mathematics, Nistarini College, Purulia-723101, India
E-mail: manaskumbhakar@gmail.com

A. K. Bhuniya
Department of Mathematics, Visva-Bharati, Santiniketan-731235, India
E-mail: anjankbhuniya@gmail.com

Acta Math. Hungar.
https://doi.org/10.1007/s10474-019-00928-3

UNIQUENESS OF PRIMARY DECOMPOSITIONS IN LASKERIAN le-MODULES

A. K. BHUNIYA[1] and M. KUMBHAKAR[2,*]

[1]Department of Mathematics, Visva-Bharati, Santiniketan-731235, India
e-mail: anjankbhuniya@gmail.com

[2]Department of Mathematics, Nistarini College, Purulia-723101, India
e-mail: manaskumbhakar@gmail.com

(Received September 27, 2018; revised January 1, 2019; accepted January 3, 2019)

Abstract. We introduce and study a new algebraic structure, which we call le-modules. An le-module M over a commutative ring R is a complete lattice ordered monoid $(M, +, \leqslant, e)$ with greatest element e and module like action of R on it. Our motivation comes from abstract ideal theory and the theory of lattice modules, and with a desire to develop an alternative abstract submodule theory. An le-module M over R abstracts the set of all subsets of a module over R and submodules are characterized as distinguished elements in M. Here we introduce prime and primary elements in an le-module and establish two uniqueness theorems for primary decompositions of a submodule element in a Laskerian le-module.

1. Introduction

The observation by W. Krull [16] that many results in the ideal theory of commutative rings [20] do not depend on the fact that the ideals are composed of elements, leads to abstract ideal theory. Many researchers chose the system, namely lattice ordered semigroups, where an element represents an ideal of the ring as an undivided entity. There are numerous publications dealing with lattice ordered commutative semigroups [3,5,8] and multiplicative lattices [2,7,22,32–34], generalizing commutative ideal theory. Success achieved in abstract ideal theory leads researchers to the theory of lattice modules, introduced by E. W. Johnson and J. A. Johnson [11,14]. A lattice module M is a complete lattice together with an action of a multiplicative

* Corresponding author.

Key words and phrases: le-module, submodule element, prime, radical, primary decomposition.

Mathematics Subject Classification: 13C99, 06F25.

lattice L on M similar to the action of a ring on a module. A lattice module M abstracts the complete lattice $\mathrm{Sub}(A)$ of all submodules of a module A over a ring R and the multiplicative lattice L stands for the lattice of all ideals of the ring R. Johnson and Johnson [11,14] studied Noetherian lattice modules as well as lattice modules over semi-local Noetherian lattice. Localization in lattice modules was considered by Nakkar and Anderson [28]. Whitman defined principal elements in a lattice module and extended Nagata's principle of idealization to lattice modules [36]. Also there are many articles on lattice modules [1,4,11–15,23,24,26,27,35,36].

In this article we introduce a new algebraic structure, namely le-modules over a commutative ring, with a view towards an alternative "abstract submodule theory". To choose an algebraic system, suitable for our purpose, we take care of our two goals. First is to make it possible to distinguish submodules from an ordinary subset of a module, so that it becomes possible to generalize the features of particular types of submodules of a module. Second is to create an avenue to study structure of rings more directly than the existing theory of lattice modules. So we consider an le-module M as if it stands for the lattice $P(A)$ of all subsets of a module A over a ring R and the action considered on M is of the ring R. Since the sum of any two submodules of A induced by the addition in A, is their join in the lattice $\mathrm{Sub}(A)$, consideration of a complete lattice order in a lattice module is sufficient to hold the additive feature of A. But the situation is not similar in the complete lattice $P(A)$, and hence we need to consider an "addition" on $P(A)$ in addition to the complete lattice order $\subseteq$, to catch the additive feature of A. Thus the algebraic system, we choose, is a complete lattice ordered additive monoid M together with an action of a ring R satisfying a set of suitable axioms (see Section 2). This enables us to characterize 'submodules' as distinguished elements in le-modules, namely "submodule elements"; and it becomes possible to generalize the features of particular types of submodules of a module, such as prime submodules, semiprime submodules, primary submodules etc in the framework of le-modules [17–19]. The radical of a submodule element n of ${}_RM$ is defined to be an ideal of the ring R, and so associated primes of n are prime ideals of R. Thus we found direct ways of interaction between rings and le-modules.

This article is organized as follows. In Section 2, we give the definition of an le-module and introduce the notion of submodule elements in le-modules. Also we prove a number of basic results characterizing submodule elements. Section 3 is devoted to characterizing prime and primary submodule elements. We study the primary decomposition of a submodule element and their uniqueness in Section 4.

2. Definition and basic properties of le-modules

Throughout the article, $\mathbb{N}$ denotes the set of all natural numbers and R stands for a commutative ring with 1. For results on rings and modules we refer to [6,20,21,25,30].

An *le-semigroup* $(M, +, \leqslant, e)$ is a commutative monoid with the zero element 0_M which at the same time is a complete lattice with the greatest element e that satisfies

(S) $m + \big(\bigvee_{i\in I} m_i\big) = \bigvee_{i\in I}(m + m_i)$, for all $m, m_i \in M$, $i \in I$.

Definition 2.1. Let $(M, +, \leqslant)$ be an le-semigroup with the zero element 0_M and R be a commutative ring. Then M is called an le-module over R if there is a mapping $R \times M \longrightarrow M$ satisfying

(M1) $r(m_1 + m_2) = rm_1 + rm_2$,

(M2) $(r_1 + r_2)m \leqslant r_1m + r_2m$,

(M3) $(r_1r_2)m = r_1(r_2m)$,

(M4) $1_Rm = m$; $0_Rm = r0_M = 0_M$,

(M5) $r\big(\bigvee_{i\in I} m_i\big) = \bigvee_{i\in I} rm_i$, for all $r, r_1, r_2 \in R$ and $m, m_1, m_2, m_i \in M$ and $i \in I$.

We denote an le-module M over R by ${}_RM$ or by M, whenever possible. From (M5), we have

(M5)′ $m_1 \leqslant m_2 \Rightarrow rm_1 \leqslant rm_2$, for all $r \in R$ and $m_1, m_2 \in M$.

An element n of an le-module M is said to be a *submodule element* if $n + n, rn \leqslant n$, for all $r \in R$. We call n proper if $n \neq e$. Observe that $0_M = 0_Rn \leqslant n$, for every submodule element n of M. We denote $(-1)n = -n$. The readers should note that $-n$ is not additive inverse of n. In spite of $0_Rm = 0_M$, this happens because $(r_1 + r_2)m$ and $r_1m + r_2m$ are in general not equal. For every submodule element n of M, we have $n = -n$, and so $-n$ is also a submodule element of M. Also $n + n = n$, i.e. every submodule element of M is an idempotent.

Let ${}_RM$ be an le-module and n be a submodule element of M. For any element r of R we set,

$$(n : r) = \bigvee\{x \in M : rx \leqslant n\}.$$

Then $(n : r)$ is a submodule element of M. One can check that $n \leqslant (n : r)$ and $r(n : r) \leqslant n$. Also for every $x \in M$ and $r \in R$, $rx \leqslant n$ if and only if $x \leqslant (n : r)$.

Let ${}_RM$ be an le-module. If l is a submodule element of M and $n \in M$, we denote

$$(l : n) = \{r \in R : rn \leqslant l\}$$

Then $(l : n)$ is an ideal of R.

Now we have the following useful results:

PROPOSITION 2.2. *Let ${}_RM$ be an le-module and $x \in M$. Then for submodule elements k, l, n and $\{n_i\}_{i\in I}$ of M,*

(i) $l \leqslant n \Rightarrow (l : x) \subseteq (n : x)$ *and* $(k : n) \subseteq (k : l)$;
(ii) $\left(\bigwedge_{i\in I} n_i : x\right) = \bigcap_{i\in I}(n_i : x)$;
(iii) $((l \wedge n) : k) = (l : k) \cap (n : k)$;
(iv) $(k : l + n) = (k : l) \cap (k : n)$;
(v) $(k : l) \cap (k : n) = (k : l \vee n)$.

PROOF. (i) Let $r \in (l : x)$. Then $rx \leqslant l \leqslant n$ implies that $r \in (n : x)$. So $(l : x) \subseteq (n : x)$. Now let $r \in (k : n)$. Then $rn \leqslant k$ and since $l \leqslant n$, so $rl \leqslant rn \leqslant k$. Thus $r \in (k : l)$. Therefore $(k : n) \subseteq (k : l)$.

(ii) Let $r \in \left(\bigwedge_{i\in I} n_i : x\right)$. Then $rx \leqslant \bigwedge_{i\in I} n_i \leqslant n_i$, for each $i \in I$, implies that $r \in (n_i : x)$, for each $i \in I$. Thus $r \in \bigcap_{i\in I}(n_i : x)$. Now let $r \in \bigcap_{i\in I}(n_i : x)$. Then $r \in (n_i : x)$, for each $i \in I$. Thus $rx \leqslant n_i$, for each $i \in I$, and so $rx \leqslant \bigwedge_{i\in I} n_i$. Therefore $\bigcap_{i\in I}(n_i : x) \subseteq \left(\bigwedge_{i\in I} n_i : x\right)$. Hence $\left(\bigwedge_{i\in I} n_i : x\right) = \bigcap_{i\in I}(n_i : x)$.

(iii) $r \in ((l \wedge n) : k)$ if and only if $rk \leqslant l \wedge n$ if and only if $rk \leqslant l$ and $rk \leqslant n$ if and only if $r \in (l : k)$ and $r \in (n : k)$ if and only if $r \in (l : k) \cap (n : k)$. Thus $((l \wedge n) : k) = (l : k) \cap (n : k)$.

(iv) Let $r \in (k : l + n)$. Then $r(l + n) \leqslant k$, i.e., $rl + rn = r(l + n) \leqslant k$. Now $rl = rl + 0_M \leqslant rl + rn \leqslant k$, (since rn is a submodule element) and $rn = 0_M + rn \leqslant rl + rn \leqslant k$ shows that $r \in (k : l)$ and $r \in (k : n)$. So $r \in (k : l) \cap (k : n)$. Thus $(k : l + n) \subseteq (k : l) \cap (k : n)$. Now let $r \in (k : l) \cap (k : n)$. Then $rl \leqslant k$ and $rn \leqslant k$. Thus $r(l + n) = rl + rn \leqslant k + k = k$,(since k is a submodule element), i.e., $r \in (k : l + n)$. Therefore $(k : l) \cap (k : n) \subseteq (k : l + n)$. Hence $(k : l + n) = (k : l) \cap (k : n)$.

(v) Let $r \in (k : l \vee n)$. Then $rl \vee rn = r(l \vee n) \leqslant k$. Now $rl \leqslant rl \vee rn \leqslant k$ implies that $r \in (k : l)$. Similarly $r \in (k : n)$. Therefore $r \in (k : l) \cap (k : n)$. Thus $(k : l \vee n) \subseteq (k : l) \cap (k : n)$. Now let $r \in (k : l) \cap (k : n)$. Then $rl \leqslant k$ and $rn \leqslant k$. It follows that $rl \vee rn \leqslant k$, i.e., $r(l \vee n) \leqslant k$. So $r \in (k : l \vee n)$. Thus $(k : l) \cap (k : n) \subseteq (k : l \vee n)$. Hence $(k : l) \cap (k : n) = (k : l \vee n)$. □

3. Prime and primary elements

In this section we introduce and characterize the prime and primary elements in an le-module.

DEFINITION 3.1. Let ${}_RM$ be an le-module and n be a proper submodule element of M. Then n is called a primary element of M if for any $a \in R$ and $x \in M$, $ax \leqslant n$ implies that either $x \leqslant n$ or $a^m e \leqslant n$, i.e., either $x \leqslant n$ or $a^m \in (n : e)$, for some $m \in \mathbb{N}$.

Recall that if I is an ideal of a ring R, then

$$\mathrm{Rad}(I) = \big\{ a \in R : a^n \in I, \text{ for some positive integer } n \big\}$$

is an ideal of R and we call $\mathrm{Rad}(I)$ the *radical* of the ideal I in R. An ideal I of R is called a *radical ideal* if $I = \mathrm{Rad}(I)$.

Let ${}_RM$ be an le-module and n be a submodule element of M. Then $(n : e)$ is an ideal of R. Now we set

$$\mathrm{Rad}(n) = \mathrm{Rad}(n : e),$$

and we call $\mathrm{Rad}(n)$ the *radical* of the submodule element n. It is easy to check that for submodule elements l and n of M, $l \leqslant n \Rightarrow \mathrm{Rad}(l) \subseteq \mathrm{Rad}(n)$; and $\mathrm{Rad}(\mathrm{Rad}(n)) = \mathrm{Rad}(n)$.

PROPOSITION 3.2. *Let ${}_RM$ be an le-module and $x \in M$. If $n_1, n_2, \ldots, n_k$ are submodule elements of M, then*

$$\mathrm{Rad}\left(\bigwedge_{i=1}^{k} n_i : x \right) = \mathrm{Rad}(n_1 : x) \cap \mathrm{Rad}(n_2 : x) \cap \cdots \cap \mathrm{Rad}(n_k : x).$$

PROOF. Let $a \in \mathrm{Rad}\big(\bigwedge_{i=1}^{k} n_i : x \big)$. Then $a^m x \leqslant \bigwedge_{i=1}^{k} n_i \leqslant n_i$, for some $m \in \mathbb{N}$. This shows that $a \in \mathrm{Rad}(n_i : x)$, for each i and hence $a \in \mathrm{Rad}\,(n_1 : x) \cap \mathrm{Rad}(n_2 : x) \cap \cdots \cap \mathrm{Rad}(n_k : x)$. Thus $\mathrm{Rad}\big(\bigwedge_{i=1}^{k} n_i : x \big) \subseteq \mathrm{Rad}(n_1 : x) \cap \mathrm{Rad}(n_2 : x) \cap \cdots \cap \mathrm{Rad}(n_k : x)$. Now let $a \in \mathrm{Rad}(n_1 : x) \cap \mathrm{Rad}(n_2 : x) \cap \cdots \cap \mathrm{Rad}(n_k : x)$. Then $a^{m_1} x \leqslant n_1, a^{m_2} x \leqslant n_2, \ldots, a^{m_k} x \leqslant n_k$, for some $m_1, m_2, \ldots, m_k \in \mathbb{N}$. Let $r = \max\{m_1, m_2, \ldots, m_k\}$. Then $a^r x \leqslant n_i$, for each i, i.e., $a^r x \leqslant \bigwedge_{i=1}^{k} n_i$. Therefore $a \in \mathrm{Rad}\big(\bigwedge_{i=1}^{k} n_i : x \big)$ and it follows that

$$\mathrm{Rad}(n_1 : x) \cap \mathrm{Rad}(n_2 : x) \cap \cdots \cap \mathrm{Rad}(n_k : x) \subseteq \mathrm{Rad}\left(\bigwedge_{i=1}^{k} n_i : x \right).$$

Hence

$$\mathrm{Rad}\left(\bigwedge_{i=1}^{k} n_i : x \right) = \mathrm{Rad}(n_1 : x) \cap \mathrm{Rad}(n_2 : x) \cap \cdots \cap \mathrm{Rad}(n_k : x). \quad \square$$

PROPOSITION 3.3. *Let q be a primary element of an le-module ${}_RM$. Then $\mathrm{Rad}(q)$ is a prime ideal of R.*

PROOF. Let $a, b \in \mathrm{Rad}(q)$. Then $a^m e \leqslant q$ and $b^n e \leqslant q$, for some $m, n \in \mathbb{N}$. So

$$(a - b)^{m+n} e = \sum_{k=0}^{m+n} (-1)^k \binom{m+n}{k} a^{m+n-k} b^k e \leqslant q$$

since either $m+n-k \geqslant m$ or $k \geqslant n$, and q is a submodule element. Thus $a-b \in \mathrm{Rad}(q)$. Also for any $a \in \mathrm{Rad}(q)$ and $r \in R$, $(ra)^m e = r^m a^m e \leqslant q$ shows that $ra \in \mathrm{Rad}(q)$. Hence $\mathrm{Rad}(q)$ is an ideal of R. Let $ab \in \mathrm{Rad}(q)$ and $b \notin \mathrm{Rad}(q)$. Then $(ab)^n = a^n b^n \in (q:e)$, for some $n \in \mathbb{N}$, i.e., $a^n b^n e \leqslant q$. Since $b \notin \mathrm{Rad}(q)$ so $b^r \notin (q:e)$, for every $r \in \mathbb{N}$. In particular $b^n \notin (q:e)$, i.e., $b^n e \nleqslant q$. But q is a primary element and so $(a^n)^k e \leqslant q$, for some $k \in \mathbb{N}$. Thus $a \in \mathrm{Rad}(q)$ and hence $\mathrm{Rad}(q)$ is a prime ideal of R. □

In fact, $\mathrm{Rad}(q)$ is the smallest prime ideal containing $(q:e)$. If q is a primary element of an le-module ${}_RM$ and $\mathrm{Rad}(q) = P$, we say that q is P-primary. One can check that if $q_1, q_2, \ldots, q_r$ be P-primary elements of M, then $q_1 \wedge q_2 \wedge \cdots \wedge q_r$ is P-primary.

The following result characterizes primary elements of an le-module. Also the result is needed to prove the 1st uniqueness theorem.

THEOREM 3.4. *Let q be a P-primary element of an le-module ${}_RM$ and $n \in M$. Then the following results hold*:

(i) *If $n \leqslant q$ then $(q:n) = R$.*

(ii) *If $n \nleqslant q$ then $(q:n)$ is a P-primary ideal of R.*

PROOF. (i) Let $n \leqslant q$ and $r \in R$. Then $rn \leqslant rq \leqslant q$ implies that $r \in (q:n)$ for every $r \in R$. Therefore $(q:n) = R$.

(ii) We have $(q:n)$ is an ideal of R. Let $a, b \in R$ be such that $ab \in (q:n)$ and $b \notin (q:n)$. Then $abn \leqslant q$ and $bn \nleqslant q$. Since q is primary, $a^m e \leqslant q$, for some $m \in \mathbb{N}$. Now $a^m n \leqslant a^m e \leqslant q$ implies that $a^m \in (q:n)$. Thus $(q:n)$ is a primary ideal of R. To show $\mathrm{Rad}(q:n) = P$, let $a \in \mathrm{Rad}(q:n)$. Then $a^m n \leqslant q$, for some $m \in \mathbb{N}$. Since q is primary and $n \nleqslant q$, so $(a^m)^k e \leqslant q$, for some $k \in \mathbb{N}$. Thus $a \in \mathrm{Rad}(q)$, and hence $\mathrm{Rad}(q:n) \subseteq P$. Now let $a \in P$. Then $a^m \in (q:e)$, for some $m \in \mathbb{N}$ implies that $a^m n \leqslant a^m e \leqslant q$. Hence $a \in \mathrm{Rad}(q:n)$ and so $P \subseteq \mathrm{Rad}(q:n)$. Therefore $\mathrm{Rad}(q:n) = P$. Hence $(q:n)$ is a P-primary ideal of R. □

Now we introduce prime submodule elements of an le-module ${}_RM$.

DEFINITION 3.5. A proper submodule element p of an le-module ${}_RM$ is said to be a prime submodule element if for every $r \in R$ and $n \in M$, $rn \leqslant p$ implies that $r \in (p:e)$ or $n \leqslant p$.

In the following result we characterize the relationship of the prime submodule elements of M with the prime ideals of the ring R.

THEOREM 3.6. *Let p be a prime submodule element of an le-module ${}_RM$ and $x \in M$. Then $(p:x)$ is a prime ideal of R for every $x \in M$.*

PROOF. We have $0 \in (p:x)$ and so $(p:x) \neq \emptyset$. Let $a, b \in (p:x)$. Then $ax \leqslant p$ and $bx \leqslant p$ implies that $(a-b)x \leqslant ax + (-b)x \leqslant p + (-p) \leqslant p + p \leqslant p$ and so $a - b \in (p:x)$. Also $(ra)x = r(ax) \leqslant rp \leqslant p$ implies that $ra \in$

$(p : x)$. Thus $(p : x)$ is an ideal of R. Let $a, b \in R$ be such that $ab \in (p : x)$. Then $(ab)x \leqslant p$, i.e. $a(bx) \leqslant p$. Since p is a prime submodule element, so $a \in (p : e) \subseteq (p : x)$ or $bx \leqslant p$, i.e. $a \in (p : x)$ or $b \in (p : x)$. Hence $(p : x)$ is a prime ideal of R. □

In particular we have:

COROLLARY 3.7. *If p is a prime submodule element of an le-module ${}_RM$, then $(p : e)$ is a prime ideal of R.*

The converse of the above corollary does not hold, in general. In the next theorem we prove that if, in addition, p is assumed to be primary then the converse holds. This result also characterizes when a primary element becomes a prime submodule element.

THEOREM 3.8. *Let p be a proper submodule element of an le-module ${}_RM$. If $(p : e)$ is a prime ideal of R and p is primary, then p is a prime submodule element.*

PROOF. Let $rn \leqslant p$ and $n \nleqslant p$ for $r \in R$ and $n \in M$. Since p is primary so $r^m e \leqslant p$, for some $m \in \mathbb{N}$, i.e., $r^m \in (p : e)$. Since $(p : e)$ is a prime ideal of R so $r \in (p : e)$. Consequently, p is a prime submodule element. □

4. Primary decomposition in Laskerian le-modules

An R-module M is called Laskerian if each submodule is a finite intersection of primary submodules. Many authors assumed Laskerian modules to be finitely generated. For further information on Laskerian modules readers are referred to [9,10,29,31].

Let ${}_RM$ be an le-module and n be a submodule element of M. Then n is said to have a primary decomposition if there exist primary elements q_1, q_2, …, q_k of M such that

$$n = q_1 \wedge q_2 \wedge \cdots \wedge q_k$$

A primary decomposition is called *reduced* if:

(i) $q_1 \wedge q_2 \wedge \cdots \wedge q_{i-1} \wedge q_{i+1} \wedge \cdots \wedge q_k \nleqslant q_i$, for all $i = 1, 2, \ldots, k$.

(ii) $\mathrm{Rad}(q_i) \neq \mathrm{Rad}(q_j)$ for $i \neq j$.

An le-module ${}_RM$ is said to be *Laskerian* if every submodule element of ${}_RM$ has a primary decomposition.

Throughout the rest of the article, every le-module ${}_RM$ is Laskerian. It is easy to observe that if a submodule element n of an le-module ${}_RM$ has a primary decomposition then it has a reduced primary decomposition.

The following result characterizes a relationship between prime submodule elements of an le-module ${}_RM$ and radical ideals of the ring R using primary decomposition.

THEOREM 4.1. *Let n be a proper submodule element of an le-module M which has a reduced primary decomposition $n = q_1 \wedge q_2 \wedge \cdots \wedge q_k$. Then every q_i is a prime submodule element of M if and only if $(n : e)$ is a radical ideal of R.*

PROOF. First assume that each q_i is a prime submodule element. We have $(n : e) \subseteq \mathrm{Rad}(n)$. Now let $a \in \mathrm{Rad}(n)$. Then $a^m e \leqslant n = \bigwedge_{i=1}^{k} q_i$, for some $m \in \mathbb{N}$. Therefore $a^m e \leqslant q_i$, for each i. Since q_i is prime so $ae \leqslant q_i$ or $a^{m-1}e \leqslant q_i$, for each i. If $ae \leqslant q_i$ then $a \in (q_i : e)$. Otherwise $a^{m-1}e \leqslant q_i$ implies $ae \leqslant q_i$ or $a^{m-2}e \leqslant q_i$. Continuing in this way we get $a \in (q_i : e)$, for each i. Thus $a \in (q_1 : e) \cap (q_2 : e) \cap \cdots \cap (q_k : e)$, i.e., $a \in (n : e)$. Hence $\mathrm{Rad}(n) = (n : e)$. Therefore, $(n : e)$ is a radical ideal of R.

Conversely, assume that $(n : e)$ is a radical ideal of R, i.e. $\mathrm{Rad}(n) = (n : e)$. Let $\mathrm{Rad}(q_i) = P_i$. We claim that $\mathrm{Rad}(q_i) = (q_i : e)$. Let $a \in P_i$. Since $\bigcap_{i=1}^{k} P_i$ is reduced, there exists $b \in \cap P_j$ but $b \notin P_i$ in R. Now

$$ab \in \bigcap_{i=1}^{k} P_i = \bigcap_{i=1}^{k} \mathrm{Rad}(q_i) = \mathrm{Rad}(n) = (n : e) = \bigcap_{i=1}^{k} (q_i : e)$$

implies $abe \leqslant q_i$, for each i. Since q_i is primary and $b \notin P_i$, so $ae \leqslant q_i$, i.e., $a \in (q_i : e)$. Consequently, $P_i = (q_i : e)$. Hence by Theorem 3.8, each q_i is a prime submodule element. □

Let I be an ideal of a ring R. A prime ideal P is called a *minimal prime divisor* of I if it is minimal among all prime ideals containing I. If I is a prime ideal, then I is the only minimal prime divisor of I. Thus a prime ideal P of R is a minimal prime divisor of I if $I \subseteq P$ and if there is no prime ideal P' of R such that $I \subseteq P' \subset P$.

Let n be a submodule element of M. Then the minimal prime divisors of $(n : e)$ are called *minimal prime divisors* of n. Immediately we have $\mathrm{Rad}(n) = \bigcap P$ where the intersection is over all minimal prime divisors of n. We omit the proof since it is similar to the analogous result in the ideal theory of rings.

Let $n = q_1 \wedge q_2 \wedge \cdots \wedge q_m$ be a reduced primary decomposition of a submodule element n of ${}_RM$ and let $P_i = \mathrm{Rad}(q_i)$, for $i = 1, 2, \ldots, m$. The prime ideals P_1, P_2, …, P_m are called *prime divisors* of n or *associated primes* of n.

THEOREM 4.2. *Let n be a proper submodule element of an le-module M which has a reduced primary decomposition $n = q_1 \wedge q_2 \wedge \cdots \wedge q_k$ and $P_i = \mathrm{Rad}(q_i)$ be the associated prime ideals of n. Let P be a prime ideal of R then $(n : e) \subseteq P$ if and only if $P_i \subseteq P$ for some $i = 1, 2, \ldots, k$.*

PROOF. Let $(n : e) \subseteq P$. Then, by Proposition 2.2, $\bigcap_{i=1}^{k} (q_i : e) \subseteq P$ which implies that $(q_i : e) \subseteq P$, for some i. Now P_i is the smallest prime ideal

containing $(q_i : e)$, hence $P_i \subseteq P$, for some i. Conversely suppose $P_j \subseteq P$, for some j. Then

$$(n : e) = \bigcap_{i=1}^{k} (q_i : e) \subseteq \bigcap_{i=1}^{k} \mathrm{Rad}(q_i) \subseteq \mathrm{Rad}(q_j) = P_j \subseteq P. \quad \square$$

COROLLARY 4.3. *Let n be a submodule element of an le-module M. Then every minimal prime divisor of n is a prime divisor of n and is minimal in the set of prime divisors of n.*

THEOREM 4.4 (1st uniqueness theorem). *Let n be a submodule element of an le-module ${}_RM$ and assume that n has a reduced primary decomposition $n = q_1 \wedge q_2 \wedge \cdots \wedge q_r$. Let P be a prime ideal of R. Then $P = \mathrm{Rad}(q_i)$ for some i if and only if $(n : x)$ is a P-primary ideal of R for some $x \nleqslant n$. Hence the set of all associated primes is independent of primary decomposition of n.*

PROOF. Let $P_i = \mathrm{Rad}(q_i)$, for $i = 1, 2, \ldots, m$. Without loss of generality, we assume that $P = P_1$. Since the decomposition is reduced, in particular $q_2 \wedge q_3 \wedge \cdots \wedge q_m \nleqslant q_1$. Let $x = q_2 \wedge q_3 \wedge \cdots \wedge q_m$. Then $x \nleqslant n$ and

$$(n : x) = (q_1 \wedge q_2 \wedge \cdots \wedge q_m : x) = (q_1 : x) \cap (q_2 : x) \cap \cdots \cap (q_m : x).$$

By Theorem 3.4, $(q_i : x) = R$, for $i = 2, 3, \ldots, m$ and whence $(n : x) = (q_1 : x)$. Thus $(n : x)$ is a P-primary ideal of R, by Theorem 3.4.

Conversely suppose that $(n : x)$ is a P-primary ideal of R, for some $x \nleqslant n$. We have

$$P = \mathrm{Rad}(n : x) = \mathrm{Rad}(q_1 : x) \cap \mathrm{Rad}(q_2 : x) \cap \cdots \cap \mathrm{Rad}(q_m : x).$$

Now $x \nleqslant n$ implies that $x \nleqslant q_i$, for some i say $x \nleqslant q_k$; $1 \leqslant k \leqslant m$. Then by the fact that $(q_i : x) \subseteq \mathrm{Rad}(q_i : x)$ and by Theorem 3.4, we have, for each i, $\mathrm{Rad}(q_i : x) = P_i$ or R, and is equal to P_i for $i = k$. Hence P is the intersection of some prime ideals $P_{i_1}, P_{i_2}, \ldots, P_{i_h}$ $(1 \leqslant h \leqslant m)$.i.e., $P = P_{i_1} \cap P_{i_2} \cap \cdots \cap P_{i_h}$. Thus $P = P_i$, for some i. $\square$

The following consequence is immediate.

COROLLARY 4.5. *Let n be a submodule element of an le-module ${}_RM$ and assume that n has a primary decomposition. If*

$$n = q_1 \wedge q_2 \wedge \cdots \wedge q_r = q_1' \wedge q_2' \wedge \cdots \wedge q_s'$$

are two reduced primary decompositions of n, then $r = s$ and the q_i and q_i' can be so numbered that $\mathrm{Rad}(q_i) = \mathrm{Rad}(q_i')$ for $i = 1, 2, \ldots, r$.

Let S be a multiplicatively closed set in R and n be a submodule element of an le-module M. We define

$$n_S = \bigvee \{ x \in M : sx \leqslant n, \text{ for some s } \in S \}$$

Note that if $(n : e) \cap S \neq \emptyset$ then $n_S = e$. Thus if $0 \in S$, then $n_S = e$. If n is a submodule element of M then n_S is a submodule element of M. We call the submodule element n_S the *S-component* of n.

The following result gives a connection between a multiplicative closed subset S in R and the S-component of a submodule element of M having a primary decomposition. Also the result is very useful for the 2nd uniqueness theorem.

PROPOSITION 4.6. *Let ${}_RM$ be an le-module and n be a submodule element M having a primary decomposition $n = q_1 \wedge q_2 \wedge \cdots \wedge q_m$ where q_i are P_i-primary. If S is a multiplicatively closed set in R such that $P_i \cap S = \emptyset$, for $i = 1, 2, \ldots, k$ and $P_i \cap S \neq \emptyset$, for the remaining i then $n_S = q_1 \wedge q_2 \wedge \cdots \wedge q_k$.*

PROOF. Let $T = \{x \in M : sx \leqslant n, \text{ for some } s \in S\}$. Then $n_S = \bigvee T$. Let $x \in T$. Then there exists $s \in S$ such that $sx \leqslant n = \bigwedge_{i=1}^{m} q_i \leqslant q_i$, for $i = 1, 2, \ldots, m$. Since $P_i \cap S = \emptyset$, $s \notin P_i$ and hence $x \leqslant q_i$, for $i = 1, 2, \ldots, k$. It follows that $n_S = \bigvee T \leqslant q_1 \wedge q_2 \wedge \cdots \wedge q_k$.

Now denote $q = q_1 \wedge q_2 \wedge \cdots \wedge q_k$. If $k = m$, then $q = n \in T$ implies that $q_1 \wedge q_2 \wedge \cdots \wedge q_k = q \leqslant \bigvee T = n_S$. Thus $n_S = q_1 \wedge q_2 \wedge \cdots \wedge q_k$. If $k \neq m$, then for $j = k+1, k+2, \ldots, m$ choose $s_j \in P_j \cap S$ and so $s_j^{r_j} e \leqslant q_j$ for some $r_j \in \mathbb{N}$. Then for large enough $r \in \mathbb{N}$, we have

$$(s_{k+1} \cdot s_{k+2} \cdots s_m)^r e \leqslant q_{k+1} \wedge q_{k+2} \wedge \cdots \wedge q_m$$

and hence

$$(s_{k+1} \cdot s_{k+2} \cdots s_m)^r q \leqslant (s_{k+1} \cdot s_{k+2} \cdots s_m)^r e \leqslant q_{k+1} \wedge q_{k+2} \wedge \cdots \wedge q_m.$$

Also

$$(s_{k+1} \cdot s_{k+2} \cdots s_m)^r q = (s_{k+1} \cdot s_{k+2} \cdots s_m)^r (q_1 \wedge q_2 \wedge \cdots \wedge q_k)$$
$$\leqslant (s_{k+1} \cdot s_{k+2} \cdots s_m)^r q_1 \wedge (s_{k+1} \cdot s_{k+2} \cdots s_m)^r q_2 \wedge \cdots \wedge (s_{k+1} \cdot s_{k+2} \cdots s_m)^r q_k$$
$$\leqslant q_1 \wedge q_2 \wedge \cdots \wedge q_k,$$

since S is multiplicatively closed and q_i's are submodule elements. Thus

$$(s_{k+1} \cdot s_{k+2} \cdots s_m)^r q \leqslant q_1 \wedge q_2 \wedge \cdots \wedge q_m = n$$

which implies that $q \in T$ and so $q \leqslant n_S$. Therefore $q_1 \wedge q_2 \wedge \cdots \wedge q_k \leqslant n_S$. Hence $n_S = q_1 \wedge q_2 \wedge \cdots \wedge q_k$. $\square$

Let ${}_RM$ be an le-module and q be a submodule element of M which has a reduced primary decomposition $q = q_1 \wedge q_2 \wedge \cdots \wedge q_n$ and $P_i = \mathrm{Rad}(q_i)$, for $i = 1, 2, \ldots, n$. Then P_i is called an *isolated prime divisor* of n if P_i is minimal in the set of all prime divisors of n, i.e., P_i does not contain properly any P_j, $(i \neq j)$. If P_i is an isolated prime divisor of n then q_i is called an *isolated component* of n. In the next theorem we show that the isolated components of n are uniquely determined by n.

THEOREM 4.7. *Let ${}_RM$ be an le-module and n a proper submodule element of M which has a reduced primary decomposition $n = q_1 \wedge q_2 \wedge \cdots \wedge q_m$ and $P_i = \mathrm{Rad}(q_i)$. Then*

$$q_i' = \bigvee \{x \in M : (n : x) \not\subseteq P_i\}$$

is a submodule element of M which is contained in q_i. If q_i is an isolated primary component of n then $q_i = q_i'$.

PROOF. Let $T = \{x \in M : (n : x) \not\subseteq P_i\}$. Consider $x, y \in T$ and $r \in R$. Then $(n : x) \not\subseteq P_i$ and $(n : y) \not\subseteq P_i$ and so there exist $a, b \in R$ such that $ax \leqslant n$ and $by \leqslant n$ but $a, b \notin P_i$. Therefore $ab(x + y) = (ab)x + (ab)y \leqslant bn + an \leqslant n + n = n$ implies that $ab \in (n : x + y)$. Since P_i is a prime ideal and $a, b \notin P_i$, $ab \notin P_i$. Thus $(n : x + y) \not\subseteq P_i$ and hence $x + y \in T$. Also $arx = rax \leqslant rn \leqslant n$ implies that $a \in (n : rx)$. But $a \notin P_i$ and so $(n : rx) \not\subseteq P_i$. Thus $rx \in T$. Hence

$$q_i' + q_i' = \bigvee_{x \in T} x + \bigvee_{y \in T} y = \bigvee_{x,y \in T} (x + y) \leqslant q_i'$$

and

$$rq_i' = r\left(\bigvee_{x \in T} x\right) = \bigvee_{x \in T} (rx) \leqslant q_i'$$

implies that q_i' is a submodule element of M. Let $x \in T$. Then $(n : x) \not\subseteq P_i$, and so there exists $a \in (n : x)$ such that $a \notin P_i$. Thus $ax \leqslant n \leqslant q_i$ which implies that $x \leqslant q_i$, since q_i is a primary element. Hence $q_i' = \bigvee_{x \in T} x \leqslant q_i$.

If q_i is an isolated primary component of n then $\mathrm{Rad}(q_i) = P_i$ is a minimal associated prime of n and so $P_j \not\subseteq P_i$ for $i \neq j$. Then there exists $a_j \in P_j$ such that $a_j \notin P_i$. Thus $a_j^{r_j} e \leqslant q_j$ for some $r_j \in \mathbb{N}$. Let $a = \prod_{j \neq i} a_j^{r_j}$. Then $ae \leqslant \bigwedge_{j \neq i} q_j$ but $a \notin P_i$, since P_i is prime ideal. Now $aq_i \leqslant ae \leqslant \bigwedge_{j \neq i} q_j$ and $aq_i \leqslant q_i$ implies that $aq_i \leqslant \bigwedge_{i=1}^{m} q_i = n$ and hence $a \in (n : q_i)$. Thus $(n : q_i) \not\subseteq P_i$ and so $q_i \in \{x \in M : (n : x) \not\subseteq P_i\}$. Hence $q_i \leqslant q_i'$ and it follows that $q_i = q_i'$. $\square$

Let ${}_RM$ be an le-module and n a proper submodule element of M which has a reduced primary decomposition $n = q_1 \wedge q_2 \wedge \cdots \wedge q_m$. We have

$$\begin{aligned}\operatorname{Rad}(n) &= \operatorname{Rad}(q_1 \wedge q_2 \wedge \cdots \wedge q_m)\\ &= \operatorname{Rad}(q_1) \cap \operatorname{Rad}(q_2) \cap \cdots \cap \operatorname{Rad}(q_m) = P_1 \cap P_2 \cap \cdots \cap P_m,\end{aligned}$$

where $P_i = \operatorname{Rad}(q_i)$ are prime divisors of n. If some P_j is not isolated then $P_i \subseteq P_j$ for some P_i and hence we can delete such P_j from the above. Thus $\operatorname{Rad}(n)$ is the intersection of isolated prime divisors of n. As a consequence it follows that, $\operatorname{Rad}(n)$ is a prime ideal of R if and only if n has a single isolated prime divisor.

THEOREM 4.8 (2nd uniqueness theorem). *Let ${}_RM$ be an le-module and n a submodule element of M. If $\{P_{i_1}, P_{i_2}, \ldots, P_{i_k}\}$ is a set of isolated prime divisors of n then $q_{i_1} \wedge q_{i_2} \wedge \cdots \wedge q_{i_k}$ depends only on this set and not on the particular reduced primary decomposition of n.*

PROOF. Let $S = R\backslash(P_{i_1} \cup P_{i_2} \cup \cdots \cup P_{i_k})$. Then S is a multiplicatively closed set in R. To prove the theorem it is sufficient to show $n_S = q_{i_1} \wedge q_{i_2} \wedge \cdots \wedge q_{i_k}$. For this we only need to show that $S \cap P_i = \emptyset$, for $i = i_1, i_2, \ldots, i_k$, and $S \cap P_i \neq \emptyset$, for $i \neq i_1, i_2, \ldots, i_k$, rest will follow from the Theorem 4.6. The former is certainly true. Let $i \neq i_1, i_2, \ldots, i_k$. Since $\{P_{i_1}, P_{i_2}, \ldots, P_{i_k}\}$ is a set of isolated prime divisors of n, we have $P_i \nsubseteq P_{i_j}$, for $j = 1, 2, \ldots, k$, and hence $P_i \nsubseteq \bigcup_{j=1}^{k} P_{i_j}$. Thus $S \cap P_i \neq \emptyset$. □

The following consequence of the uniqueness of primary components corresponding to minimal prime divisors of a submodule element is immediate from Theorem 4.6 and Theorem 4.8.

COROLLARY 4.9. *Suppose that n is a submodule element of an le-module M and let P be a minimal prime divisor of n. If a P-primary element q occurs in a reduced primary decomposition of n, then q occurs in every reduced primary decomposition of n.*

References

[1] E. A. Al-Khouja, Maximal elements and prime elements in lattice modules, *Damascus Univ. J. of Basic Sciences*, **19** (2003), 9–21.

[2] D. D. Anderson, *Multiplicative lattices*, Dissertation, University of Chicago (1974).

[3] D. D. Anderson, Abstract commutative ideal theory without chain condition, *Algebra Universalis*, **6** (1976), 131–145.

[4] D. D. Anderson, Fake rings, fake modules, and duality, *J. Algebra*, **47** (1977), 425–432.

[5] D. D. Anderson and E. W. Johnson, Abstract ideal theory from Krull to the present, in: *Ideal Theoretic Methods in Commutative Algebra*, (Columbia, MO, 1999), Lecture notes in Pure and Appl. Math., 220, Marcel Dekker (New York, 2001), pp. 27–47.

[6] M. F. Atiyah and I. G. MacDonald, *Introduction to Commutative Algebra*, Addison-Wesley Publishing Company (1969).
[7] R. P. Dilworth, Abstract commutative ideal theory, *Pacific J. Math.*, **12** (1962), 481–498.
[8] L. Fuchs and R. Reis, On lattice-ordered commutative semigroups, *Algebra Universalis*, **50** (2003), 341–357.
[9] W. Heinzer and D. Lantz, The Laskerian property in commutative rings, *J. Algebra*, **72** (1981), 101–114.
[10] C. Jayaram and U. Tekir, Q-modules, *Turk. J. Math.*, **33** (2009), 215–225.
[11] J. A. Johnson, a-adic completion of Noetherian lattice module, *Fund. Math.*, **66** (1970), 341–371.
[12] J. A. Johnson, Noetherian lattice modules and semi-local completions, *Fund. Math.*, **73**, (1970), 93–103.
[13] J. A. Johnson, Quotients in Noetherian lattice modules, *Proc. Amer. Math. Soc.*, **28** (1971), 71–74.
[14] E. W. Johnson and J. A. Johnson, Lattice modules over semi-local Noether lattices, *Fund. Math.*, **68** (1970), 187–201.
[15] E. W. Johnson and J. A. Johnson, Lattice modules over principal element domains, *Comm. Algebra*, **31** (2003), 3505–3518.
[16] W. Krull, Axiomatische begrundung der allgemeinen idealtheorie, *Sitzungsber. phys.-med. Soz. Erlangen*, **56** (1924), 47–63.
[17] M. Kumbhakar and A. K. Bhuniya, On the prime spectrum of an le-module, arXiv:1807.04024[math.RA].
[18] M. Kumbhakar and A. K. Bhuniya, On Noetherian pseudo-prime spectrum of a topological le-module, communicated.
[19] M. Kumbhakar and A. K. Bhuniya, On irreducible pseudo-prime spectrum of topological le-modules, *Quasigroups Related Systems*, **26** (2018), 251–262.
[20] M. D. Larsen and P. J. McCarthy, *Multiplicative Theory of Ideals*, Pure and Applied Mathematics, 43, Academic Press (New York–London, 1971).
[21] C. P. Lu, Prime submodules of modules, *Comment. Math. Univ. St. Paul.*, **22** (1984), 61-69.
[22] D. J. Majcherek, *Multiplicative lattice versions of some results from Noetherian commutative rings*, Dissertation, University of California, Riverside (2014).
[23] C. S. Manjarekar and A. V. Bingi, Absorbing elements in lattice modules, *Int. Electron. J. Algebra*, **19** (2016), 58–76.
[24] C. S. Manjarekar and U. N. Kandale, Primary decomposition in lattice modules, *European J. Pure Appl. Math.*, **7** (2014), 201–209.
[25] R. L. McCasland and M. E. Moore, Prime submodules, *Comm. Algebra*, **20** (1992), 1803–1817.
[26] H. M. Nakkar, Localization in multiplicative lattice modules, *Mat. Issled.*, **2** (1974), 88–108 (in Russian).
[27] H. M. Nakkar and D. D. Anderson, Associated and weakly associated prime elements and primary decomposition in lattice modules, *Algebra Universalis*, **25** (1988), 196–209.
[28] H. M. Nakkar and D. D. Anderson, Localization of associated and weakly associated prime elements and supports of lattice modules of finite length, *Studia Sci. Math. Hungar.*, **25** (1990), 263–273.
[29] N. Radu, Sur les anneaux coherents Laskeriens, *Rev. Roum. Math. Pures Appl.*, **11** (1966), 865–867.
[30] P. F. Smith, Uniqueness of primary decompositions, *Turk. J. Math.*, **27** (2003), 425–434.
[31] S. Visweswaran, Laskerian pairs, *J. Pure Appl. Algebra*, **59** (1989), 87–110.

[32] M. Ward and R. P. Dilworth, Residuated lattices, *Trans. Amer. Math. Soc.*, **35** (1939), 335–354.
[33] M. Ward and R. P. Dilworth, Lattice theory of ova, *Ann. of Math.*, **40** (1939), 600–608.
[34] M. Ward and R. P. Dilworth, Evaluations over residuated structures, *Ann. of Math.*, **40** (1939), 328–338.
[35] D. G. Whitman, Ring theoretic lattices modules and the Hilbert polynomial, Dissertation, University of California, Riverside (1967).
[36] D. G. Whitman, On ring theoretic lattice modules, *Fund. Math.*, **70** (1971), 221–229.

ISSN - 0976-9536

Yearly Shakespeare 2019

AN INTERNATIONAL
PEER-REVIEWED JOURNAL

Vol – XVII/ Issue 17

Edited by
GOUTAM GHOSAL

Sri Aurobindo Study Centre
Santiniketan – 731235
INDIA

Edited and published by Goutam Ghosal on behalf of
Sri Aurobindo Study Centre
Sri Aurobindo Nilay
Santiniketan – 731235
India
E-Mail : gghosal87@gmail.com
Mobile : 0-9832852705

A non-profit publication

Dedicated
To
The Mother

Acknowledgement :

Manoj Dasgupta, Matriprasad, Abhijit Bajpayee, Biswajit Ganguly and Sambit Sinha.

250/-

CONTENTS

USE OF SHAKESPEARE FOR ISSUING CULTURAL DIFFERENCE IN SALMAN RUSHDIE'S NOVELS

Indrajit Mukherjee

Whenever we think of history as an international discourse, it reminds us of Dipesh Chakrabarty's dictum "'Europe' remains the sovereign, theoretical subject of all histories, including the ones we call 'Indian', 'Chinese', 'Kenyan' and so on" (Chakrabarty 1992: 1), thereby summing up the complex relationship between the Colonizer and the Colonized, the Black and the White, the Occident and the Orient, in terms of power, domination, and varying degrees of complicated hegemony. Intertextuality, a self-conscious, self-contradictory and self-undermining use of the inter-involvement of literary texts with one another, a stylistic way of talking about allusions and influence, with a deliberate purpose to politicize representation in order to unsettle all accepted beliefs and ideologies, and problematize the parameters of one's own writing, is central to the discussion of the postmodern novel in order to totalizing solutions to the contradiction of society. T. S. Eliot in his landmark essay "Tradition and Individual Talent" shows us that literature is highly plagiaristic because "the most individual parts of a poet's work may be those in which the dead poets, his ancestors, assert their immortality most vigorously" (Eliot 1975: 38), illustrating that they are using other's ideas and quotations to enhance their own ideas, not simply plagiarizing them. Graham Allen looks upon intertextuality in the space of a given text "as a split, multiple concepts, which poses questions and requires one to engage with them rather than forcing one to produce definite answers" (2000: 59-60); Umberto Echo notes, "Works are created by works, texts are created by texts, all together they speak to each other independently of the intention of their authors" (1986: 200); Ihab Hassan describes "intertextuality" as a "patina of thoughts, of signifiers, of 'connections', now lies on everything the mind touches" (1987: 172). Taking cue from Barthes, Foucault, Kristeva, Deleuze, and Guattari's critical notion we may assume that 'intertextuality' or 'repetition' has been consciously used as a postcolonial implement for issuing a new discourse in the creation of the identity of the colonized, and in this sense Shakespeare's canonical texts, such as *Macbeth*, *Othello*, *The Tempest*, have been reworked by Gail Jones in *Sorry* (2007), George Lamming in *Water with Berries* (1971), Salman Rushdie in *The Moor's Last Sigh* (1995) respectively, thereby rendering the Renaissance Elizabethan playwright relevant all over again. Applying the

Regn. No.: B-731/06
20-04/06

ISSN no.: ISSN0975-167X

HETEROGLOSSIA

the creative and the critical eye
(a refereed journal)

Volume: IX, 2019

A Special Issue on Ancient Classical Literature

EDITED BY
INDRANI DEB

NISTARINI COLLEGE
PURULIA

Distributed by
Books Way
Publishers and Distributors
86A, College Street (Y.M.C.A. Building)
Kolkata - 700 073
Ph. : 91-33-22572476/2423
E-mail : bookswaypub@gmail.com
Visit us: www.booksway.in

9th Volume Special Issue : 2019

Price: Rupees **Three Hundred** Only (Single Copy)

Printed by
D. G. Offset
36/N, Maharani Indra Devi Road
Kolkata 700060, INDIA

CONTENTS

Starks-Estes, Lisa S. 2014. "Coda: Philomela's Song: Transformations of Ovid, Trauma, and Masochism in *A Midsummer Night's Dream* and *Cymbeline*." In Lisa S. Starks-Estes. *Violence, Trauma and Virtus in Shakespeare's Roman Poems and Plays Transforming Ovid*. Hampshire and New York: Palgrave Macmillan, 160-83.

—. 2014. "Introduction." In Lisa S. Starks-Estes. *Violence, Trauma and Virtus in Shakespeare's Roman Poems and Plays Transforming Ovid*. Hampshire and New York: Palgrave Macmillan, 1-59.

—. 2014. *Violence, Trauma and Virtus in Shakespeare's Roman Poems and Plays Transforming Ovid*. Hampshire and New York: Palgrave Macmillan.

Weller, Barry. "Identity Dis-figured: "*A Midsummer Night's Dream*"." *The Kenyon Review* 7.3 (Summer, 1985): 66-78. URL: www.jstor.org/stable/4335604. Accessed on 6th December, 2018.

Wyrick, Deborah Baker. "The Ass Motif in *The Comedy of Errors* and *A Midsummer Night's Dream*." *Shakespeare Quarterly* 33.4 (Winter, 1982): 432-48. URL: www.jstor.org/stable/2870124. Accessed on 6th December, 2018.

Echoes of Virgil in Marlowe's Underrated Text

Indrajit Mukherjee

> Dido, and her Aeneas, shall want troops,
> And all the haunt be ours.
> Shakespeare: *Antony and Cleopatra* (IV.14.53-54)

"Influence", according to Harold Bloom, "is a metaphor, one that implicates a matrix of relationships—imagistic, temporal, spiritual, psychological—all of them ultimately defensive in their nature" (1997: xxiii). Marlowe (1564-'93), the most striking personality and the most impressive dramatist among the University Wits, used his classical background to create his "mighty lines" whose heightened rhetoric matches the hugely spectacular dramatic intentions of the oeuvre. *The Tragedie of Dido Queene of Carthage: Played by the Children of her Maiesties Chappell. Written by Christopher Marlowe, and Thomas Nash. Gent,* as the title page indicates, finds its fountain in classical epic, dramatizing Book I, II and IV of Virgil's Aeneid with a veneer of Ovidian shading from the *Heroides* Book *VII*. Virgil's *Dido,* which "has been read variously as a paradigm of chaste widowhood, the protagonist of a tragic tale as well as a Medea-like queen seducing AEneas" (2001-2002:19-20), finds a prominent position in an era of Renaissance in which the motto was *Homo sum: humani nil a me alienum puto* (" I am a man and nothing that touches humanity is alien to me") through the Petrarchan sonnets, and through the plays of Alessandro Pazzi, John Rightwise, Glambattista Giraldi Cinthio and Lodovico Dolce. Marlowe's *Dido, Queen of Carthage* (probably composed around 1585-1586) is based on a myth which was exceptionally important to the English Renaissance, the story of the tragic fall on the ringing plains of windy Troy and its aftermath. It is the central material of both the Greek and Roman national epics, and it is also the story which Shakespearean Hamlet asks the Player King to recite: "One speech in't I chiefly lived;' twas AEneas' tale to Dido, and thereabout